INFORMATION TO USERS

This manuscript has been reproduced from the microfilm master. UMI films the text directly from the original or copy submitted. Thus, some thesis and dissertation copies are in typewriter face, while others may be from any type of computer printer.

The quality of this reproduction is dependent upon the quality of the copy submitted. Broken or indistinct print, colored or poor quality illustrations and photographs, print bleedthrough, substandard margins, and improper alignment can adversely affect reproduction.

In the unlikely event that the author did not send UMI a complete manuscript and there are missing pages, these will be noted. Also, if unauthorized copyright material had to be removed, a note will indicate the deletion.

Oversize materials (e.g., maps, drawings, charts) are reproduced by sectioning the original, beginning at the upper left-hand corner and continuing from left to right in equal sections with small overlaps. Each original is also photographed in one exposure and is included in reduced form at the back of the book.

Photographs included in the original manuscript have been reproduced xerographically in this copy. Higher quality 6" x 9" black and white photographic prints are available for any photographs or illustrations appearing in this copy for an additional charge. Contact UMI directly to order.

UMI

A Bell & Howell Information Company
300 North Zeeb Road, Ann Arbor MI 48106-1346 USA
313/761-4700 800/521-0600

Phosphinoorganosilane Synthesis and Bis(phosphinoorgano)silyl Complexes of Ruthenium

by

Xiaobing Zhou
B.Sc., Beijing University, 1989

A Dissertation Submitted in Partial Fulfillment of the
Requirements for the Degree of

DOCTOR OF PHILOSOPHY

in the Department of Chemistry

We accept this dissertation as conforming
to the required standard

Dr. S.R. Stobart, Supervisor (Department of Chemistry)

Dr. R.H. Mitchell, Departmental Member (Department of Chemistry)

Dr. D.J. Berg, Departmental Member (Department of Chemistry)

Dr. C.E. Picciotto, Outside Member (Department of Physics and Astronomy)

Dr. M.D. Fryzuk, External Examiner (Department of Chemistry, University of British Columbia)

Supervisor: Dr. S.R. Stobart

Abstract

Hydrozirconation and subsequent phosphination have been developed into a versatile synthetic methodology leading to formation of phosphorus-carbon bonds. A family of phosphinoalkylsilane ligand precursors $SiHMe_n(CH_2CH_2CH_2PPh_2)_{3-n}$ (ChelH, **I**: n = 2; biPSiH, **II**: n = 1; triPSiH, **III**: n = 0) previously prepared via a photo-chemical route were synthesized in this way and the phosphination step has been shown to be dependent on steric factors. Similar methods have been used to obtain a group of new ligand precursors, the poly(silaalkyl)phosphines $PPh_n(CH_2CH_2CH_2PR_2)_{3-n}$ (**12**: n = 1; **13**: n = 0), which have been isolated and fully characterized. Analogues $PPh_n(o\text{-}C_6H_4SiMe_2H)_{3-n}$ (**21**: n = 1; **22**: n = 0) containing more rigid benzylic backbones have been prepared from the corresponding (*o*-tolyl)phosphines via polylithiation and shown to exhibit temperature dependent NMR behavior. Poly(silaalkyl)phosphine coordination chemistry has been explored, yielding an unprecedented *trans*-bis(silyl) Pt(II) complex $Pt[PhP(o\text{-}C_6H_4CH_2SiMe_2)_2]PPh_3$ (**25**) which was isolated and characterized by using spectroscopic methods.

The chemistry of [bis(diphenylphosphinopropyl)silyl] hydrido dicarbonyl ruthenium(II), $RuH(biPSi)(CO)_2$ (**26**), has been investigated in detail. The two diastereomers, *syn* and *anti*, were observed to exchange slowly with the two CO groups also scrambling at a comparable rate. A kinetic study of these two intramolecular isomerization processes suggests the involvement of dissociation and re-association of the chelate (biPSi) phosphines. Oxygen atom insertion into the Ru-Si bond of **26** occurs both

in a hydrolysis process and direct oxidation by dioxygen. A labeling experiment suggests the former may involve a molecular dihydrogen intermediate, while the latter leads to insertion of oxygen atoms into both Ru-Si and Si-C bonds. Chlorination of **26** and subsequent thermal loss of a CO group afforded a novel 16e five coordinate Ru(II) species RuCl(biPSi)(CO) (**42**). Reaction of **42** with $NaBH_4$ or $LiAlH_4$ gave a mononuclear borohydride complex Ru(biPSi)(CO)(μ-η^2-H_2BH_2) (**43**) or a rare hydrido anionic complex [*fac*-Ru$(H)_2$(biPSi)(CO)]$^-$ (**44**), both of which are extremely sensitive and have been identified *in situ* by using solution NMR spectroscopy. The silyl group in **26** was found to exert a stronger *trans* effect than hydride.

Examiners:

Dr. S.R. Stobart, Supervisor (Department of Chemistry)

Dr. R.H. Mitchell, Departmental Member (Department of Chemistry)

Dr. D.J. Berg, Departmental Member (Department of Chemistry)

Dr. C.E. Picciotto, Outside Member (Department of Physics and Astronomy)

Dr. M.D. Fryzuk, External Examiner (Department of Chemistry, University of British Columbia)

Table of Contents

List of Compounds

I $SiHMe_2CH_2CH_2CH_2PPh_2$ (ChelH)

II $SiHMe(CH_2CH_2CH_2PPh_2)_2$ (biPSiH)

III $SiH(CH_2CH_2CH_2PPh_2)_3$ (triPSiH)

IV $Ph_2PCH_2CH_2CH_2Cl$

V $(EtO)_3SiCH_2CH_2CH_2PPh_2$

VI $SiHMe(o\text{-}CH_2C_6H_4PPh_2)_2$ (mcbiPSiH)

1 $ZrCp_2(CH_2CH_2SiEt_3)Cl$

2 $Et_3SiCH_2CH_2PPh_2$

3 $ZrCp_2(CH_2CH_2CH_2SiMe_2H)Cl$

4 $SiHMe_2CH_2CH_2CH_2Br$

5 $SiHMe_2CH_2CH_2CH_2I$

6 $SiHMe^nPr(CH_2CH_2CH_2PPh_2)$

7 $SiH^nPr_2(CH_2CH_2CH_2PPh_2)$

8 $SiH^nPr(CH_2CH_2CH_2PPh_2)_2$

9 $SiH_2(CH_2CH_2CH_2PPh_2)_2$

10 $SiHMe(CH_2CH_2CH_2P^nhex_2)_2$ [biP(^{n}hex)$_2$SiH]

11 $SiHMe(CH_2CH_2CH_2PPhBz)_2$ [biP(PhBz)SiH]

12 $PhP(CH_2CH_2CH_2SiMe_2H)_2$

13 $P(CH_2CH_2CH_2SiMe_2H)_3$

14 $Ph_2PCH_2CH_2CH_2Br$

15 $Ph_2PCH_2CH_2CH_2CH_2Br$

16 $Ph_2PCH_2CH_2CH_2CH_2CH_2Br$

17 $Ph_2PCH_2CH_2CH_2CH_2CH_2CH_2Br$

18 $Ph_2P(=O)CH_2CH_2CH_2CH_2Br$

19 $Ph_2P(=O)CH_2CH_2CH_2CH_2CH_2Br$

20 $Ph_2P(=O)CH_2CH_2CH_2CH_2CH_2CH_2Br$

21 $PhP(o\text{-}C_6H_4CH_2SiMe_2H)_2$

22 $P(o\text{-}C_6H_4CH_2SiMe_2H)_3$

23 $Pt[biP(^nhex)_2Si]Cl$

24 $Pt[PhP(CH_2CH_2CH_2SiMe_2)(CH_2CH_2CH_2SiMe_2H)]$

25 $Pt[PhP(o\text{-}C_6H_4CH_2SiMe_2)_2]PPh_3$

26a *syn*-$RuH(biPSi)(CO)_2$

26b *anti*-$RuH(biPSi)(CO)_2$

27 $RuH(biPSi)(CO)[P(OMe)_3]$

28 $RuH(biPSi)[P(OEt)_3]_4$

29 $RuH(biPSi)(CO)[P(OEt)_3]$

30 $RuH(biPSiO)(CO)(NHC_5H_{10})$

31 $RuH(biPSiO)(CO)_2$

32 $RuH(biPSiO)(CO)[P(OMe)_3]$

33 $RuH(biPSiO)(CO)(CN^tBu)$

34 $RuH(biPSiO)(CO)(PPh_3)$

35 $RuH(biPSiO)(CO)(NC_5H_5)$

List of Tables

List of Figures

List of Schemes

Abbreviations

Å	angstrom unit, 10^{-10} m
acac	acetylacetonato anion
AIBN	azoisobutyronitrile
9-BBN	9-borabicyclo[3,3,1]nonane
BHT	2,6-di-(*tert*-butyl)-4-methylphenol
Bu	butyl
^{t}Bu	*tert*-butyl
Bz	benzyl
COD	cycloocta-1,5-diene
cosy	correlation spectroscopy
Cp	cyclopentadienyl
Cy	cyclohexyl
d	doublet
dd	doublet of doublet
diglyme	diethylene glycol dimethyl ether, $CH_3O(CH_2CH_2O)_2CH_3$
DMPE	1,2-bis(dimethylphosphino)ethane
dppe	1,2-bis(diphenylphosphino)ethane
dt	doublet of triplet
EA	elemental analysis
Et	ethyl

FT	Fourier transform (for NMR or IR)
^{n}hex	n-hexyl
IR	infrared spectroscopy
L	ligand
M	central (usually metal) atom in compound
Me	methyl
NBS	N-bromosuccinimide
NHPI	N-hydroxyphthalimide
NMR	nuclear magnetic resonance
Ph	phenyl
^{i}Pr	iso-propyl
^{n}Pr	n-propyl
PPN	bis(triphenylphosphine)iminium
t	triplet
tmeda	N, N, N', N'-tetramethylethylenediamine

Acknowledgement

I would like to thank my supervisor, Dr. S.R. Stobart, for his advice and encouragement throughout the course of this work.

to my parents and wife

Chapter 1

INTRODUCTION

The electronegativities of Si and H are estimated at 1.8 and 2.1 respectively, i.e., the silicon atom in the Si-H bond is more electropositive than hydrogen. The polarity of the bond depends on the character of the other substituents on silicon. The lengths of most Si-H bonds lie in the range 1.47-1.55 Å[1] with a bond energy of approximately 323 $kJmol^{-1}$. The Si-H bond is weaker than C-H but is stronger than Si-C bonds (in the range 250-335 $kJmol^{-1}$).[2a]

Like hydroboration,[2b] the Si-H bond can be added across a variety of unsaturated linkages, such as C=C, C≡C, C≡N and C=O. Olefins usually give the terminal product, i.e., *anti*-Markovnikov addition of $SiHR_3$. The reaction can be initiated by free radical initiators, or can be catalyzed by transition metal complexes of which chloroplatinic acid, H_2PtCl_6, (commonly referred to as Speier's Catalyst), is the most well-known. Other effective transition metal catalysts that have been discovered include various complexes of Co, Rh, Ir, Pd and Pt. The mechanisms are believed to involve oxidative addition of the Si-H bond to the low-valent transition metal atom in a reaction that can also be referred to as hydrosilylation at transition metal centers.[2c]

Oxidative addition to a late transition metal center begins by nucleophilic attack of the latter on an external substrate. It can be written generally as $M^nLy + XY = M^{n+2}Ly(X)(Y)$. The reverse reaction is termed reductive elimination. For the oxidative addition to occur, the following three prerequisites should be met:

(a) There is nonbonding electron density on the metal

(b) There exist two vacant coordination sites on the complex to allow formation of two new bonds

(c) The metal has stable oxidation states separated by two units

The most studied complexes are those of low valent transition metals, e.g., Cr(0), Fe(0), Ru(0), Os(0), Rh(I), Ir(I), Ni(0), Pd(0), Pt(0), Pd(II) and Pt(II).

Oxidative addition to 16-electron systems produces 18-electron systems. 18-electron species can not normally undergo oxidative addition without the expulsion of a ligand.

In some cases, oxidative addition and reductive elimination establish an equilibrium with one another. Whether the equilibrium lies on the reduced or the oxidized side depends on (a) the nature of the metal and its ligands, (b) the nature of the added molecule and the strength of the newly formed metal ligand bonds and (c) the medium in which the reaction is conducted.

The higher oxidation states are usually more stable for the heavier than for the lighter metals. In a given triad, the ligands that tend to increase electron density on the metal favor the oxidation reaction. Steric properties of ligands are also important. Very bulky ligands tend to decrease the ease of oxidative addition.

Oxidative addition can lead to the formation of isomers. The distribution depends on the coordination pattern of the molecule, XY, to metals, thermodynamic stabilities of products, experimental conditions including solvent, temperature, pressure and so on. In some cases, the initial kinetic products isomerize to a final thermodynamic distribution.[3]

Oxidative addition is often used as a route to synthesize silicon-containing transition metal complexes. These complexes with silicon atoms bonded to metal centers are potential silylation reagents or effective catalysts in dehydrogenative double silylation,[4] hydrosilylation,[5] hydroformylation[6] or oxidation reactions.[7] For the oxidative addition reaction, both electronic and steric effects are significant factors in the Si-H bond addition at a transition metal atom. Oxidative addition proceeds more readily if the silicon group can distribute electrons on the metal more effectively, or if it is less bulky.[8] To date, the oxidative addition reaction of Si-H bonds has been successfully applied in Cr, Mn, Fe, Co and Ni groups.

Compared to the oxidative addition of the Si-H bonds, the oxidative addition of C-H bonds in saturated hydrocarbons at transition metals is rare while the oxidative addition of arene C-H bonds at transition metals has been known for some time (eq 1-1).[9]

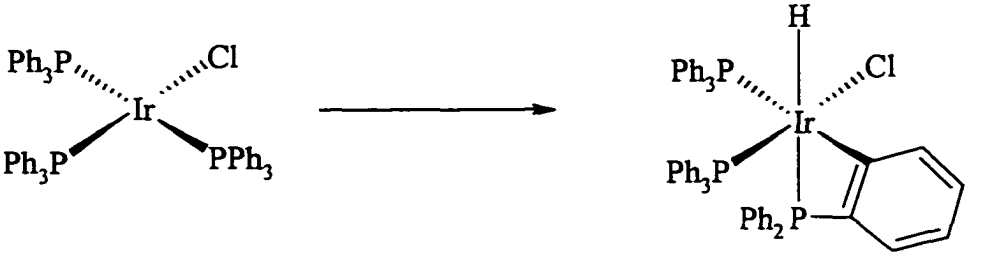

(1-1)

In most cases, the oxidative addition of C-H bonds in alkanes, the decisive step for the activation of C-H bonds, is thermodynamically unfavorable and thus the reverse reaction, the reductive elimination of M-C and M-H bonds to liberate alkanes, is spontaneous. The activation of aliphatic C-H bonds has been an active area since Bergman and Graham first

discovered the photo activation of C-H bonds in alkanes (Scheme 1-1).[10] The complexes of low coordination number and high electron density at the central metal are required for the reaction of non-activated aliphatic C-H bonds. The inert C-H bonds in alkanes can be activated under mild conditions by some positively charged Ir(III) complexes.[11a] The recent use of ultrafast infrared spectroscopy intercepts and characterizes the intermediates of the activation reaction of C-H bonds by a dicarbonyl Rh(I) complex with a trispyrazolyl borate ligand and proves the involvement of dissociation of one pyrazolyl arm before the C-H bond breaks.[11b]

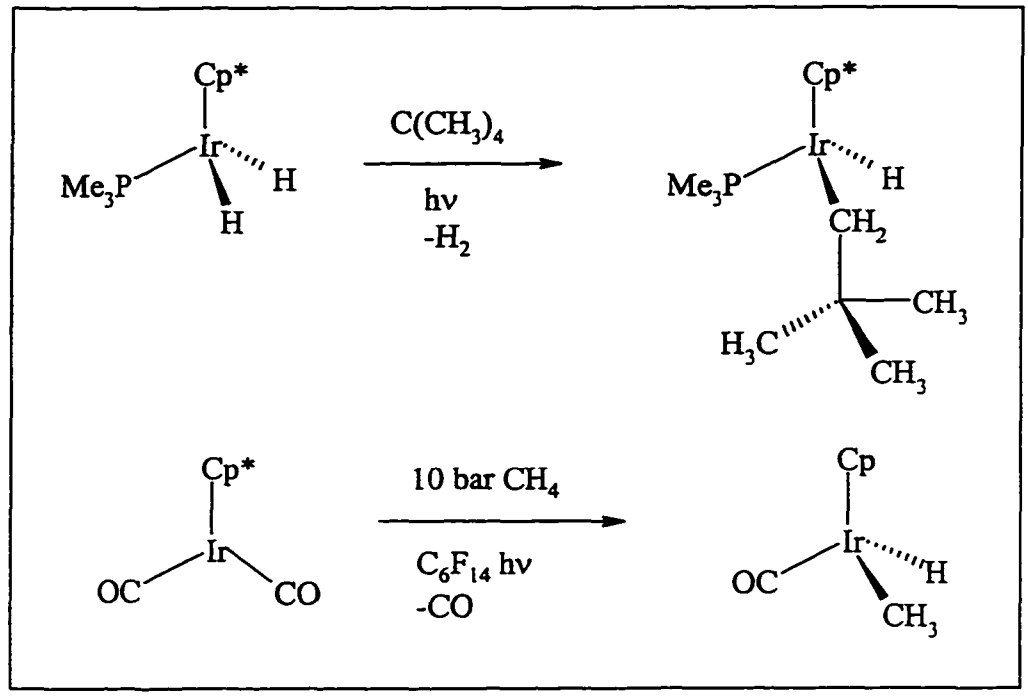

Scheme 1-1. Activation of C-H bonds in alkanes

Some metal complexes containing two, three or even four silyl groups have been prepared. The most investigated metals include Fe, Ru, Os, Co, Rh, Ir, Ni, Pd and Pt.[12]

The poly(silyl) groups can be offered by monodentate or chelate ligands. The poly(silyl) ligand precursors not only form stable metal complexes of low oxidation states, but also stabilize unusual high oxidation states, such as Ir(V), Rh(V), Ni(IV), Pd(IV) or Pt(IV).

The widely used bifunctional hydridosilanes are listed in Figure 1-1, some of which are substituted benzenes.[13] They can go through double oxidative addition with the liberation of hydrogen gas to afford 4, 5 or 6 membered disilametallacyclic units with $PtL_2(\eta\text{-}C_2H_4)$ [L = PPh_3 or dppe; dppe = 1,2-bis(diphenylphosphino)ethane],[14] $Fe(CO)_5$,[15] $Ru_3(CO)_{12}$,[15a] $Os_3(CO)_{12}$,[15a] $CpCo(\eta\text{-}C_2H_4)_2$,[16] $Co_2(CO)_8$,[15a] or $Rh(SPh)(PMe_3)_3$.[17] Some typical reaction with Pt precursors are shown in Scheme 1-2. The formation of poly(silyl) metal complexes is favored by the chelate effect.

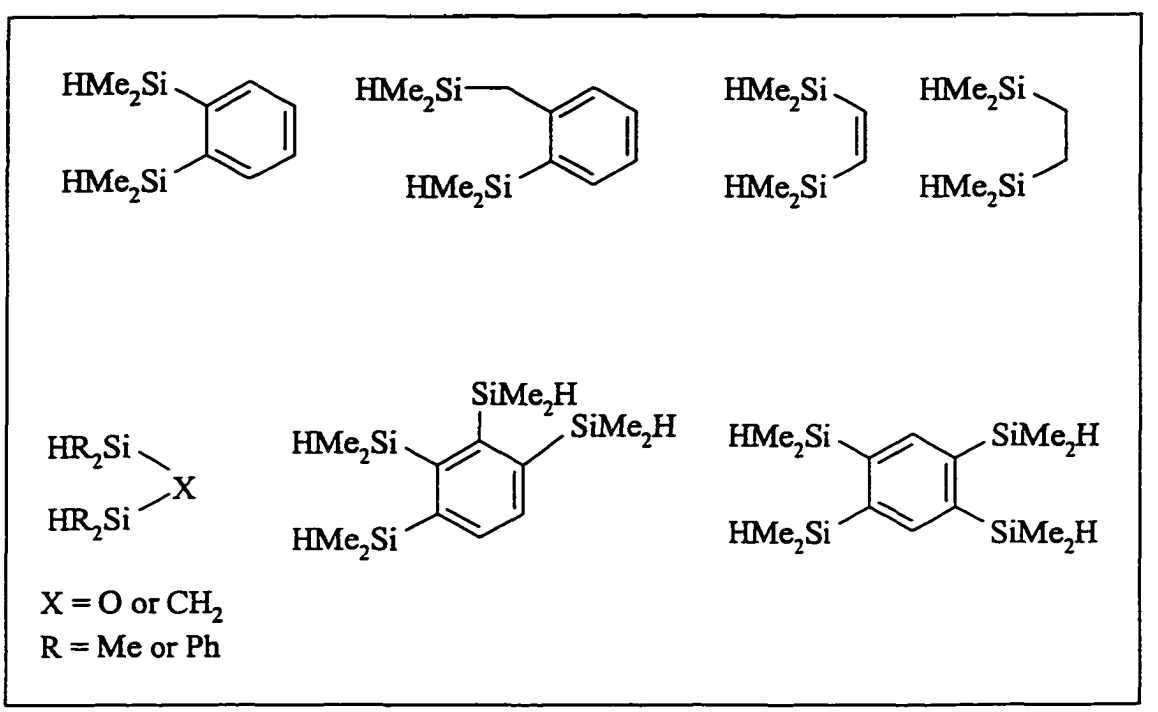

Figure 1-1. Examples of bifunctional hydridosilanes

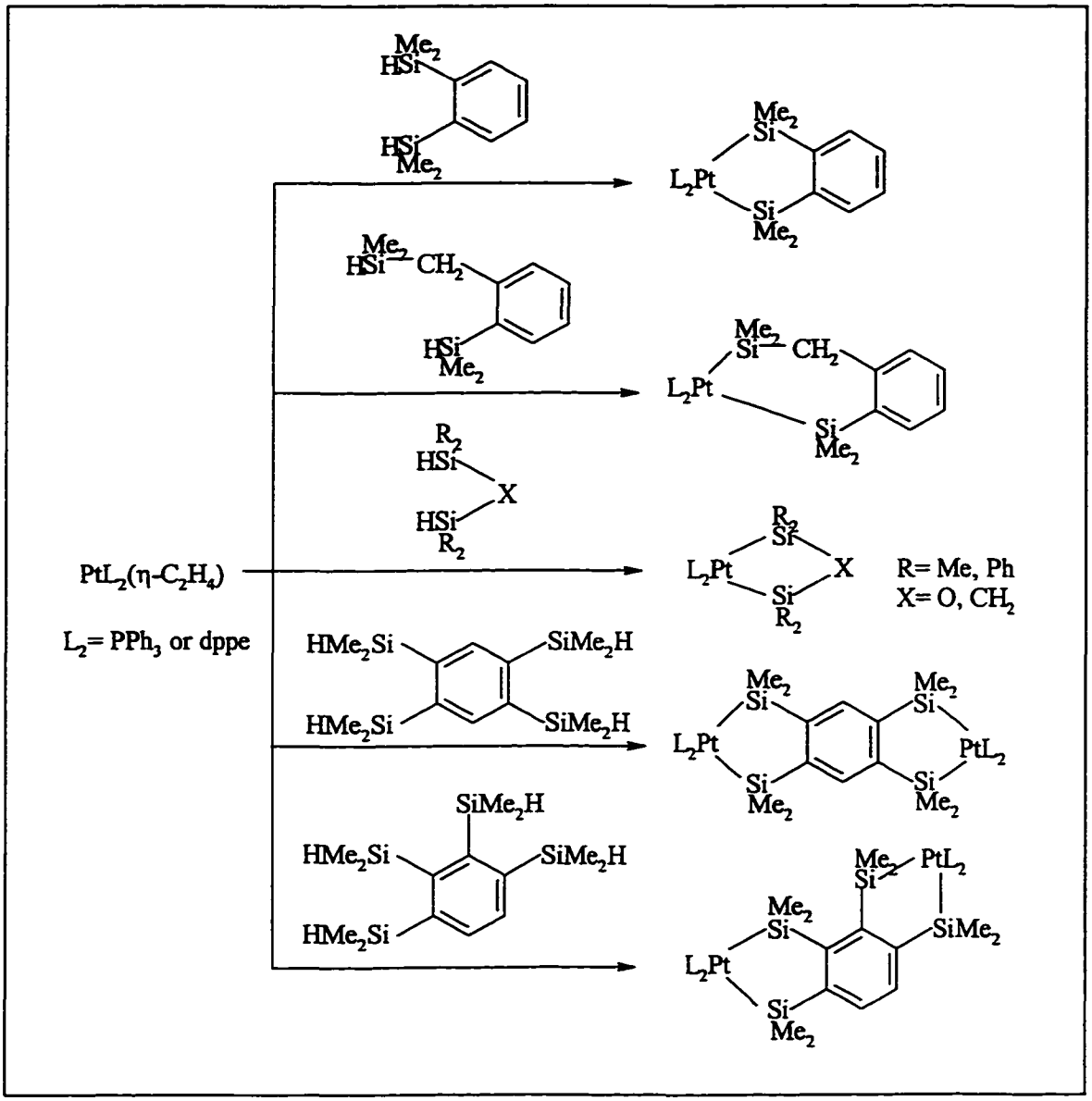

Scheme 1-2. Synthesis of some bis(silyl) Pt(II) complexes

Chelate bis(silyl) metal complexes have been found to catalyze dehydrogenative single or double silylation. Some Ni[18] and Rh[19] complexes were first investigated. Recent work shows that bis(silyl) Pt(II) complexes efficiently catalyze the dehydrogenative double silylation of acetylenes, olefins, dienes, aldehydes, ketones and nitriles (see

Scheme 1-3 for some examples).[20] The Pt(0) species, (η^2-ethylene)bis(triphenylphosphine)platinum(0), is the commonly used catalyst precursor.

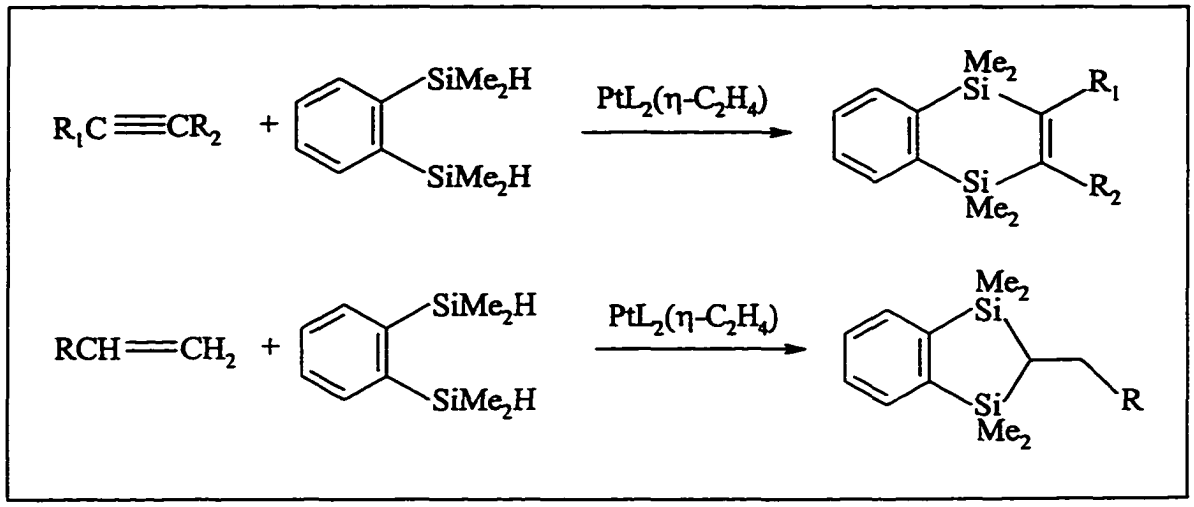

Scheme 1-3. Some examples for dehydrogenative double silylation

High valent Ir(V), Rh(V), Ni(IV), Pd(IV) or Pt(IV) states are most usually stabilized as halides because halogens with strong electron-withdrawing abilities can attract electrons from metals and meanwhile donate p electrons to form a π bond with the d orbitals of the metal. The metal complexes of high oxidation states containing less polar covalent bonding are rare. The very electron-deficient metal centers strongly attract electrons from the electron rich and reductive ligands. Thus only those ligands that can donate electrons and simultaneously hold the shared electrons to form covalent bonds can stabilize such high valent species. Maitlis[19a, 21] and Perutz[22] demonstrated that both Ir(V) and Rh(V) species could be formed through the coordination by the bulky Cp group (Cp = cyclopentadienyl) and multiple interactions with good σ-donors like hydride or silyl groups. A representative structure of the type is shown as structure 1-A. Further work

done by Crabtree showed that these high oxidition state species could be stabilized by less bulky ligands than the Cp group (structure 1-B).[23] The Ni(IV), Pd(IV) and Pt(IV) species stabilized by poly(silyl) groups have been isolated and characterized by Tilley and Tanaka (structure 1-C).[24, 25]

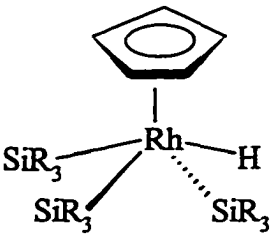

R = Me or Et

(1-A)

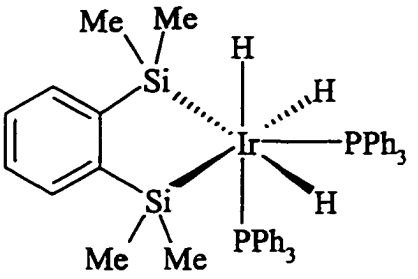

(1-B)

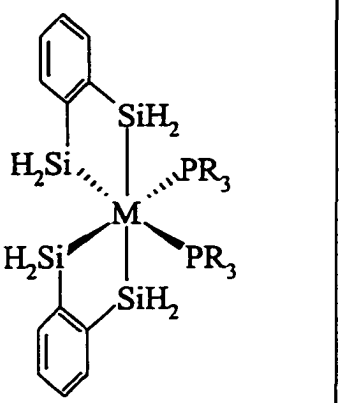

M = Ni, Pd or Pt
R = Et or Ph

(1-C)

The *trans* effect is defined by the way in which a ligand facilitates substitution in the position *trans* to itself.[26a] It is a kinetic phenomenon, depending on activation energies, and the stabilities of both the ground state and the activated complex. The approximate order of ligands according to the strength of their *trans* effects in square planar geometry is: CO, CN^-, C_2H_4 > PR_3, H^- > CH_3^- > $C_6H_5^-$, NO_2^-, I^-, SCN^- > Br^-, Cl^- > py, NH_3, OH^-, H_2O. The ligands that can form stronger π back bonding with metals in the transition states exert a stronger *trans* effect. Occasionally, *trans* labilization is also used to describe the ligands that have a strong *trans* effect. In six coordinate octahedral systems, hydride, silyl, germyl, stannyl and alkyl groups also show strong *trans* effects.

The *trans* influence is defined as the influence of one ligand on the strength of the bond to the ligand that is *trans* to it. It is a ground state property and can be evaluated from bond lengths or M-L stretching frequencies. *Trans* influence is attributable to the fact that bonding of two *trans* ligands will both depend on the participation of one metal orbital, and the more one ligand pre-empts this orbital, the weaker will the bond to the other ligand be. The order of some ligands with regard to their *trans* influence in square planar geometry is: H^- > PR_3 > SCN^- > I^-, CH_3^-, CO, CN^- > Br^- > Cl^- > NH_3 > OH^-.

It is believed that different mechanisms are involved in the *trans* effect and *trans* influence for σ-donors (such as hydride, silyl and alkyl groups) and π acids (such as CO and ethylene).[26b, 26c] The *trans* effect is equivalent to the *trans* influence if only σ donors are compared.

Alkylsilyl groups have been found to act mainly as σ-donors[27] and have stronger *trans* influence (and also *trans* effect) than other σ-donors like hydrides, alkyl groups,

amines and halides.[28] The trichlorosilyl group, -$SiCl_3$, has significant ability to accept π back donation.[29] The labilization of the ligands *trans* to silicon atoms can be observed in many complexes with square planar or octahedral geometry.[28, 29]

As a result of competitive *trans* influences, the strong σ-donors prefer to avoid being *trans* to other good σ-donors on complexation. This rule applies in both four coordinate square planar[24, 30-33] and six coordinate octahedral geometries.[34-36] and has been confirmed by a large number of experimental observations. In the reaction of (diphenylphosphinoethyl)dimethylsilane with $Pt(COD)_2$ or $Pt(COD)Cl_2$ (COD = cycloocta-1,5-diene), for example, only one thermodynamically favored product (eq 1-2) can be isolated in which silyl groups are *trans* to the phosphine groups, which are relatively weaker σ-donors and weak π-acceptors.[37, 38]

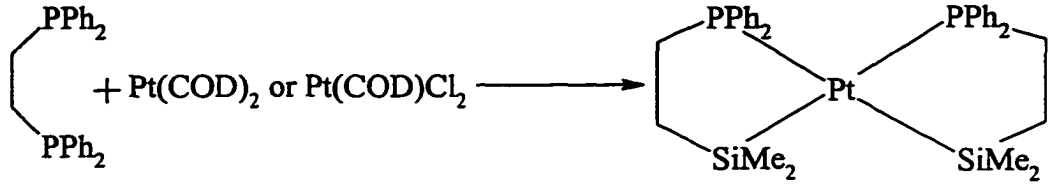

(1-2)

Coordinatively unsaturated metal complexes are at the center of transition metal chemistry and catalysis, since the unoccupied sites remain reactive and can be attacked by other substrates. In some situations, the unsaturated species are so reactive that their isolation requires the use of inert atmosphere techniques or interim stabilization by some weakly bonded ligand such as polar solvent molecules. There also exist certain unsaturated complexes that would be considered to be thermodynamically unfavored

without the involvement of unusual electronic interactions, such as the agostic interaction. Agostic interaction refers to the weak σ-donation from saturated bonds, e.g., C-H or Si-H, to coordinatively unsaturated metal centers.[39] This kind of bonding has been found to be common in early transition metal complexes, but is comparatively rare in late transition metal complexes. It is considered as the early stage along the kinetic pathway for C-H or Si-H activation. Coordinatively unsaturated complexes can also be stabilized by ligands with large steric effects. Wrapping metal centers in bulky ligand geometries can prevent them from contacting other reactive reagents. Such a strategy is being widely used in current research aimed at ligand design.

The 16-electron, five coordinate state for Ru(II) is known to be reactive, readily associating with one more ligand to achieve coordinative saturation. However a range of five coordinate Ru(II) species containing Ru-X bonds (X = I, Br, Cl, OR, NR_2, SR, C_2R or C_2H_2R) can be isolated and have been characterized.[40-44] In the complexes with the molecular formula $RuHX(CO)(P^tBu_2Me)_2$, no agostic interaction is observed to stabilize the 16-electron system. Based on *ab initio* calculations, Eisenstein and Caulton have suggested that the electron deficiency in these coordinatively unsaturated complexes could be efficiently compensated primarily by the powerful σ-donating group H and secondarily by the push-pull interaction involving the p lone pair(s) of X, the occupied d metal orbital, and the π^*_{CO} orbitals.[45] The weak π bonding simply finely tunes electron availability in these 16 electron species and does not prohibit the complexes from undergoing an addition reaction. Through comparison of the IR frequencies of CO groups, a ranking of total ligand donor power (δ + π) has been assigned: OEt > $OCPh_3$ >

$OSiMe_3 > OSiMe_2Ph > OSiPh_3 > F \cong OCH_2CF_3 > OH \cong OB(Mesityl)_2 > NHPh \cong OPh > SPh \cong Cl > C_2Ph \cong Br > I$. These complexes adopt a square pyramidal geometry with the hydride in the apical position. The analogues $Ru(SiR_3)Cl(CO)(PPh_3)_2$ containing silyl groups which are stronger σ-donors than hydrides and weak π-acceptors, are found to adopt similar square pyramidal structures (structure 1-D).[46, 47]

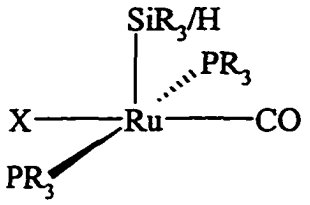

(1-D)

Strong σ-donors appear to be essential to stabilize the five coordinate Ru(II) species. This is why some novel five coordinate Ru(II) species, such as $Ru(H)_2(CO)(P^tBu_2Me)_2$ and $RuH(SiHPh_2)(CO)(P^tBu_2Me)_2$ (structure 1-E), are observed to be surprisingly stable. The dihydride complex $Ru(H)_2(CO)(P^tBu_2Me)_2$ is prepared *in situ* from dehydrohalogenation of $RuHCl(CO)(P^tBu_2Me)_2$ using ^{t}BuLi in toluene, see eq 1-3. It has a square pyramidal geometry where one hydride lies in an apical

$$RuHCl(CO)(P^tBu_2Me)_2 + {}^t\text{BuLi} \longrightarrow Ru(H)_2(CO)(P^tBu_2Me)_2 + LiCl + CH_2{=}CMe_2 \quad \textbf{(1-3)}$$

position while the other is *trans* to CO. The two hydride sites exchange, resulting in dynamic line broadening above -30°C.[45b] The oxidative addition of SiH_2Ph_2 to this reactive dihydride precursor affords $RuH(SiHPh_2)(CO)(P^tBu_2Me)_2$.[48] The X-ray diffraction analysis of $RuH(SiHPh_2)(CO)(P^tBu_2Me)_2$ shows that this molecule is square pyramidal with the silyl group occupying the apical site. There is no agostic interaction acting to increase the coordination number. In the IR spectra, ν_{CO} is found at 1925cm^{-1}, a value that suggests that the SiHPh group has a net (σ + π) electron donor power considerably less than that of iodide (ν_{CO} at 1908cm^{-1}). The fact that the silyl adopts a site *cis* to CO also suggests that the silyl group is not a significant π-donor. In these two complexes, the bulky ligands also contribute to the stabilization.

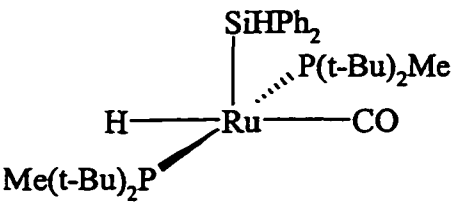

(1-E)

The platinum group metals are electron rich and behave as "soft" base centers in the Basolo and Pearson sense, so that low-oxidation state chemistry for these elements is dominated by complex formation with "soft" donors, especially organophosphines PR_3. To take advantage of the strongly electron-releasing character of silyl groups, attachment of the latter in a polyfunctional ligand framework is advantageous to avoid subsequent elimination chemistry. This idea has led to the synthesis of a family of multidentate

ligand precursors containing one, two or three terminal phosphines together with one hydridosilane core. This provided access to chelate complexes in which phosphine and silyl ligand centers are connected by one, two or three methylene units (see Figure 1-2 for the latter two). The short backbones formed by only one CH_2 unit favored the formation of dimers instead of mononuclear complexes on complexation.[49]

The UV irradiation of a mixture of a secondary phosphine PHR_2 with a vinyl- or allyl-silane provided a successful synthesis of the target chelate precursors in high yield (eq 1-4).[6, 50] The reaction with allylsilanes is significantly slower than with vinylsilanes (weeks *vs* days). This difference can be explained by the existence of what is referred to as the β-effect of silicon atoms. The empty 3d orbitals of the latter can participate in the delocalization of electron density in the radical intermediates (Scheme 1-4).

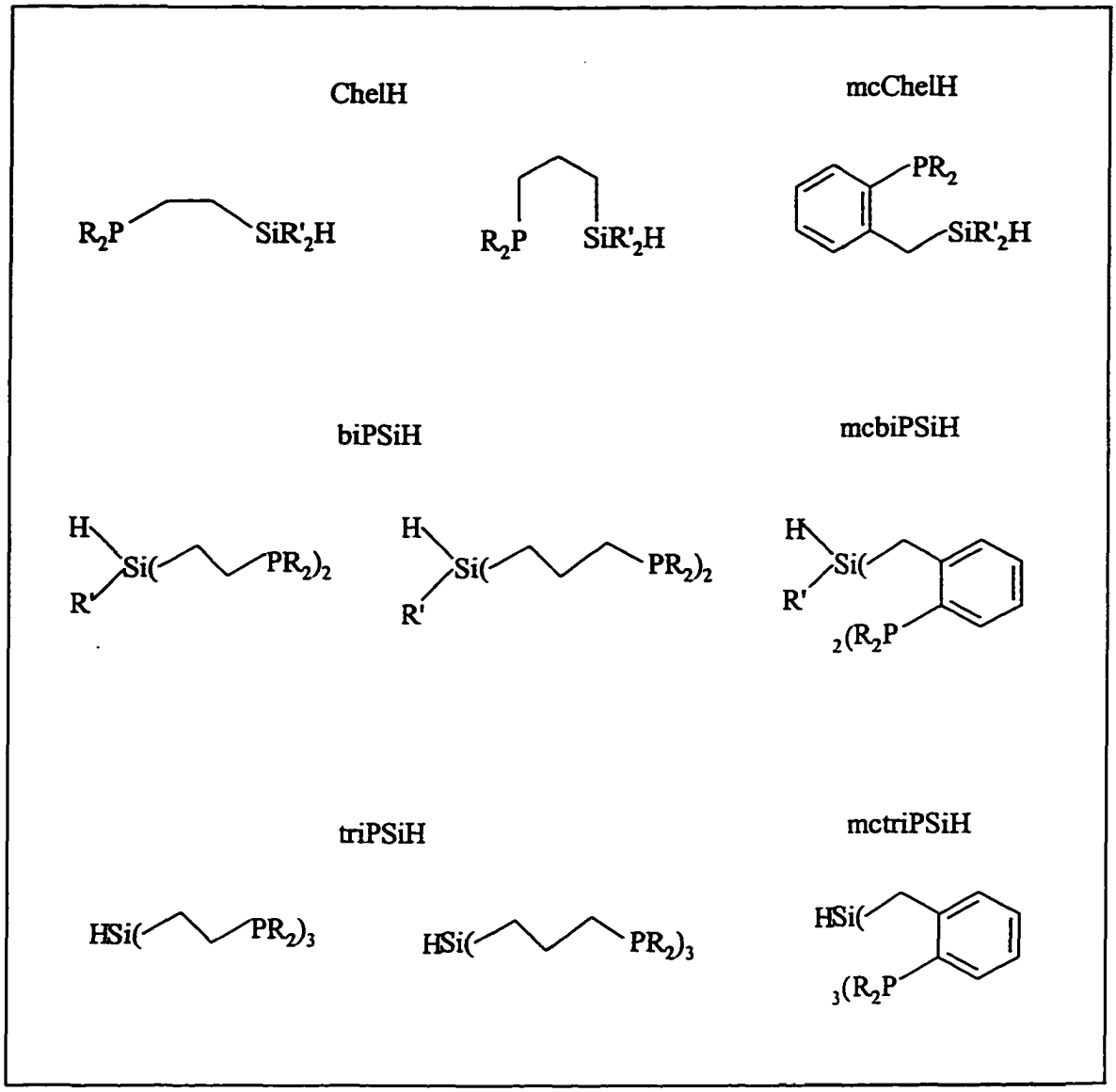

Figure 1-2. The PSiH and mcPSiH ligand precursors

Such a photochemical addition of P-H bonds to unsaturated bonds via a free radical pathway has recently been well developed into a versatile synthetic method towards primary, secondary and tertiary phosphines (see Scheme 1-5 for an example).[51]

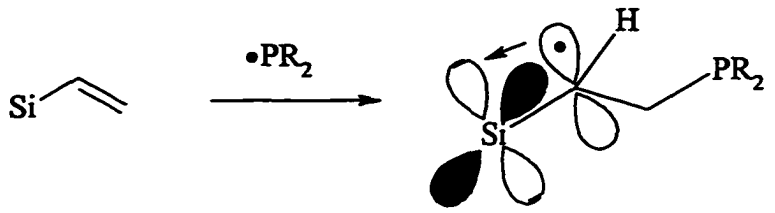

Scheme 1-4. The description of β-effect of silicon atoms

$$SiHR_x[(CH_2)_nCH{=}CH_2]_{3-x} + (3\text{-}x)PR'_2H \xrightarrow{h\nu} SiHR_x[(CH_2)_nCH_2CH_2PR'_2]_{3-x} \quad (1\text{-}4)$$

n = 0 or 1; x = 0, 1 or 2
R = alkyl or phenyl; R' = alkyl or phenyl

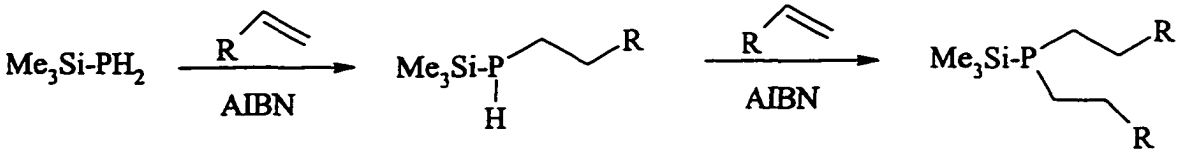

Scheme 1-5. Photoaddition of P-H bonds cross unsaturated bonds

This photochemical synthesis of phosphinopropylsilanes according to eq 1-4 is inconvenient for large-scale operation, and has limited the exploration of the corresponding phosphinoalkylsilyl chemistry. An alternative chemical synthesis was recently developed that yields a series of similar ligand precursors (mcPSiH) in which a more rigid backbone formed from a benzylic fragment connects P to Si (Scheme 1-6).[52] Thus the metallation of (*o*-tolyl)diphenylphosphine using ^{n}BuLi in the presence of tmeda (tmeda = N, N, N', N'-tetramethylethylenediamine) results in quantitative formation of an organolithium reagent[53] which can be quenched with chlorodimethylsilane,

dichloromethylsilane or trichlorosilane to afford the modified chelate analogues mcChelH, mcbiPSiH and mctriPSiH of ChelH, biPSiH and triPSiH. A different family of chelate precursors in which the benzene ring is adjacent to silicon may be synthesized similarly starting from an alternate lithium reagent (eq 1-5).[54, 55]

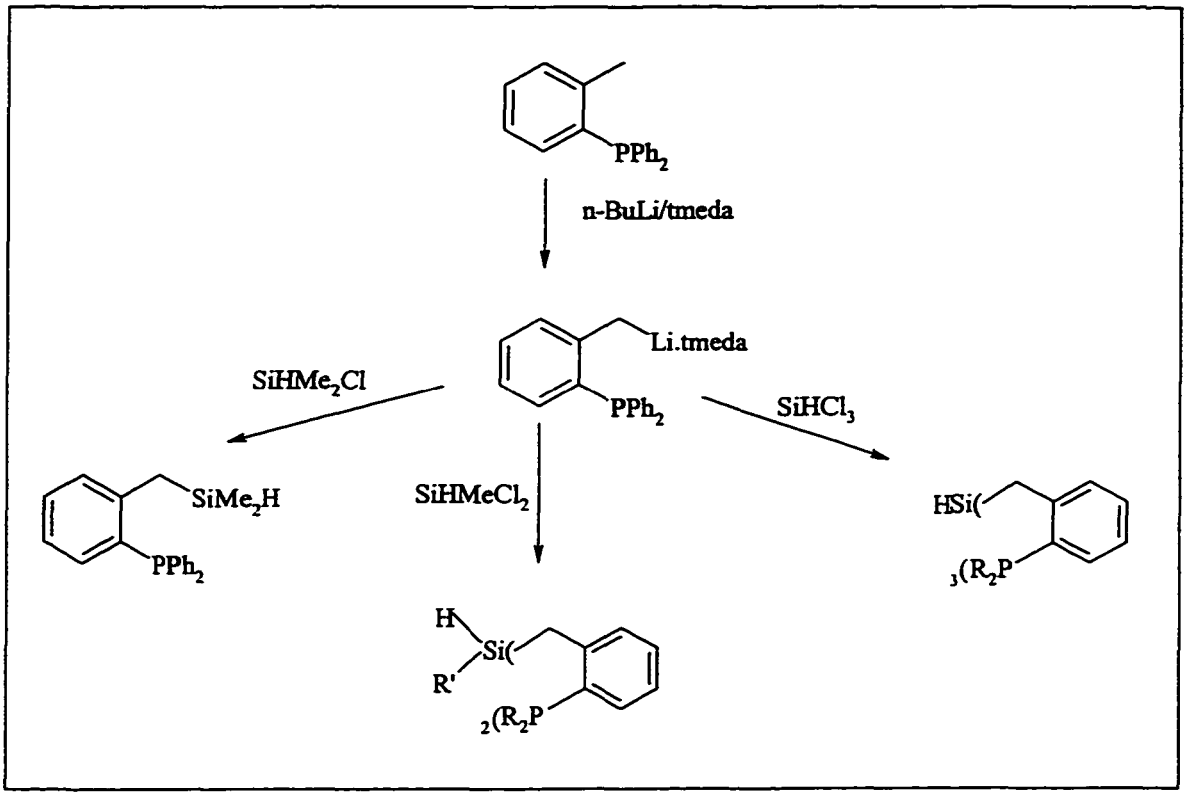

Scheme 1-6. Synthesis of mcChelH, mcbiPSiH and mctriPSiH

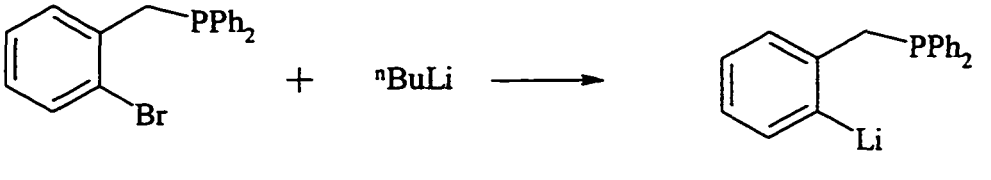

(1-5)

Complexation of phosphinoorganosilanes at platinum group metal centers to form chelate complexes has been investigated by earlier workers in this laboratory. In particular, six coordinate octahedral Ru(II) and Os(II) complexes have been isolated

from reactions with $M_3(CO)_{12}$ (M = Ru or Os)[34, 56] and, much more recently (see Chapter 4), from reactions of $Ru(PPh_3)_2(CO)_3$ or $Os(PPh_3)_3(CO)_2$ with tridentate biPSiH or mcbiPSiH precursors (Figure 1-3: structures A and B). Related reactions with platinum precursors such as $Pt(COD)_2$, $Pt(COD)Cl_2$ or $Pt(COD)Me_2$ lead to the formation of square planar Pt(II) species (Figure 1-3: structures C and D).[38, 49, 52, 37] Complexation with Ir or Rh precursors, $[M(COD)Cl]_2$ or *trans*-$M(CO)(Cl)(PPh_3)_2$, produces either five or six coordinate products (Figure 1-3: structures E, F, G, H, I, J and K),[19, 57] of which the first group possesses unusual structures and reactivity.

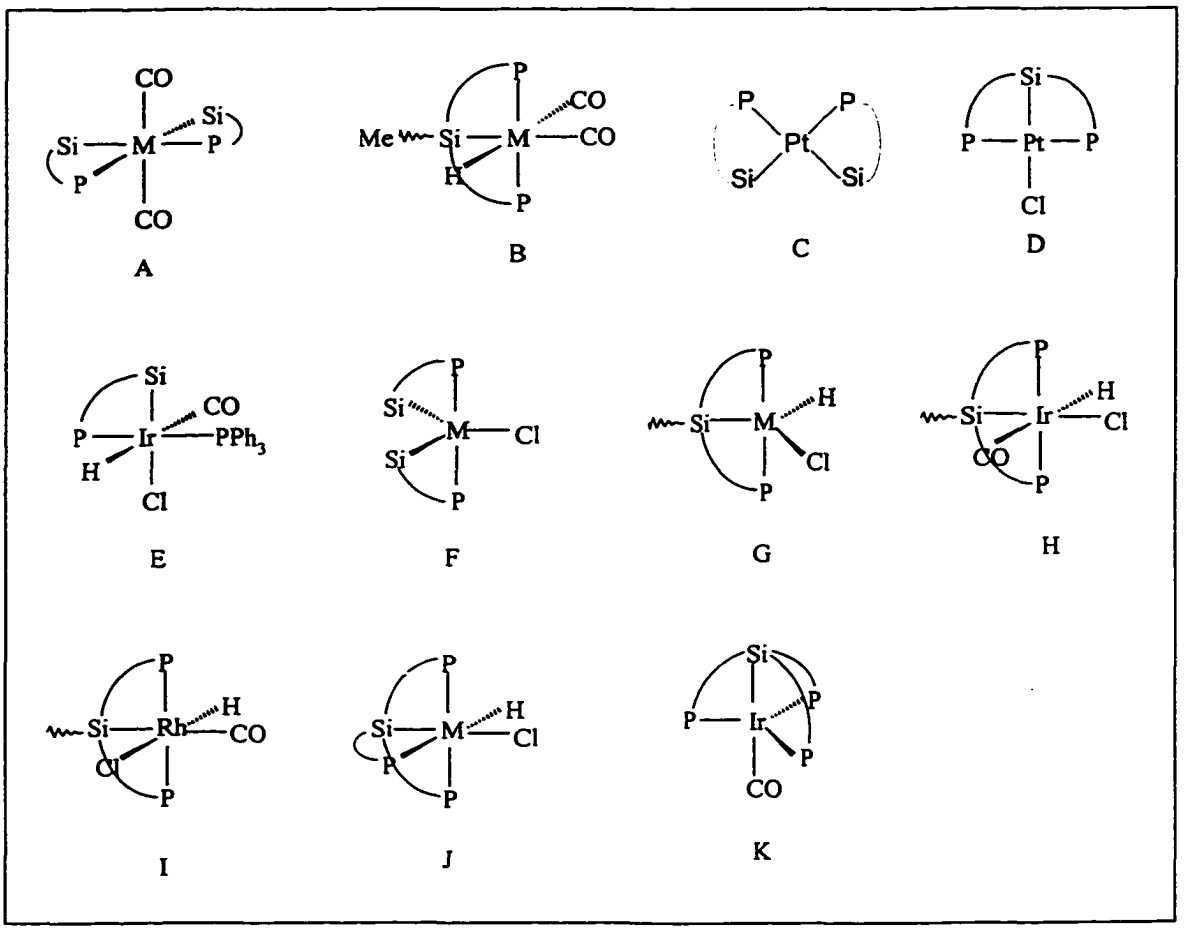

Figure 1-3. Structures of chelate phosphinoorganosilyl complexes of the platinum group metals

Coordination of chelate phosphinoorganosilyl ligands may lead to either *mer* or *fac* configurations, and *syn* or *anti* diastereomers (Figure 1-4). In general, the *mer* configuration has been commonly observed in thermodynamically favored products. The relative stability of *syn* and *anti* isomers is less clear: either of them could be the thermodynamically favored geometry. In the range of known poly(silyl) metal complexes, silyl groups are almost never found *trans* to each other. This observation is explained by the fact that silyl groups exert a very strong *trans* influence. Two carbonyl groups are found to be chemically inert if they are *trans* to each other in six coordinate Ru(II) complexes (Figure 1-3: structure A),[34] and thus can not be substituted by other stronger neutral ligands such as phosphites. The structure F in Figure 1-3 where M is either Ir or Rh shows a distorted trigonal bipyramidal (tbp) geometry,[57b] in which the Si-M-Si angle is found to be unusually small (<90°). An *ab initio* calculation has predicted that molecules which contain four strong σ-donor ligands and one weak donor ligand bound at a coordinatively unsaturated d^6 metal center will have a distorted tbp geometry, with a narrow angle between the two strong donors in the equatorial plane.[58] The weak donor is also predicted to be located in the equatorial plane and to further stabilize the complex by enhanced π-bonding interactions.

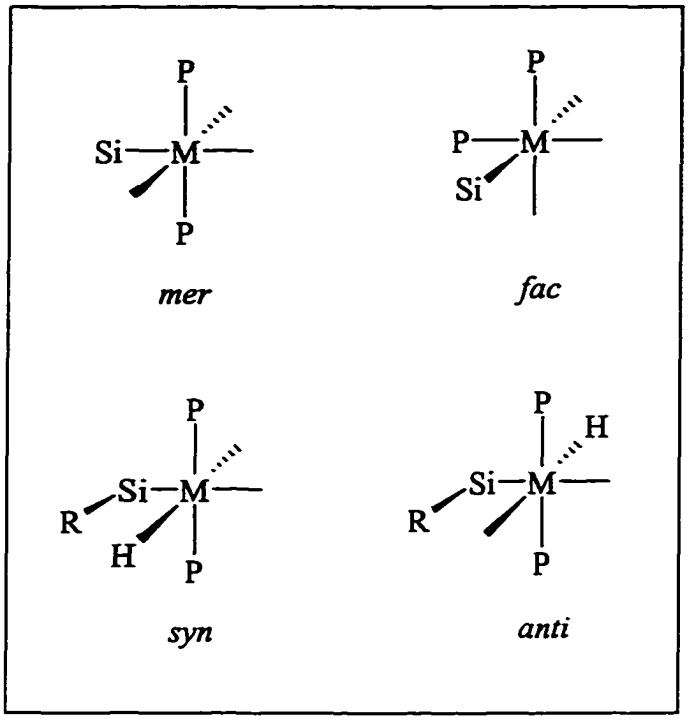

Figure 1-4. Description of *mer*, *fac*, *syn* and *anti* relationships

Chapter 2

FORMATION OF P-C BONDS VIA HYDROZIRCONATION AND PHOSPHINATION

2.A. Hydrozirconation of Allylsilanes and Synthesis of (Phosphinopropyl)silane Ligand Precursors

2.A.i. Synthesis of (Diphenylphosphinopropyl)silanes, ChelH (I), biPSiH (II) and triPSiH (III)

As discussed in Chapter 1, a series of phosphinoalkylsilanes (precursors to PSi ligands) which form mononuclear metal complexes via oxidative addition of Si-H bonds have been synthesized through photochemical P-H bond addition to allyl or vinylsilanes. While this method is very efficient in terms of overall conversion and tolerates some changes in organic functionality at Si or P, long reaction times and awkward scaleup logistics have led to a search for an alternate preparative strategy. Molecules in which the same type of connection between P and Si is made through a planar benzenoid skeleton (mcPSiH ligand precursors) can readily be constructed from benzylic carbanions, but this is an approach that cannot easily be adapted to assemble unsubstituted polymethylene backbones. Framework flexibility has been shown to be an important influence on structures and reactivities of metal complexes.[59] So in spite of the availability of the skeletally more rigid mcPSiH analogues, the unmodified PSiH series remain desirable targets.

Hydrosilylation and hydroboration are two well developed synthetic methods to add hetero atoms to unsaturated carbon chains. The former is usually catalyzed by metal

complexes, of which Speier's Catalyst (PtH_2Cl_6) is the most well-known, but the presence of organophosphine ligands can kill the activity of the catalyst through coordination to the Pt center. Such a poisoning mechanism will obviously limit the application of metal catalyzed hydrosilylation in phosphine synthesis. Recently it was shown in this laboratory by Gossage that 9-BBN (see structure 2-A) or $BHCl_2 \cdot SMe_2$ can be used for hydroboration of allylsilanes to give the terminal adducts. However, while the subsequent replacement of the boryl group with chlorophosphines afforded a mixture in which phosphinopropylsilanes can be detected, separation of the latter from other by-products was found to be problematic.[55]

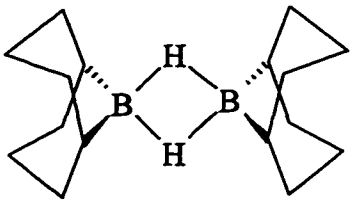

(2-A)

Zirconium complexes have been successfully applied as catalysts or intermediates in organic synthesis for decades.[60, 61, 62a] Most of them are air and water sensitive and are usually prepared via transmetallation, oxidative coupling, carbozirconation, oxidative addition, metal-hydrogen exchange or hydrozirconation (Scheme 2-1),[63, 64] of which the last was first investigated by Schwartz's group in the late 1970s.[62b-e]

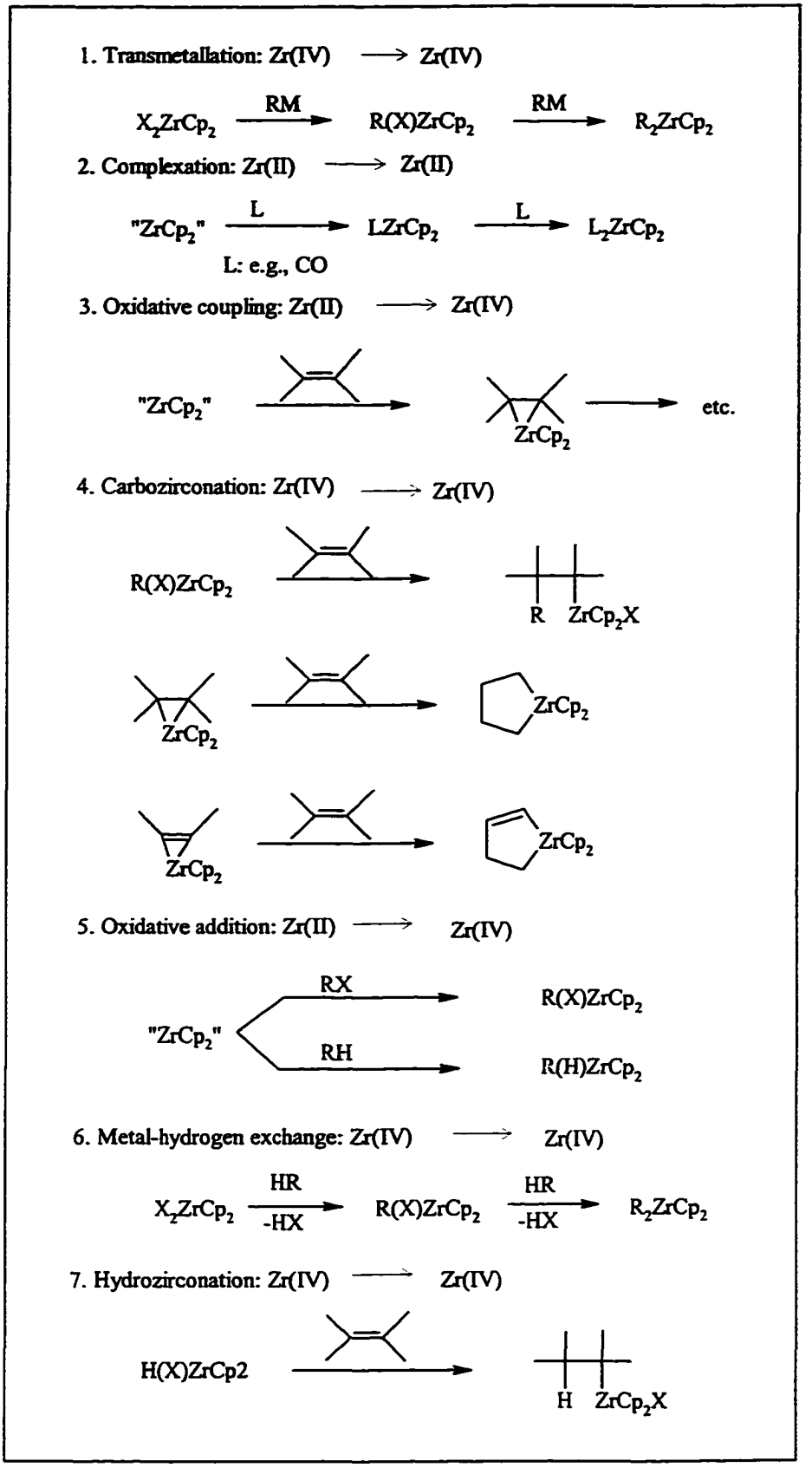

Scheme 2-1. Preparation of zirconium compounds

Hydrozirconation is the process in which a Zr-H bond is added across an unsaturated fragment regioselectively, usually to give terminal adducts. It has been proposed that the addition reaction proceeds through a four-center intermediate (see structure 2-B).[65] The best known hydrozirconation reagent is zirconocene chloride hydride, also known as Schwartz's reagent.

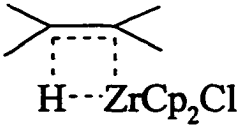

(2-B)

Zirconocene chloride hydride can be prepared on a large scale (~100g) via the reduction of zirconocene dichloride, Cp_2ZrCl_2, using lithium aluminum hydride.[66] It is a white, moderately air-sensitive powder with a polymer structure that results in poor solubility in all solvents.[67] It slowly turns to purple while exposed to light, which is attributed to a structural change of the polymeric lattice. The purple isomer has the same reactivity as the white product. The purity of the reagent can be measured by reaction with a quantitative amount of acetone.[66a] The Zr-H bond in zirconocene chloride hydride has a strong IR absorption at 1390 cm^{-1}.[67a]

Schwartz also discovered that the zirconium groups in hydrozirconated compounds can be substituted by nucleophiles including halogens and other heteroatom reagents (Scheme 2-2).

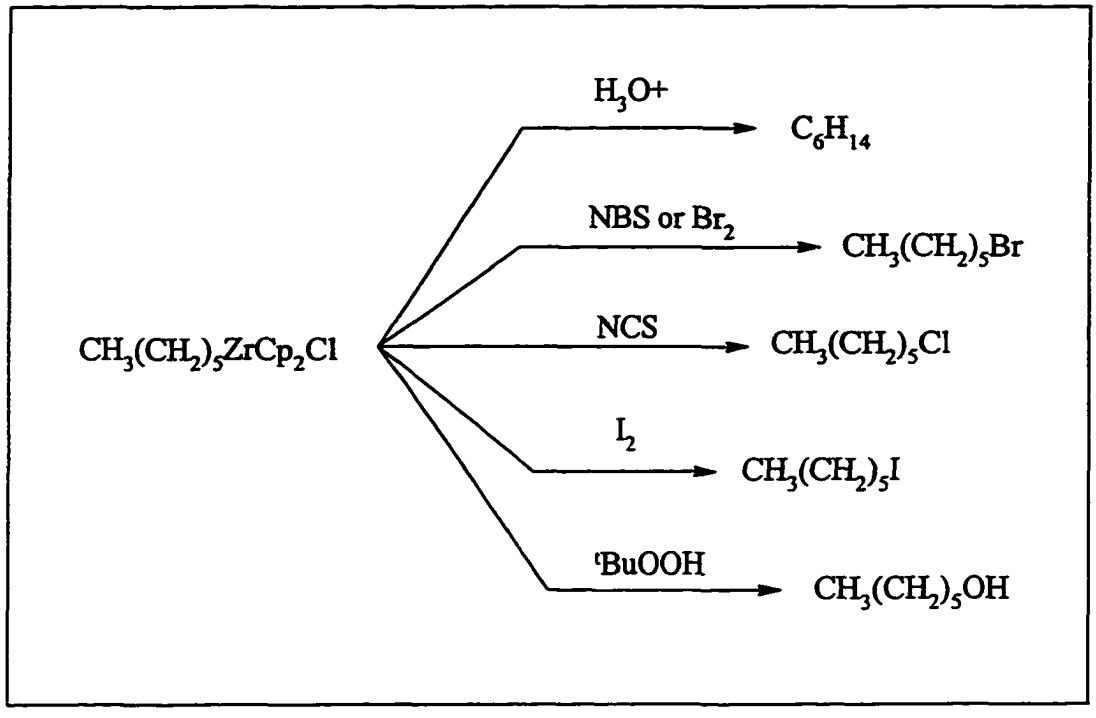

Scheme 2-2. Substitution of zirconium groups with other hetero atoms

The synthesis of phosphines via zirconium intermediates and phosphination has recently been developed into an efficient synthetic method for the formation of carbon-phosphorus bonds.[68] It is believed that phosphination also goes through a four-center transition states in which the electronegative chlorine atom attacks a partially positive Zr center, while the electropositive phosphorus atom attaches to the negative alkyl residue. The formation of stable Zr-Cl bonds in the reaction is also a strong driving force. Pioneering research work in this area has been reported by Fryzuk, *et al*[69] and by Nugent, *et al.*[71] Fryzuk demonstrated that regioselective hydrozirconation can convert substituted enyne molecules to functionalized dienes having Zr substituents at the 1-position and that the Zr-containing groups could subsequently be replaced with -PMe_2 and -PPh_2 or other main group hetero atoms like boron, selenium and tin (Scheme 2-3). By using PCl_3 or

$C_6H_5PCl_2$, Nugent and colleagues isolated secondary or tertiary phosphines via the one-pot double phosphination (metallacycle transfer) of cyclic dialkyl Zr intermediates first prepared by Negishi[70] (Scheme 2-3).[71] They also found such a multiple substitution reaction worked well with sulfur, selenium, arsenic, antimony and bismuth di- or tri-halides. This synthetic methodology has been extended by other research groups to give a broadly useful synthetic route to heteroles and other heterocycles of the group 13-16 elements.[72-74]

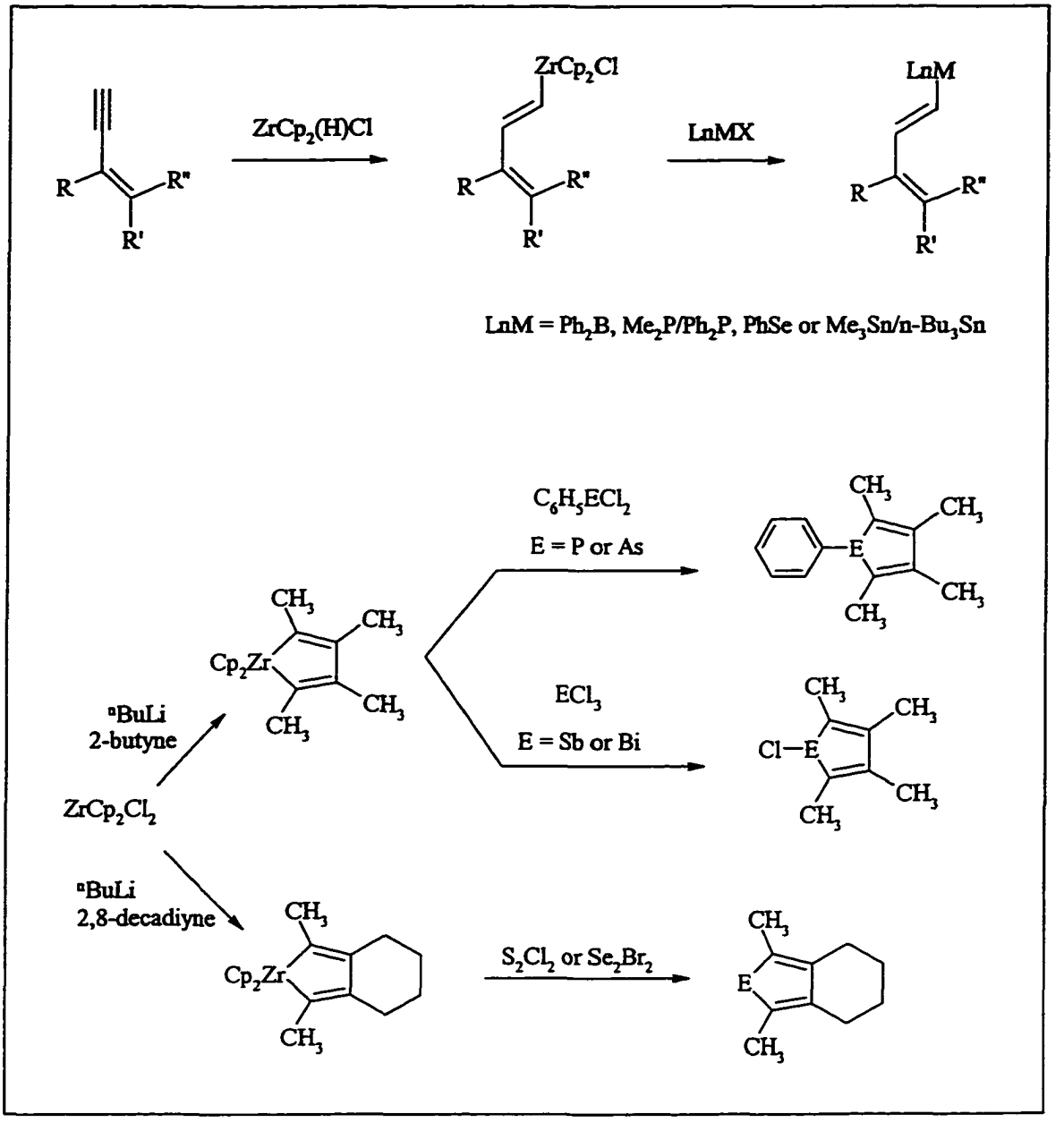

Scheme 2-3. Substitution of zirconium groups with main group atoms

How the presence of other hetero atoms influences hydrozirconation and subsequent substitution has not been given much attention, although Majoral, *et al* have described the normal terminal hydrozirconation of vinylphosphines and vinylphosphine oxides/sulfides and the unexpected substitution by chlorophosphines at α positions (Scheme 2-4).[75]

Unlike the hydrocyanation of 2-vinylfuran (Scheme 2-4), in which the oxygen atom of the furan group acts as a donor site to force the zirconium group to add to the internal carbon of the vinyl system, the phosphorus lone pair does not participate in the same way as the oxygen of the furan group. The reason why the phosphination takes place at α position is proposed to be due to migration of the zirconium group along the carbon chain by a sequence of facile reversible additions and β-hydrogen elimination.[76] Development of a related strategy that uses hydrozirconation and subsequent phosphination as a method for phosphinoalkylsilane synthesis is the subject of this chapter.

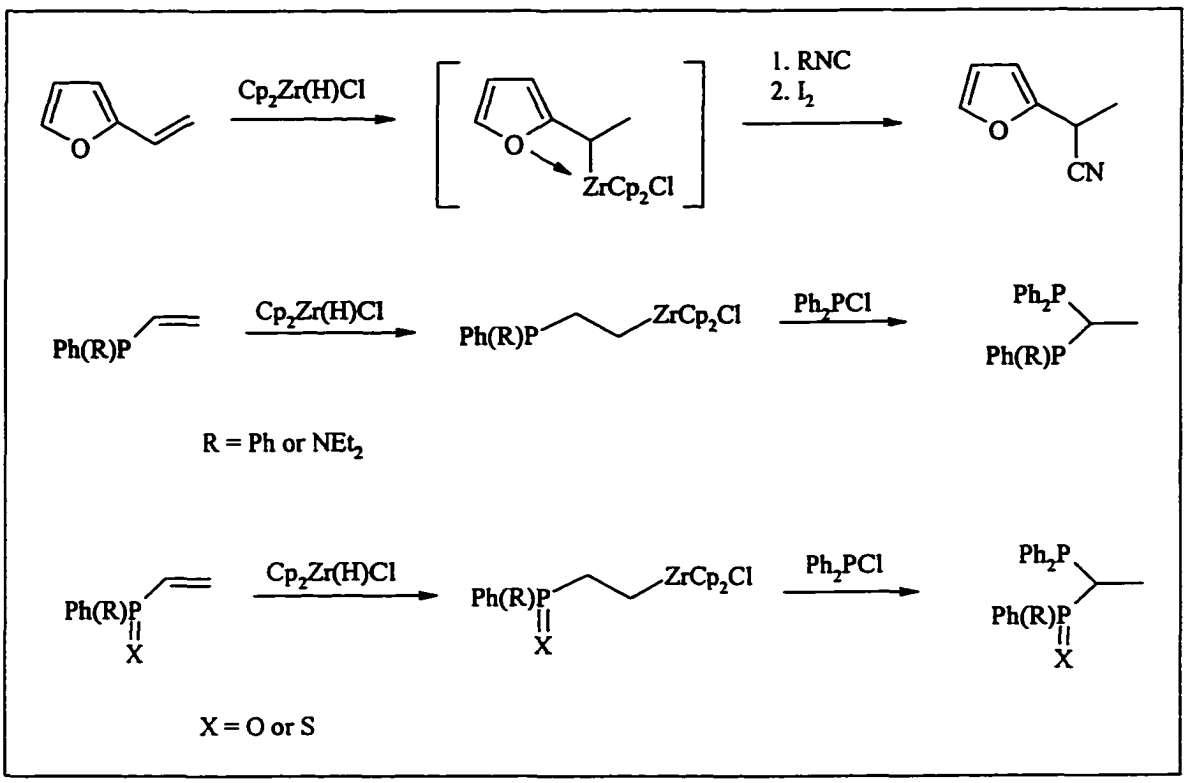

Scheme 2-4. Unusual behavior of hydrozirconation and phosphination of vinyl phosphines and vinyl phosphine oxides/sulfides

In a preliminary experiment, hydrozirconation of triethylvinylsilane was investigated. This substrate was added to a slurry in dry benzene of zirconocene chloride hydride, after which NMR spectroscopy suggested that the yellow, very air-sensitive powder recovered from the clear yellow solution that resulted was a (triethylsilyl)ethylzirconocene derivative 1 (eq 2-1).

$$ZrCp_2HCl + SiEt_3(CH{=}CH_2) \longrightarrow \underset{\underline{1}}{ZrCp_2(CH_2CH_2SiEt_3)Cl} \qquad \textbf{(2-1)}$$

Further reaction with PPh_2Cl (1 mol equiv) led to the detection (see Tables 2-1 and 2-2 for NMR data) of Cp_2ZrCl_2 and to the isolation in high yield (>75%) of colorless, liquid (diphenylphosphino)ethyl(triethyl)silane 2 (eq 2-2), *i.e.* to successful formation of the desired Si-polymethylene-P connectivity.

$$\underset{\underline{1}}{ZrCp_2(CH_2CH_2SiEt_3)Cl} + PPh_2Cl \longrightarrow \underset{\underline{2}}{PPh_2CH_2CH_2SiEt_3} + ZrCp_2Cl_2 \qquad \textbf{(2-2)}$$

In each of the two consecutive reactions, equimolar stoichiometry [of $Cp_2Zr(H)Cl$ and PPh_2Cl] was used in order to avoid any side reaction between these two (eq 2-3). The latter was identified independently in a separate reaction, in which a singlet at δ 5.88 in the ^1H NMR spectrum confirmed the formation of Cp_2ZrCl_2 and a ^{31}P NMR signal was

found at δ -40 due to PPh_2H.[77] This chemistry is fast enough to compete with the phosphination of the silaalkyl zirconium species, (eq 2-3). Formation of the final product (2) is stoichiometric (rather than catalytic), but the residual zirconium-containing material (mainly Cp_2ZrCl_2 plus some hydrolyzed species) can in principle be recycled to $Cp_2Zr(H)Cl$ although this was not attempted.

$$ZrCp_2(H)Cl + PPh_2Cl \longrightarrow ZrCp_2Cl_2 + PHPh_2 \qquad \textbf{(2-3)}$$

Successful synthesis of 2 using hydrozirconation suggests that a similar approach could be used as a route to phosphinoethylsilanes. To test the regioselectivity as well as the generality of this chemistry, hydrozirconation using Cp_2ZrHCl of allyl(dimethyl)silane (CH_2=$CHCH_2SiHMe_2$, *i.e.* already incorporating the Si-H functionality required for oxidative complexation at a low-valent transition-metal center) was investigated. This affords exclusively the (dimethylsilyl)propyl analogue 3 of 1 (see eq 2-4), immediately distinguishable from its [2-(methylsilyl)ethyl]zirconium regioisomer in the ^{1}H NMR spectrum (Table 2-1).

$$ZrCp_2HCl + SiHMe_2(CH_2CH{=}CH_2) \longrightarrow \underset{\underline{3}}{ZrCp_2(CH_2CH_2CH_2SiHMe_2)Cl} \qquad \textbf{(2-4)}$$

In the δ 0-5 range, the Si*Me* signal is split into a doublet by coupling (^3J = 3.7 Hz) to Si*H*, the latter appearing as an apparent nonet at δ 4.22 split equally by six protons in two

neighboring Si*Me* groups and two protons in one SiCH_2 group, accompanied by three well separated methylene resonances at δ 0.70, 1.17 and 1.72. Direct comparison of the appearance of this region with that illustrated elsewhere[50a] for $Ph_2P(CH_2)_3SiMe_2H$ (*i.e.* chelH, I: Tables 2-1, 2-2) highlights an upfield shift (1.17) for the CH_2 protons adjacent to the electropositive Zr center, to a position between the methylene hydrogens that are α and β to Si (δ 0.70, 1.72 respectively). The identity of 3 was further confirmed by its characteristic reactivity:[78] with traces of moisture, progressive replacement of the C_5H_5 NMR signal of 3 (δ 5.80) by a new Cp peak at δ 6.05 occurred, together with accumulation of a prominent triplet at δ 0.96 attributable to the CH_3 resonance of the triorganosilane $SiHMe_2Pr^n$ (Pr^n = n-propyl). Similarly, when dry HCl was bubbled into a solution of 3 in C_6D_6, the yellow color was discharged with precipitation of white Cp_2ZrCl_2 (observed at δ 5.88) and the pattern of multiplets due to $SiHMe_2Pr^n$ was again evident. This demonstrates cleavage of the latter from the Zr center that is similar to the behavior of simple alkylzirconium complexes, which can be protonated to release alkanes.. More prolonged exposure to HCl leads to gradual diminishment of the Si-H signal and appearance of a new unsplit Si*Me* signal at δ 0.18, shifted 0.17 down field, consistent with conversion of Si-H bonds to Si-Cl bonds. Such substitution with dry HCl gas is a well known reaction in silicon chemistry.

Oxidative cleavage by addition to solutions of 3 of either N-bromosuccinimide (NBS) or di-iodine (1 mol equiv) afforded products identified by ^{1}H NMR as (3-halogenopropyl)(dimethyl)silanes, 4 or 5 respectively. Each of these shows a characteristic triplet, at δ 3.40 and 3.10 respectively, assigned to the methylene groups

bonded to the electronegative atoms Br or I, see Scheme 2-5. The bromide 4 was isolated in poor yield while the iodide 5 was identified only in a mixture by solution NMR spectroscopy. Cleavage of both Si-H and Si-C bonds is possible with strong oxidants like NBS and I_2, so that competing side reactions may account for the low yield of compounds 4 and 5. The isolated bromide 4 represents a new type of useful precursor that could be used to prepare some unusual silanes by making use of the reactive bromide functionality, although this field has not been further investigated yet.

Following a procedure similar to that of eq 2-4, addition of PPh_2Cl to a yellow solution in benzene of the silylpropyl zirconium species 3 led again to discharge of the color, to formation of Cp_2ZrCl_2, and to the isolation in high yield (~80%) of the known phosphinoalkylsilane $Ph_2PCH_2CH_2CH_2SiMe_2H$, I (Scheme 2-5) which was first prepared via a photochemical route and reported by Stobart *et al*[50a] in the early 1980s.

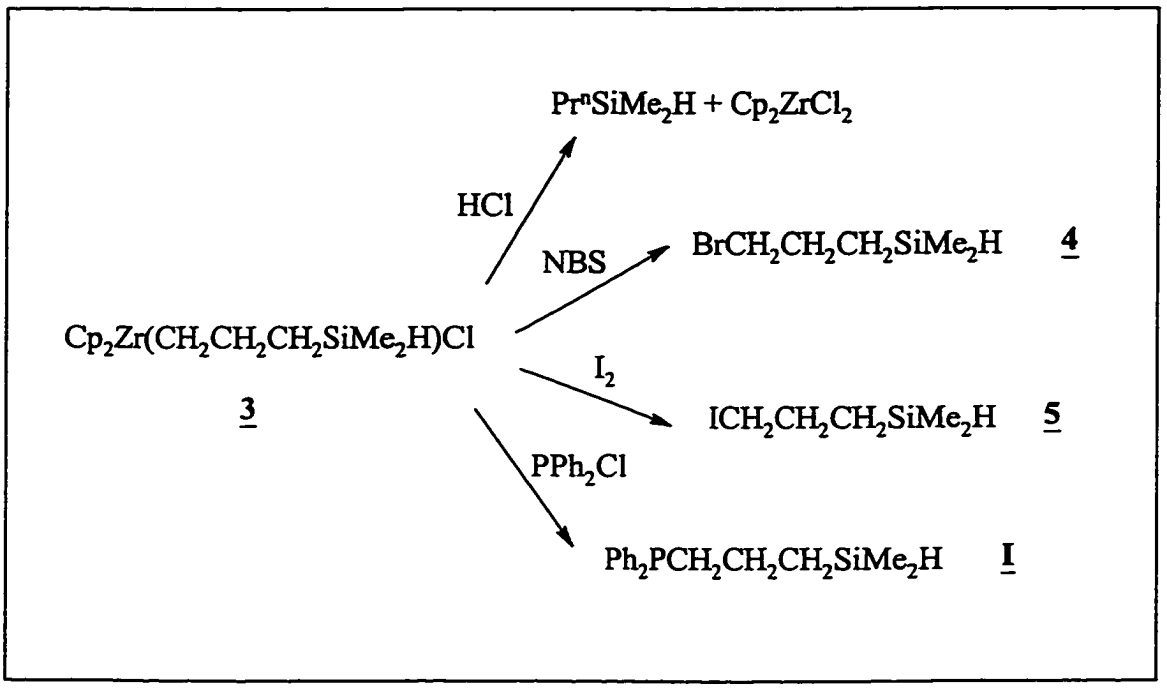

Scheme 2-5. Reactivity of intermediate 3

Access using parallel operations to the poly(phosphinoalkyl)silanes biPSiH, **II** (Figure 2-1: ^{1}H NMR spectrum), or triPSiH, **III**, requires that hydrozirconation occurs across each terminal alkenyl group in a diallyl- or triallyl-silane (Scheme 2-6). Both **II** and **III** were previously prepared by the slow photochemical addition of PPh_2H to corresponding polyallylsilanes.[50b] After a solution in benzene of $SiH(Me)(CH_2CH{=}CH_2)_2$ was added to Cp_2ZrHCl (2 mol equiv), ^{1}H NMR showed that all allyl groups had reacted since no signals due to alkenyl hydrogens remained, clearly establishing that multiple hydrozirconation of the precursor silane is possible. New signals at δ 0.15, 0.30 (doublets) and δ 4.17, 4.34 (multiplets) are attributable to the $SiCH_3$ and SiH hydrogens respectively of mono- and bis-zirconated intermediates related to **3**. A characteristic triplet (δ 1.03) due to Pr^n attached to Si in the monosubstituted species confirms that it originates from partial hydrolysis, and although its formation could be suppressed it was never eliminated under the experimental conditions employed. Thus in a typical further reaction with PPh_2Cl an oily mixture (*ca* 2:1) of the known biPSiH (**II**) and a propyl analogue $Ph_2PCH_2CH_2CH_2SiMe(Pr^n)H$ (**6**, triplet at δ 0.91: Pr^n group) of **I** was formed; these two compounds proved to be separable by distillation, giving pure **II** in ~50% yield. A similar sequence, see Scheme 2-5, converted $SiH(CH_2CH{=}CH_2)_3$ to a mixture (*ca* 5:2:1 ratio) of the known triPSiH (**III**), a new biPSiH analogue $SiH(Pr^n)(CH_2CH_2CH_2PPh_2)_2$ (**7**), and a further analogue $Ph_2PCH_2CH_2CH_2SiHPr^n_2$ (**8**) of **I**. These three products, of which only **8** has a low boiling point and could be obtained pure by distillation *in vacuo*, were shown by using *in situ* ^{1}H NMR to be formed from tris-,

bis-, and mono-zirconated intermediates characterized by Si*H* resonances at δ 4.44, 4.31, 4.18 (apparent octets) respectively.

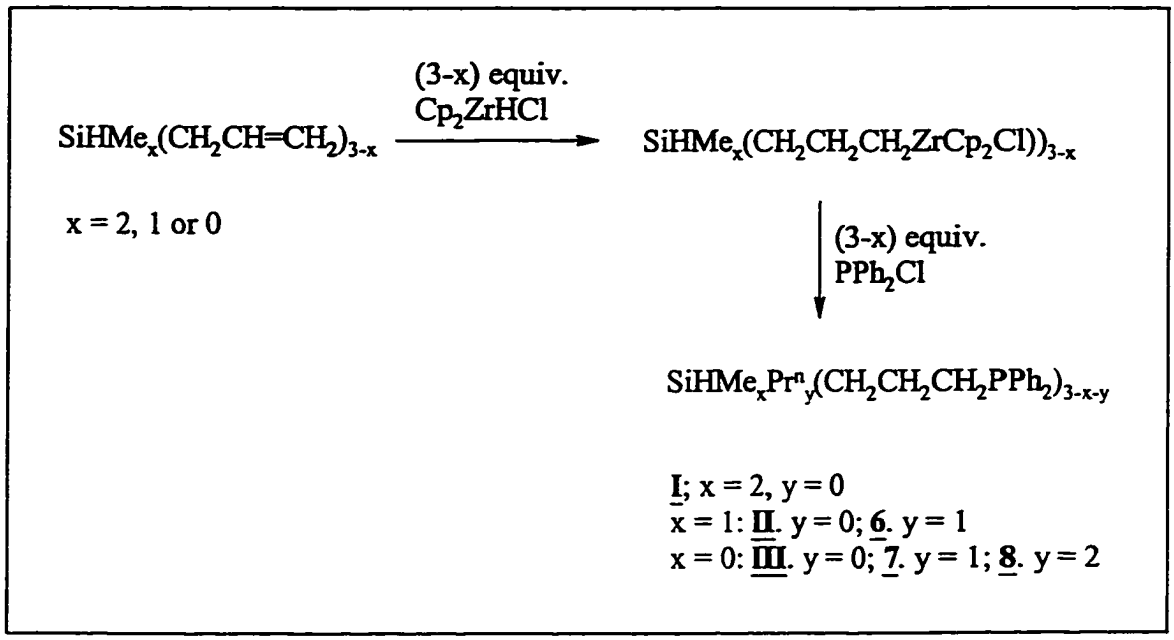

Scheme 2-6. Synthesis of ChelH (I), biPSiH (II) and triPSiH (III)

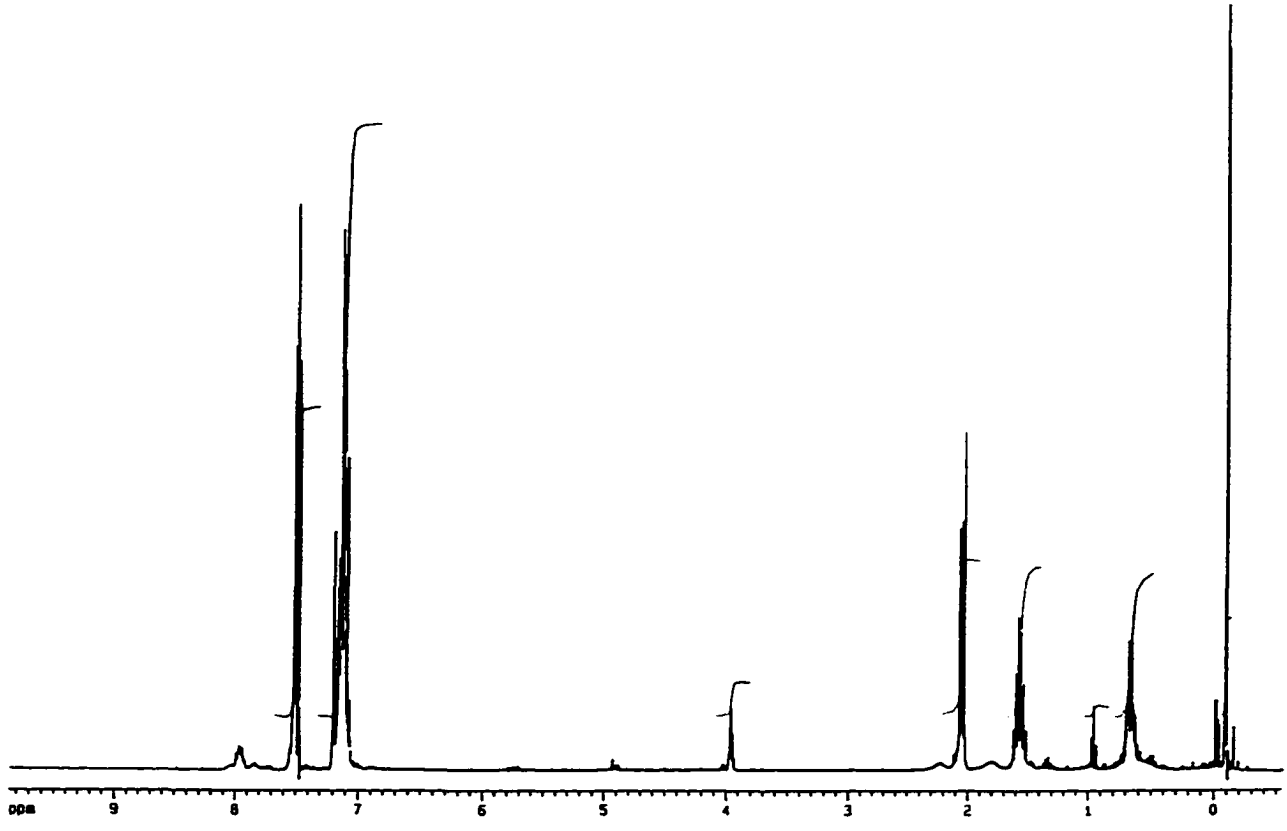

Figure 2-1. ^{1}H NMR spectrum for biPSiH (II)

A further analogue $SiH_2(CH_2CH_2CH_2PPh_2)_2$ (9) of biPSiH (II) was also prepared similarly, starting from diallylsilane $SiH_2(CH_2CH{=}CH_2)_2$. NMR data for 7-9 are included in Table 2-1 (^{1}H, ^{31}P and ^{29}Si) and Table 2-2 (^{13}C). The coordination behavior of 9 is expected to be different from biPSiH (II) since one or both of Si-H bonds can be involved in coordination to metal centers. In the complexes $ML_m(SiHR_2)$ where a hydridosilyl group is coordinated, the Si-H bond should be weaker and more reactive[12] than that in uncomplexed hydridosilanes, such as 9. Weakening of Si-H bond can be

spectroscopically confirmed by the reduction of IR stretching frequency of Si-H bond and of NMR coupling constants $^1J_{SiH}$.

It should be noted that neither $SiMe_3Cl$ nor $SiHMe_2Cl$ leads to cleavage of 3 or other alkylzirconium derivatives in a manner similar to that effected by the phosphorus halides. Nugent *et al* have demonstrated that a zirconium group can be substituted by the silicon atom in silicon tetrabromide under much more vigorous conditions in low yield (eq 2-5). Similar substitution by germanium tetrachloride was found to be much easier.

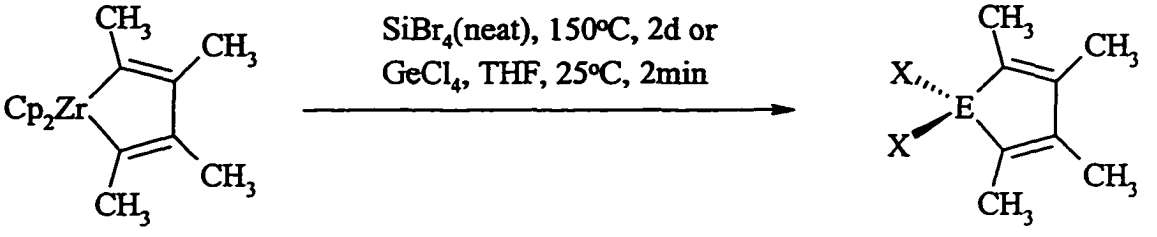

E = Si, X = Br, ca. 28%
E = Ge, X = Cl, 83%

(2-5)

Table 2-1. ^1H, ^{31}P and ^{29}Si NMR Data[a] for Compounds 1-11 and I, II

	^{31}P	^{29}Si	^1H					
Compd	$\delta(PR_2)$	$\delta(SiR_3)$	$\delta(X^bCH_2)$	$\delta(XCH_2CH_2)$	$\delta(SiCH_2)$	$\delta(SiH)$	$\delta(SiCH_3)$	$^3J(CHSiH)$
1[c]	-	-	0.94	-	0.49	-	-	-
2[d]	-9.2	7.9(d)	2.06	-	0.72	-	-	-

3	-	-	1.17	1.72	0.70	4.22	0.14	3.7
4	-	-	3.40	1.88	0.69	3.86	0.09	3.6
5	-	-	3.10	1.59	0.42	3.94	-0.09	3.6
I	-16.5	-13.8	2.04	1.57	0.67	4.03	-0.06	3.5
6[e]	-17.1	-11.1	2.05	1.58	0.70	3.98	-0.06	3.7
7[f]	-17.1	-8.9	2.03	1.53	0.68	3.89	-	3.5
II	-17.0	-11.3	2.04	1.57	0.67	3.96	-0.10	3.9
8[g]	-17.1	-8.3	2.08	1.60	0.74	3.94	-	-
9	-16.9	-30.4	1.99	1.53	0.63	3.75	-	3.7
10[h]	-32.8	-10.9	1.49	1.64	0.78	4.11	0.09	3.7
11[i]	-19.9	-11.3	1.64	1.39	0.50	3.86	-0.18	3.5

[a] C_6D_6 was used as solvent except compound 4 ($CDCl_3$); ^{31}P chemical shifts vs external 85% H_3PO_4; ^{29}Si chemical shifts vs external tetramethylsilane; coupling constants were measured in Hz.

[b] X = Zr in compound 1 and 3; X = Br in compound 4; X = I in compound 5; X = P in compound 2, 6-11 and I, II.

[c] NMR data for ethyl group: ^{1}H, δ(SiCH_2) = 0.61, δ(SiCH$_2$CH_3) = 1.08.

[d] NMR data for ethyl group: ^{1}H, δ(SiCH_2) = 0.44, δ(SiCH$_2$CH_3) = 0.87; ^{29}Si, $^3J_{PSi}$ = 19.8 Hz.

[e] NMR data for propyl group: ^{1}H, δ(SiCH_2) = 0.45, δ(SiCH$_2$CH_2) = 1.30, δ(CH_3) = 0.91.

[f] NMR data for propyl group: ^{1}H, δ(SiCH_2) = 0.42, δ(SiCH$_2$CH_2) = 1.26, δ(CH_3) = 0.89.

[g] NMR data for propyl group: ^{1}H, δ(SiCH_2) = 0.50, δ(SiCH$_2$CH_2) = 1.32, δ(CH_3) = 0.93.

[h] NMR data for hexyl group: ^{1}H, δ(PCH_2) = 1.27, δ(PCH$_2$CH_2) = 1.39, δ(PC$_2$H$_4$CH_2) = 1.39, δ(PC$_3$H$_6$CH_2) = 1.48, δ(PC$_4$H$_8$CH_2) = 1.22, δ(PC$_5$H$_{10}$CH_2) = 0.89.

[i] NMR data for benzyl group: ^{1}H, δ(PCH_2) = 2.91, $^2J_{PH}$ = 13.2 Hz.

Table 2-2. ^{13}C NMR Data[a] for Compounds 1-11 and I, II

	^{13}C						
Compd	δ(X*C*H$_2$)	$^1J_{PC}$	δ(X^{b}CH$_2$*C*H$_2$)	$^2J_{PC}$	δ(SiCH$_2$)	$^3J_{PC}$	δ(SiCH$_3$)
1[c]	46.34	-	-	-	16.04	-	-
2[d]	21.99	15.1	-	-	6.84	10.3	-
3	29.25	-	59.48	-	21.59	-	-3.89

4	36.65	-	28.30	-	13.38	-	-4.58
5	[c]						
I	32.23	13.0	21.50	18.0	16.29	12.1	-4.53
6[f]	32.37	12.8	21.61	17.7	14.97	11.9	-6.23
7[g]	32.40	13.1	21.72	17.6	13.43	12.1	-
II	32.29	12.9	21.56	17.4	14.76	12.1	-6.40
8	[c]						
9	31.88	13.3	22.43	18.2	11.09	12.2	-
10[h]	32.16	14.8	21.83	15.3	15.30	10.1	-6.10
11[i]	31.24	17.1	21.43	14.8	14.81	16.7	-6.37

[a] C_6D_6 was used as solvent except compound 4 ($CDCl_3$); coupling constants were measured in Hz.

[b] X = Zr in compound 1 and 3; X = Br in compound 4; X = I in compound 5; X = P in compound 2, 6-11 and I, II.

[c] NMR data for ethyl group: ^{13}C, $\delta(SiCH_2) = 3.10$, $\delta(SiCH_2CH_3) = 7.69$.

[d] NMR data for ethyl group: ^{13}C, $\delta(SiCH_2) = 2.96$, $\delta(SiCH_2CH_3) = 7.24$.

[e] ^{13}C NMR data not measured.

[f] NMR data for propyl group: ^{13}C, $\delta(SiCH_2) = 15.35$, $\delta(SiCH_2CH_2) = 18.26$, $\delta(CH_3) = 18.07$.

[g] NMR data for propyl group: ^{13}C, $\delta(SiCH_2) = 13.82$, $\delta(SiCH_2CH_2) = 18.39$, $\delta(CH_3) = 18.11$.

[h] NMR data for hexyl group: ^{13}C, $\delta(PCH_2) = 31.88$, $^1J_{PC} = 18.0$ Hz, $\delta(PCH_2CH_2) = 31.61$, $^2J_{PC} = 10.3$ Hz, $\delta(PC_2H_4CH_2) = 28.18$, $^3J_{PC} = 13.9$ Hz, $\delta(PC_3H_6CH_2) = 26.55$, $^4J_{PC} = 13.5$Hz, $\delta(PC_4H_8CH_2) = 22.96$, $^5J_{PC} = 8.2$ Hz, $\delta(PC_5H_{10}CH_2) = 14.29$, $^6J_{PC} = 7.9$ Hz.

[i] NMR data for benzyl group: ^{13}C, $\delta(PCH_2) = 36.91$, $^1J_{PC} = 4.9$ Hz.

2.A.ii. Steric Effect of Phosphination

The zirconium-mediated chemistry of Schemes 2-5 and 2-6 suggests that the choice of R in the reagent PR_2Cl may offer a straightforward method for varying substituent groups at P in PSiH ligand precursors. The commercially available alkylphosphine chlorides PR_2Cl (R = Pr^i or Bu^t; Pr^i = iso-propyl, Bu^t = tert-butyl) behaved differently from one another, but in reactions monitored by using NMR spectroscopy neither yielded a phosphinoalkylsilane. Thus with R = Pr^i, precursor 3 was consumed to afford a new -$SiHMe_2$ derivative that did not however contain P, together with a product tentatively identified as $P_2Pr^i_4$ (^{31}P NMR: δ = -11.2); while with R = Bu^t only slow hydrolysis of 3 was observed with no evidence for formation of Cp_2ZrCl_2. There was also no reaction of PBu^t_2Cl with a solution containing hydrozirconated

$SiH(Me)(CH_2CH{=}CH_2)_2$, but by contrast treatment of the latter with $P(^nhex)_2Cl$, *i.e.* ^{n}hex = $CH_3(CH_2)_4CH_2$-, did behave according to Scheme 2-6. This facilitated isolation in good yield of a further new biPSiH analogue $SiH(Me)[CH_2CH_2CH_2P(^nhex)_2]_2$ (**10**), and another congener $SiH(Me)(CH_2CH_2CH_2PPhBz)_2$ (**11**) was similarly recovered (~60%) by using PPhBzCl (*i.e.* Bz = $-CH_2C_6H_5$). NMR data for **10** and **11** are listed in Tables 2-1 and 2-2. The ^1H and ^{13}C NMR spectra of **10** are complicated by the overlap of signals of ^{n}hexyl groups and methylene units. Assignment of all of the NMR signals relied on the extra information obtained from the ^1H-^1H cosy and ^1H -^{13}C correlation spectra and from the comparison with the analogue biPSiH (**II**). The diastereoisomeric character of **11** (*rac vs meso*) could not be detected by ^{31}P and ^{29}Si NMR.

Mass spectrometry was used for further characterization of the new PSiH precursors **6** - **13**. Using CH_4 chemical ionization, parent ions were prominent in all cases. These silanes all have a strong SiH stretching frequency, observed in the IR spectrum in the range from 1995 to 2110 cm^{-1}.

It is clear that the silaalkyl-zirconium intermediates can be cleaved by both alkyl- and arylchlorophosphines and this cleavage is controlled by steric rather than electronic influences, as has been suggested previously.[71] The shutdown of alkyl transfer from Zr to P (accompanied by formation of Cp_2ZrCl_2) is observed to occur between PPhBzCl and PPr^i_2Cl (with PBu^t_2Cl totally unreactive), *i.e.* follows expectations based on phosphine group 'cone angle'[79] considerations. The concept of a cone angle was introduced by Tolman in order to quantitatively describe the size of a ligand. It is defined as the apex angle of a cylindrical cone when all ligand substituents are arranged so as to occupy as little space as possible (Figure 2-2). The cone angles of some relevant tertiary phosphines

are listed in Table 2-3. An ordering of the steric effect of the phosphine subsituents is -P^tBu_2 > -P^iPr_2 > -PPhBz > PPh_2 > P^nhexyl$_2$. This conclusion suggests in particular that -PMe_2 groups could be introduced into PSiH ligand precursor system in this way although this has not been investigated.

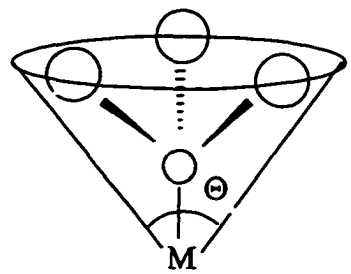

Θ: cone angle

Figure 2-2. Tolman's cone angle

Table 2-3. The cone angles of some relevent tertiary phosphines

Ligand	PMe_3	PEt_3	PPh_3	P^iPr_3	PBz_3	PCy_3	P^tBu_3
Cone angle (°)	118	132	145	160	165	170	182

Coordination of **10** at platinum(II) was investigated using an NMR scale reaction for comparison with the behavior of biPSiH (**II**). Addition of 1 mol equiv of **10** to Pt(COD)Cl_2 in the presence of excess triethylamine (~5 x) in benzene gave immediately a white precipitate. After removal of volatiles, the residue was extracted with C_6D_6 and ^1H and ^{31}P NMR spectra were recorded. The product **23** was found to have a singlet (δ 0.52)

with ^{195}Pt side bands ($^{3}J_{PtH}$ = 27 Hz) assigned to silylmethyl groups in the ^{1}H NMR spectrum, with a singlet (δ 0.51) showing ^{195}Pt satellites ($^{1}J_{PtP}$ = 2607 Hz) in the ^{31}P NMR spectrum. The $^{1}J_{PtP}$ value is close to those measured for the known compounds $Pt[Si(Me)(CH_2CH_2CH_2PPh_2)_2]Cl$ and $Pt[Si(Me)(CH_2CH_2CH_2PCy_2)_2]Cl$ (2825 and 2714 Hz respectively).[80] Thus complex **23** is assumed to have a similar structure.

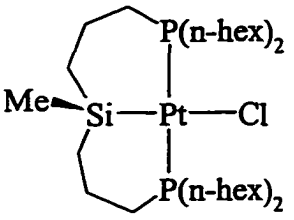

23

It is apparent that hydrozirconation using $Cp_2Zr(H)Cl$ opens up a new route to 1-phosphino, 3-silylpolymethylene connectivity by cleavage using halogenophosphines of silaalkylzirconium complexes that are formed as intermediates from poly- as well as mono-alkenylsilanes. This acts as a convenient and versatile chemical synthesis of phosphinoalkylsilanes that are required as precursors to transition metal PSi complexes. Thus in the silane $SiHR^1_x[(CH_2)_nPR^2_2]_{3-x}$, with R^1 and n determined by appropriate choice of alkenylsilane precursor (with silaalkyl attachment at Zr expected to be independent of n), it has been shown here that x can be varied at the intermediate stage, by using poly(hydrozirconation), Scheme 2-6; and that R^2 can be introduced as alkyl (^{n}hex) instead of aryl (Ph).

2.B. Synthesis of Poly[3-(dimethylsilyl)propyl]phosphines, $PR_n(CH_2CH_2CH_2SiMe_2H)_{3-n}$ (12): n = 1, R = Ph; (13): n = 0

Under the conditions similar to those that lead to ChelH (I), biPSiH (II) and triPSiH (III), reaction of 3 with either $PPhCl_2$ or PBr_3 afforded (Scheme 2-7) the corresponding bis- or tris- silylpropylphosphines $PhP(CH_2CH_2CH_2SiMe_2H)_2$ (12), $P(CH_2CH_2CH_2SiMe_2H)_3$ (13) as colorless or yellow oily liquids that were purified by using short-path distillation at reduced pressure onto a cold finger assembly. These new polysilyls showed strong IR absorption near 2100 cm^{-1}, (ν_{SiH}), and were further characterized by the NMR data listed in Tables 2-4 and 2-5: in the ^1H NMR, the methylene hydrogens α and β to Si are essentially invariant while the γ protons (*i.e.* to P) shift progressively to higher field as Ph at P is replaced by $-CH_2CH_2CH_2SiMe_2H$; while the distinctive multiplet family due to this latter group make up the entire spectrum for 13, which is a homoleptic trialkyl phosphine. As has been observed before for related compounds including I, in the ^{13}C NMR coupling to ^{31}P persists for all successive carbons of the polymethylene chain; by contrast the ^{29}Si resonances are observed as sharp singlets, although for $Ph_2PCH_2CH_2SiEt_3$ (*i.e.* with Si and P separated by only two methylene units) $^3J_{SiP}$ = 19.8 Hz (Table 2-1). The ^1H and ^{13}C NMR spectra for compounds 12 and 13 are shown in Figures 2-3, 2-4, 2-5 and 2-6.

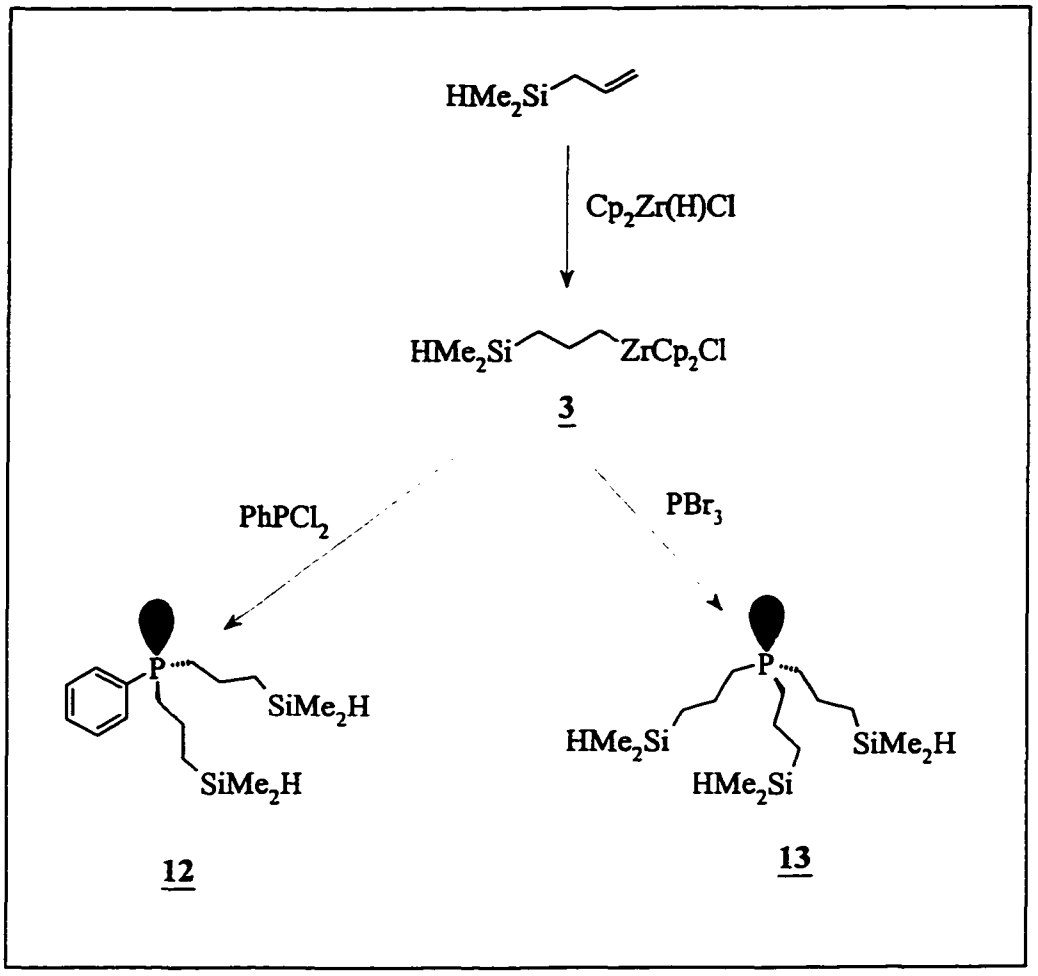

Scheme 2-7. Synthesis of 12 and 13

Table 2-4. ^{1}H, ^{31}P and ^{29}Si NMR Data[a] for Compounds 12 and 13

	^{31}P	^{29}Si	^{1}H					
Compd	$\delta(PR_2)$	$\delta(SiR_3)$	$\delta(PCH_2)$	$\delta(PCH_2CH_2)$	$\delta(SiCH_2)$	$\delta(SiH)$	$\delta(SiCH_3)$	$^{3}J(CHSiH)$
							-0.04	
12	-27.1	-13.8	1.71	1.53	0.65	4.07	-0.05	3.6
13	-34.6	-13.7	1.46	1.60	0.70	4.13	0.04	4.5

[a] C_6D_6 was used as solvent; ^{31}P chemical shifts vs external 85% H_3PO_4; ^{29}Si chemical shifts vs external tetramethylsilane; coupling constants were measured in Hz.

Table 2-5. ^{13}C NMR Data[a] for Compounds 12 and 13

	^{13}C						
Compd	$\delta(PCH_2)$	$^{1}J_{PC}$	$\delta(PCH_2CH_2)$	$^{2}J_{PC}$	$\delta(SiCH_2)$	$^{3}J_{PC}$	$\delta(SiCH_3)$
							-4.82
12	32.34	12.7	21.23	15.9	16.03	10.9	-4.85
13	32.06	14.6	21.71	15.0	16.62	10.5	-4.40

[a] C_6D_6 was used as solvent; coupling constants were measured in Hz.

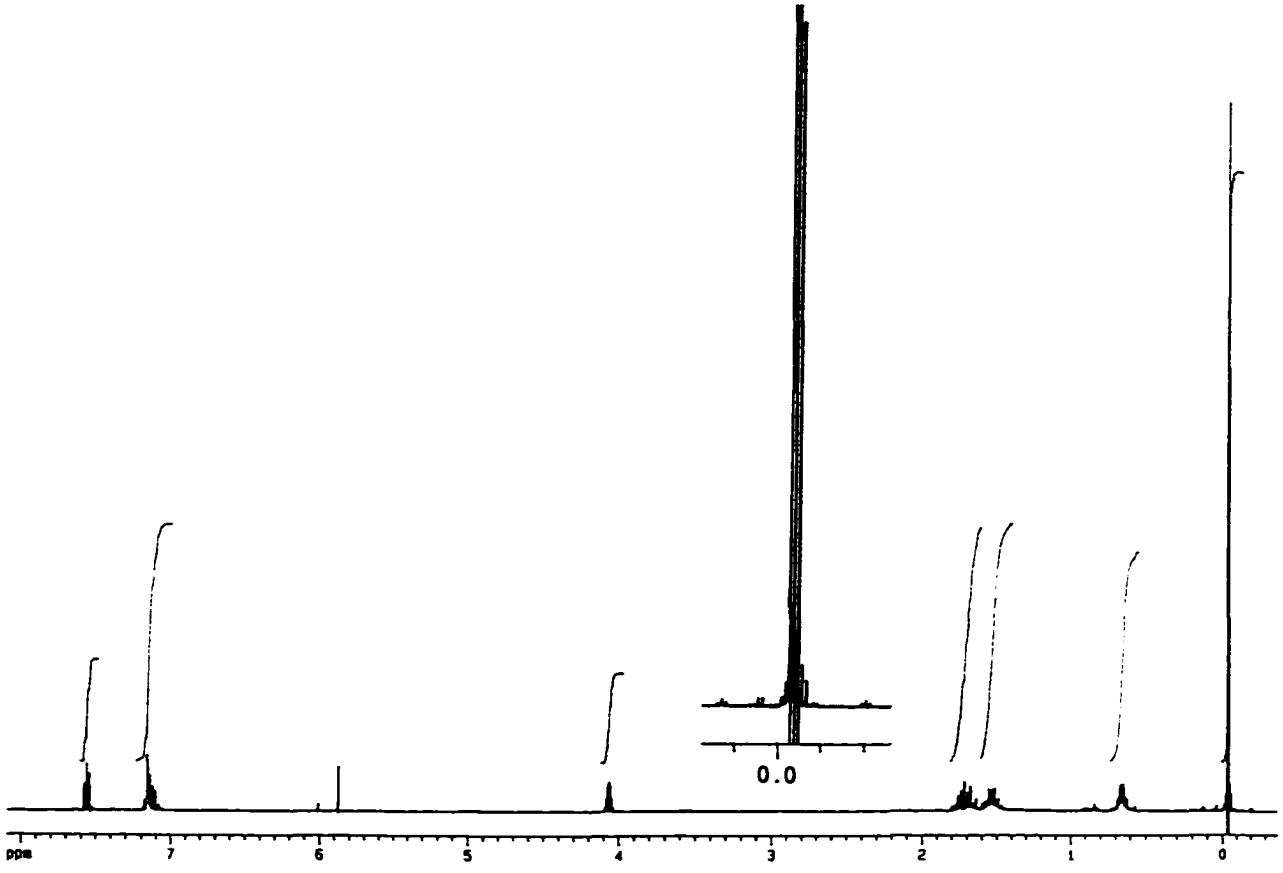

Figure 2-3. ^{1}H NMR spectrum for compound **12**

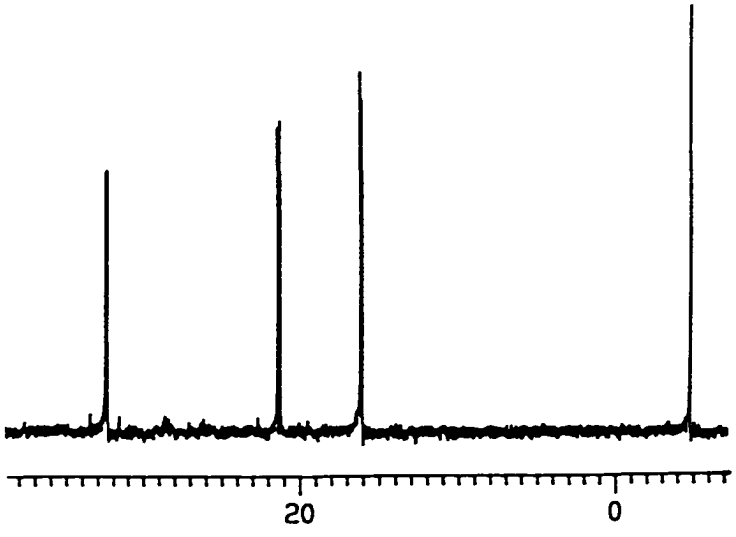

Figure 2-4. ^{13}C NMR spectrum for compound **12**

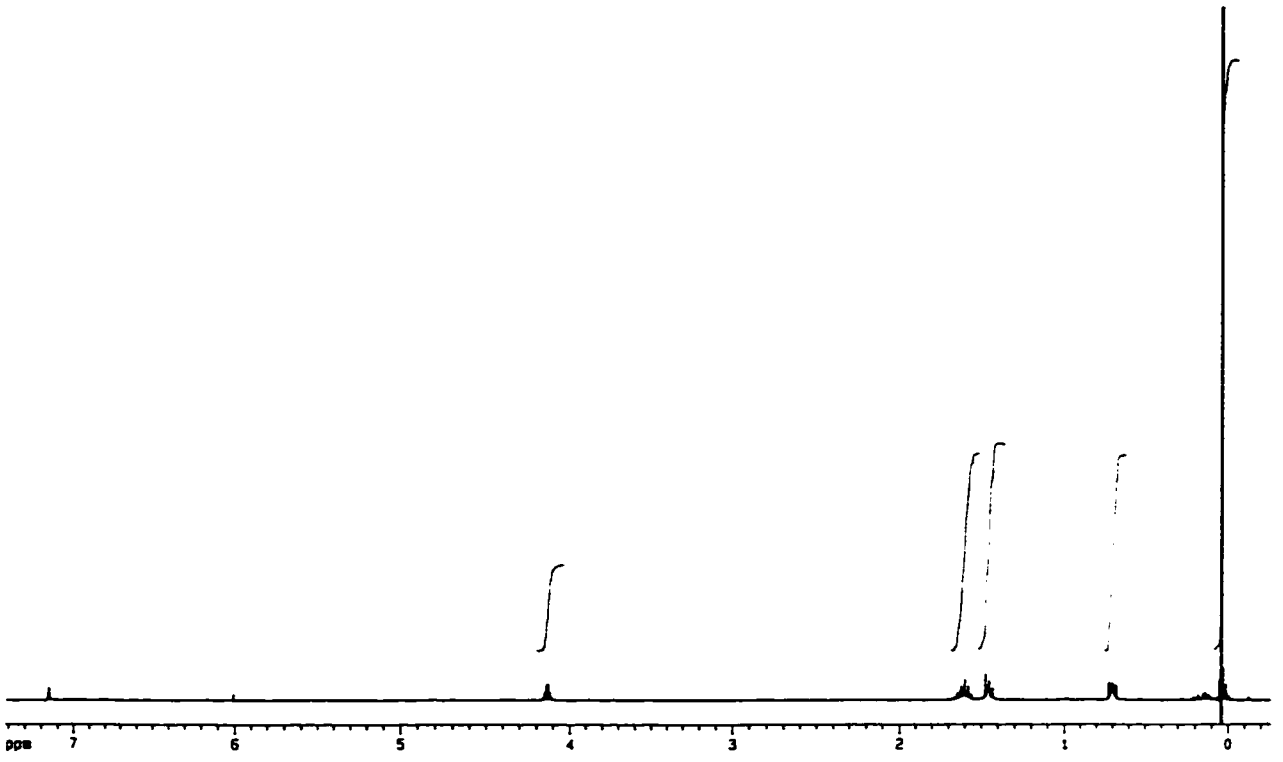

Figure 2-5. ^{1}H NMR spectrum for compound 13

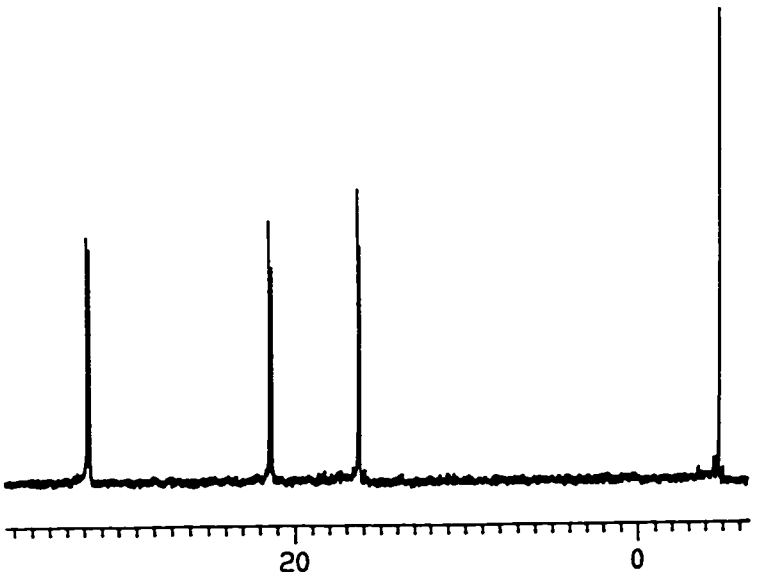

Figure 2-6. ^{13}C NMR spectrum for compound 13

Successive substitution of aryl by alkyl at P along the family I, 12, 13 results in monotonic changes in ^{31}P and PCH_2 NMR shifts as is expected (Tables 2-4 and 2-5). Two methyl resonances are observed in both ^{1}H and ^{13}C NMR spectra for compound 12, a reflection[50a] of its low molecular symmetry (C_S) *vs* that of the trisubstituted compound 13 (the idealized geometry of which belongs to the point group C_{3v}; Figure 2-7). A plane can be drawn through the -PPh fragment in 12 that relates the two $-CH_2CH_2CH_2SiMe_2H$ chains. One of the two protons (H) in each methylene group is equivalent to its partner (H) in the corresponding methylene group of the other chain but is inequivalent to the other proton (H') on the same methylene carbon. Similarly, one of the two methyl groups (Me) on one silicon atom is symmetry related to a partner on the other silicon atom while the two methyl groups on the same silicon atom are different from each other. H and H' can not be differentiated in the ^{1}H NMR spectrum because of the overlap and non-first-order feature of signals, but the two silicon methyl groups are well resolved and show up as two different signals in both ^{1}H and ^{13}C NMR spectra. A three-fold rotation axis and three mirror planes exist for 13 so that the two hydrogen atoms on each methylene carbon are equivalent to one another as well as to corresponding methylene hydrogen atoms on different chains. Also as a consequence of C_{3v} symmetry, all the six silicon methyl groups are equivalent giving only one methyl signal for 13 in both ^{1}H and ^{13}C NMR spectra. The formation of 12 and 13 was further confirmed by mass spectroscopy. In each case, the only abundant ions were those corresponding to loss of one or two 'arms' from P.

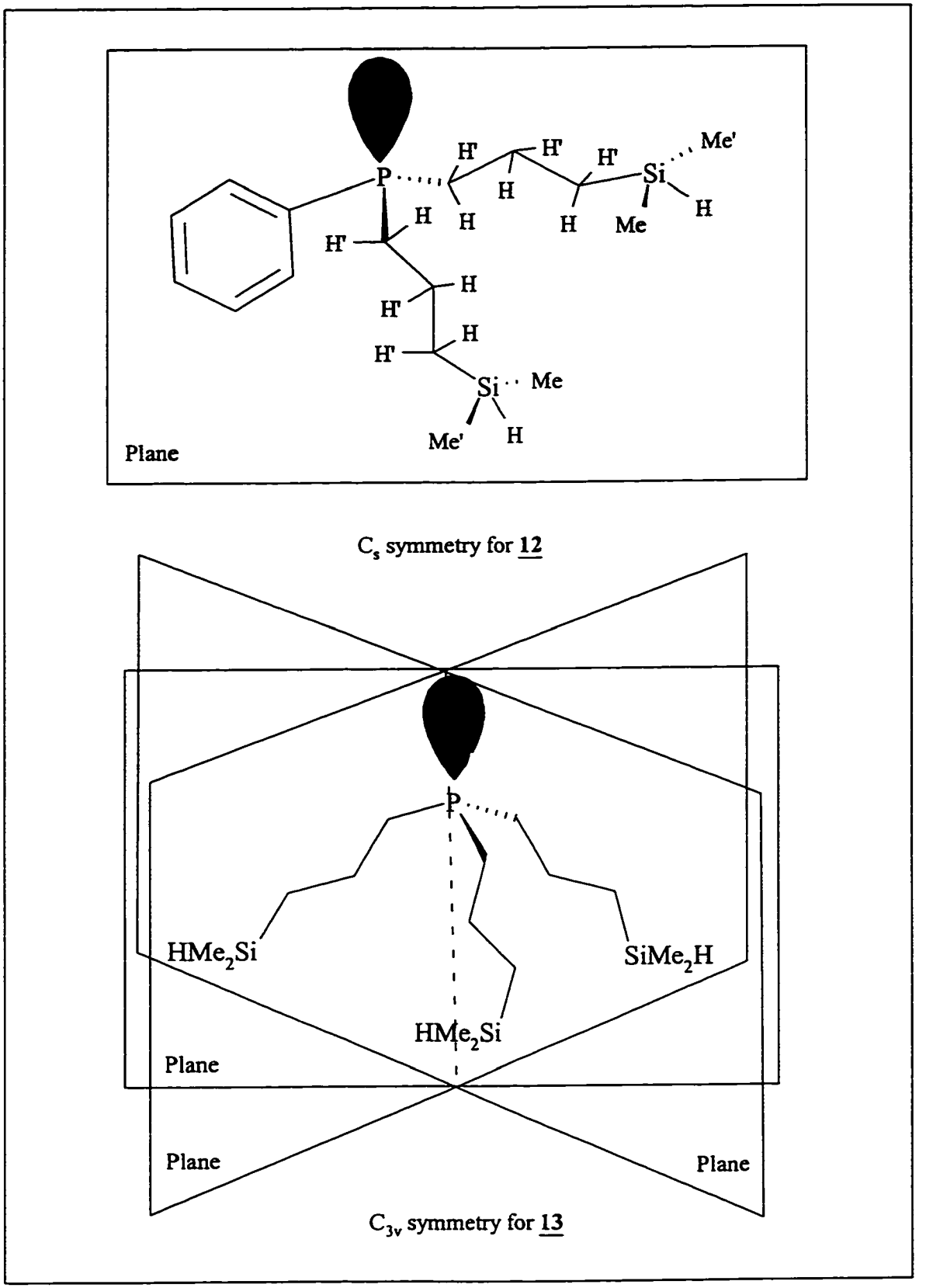

Figure 2-7. Description of the symmetries of compounds 12 and 13

The overall yields for compound 12 and 13 remained below 30% even after many attempts to optimize the experimental conditions. Phosphination of intermediate 3 with PCl_3 rather than PBr_3 led to an even poorer yield (~10% *vs* ~20%) of 13, which may be a result of relative P-X bond strengths. Both 12 and 13 are very air sensitive since they are alkyl (rather than aryl) phosphines.

Poly(silylpropyl)phosphines, $PhP(CH_2CH_2CH_2SiMe_2H)_2$ (12) and $P(CH_2CH_2CH_2SiMe_2H)_3$ (13), belong to an interesting new sub-group of PSiH precursors that are expected to induce chelate-assisted multiple Si-H bond addition at transition-metal centers: this chemistry is under investigation (see Chapter 3). The synthetic problems referred to above led to a search for other more accessible analogues possessing the same functionality (also Chapter 3).

2.C. Synthesis of (Haloalkyl)phosphines and (Haloalkyl)phosphine Oxides

Use of (haloalkyl)phosphines [$X(CH_2)_nPR_2$, X = halide] and their derivatives as potential ligand precursors has been given little attention since (haloalkyl)phosphines are considered to be thermodynamically unstable, transforming to penta-valent phosphonium salts via inter- or intra-molecular pathways (Scheme 2-8)[81] that interfere with attempts to isolate the products as pure compounds.

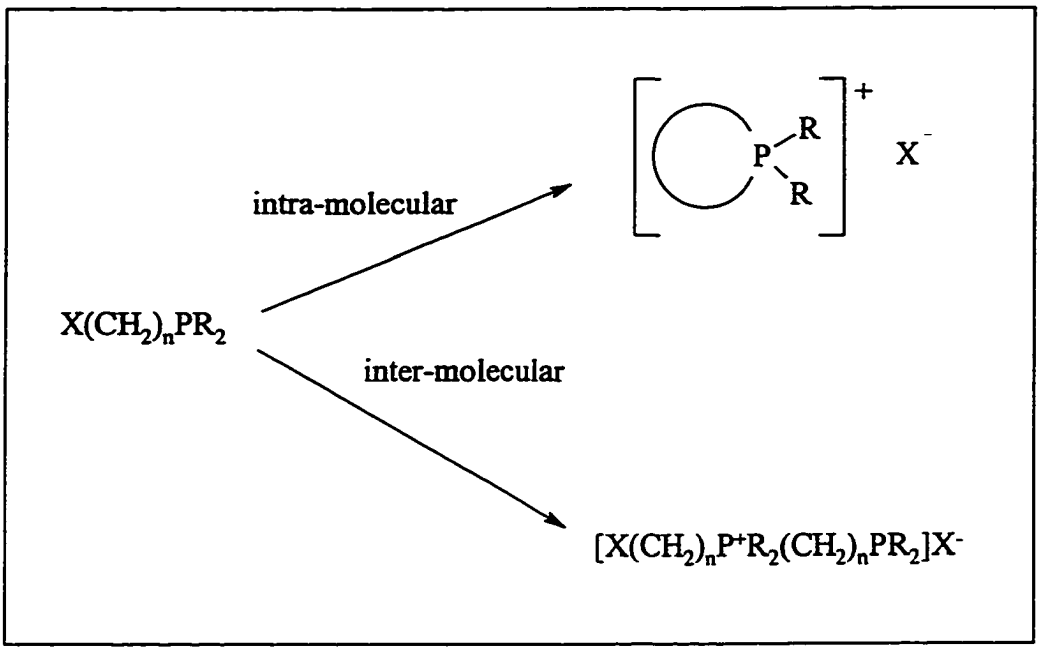

Scheme 2-8. Formation of phosphonium salts

However (chloroalkyl)diphenylphosphines, $Cl(CH_2)_nP(C_6H_5)_2$ (n = 1, 2, or 3), which can be synthesized by reaction of $(C_6H_5)_2P^-$ with polymethylene dichlorides (eq 2-6), are found to be stable even at elevated temperature because formation of phosphonium salts is slower for chlorides than for the corresponding bromides and iodides. These products have been used to prepare multidentate phosphines via Grignard reactions.[82] In this section, extension of alkene hydrozirconation to the synthesis of (haloalkyl)phosphines and their oxides will be discussed.

$$(C_6H_5)_2PNa + Cl(CH_2)_nCl \longrightarrow (C_6H_5)_2P(CH_2)_nCl \qquad (2\text{-}6)$$

n = 1, 2 or 3

Hydrozirconation of the bromoalkenes $Br(CH_2)_nCH{=}CH_2$ (n = 0, 1, 2, 3 or 4), or of 3-chloropropene was found to give the expected terminal zirconium substitution with products showing characteristic triplets at δ 3.1-3.3 in the ^1H NMR spectra assigned to the CH_2 groups adjacent to halides ($^3J_{HH} \cong 7$ Hz). Phosphination of the zirconium intermediates led to formation of the corresponding (haloalkyl)phosphines, which vary in relative stablility (Scheme 2-9): some can be isolated as colorless or yellowish liquids, while all transform to the related phosphonium salts. Formation of the latter is accompanied by transformation of the liquid phosphines to white solids and by observation of multiple ^{31}P NMR signals in the range δ 20 - 80, i.e., 30-110 downfield compared to the phosphines. It was found that pure (2-bromoethyl)diphenylphosphine was not isolable, and only white solid material insoluble in benzene was recovered from the reaction. By contrast, pure (3-bromopropyl)diphenylphosphine (**14**) is stable only for a few minutes at 25°C, while (3-choropropyl)diphenylphosphine (**IV**) is stable even at elevated temperature; and (4-bromobutyl)diphenylphosphine (**15**), and (5-bromopentyl)diphenylphosphine (**16**) are each stable for several hours at ambient temperature. Finally (6-bromohexyl)diphenylphosphine (**17**) is thermally stable for at least a day at room temperature (Figure 2-8: ^1H NMR spectrum; Figure 2-9: ^{13}C NMR spectrum). These compounds were isolated as oily liquids, and (**15**), (**16**) and (**17**) were converted to the corresponding phosphine oxides (**18**), (**19**) and (**20**) by immediate oxidation with 10% H_2O_2 (Scheme 2-9). Compounds **18**-**20** are air stable white solids that have been fully characterized by NMR spectroscopy, mass spectroscopy and elemental analysis. The ^1H NMR data for **14**-**20** and ^{13}C NMR data for **16**-**20** are collected in Tables

2-6 and 2-7 respectively. All the bromoalkylphosphines show characteristic triplets at δ 2.9-3.1 assigned to the methylene groups attached to Br in the ^{1}H NMR spectra. The methylene group bonded to P can be differentiated from the others by its typical non-first-order coupling pattern [δ 1.9 - 2.2, as has been observed for ChelH (I), biPSiH (II), triPSiH (III), 12 and 13]. The ^{13}C NMR data show that up to three-bond P-C coupling can be observed along the linear backbones for phosphines 16, 17 and IV, and that the coupling constants ($^{1}J_{PC}$, $^{2}J_{PC}$, $^{3}J_{PC}$) are similar to one another. Similar patterns can also be observed for compounds 6-13, I-III (Tables 2-1 and 2-2). For the phosphine oxides 18, 19 and 20, the two-bond coupling ($^{2}J_{PC}$) is the largest, in the range 39 - 72 Hz, while the one-bond coupling ($^{1}J_{PC}$) is from 8 to 18 Hz and the three-bond coupling ($^{3}J_{PC}$) is small at only 3-4 Hz. The chemical ionization mass spectra for the (bromoalkyl)phosphine oxides show molecular ions which are polyisotopic due to the effect of bromine (50.69% ^{79}Br, 49.31% ^{81}Br), as well as fragments arising from loss of bromine atoms as the strongest peaks.

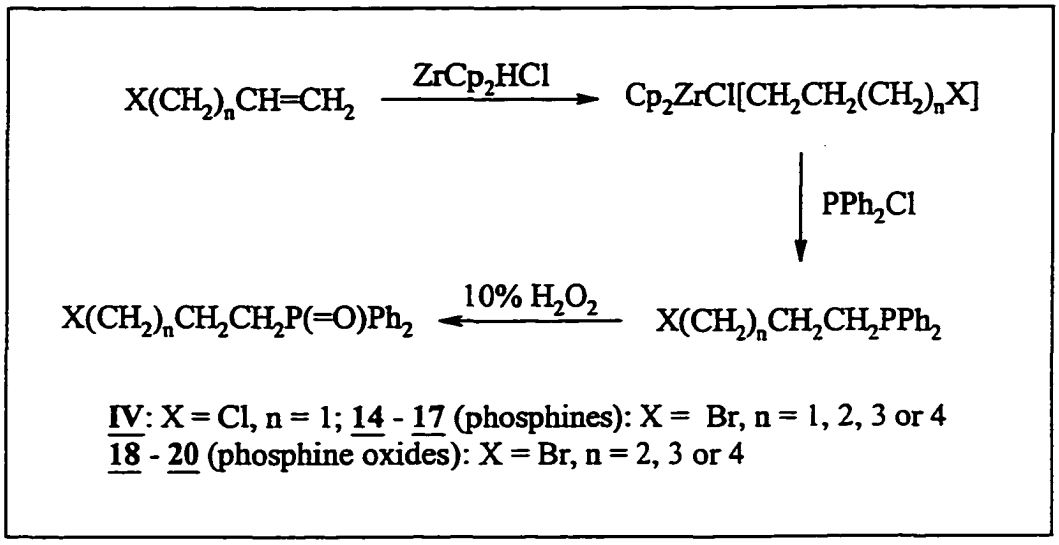

Scheme 2-9. Synthesis of (haloalkyl)phosphines and (haloalkyl)phosphine oxides

Table 2-6. ^{1}H and ^{31}P NMR Data[a] for Compounds 14 - 20 and IV

	^{31}P	^{1}H					
Compd	$\delta(PR_2)$	$\delta(X^bCH_2)$	$\delta(XCH_2CH_2)$	$\delta(XCH_2CH_2CH_2)$	$\delta[P(CH_2)_3CH_2]$	$\delta[P(CH_2)_4CH_2]$	$\delta(PCH_2)$
14	-14.6	2.94	1.94	-	-	-	1.91
IV	-17.0	3.11	1.62	-	-	-	1.92
15	-17.2	2.88	1.44	1.34	-	-	1.97
16	-16.3	2.84	1.34	1.22	1.24	-	1.81
17	-16.2	2.90	1.41	1.11	1.03	1.34	1.89

18	32.6	3.33	1.94	1.77	-	-	2.27
19	32.8	3.31	1.80	1.53	1.61	-	2.25
20	32.7	3.28	1.70	1.33	1.33	1.56	2.19

[a] C_6D_6 was used as solvent for **14**-**17** and **IV**; $CDCl_3$ was used as solvent for **18**-**20**; ^{31}P chemical shifts vs external 85% H_3PO_4

[b] X = Br for **14**-**20**; X = Cl for **IV**

Table 2-7. ^{13}C NMR Data[a] for Compounds **16**-**20** and **IV**

	^{13}C								
Compd	$\delta(X^bCH_2)$	$\delta(XCH_2CH_2)$	$\delta(XCH_2CH_2$ $CH_2)$	$\delta[X(CH_2)_3$ $CH_2]$	$\delta[X(CH_2)_4$ $CH_2]$	$\delta(PCH_2)$	$^1J_{PC}$	$^2J_{PC}$	$^3J_{PC}$
IV	45.33	25.26	-	-	-	29.08	18.3	13.2	15.3
16	33.14	32.14	25.10	27.88	-	29.47	12.5	12.9	17.1
17	33.23	32.44	27.55	25.74	28.01	30.07	13.1	12.9	16.5
18	32.57	20.31	28.74	-	-	33.44	13.8	72.0	3.0

19	33.32	32.11	20.67	29.64	-	29.11	18.0	39.2	3.7
20	33.54	32.08	27.30	21.01	29.26	29.73	8.1	65.8	3.7

[a] C_6D_6 was used as solvent for 16, 17 and IV; $CDCl_3$ was used as solvent for 18-20; coupling constants were measured in Hz

[b] X = Br for 16-20; X = Cl for IV

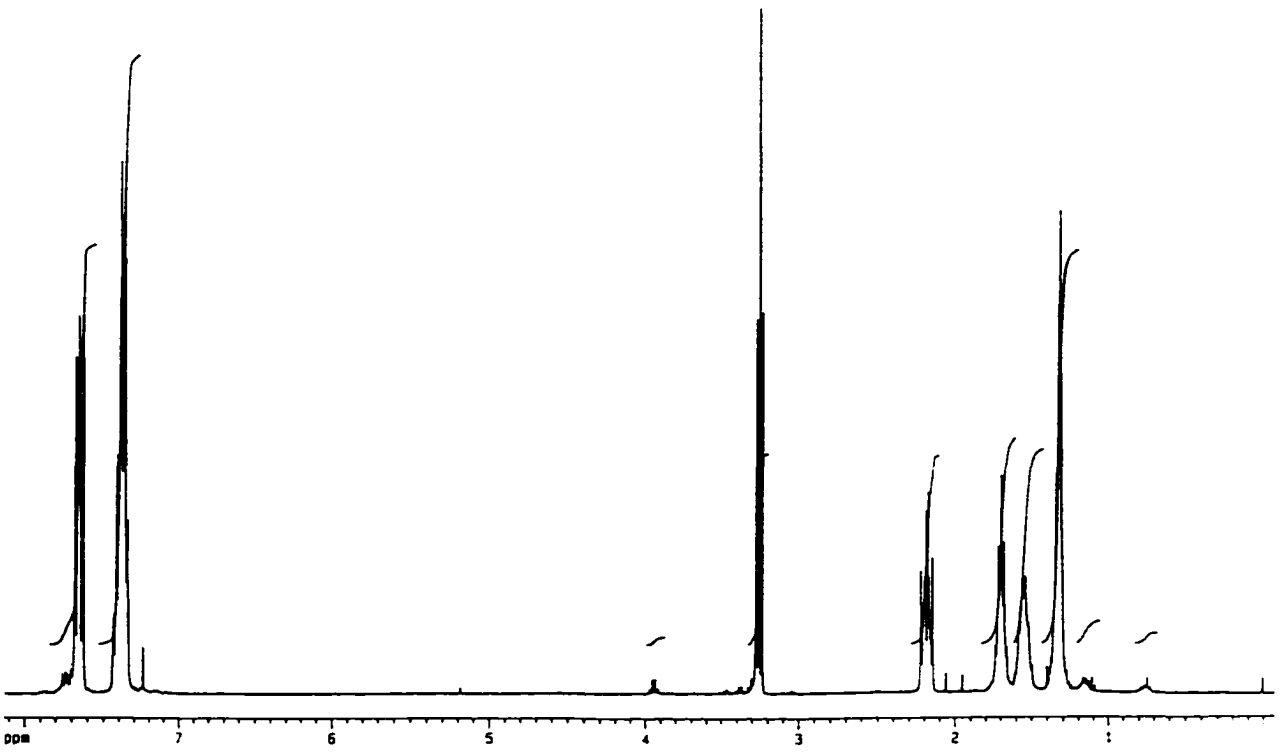

Figure 2-8. ^{1}H NMR spectrum for compound 17

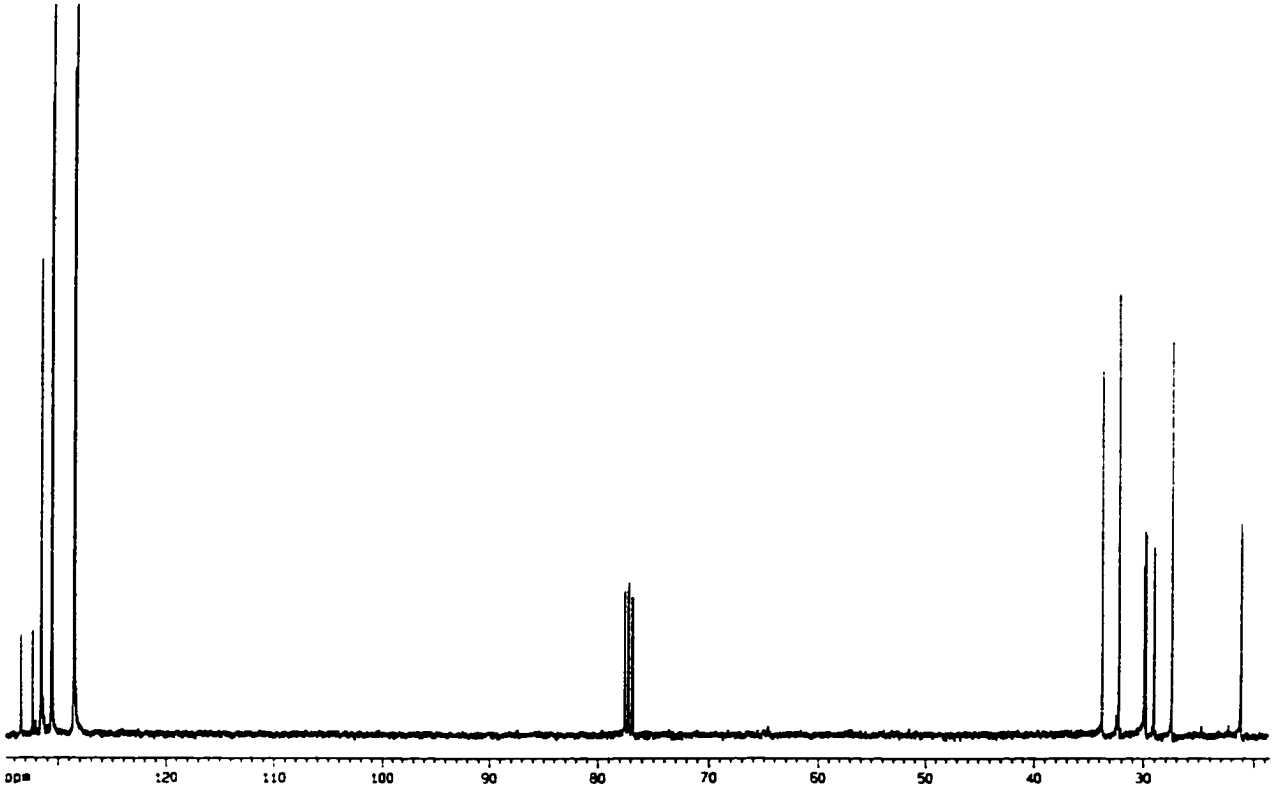

Figure 2-9. ^{13}C NMR spectrum for compound 17

The relative thermal stabilities of the (bromoalkyl)phosphines (14)-(17) strongly suggest that conversion to phosphonium salts is slowed down as the length of the chain separating the phosphine group from the bromine atom increases, suggesting that intramolecular elimination may be dominant (see Scheme 2-8). Of the isolated (bromoalkyl)phosphines, (6-bromohexyl)diphenylphosphine (17) is stable enough for use as a useful reagent and it is expected that the analogues containing more than six methylene units should be even more resistant to formation of phosphonium salts.

Grignard reagents prepared from (chloroalkyl)phosphines have been used by Grim *et al* to synthesize chelate phosphine ligands.[82b] Hydrozirconation and subsequent phosphination provides an alternative way of making the required precursor, (3-choropropyl)diphenylphosphine (IV). Related use of the other (bromoalkyl)phosphines and (bromoalkyl)phosphine oxides described above can be envisaged.

2.D. Synthesis of (Diphenyphosphinoalkyl)trialkoxylsilanes

The concept of immobilizing metal complexes on the surface of solid supports has been widely used in heterogeneous catalysis, materials science and pharmaceutical applications.[83] The (diphenyphosphinoalkyl)trialkoxylsilanes $Si(OR)_3(CH_2)_nPPh_2$ (R = Me or Et; n = 2 or 3) connect a phosphine group that can complex to metal centers with an alkoxylsilane unit that can attach to a silica surface via formation of Si-O-Si bonds.[84] This type of compound can be synthesized via nucleophilic attack of $LiPPh_2$ on bifunctional silanes,[85a, 85b] $Si(OR)_3(CH_2)_nCl$, or via photoaddition of $PHPh_2$ across vinyl or allyl silanes, $Si(OR)_3(CH_2)_nCH{=}CH_2$.[85c] Hydrozirconation-phosphination synthetic methodology related to that described in Sections 2.A.-C. has been found to offer a high yield route to one such linking reagent, $Si(OEt)_3(CH_2)_3PPh_2$ (V).

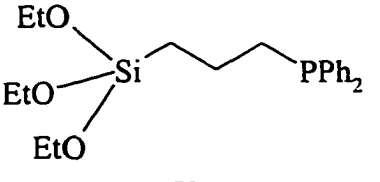

V

Following the procedure shown in Scheme 2-5, compound V was isolated as a colorless liquid in over 80% yield (Equation 2-7; see Table 2-8 for NMR data). This product appeared to be contaminated with small amount of $PPh_2(OEt)$ [$\delta(^{31}P) = 110$], formed by slow attack of PPh_2Cl at Si-OEt bond during phosphination stage. This side reaction was observed to be more significant during phosphination of the zirconium intermediate in the preparation of an analogue, $Si(OEt)_3(CH_2)_2PPh_2$, formed from the vinylsilane $Si(OR)_3CH{=}CH_2$; a mixture of products was formed in which the target compound was observed in only 60% yield.

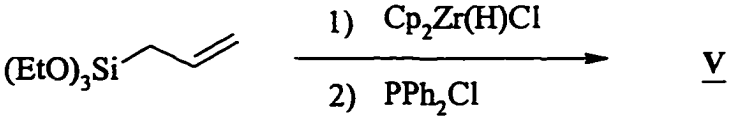

(2-7)

Table 2-8. NMR data[a] for V

	^{31}P	^{29}Si	^{1}H			^{13}C		
Compd	$\delta(PR_2)$	$\delta[SiOR]$	$\delta(PCH_2)$	$\delta(PCCH_2)$	$\delta(SiCH_2)$	$\delta(PCH)$	$\delta(PCCH_2)$	$\delta(SiCH)$
V[b]	-16.9	-46.2	2.12	1.81	0.89	31.98	20.17	12.79

[a] C_6D_6 was used as solvent;

[b] $^1J_{PC} = 12.4$ Hz, $^2J_{PC} = 18.0$ Hz, $^3J_{PC} = 12.4$ Hz; NMR data for ethoxyl group: ^1H, $\delta(OCH_2) = 3.74$ (q), $\delta(CH_3) = 1.12$ (t); ^{13}C: $\delta(OCH_2) = 58.43$, $\delta(CH_3) = 18.54$

Chapter 3

SYNTHESIS OF POLYSILAORGANOPHOSPHINES VIA LITHIATION AND COORDINATION CHEMISTRY TO FORM PLATINUM COMPLEXES

3.A. Synthesis of Poly(silylorgano)phosphines via Lithiation

Because they bind strongly to late transition metals, phosphines have been used not only as mono- and poly-dentate ligands but also to stabilize coordination by other atoms in chelate complexes. Heteroatom chelates containing one phosphorus and other main group donor centers such as N,[86] P,[87] O [88] and S [90] have been reported (Figure 3-1) and the coordination chemistry of these heteropolydentate ligands has already attracted much attention. As discussed in the previous chapter (Section 2.B.), new poly(silylpropyl)phosphines $PhP[(CH_2)_3SiMe_2H]_2$ (12) and $P[(CH_2)_3SiMe_2H]_3$ (13) can be prepared via hydrozirconation and subsequent phosphination (Scheme 2-7). Like simple phosphinoalkylsilanes (Chapters 1 and 2), these systems are also potential ligand precursors. Since both are rather air-sensitive and were isolated in only low yields (30% and 20% respectively), access to analogues having the same type of functionality has been explored. This has led to synthesis of analogues of 12 and 13 in which the saturated polymethylene backbones are replaced by benzylic fragments.

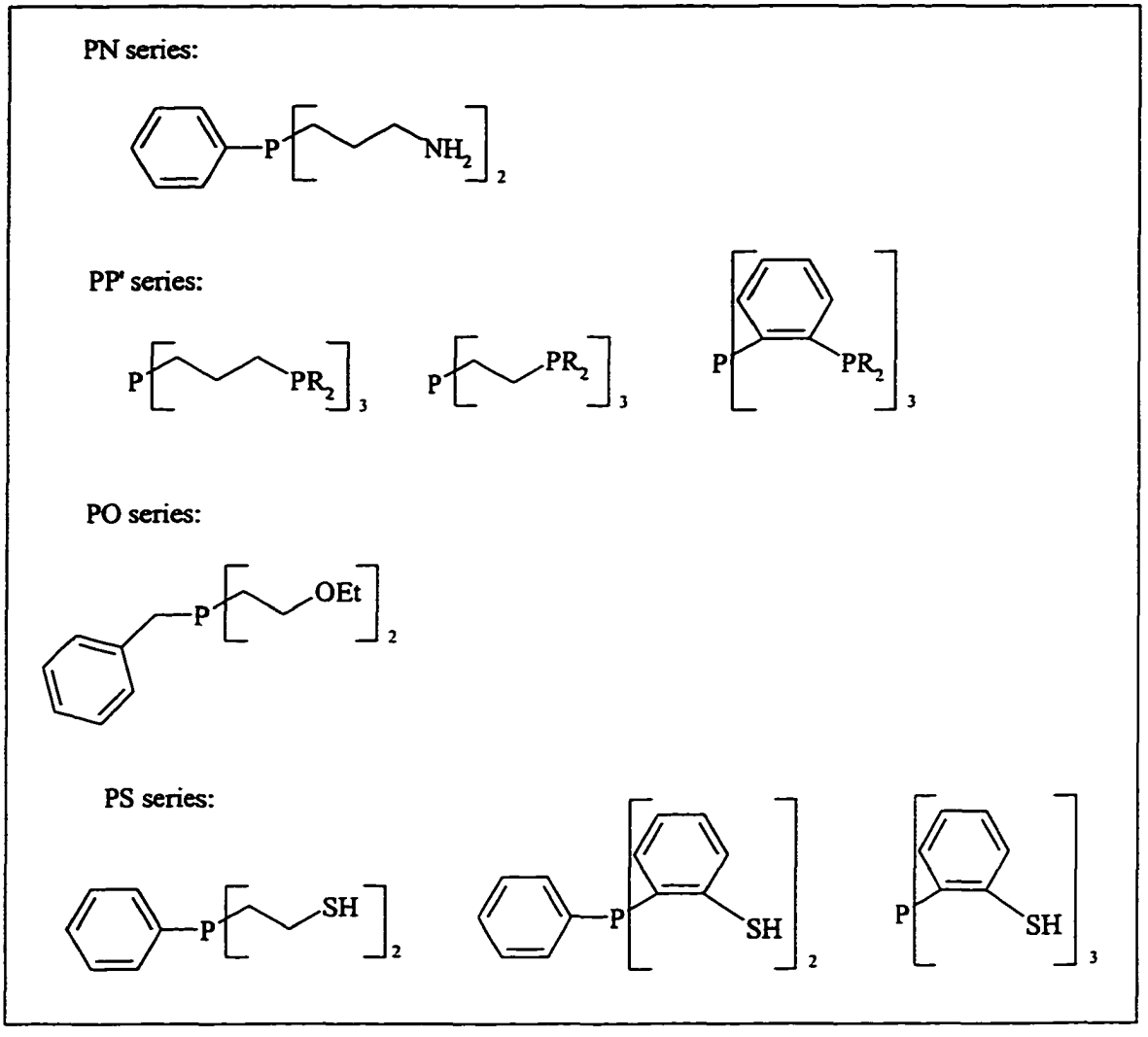

Figure 3-1. Examples of the chelate phosphines containing one P core and two or three N, P, O or S termini

Benzylic anions are more stable than their alkyl analogues because of charge-delocalization into the conjugated benzene ring system. They are readily accessible from the reaction of benzylic halides with alkali metals, which is thermodynamically driven by the formation of ionic halides. Another method commonly used for the formation of benzylic anions is the removal of the acidic hydrogen on the α-(benzylic) position using

strong bases such as n-butyl-lithium. Corresponding potassium salts are even more reactive so that under similar conditions polybenzylic anions can be prepared (eq 3-1).[90]

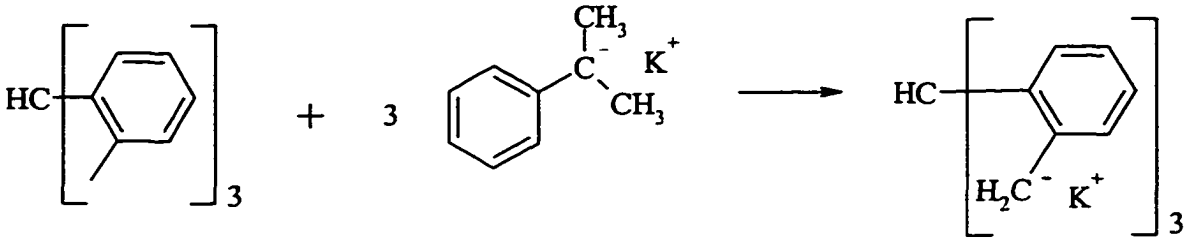

(3-1)

In the formation of benzylic anions via lithiation, one equivalent of tmeda is usually used to stabilize the lithium salts through chelating coordination of tmeda to the lithium centers. Thus the reactivity of n-butyllithium is significantly enhanced in the presence of tmeda. This synthetic methodology has been developed for stereospecific lithiation, achieved by using a chiral chelating amine (eq 3-2).[91]

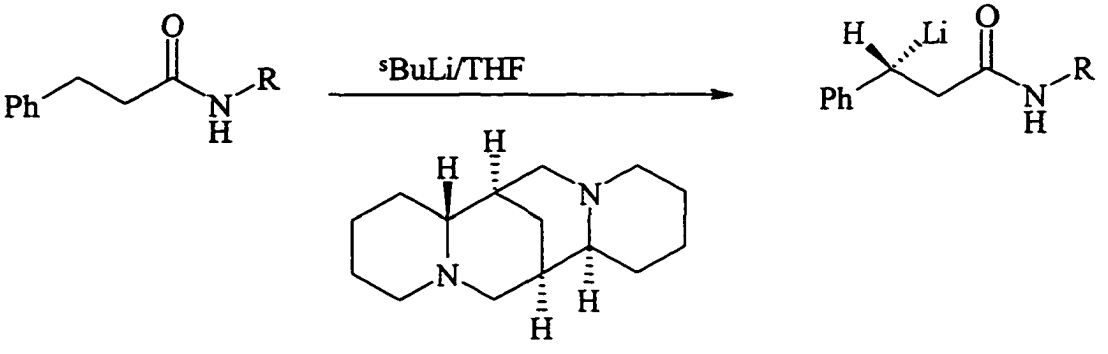

(3-2)

Synthesis of the modified mcCheH, mcbiPSiH and mctriPSiH (see Scheme 1-9) through lithiation of (*o*-tolyl)diphenylphosphine suggested that polylithiation of di(*o*-tolyl)phenylphosphine and tri(*o*-tolyl)phosphine, which are easily prepared from the reaction of (*o*-tolyl)magnesiumbromide with $PPhCl_2$ or PCl_3, might provide a route to analogues of 12 and 13. Lithiation with a slight excess of ^nBuLi in the presence of one equivalent of tmeda slowly led to the formation of red and very moisture sensitive precipitates over 12 h at room temperature. The lithiated intermediates, which may be stabilized both by chelating tmeda and by the lone pair of electrons on a phosphorus atom, were subsequently quenched with excess $SiMe_2HCl$. This led to formation of two new polysilylphosphine analogues related to 12 and 13, bis(*α*-dimethylsilyl-*o*-tolyl)phenylphosphine (21) and tris(*α*-dimethylsilyl-*o*-tolyl)phosphine(22), which were isolated pure and in quantitative yield (Scheme 3-1).

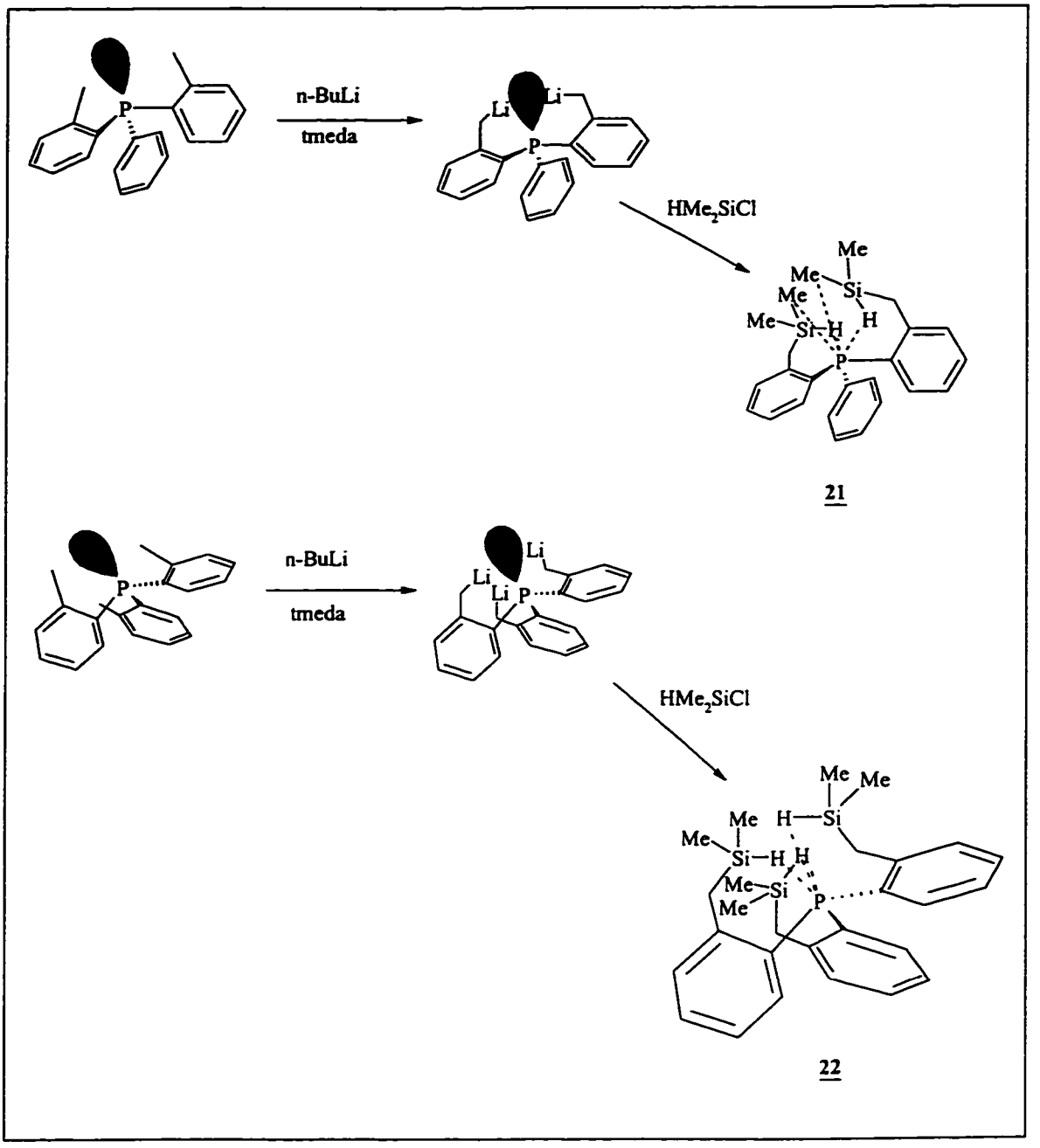

Scheme 3-1. Synthesis of compounds 21 and 22

The bis-silylated phosphine, 21 is a yellow viscous liquid, while the tris analogue, 22, is a white sticky solid. Both are much less sensitive in air than unmodified 12 and 13, and have been fully characterized by NMR (see Table 3-1 for ^{1}H, ^{31}P and ^{29}Si NMR data;

Table 3-2 for ^{13}C NMR data), mass spectrometry, IR and elemental analysis. Using CH_4 chemical ionization, parent ions were prominent along with fragments due to loss of one or two $-C_6H_4CH_2SiMe_2H$ in both cases. Compounds 21 and 22 show strong IR absorption due to SiH stretching frequencies at 2120 and 2125 cm^{-1} respectively. The ^1H and ^{13}C NMR spectra are illustrated in Figures 3-2, 3-3, 3-4 and 3-5.

Table 3-1. ^1H, ^{31}P and ^{29}Si NMR Data[a] for Compounds 21 and 22

	^{31}P	^{29}Si	^1H						
Compd	$\delta(PR_2)$	$\delta(SiH)$	$\delta(SiCH_2)$	$^3J(CHSiH)$	$\delta(SiH)$	$J(P\text{-}SiH)$	$\delta(SiCH_3)$	$^3J(CH_3SiH)$	$J(P\text{-}SiCH_3)$
21	-21.0	-11.7	2.47	3.3	4.27	1.9	0.086	3.6	0.4
			2.47				0.077	3.6	0.4
22	-26.7	-11.5	2.42	-	4.28	1.8	0.11	3.6	-

[a] C_6D_6 was used as solvent; ^{31}P chemical shifts vs external 85% H_3PO_4; ^{29}Si chemical shifts *vs* external tetramethylsilane; coupling constants were measured in Hz

Table 3-2. ^{13}C NMR Data[a] for Compounds 21-22

	^{13}C							
Compd	$\delta(SiCH_2)$	$^3J_{PC}$	$\delta(SiCH_2C)$	$^2J_{PC}$	$\delta(SiCH_2C{=}C)$	$^1J_{PC}$	$\delta(SiCH_3)$	$J(P\text{-}SiCH_3)$
21	23.56	20.5	137.28	11.2	145.52	27.1	-3.85	2.2
							-3.94	1.9
22	23.71	19.4	134.03	10.6	145.45	26.1	-3.88	-

[a] C_6D_6 was used as solvent; coupling constants were measured in Hz

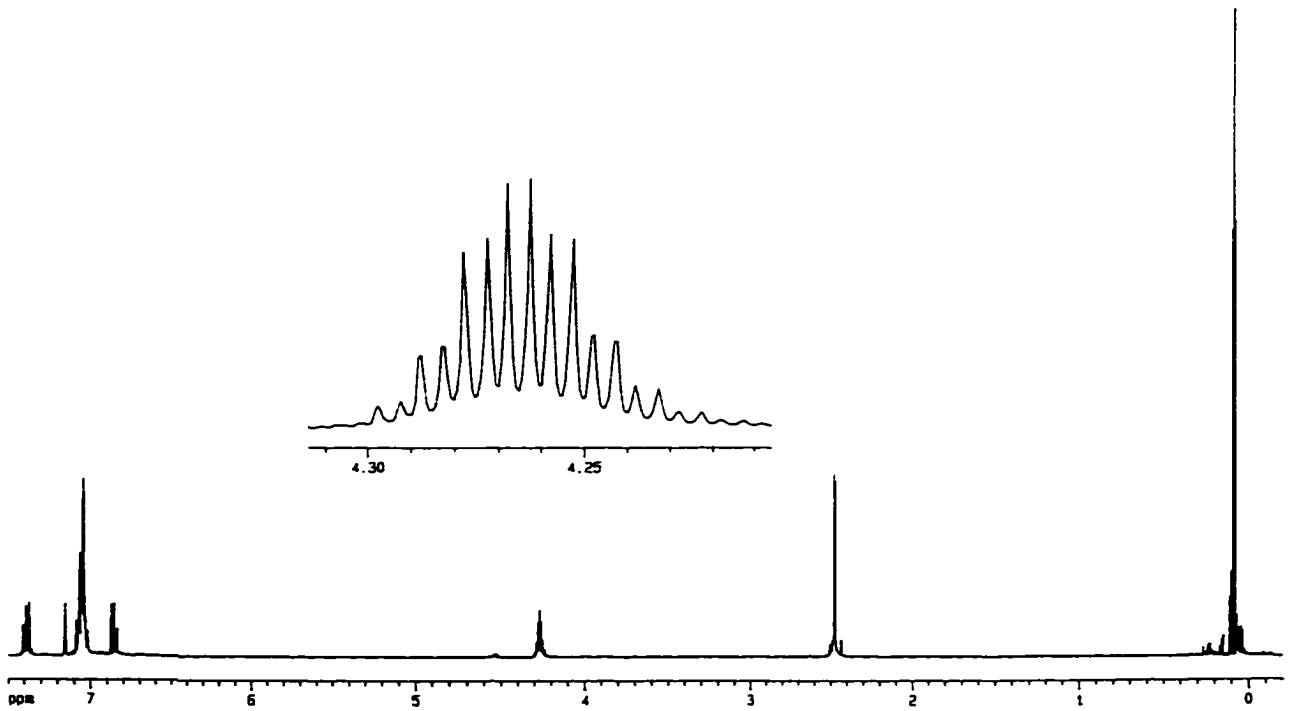

Figure 3-2. ^1H NMR spectrum for compound 21

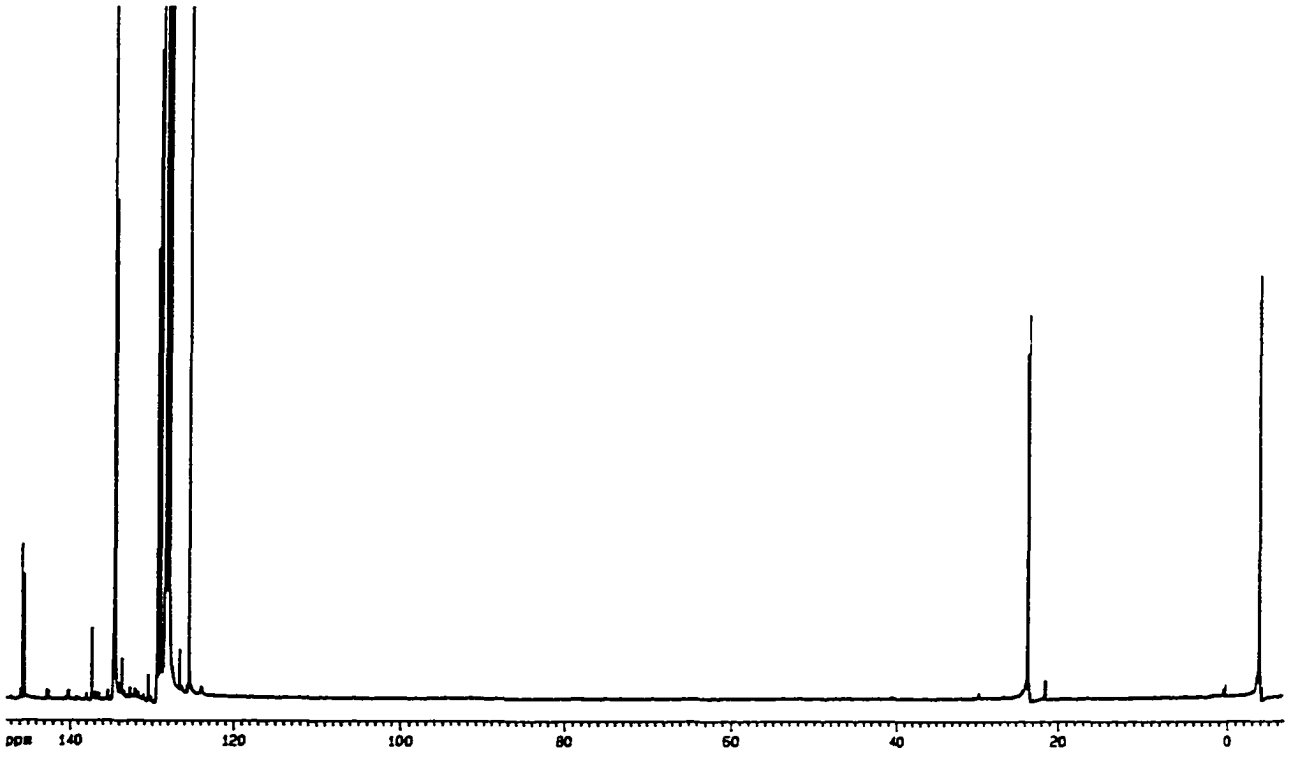

Figure 3-3. ^{13}C NMR spectrum for compound 21

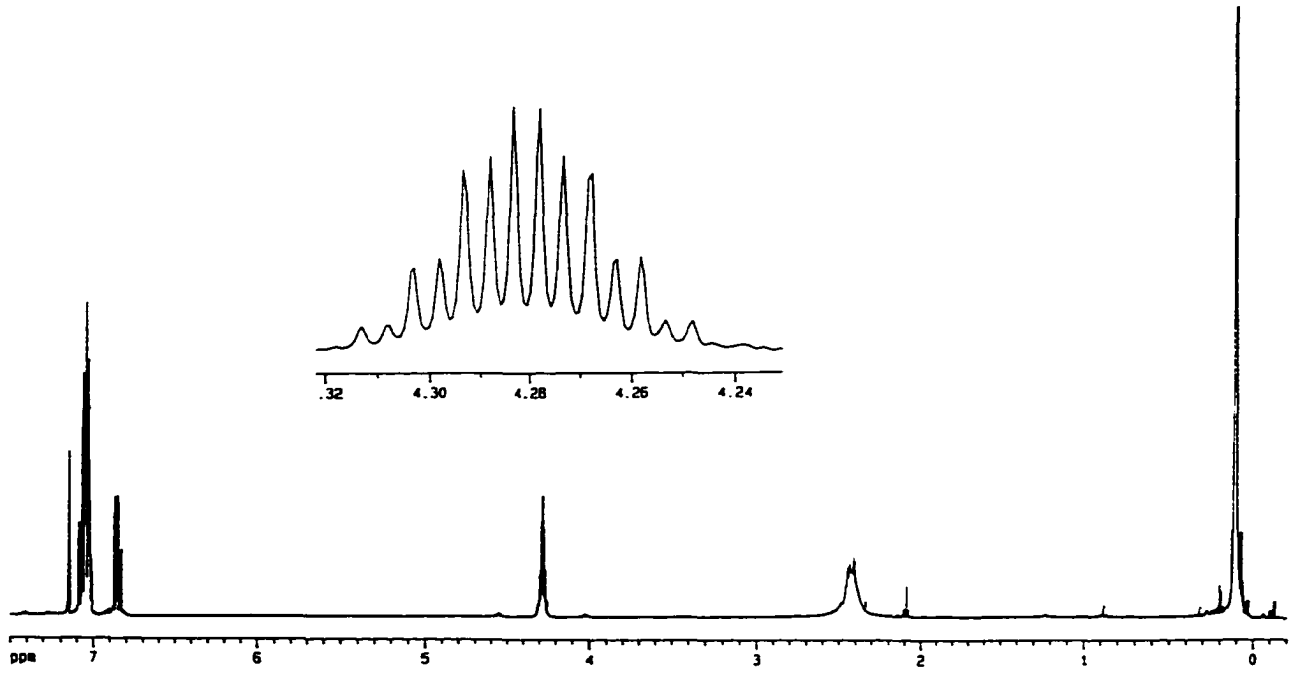

Figure 3-4. ^{1}H NMR spectrum for compound 22

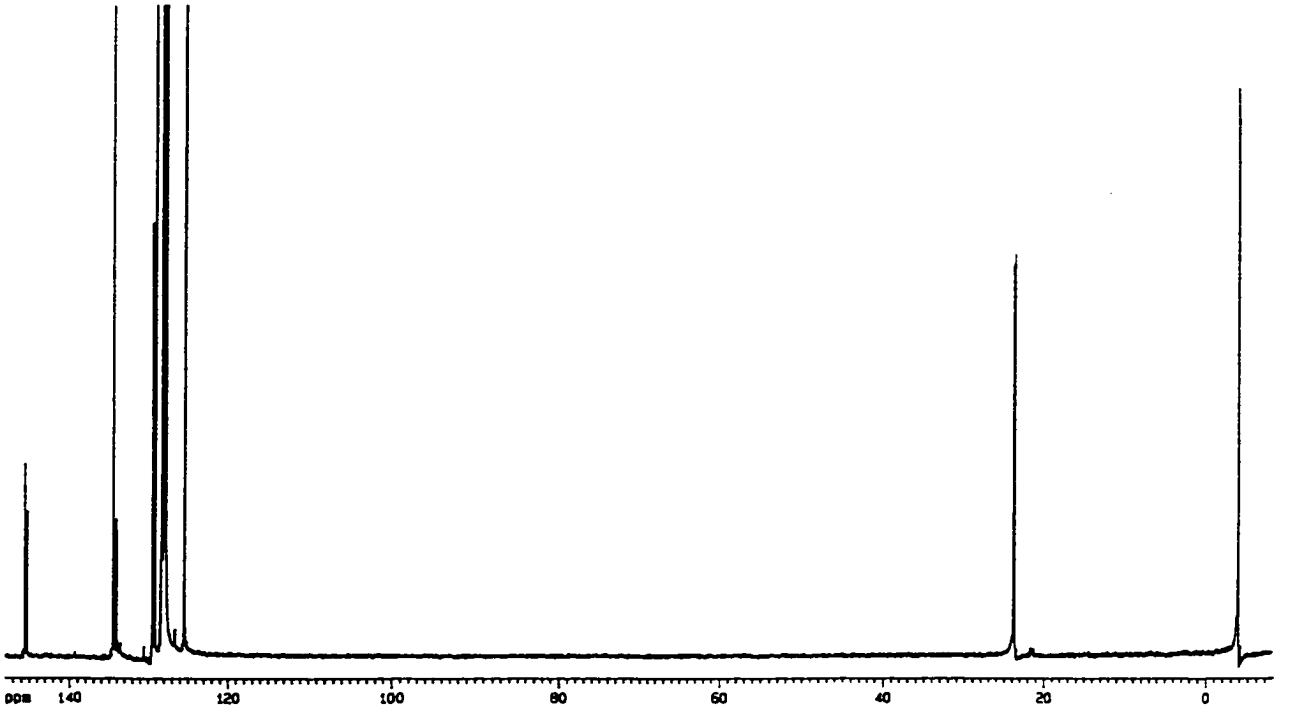

Figure 3-5. ^{13}C NMR spectrum for compound 22

In the ^{1}H NMR spectrum of compound 21, a multiplet near δ 4.3 is assigned to the silyl hydride. This signal shows fine structure that resembles a doublet of nonets; the neighboring six protons in two silyl methyl groups and one methylene group couple almost equally, with $^{3}J_{HH}$ = 3.3-3.6 Hz to afford a nine-line pattern. The small additional coupling (1.9 Hz) splitting each of the nine components must be due to coupling to phosphorus, because on irradiation at the ^{31}P resonant frequency it collapses the envelope to a simple nonet. A doublet at δ 2.4 is assigned to the benzylic CH_2 protons. These two methylene protons are magnetically inequivalent due to the low symmetry of the

molecule (C_S:Figure 3-6; compare 2.C. for the symmetry of compound **12**). The coupling constant between these two geminal hydrogen atoms is unknown. The low symmetry of the molecule is further confirmed by distinguishable Si-*Me* signals, as was also observed for the analogue **12**. The ^{13}C NMR spectrum also reflects such symmetry: two doublets around δ -4 with P-C coupling constants 2.2 and 1.9 Hz respectively are assigned to silicon methyl groups. A doublet at δ 23.6 is assigned to benzylic CH_2 split by $^3J_{PC}$ 20.5 Hz. Two carbon atoms in the skeletal benzene rings, which together with a methylene unit form the C_3 backbone are distinguishable from the other phenyl *C*H groups both by the coupling with phosphine ($^2J_{PC}$ 11.2 Hz and $^3J_{PC}$ 27.1 Hz) and by their relatively weaker intensities due to the lack of nOe enhancement (The latter expression is used for the NMR signal intensity enhancement of a nucleus when its relaxation time is shortened by interaction with other adjacent spin active nuclei such as protons).

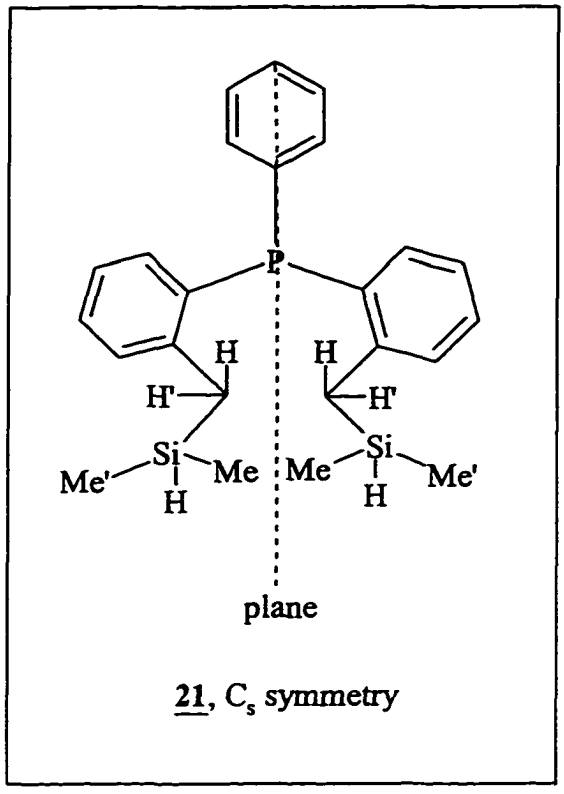

Figure 3-6. Description of C_s symmetry of compound 21

Coupling to ^{31}P is not observed for the benzylic hydrogens or for the ^{29}Si NMR signals, so small coupling to P observed in Si*H* or Si*Me* are attributed to 'through space' spin interaction (rather than $^5J_{PH}$, $^6J_{PH}$ or $^5J_{PC}$). This effect may result from interaction between the bulky substituted *o*-tolyl groups, with distortion of the molecular configuration leading to an unusually short distance between phosphorus atom and the substituents on silicon. The tri-substituted phosphine 22 shows similar coupling, although only in the Si*H* signal, which also appears as a doublet of nonets at ambient temperature.

Related electronic interaction that gives rise to 'through-space' coupling has been found in some unsaturated organic molecules and heterocycles with certain topologies.[92] The stereochemical relationship between phosphorus atoms and silyl groups in

compounds **21** and **22** make it possible that the electrons in the orbitals of SiH and SiMe groups interact with the lone pairs of phosphorus atoms to some extent. Significant bonding interaction involving 3d orbitals of phosphorus and C-H bonds of silicon methyl groups or Si-H bonds (*i.e.* bonding similar to the agostic interaction that occurs in certain transition metal complexes) can be ruled out since both $^1J_{CH}$ 119.6 Hz for silicon methyl groups and $^1J_{SiH}$ 188.2 Hz for compound **21** are in the normal range. The $^1J_{CH}$ in alkanes and $^1J_{SiH}$ in hydridosilanes are typically around 110-130 Hz and 200 Hz respectively, with a noticeable reduction of these parameters accompanying agostic-type interaction, e.g., $^1J_{SiH}$ in complexes containing Si-H-M two-electron three-center bonds is in the range 40-70 Hz; $^1J_{SiH}$ in complexes containing agostic Si-H-M interaction is approximately 100-140 Hz.[93]

The fact that no coupling between phosphorus and silicon atoms was detected also rules out the possibility of coordination of P to Si in compound **21** and **22**, though both of them are likely to have short distances between phosphino- and silyl groups and have rigid structures. There is a number of examples of silylamine derivatives[94] in which the Si atom is believed to use its empty 3d orbitals to accommodate lone pairs on nitrogen to achieve a coordination number of five[95] or six[96] ('hypervalent' systems: e.g. structure 3-A).

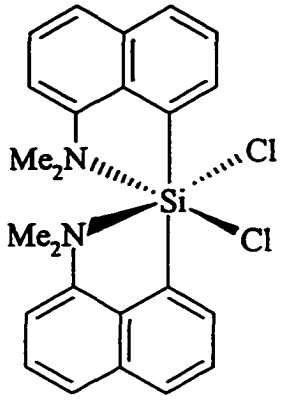

(3-A)

The idealized structure of compound **22** has C_{3v} symmetry, like its analogue **13** (see 2.C.), but a broad benzylic C*H*$_2$ resonance observed in the room temperature ^{1}H NMR spectrum implies deviation from this symmetry. When examined using variable temperature ^{1}H NMR, this compound shows interesting dynamic behavior (Figure 3-7). At elevated temperature, the broad signal sharpens at 40°C and shows a doublet structure [at 60°C ^3J(C*H*Si*H*) = 3.3 Hz] at 60°C or higher temperatures. At the same time, there is no change in coupling patterns for Si*H* and Si*Me* signals. As the temperature is lowered, the broad C*H*$_2$ signal gradually resolves into two well separated pairs of doublets consistent with an ABX coupling pattern (X = P): at -60°C ^3J(C*H*Si*H*) = 2.9 Hz, ^2J(*HCH*) = 13.6 Hz. The coalescence point T_c for these changes was *ca.* 300 K. Simultaneously the doublet assigned to silicon methyl protons first merges into a broad peak and then resolves into two independent doublets [at -60°C ^3J(C*H*Si*H*) = 3.5 Hz]. The coalescence temperature T_c for this process was *ca.* 255 K. With decreasing temperature, the well-resolved Si*H* signal gradually transforms into a broad unresolved peak. The ^{31}P and ^{13}C NMR spectra run at -60°C show only one ^{31}P signal, one methylene carbon signal

(doublet, $^3J_{PC}$ = 17.7 Hz) and two silicon methyl signals (one a doublet, J_{PC} = 1.8 Hz; and the other a singlet).

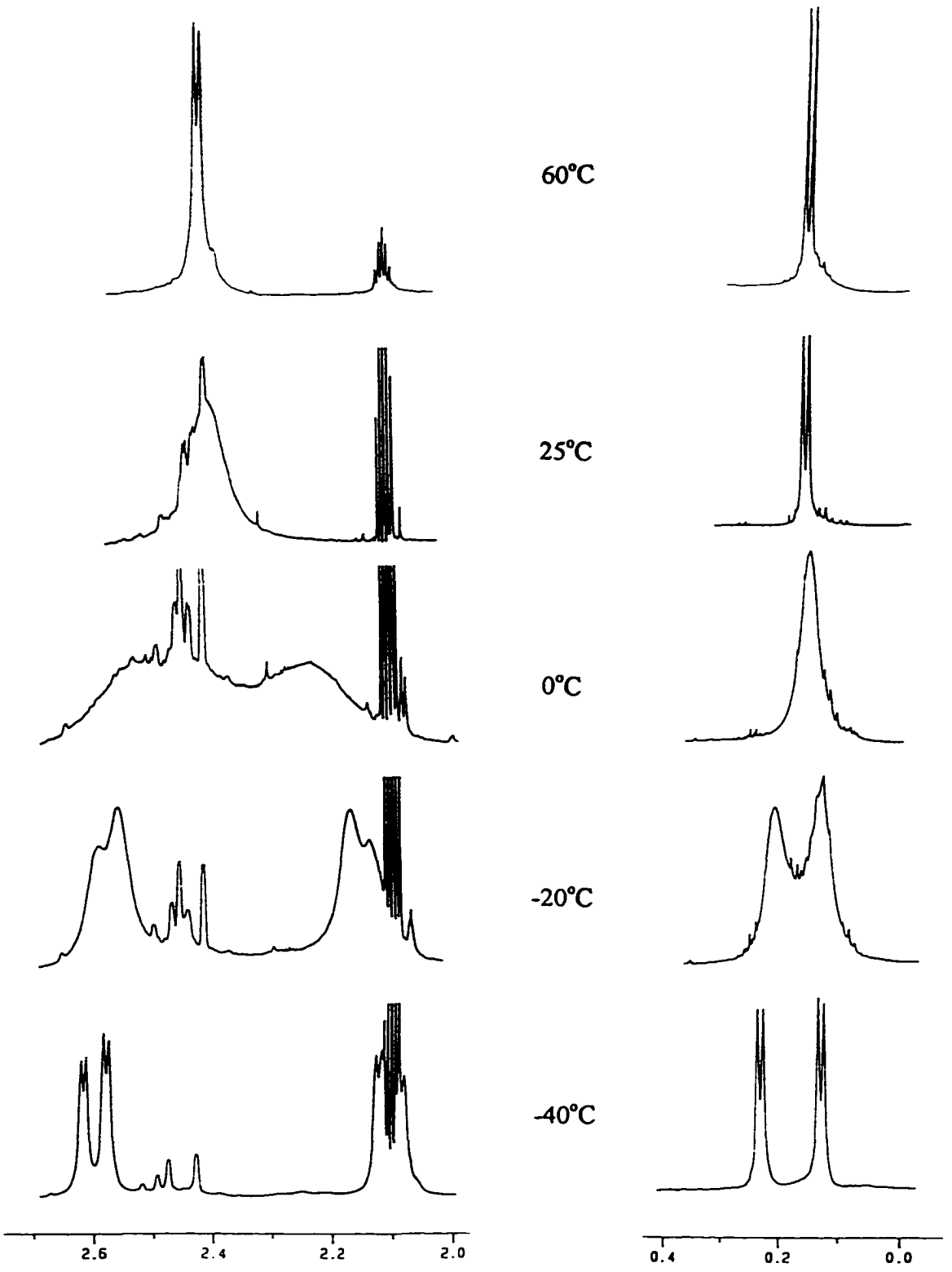

Figure 3-7. ^{1}H VT NMR spectra of compound 22

These VT NMR experiments further imply a conformationally rigid structure for 22. Tri(*o*-tolyl)phosphine is regarded as a bulky phosphine, with a 'cone angle' of 194°. Its derivative 22 is expected to be much more bulky, so that rotation of the subsituent arms is likely to be restricted. The resulting energy barrier ΔG_c^*, calculated at 54 ± 5 kJmol^{-1} based on the T_c of CH_2 signals, 52 ± 5 kJmol^{-1} based on the T_c of Si*Me* signals, is overcome at elevated temperature restoring C_{3v} molecular symmetry; however rotation about P-C bonds is frozen at low temperature, leading to a rigid distorted configuration. A possible configuration having C_3 symmetry is shown in Figure 3-8, where there are no mirror planes but only a three-fold rotation axis, so that the two protons in a methylene unit are not related by symmetry and will couple to each other, and the two methyl groups on each silicon atom are also diastereotopic. The small coupling (1.8 Hz) observed for one methyl carbon in the ^{13}C NMR spectrum can be assigned to through-space coupling with phosphorus. The similar ΔG_c^* values obtained from the coalescence temperatures of CH_2 and Si*Me* signals strongly suggests that it is rotation about P-C bonds that is restricted, rather than around =C-CH_2, H_2C-Si or Si-CH_3 bonds.

The coalescence temperature is quantitatively related to the free energy by the relationship: $\Delta G_c^* = RT_c \times [22.96 + \ln(T_c/\Delta\nu)]$ ($\Delta\nu$ is the chemical shift difference in Hz; it can be measured in the low temperature limiting spectrum).[97] For the CH_2 unit, ΔG_c^* = 54 kJmol^{-1} is calculated from a T_c of 280 K and $\Delta\nu$ = 238 Hz; for Si*Me*, ΔG_c^* = 52 kJmol^{-1} is obtained from T_c = 255 K and $\Delta\nu$ = 47 Hz.

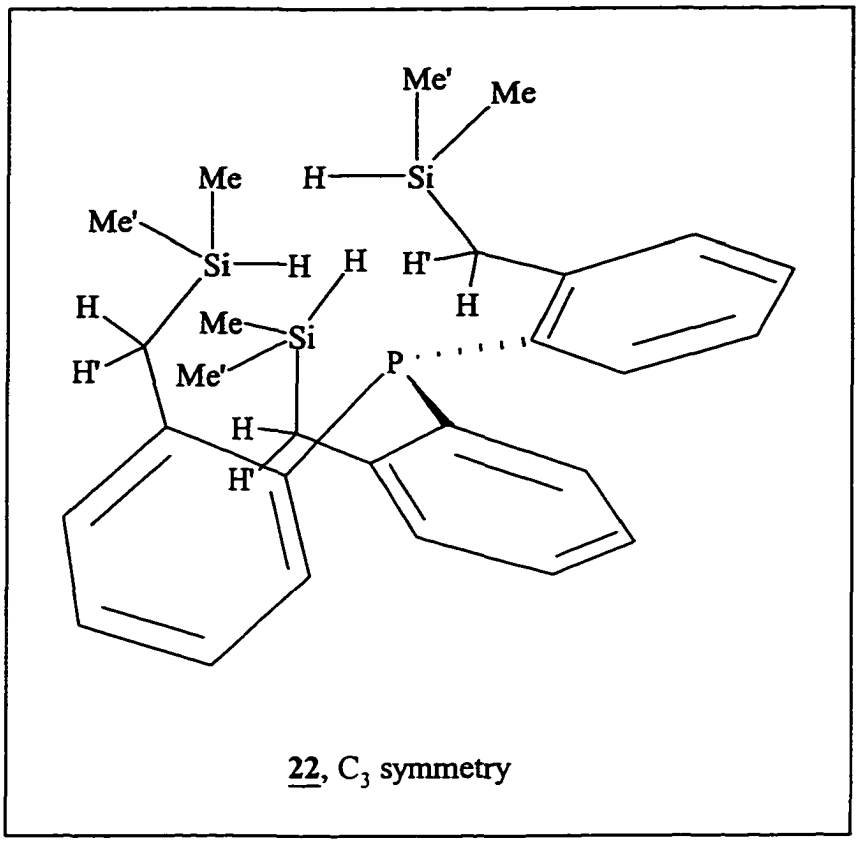

22, C_3 symmetry

Figure 3-8. The possible *C3* symmetry for compound 22 at low temperature

The bis(organosilyl)phosphine also shows temperature dependent NMR behavior (Figure 3-9). At ambient, the two protons of the methylene CH_2 unit appear as a doublet (AA'X coupling pattern), but at 60°C, there is a chemical shift difference that leads to an ABX coupling pattern. At 100°C, the two inequivalent protons are well separated by $\Delta\delta$ 0.05 and couple to each other with $^2J_{HH}$ 14.1 Hz; through-space coupling between phosphorus and Si*Me* disappears, while the Si*H* multiplet is unchanged from room temperature. The disappearance of through-space coupling at elevated temperature is consistent with an increase in molecular mobility. The AA'X or ABX patterns correspond with C_s molecular symmetry. The pattern for the methylene unit also changes to ABX on

reducing the temperature, with the doublet resolving into two overlapped 'doublets of doublets' at 0°C then into two well separated pairs of doublets at -20°C or lower temperatures. At -40°C, the $\Delta\delta$ and $^{2}J_{HH}$ were measured as δ 0.09 and 13.7 Hz respectively and the through-space couplings between phosphorus and Si*H* or Si*Me* were clearly resolvable.

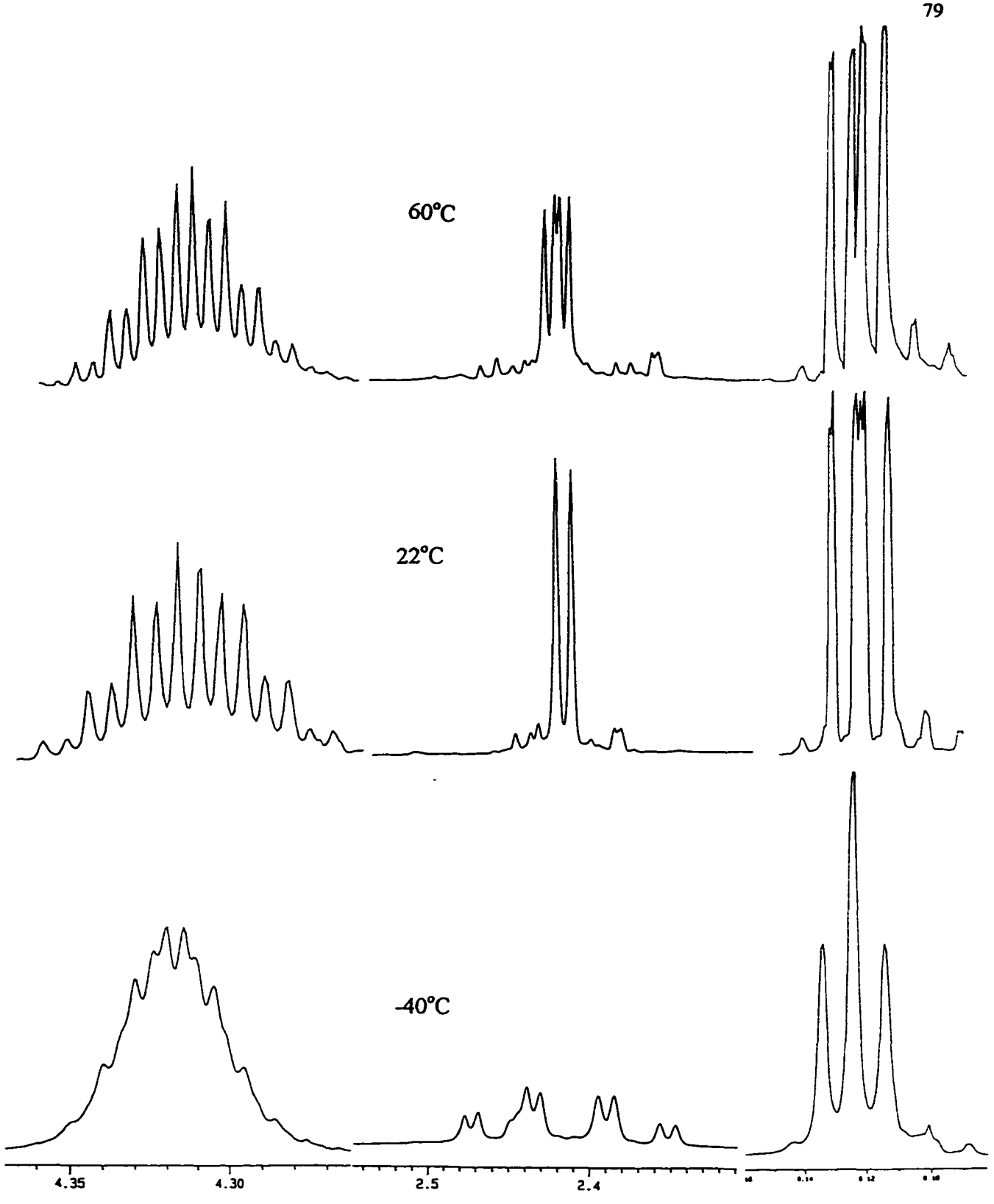

Figure 3-9. ^{1}H VT NMR spectra of compound 21

Compounds 21 and 22 therefore both show VT NMR behavior and through-space coupling which are consistent with rigidity of the backbones that connect Si and P. The polymethylene backbones in the analogues 12 and 13 are expected to be much more flexible, and this difference in rigidity for 12 *vs* 21 leads to different coordination chemistry at square platinum(II), as will be described in the following section.

3.B. Platinum Complexes of Poly(silylorgano)phosphines

Availability of the new family of chelate precursors, poly(silylorgano)phosphines 12, 13, 21 and 22, led to a preliminary investigation of coordination properties at transition metal centers, with the expectation that poly(silyl) metal complexes might be formed via a double oxidative addition which is favored by the chelate effect.

The first bis(silyl) metal complex to be made from PSiH ligand precursors was $Ir(PPh_2CH_2CH_2SiMe_2)_2(H)(CO)$ (Structure 3-B), formed in the reaction[36] of $PPh_2CH_2CH_2SiMe_2H$ with Vaska's complex, *trans*-$Ir(PPh_3)_2(CO)Cl$. It was found here, however, that a similar operation using 12 afforded a mixture in which no single complex was prominent. Reactions of 12 with another Ir(I) precursor, $[Ir(COD)Cl]_2$, and also with the Fe(0) and Ru(0) precursors $Fe(CO)_5$, $Fe(PPh_3)_2(CO)_3$ and $Ru(PPh_3)_2(CO)_3$ also did not show evidence for formation of clean products.

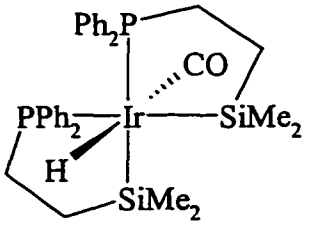

(3-B)

Poly(silyl) Pt(II) or Pt(IV) species have been known for some time (see Chapter 1). They are usually made from double or multiple oxidative addition of Si-H bonds. The characterization of these Pt complexes is facilitated by the informative ^{195}Pt chemical shifts[25a] and $^{1}J_{PtP}$ coupling constants if phosphines are also coordinated. For square planar $Pt(R_3P)_2X_2$-type of complexes (X = halides), $^{1}J_{PtP}$ is typically greater than 3000 Hz in *cis* isomers, but is usually less than 2500 Hz in the corresponding *trans* derivatives. Where strong σ-donors are coordinated *trans* to P, $^{1}J_{PtP}$ becomes even smaller, as illustrated by the examples collected in Table 3-3.

Table 3-3. $^{1}J_{PtP}$ coupling constants for some Pt(II) and Pt(IV) species containing strong σ-donors

Compound	$^{1}J_{PtP}$	atoms *trans* to P
trans-$Pt(H)_2(P^tBu_3)_2$	3003[98]	P
trans-$Pt(H)X(P^tBu_3)_2$	2904-2952[98]	P
(X = Cl, Br, I or CF_3CO_2)		
trans-$Pt(H)(Ph)(PPh_3)_2$	3128[99]	P
trans-$Pt(H)[CH(SO_2CF_3)_2](PPh_3)_2$	3060[100]	P
trans-$Pt(PPh_2CH_2CH_2CH_2SnMe_2)_2$	2664[101]	P
trans-$Pt(H)(SiH_3)(PCy_2)_2$	2615[102]	P
trans-$Pt(H)(GeH_3)(PCy_2)_2$	2638[102]	P
trans-$Pt(TePh)(SiMe_3)(PEt_3)_2$	2837[103]	P
cis-$Pt(H)[CH(SO_2CF_3)_2](PPh_3)_2$	2102, 3615[100]	H or C

cis-$Pt(PPh_2CH_2CH_2SiMe_2)_2$	1608[37]	Si
cis-$Pt(SiMePh_2)_2(PMe_2Ph)_2$	1559[37]	Si
cis-Pt(H)(Ph)(dppe)	1732, 1720[99]	H or C
cis-$Pt(o\text{-}SiH_2C_6H_4SiH_2)(PEt_3)_2$	1776[25a]	Si
cis-$Pt(PPh_2CH_2CH_2CH_2SnMe_2)_2$	2761[101]	Sn
cis-$Pt(H)\{GeH[N(SiMe_3)_2]_2\}(PEt_3)_2$	2129, 2112[104]	H or Ge
cis-$Pt(IV)(o\text{-}SiH_2C_6H_4SiH_2)_2(PEt_3)_2$	1188[25a]	Si
cis-$Pt(IV)(H)(Cl)(PPh_2CH_2CH_2SiMe_2)_2$	1084[37]	Si

The reactions of **12** with different Pt precursors led to different results. No reaction could be detected with $Pt(PPh_3)_2Cl_2$, while with $Pt(COD)Cl_2$ immediate liberation of HCl was accompanied by subsequent formation of white phosphonium salts, which was not avoidable even in the presence of added triethylamine. Formation of phosphonium salts might imply that the silyl groups were coordinated first leaving free phosphine center to be attacked by HCl. By contrast, reaction of **12** with two Pt(0) precursors, $Pt(PPh_3)_3$ and $Pt(PPh_3)_2(\eta\text{-}C_2H_4)$, afforded encouraging results. Fresh $Pt(PPh_3)_3$ [$\delta(^{31}P) = 50.7$, $^1J_{PtP} = 4460$ Hz in C_6D_6] is a bright yellowish solid which slowly decomposes in air[105] while $Pt(PPh_3)_2(\eta\text{-}C_2H_4)$ [$\delta(PtC_2H_4) = 2.64$, $J(PtC_2H_4) = 60.5$ Hz; $\delta(^{31}P) = 34.9$, $^1J_{PtP} = 3740$ Hz in C_6D_6] is a more stable white solid.[106] In solution, both release a ligand PPh_3 from $Pt(PPh_3)_3$; a C_2H_4 from $Pt(PPh_3)_2(\eta\text{-}C_2H_4)$] to form the reactive intermediate $Pt(PPh_3)_2$ [$\delta(^{31}P) = 17.7$, $^1J_{PtP} = 4080$ Hz in C_6D_6].[107] Prolonged storage of such solutions leads to a red color and loss of Pt-P coupling, the sign for decomposition.

Rapid addition of two mol equivalents of 12 in benzene to $Pt(PPh_3)_3$ immediately afforded a yellow solution in which bubbling was observed to occur. After the bubbling stopped, solvent was removed *in vacuo*, leaving a yellow sticky residue which was found to be very soluble in all common solvents and therefore difficult to purify further. The ^1H and ^{31}P NMR data suggested the presence of a *cis*-bis(silyl) Pt(II) complex 24 (Scheme 3-2) which contains two chelated silyl groups, although a number of other unidentified minor products were also clearly present. In the ^1H NMR spectrum, an unresolved multiplet at 4.05 and doublets at 0.03 and 0.08 are observed. These can be assigned to the non-coordinated ('dangling') hydridomethylsilyl groups. The coordinated Si*Me* groups (δ 0.6-0.8 range) are only partly resolved from the polymethylene envelope. In the ^{31}P NMR spectrum, a singlet at δ -1.6 showing ^{195}Pt satellites is assigned to the coordinated phosphines. The small coupling constant $^1J_{PtP}$ = 1355 Hz, which is even less than $^1J_{PtP}$ 1608 Hz[37] for the known analogue *cis*-$Pt(PPh_2CH_2CH_2SiMe_2)_2$, (Structure 3-C), confirms the *cis* configuration. By analogy with a diastereomeric analogue,[38] $Pt(PPh_2CH_2CH_2SiMePh)_2$, complex 24 exists as two diastereomers and shows *ca.* 2:1 distribution of racemic (C_2 symmetry) *vs* meso (C_S) isomers. The latter shows up in the ^{31}P NMR spectrum as a singlet at δ -0.2 with a $^1J_{PtP}$ = 1420 Hz.

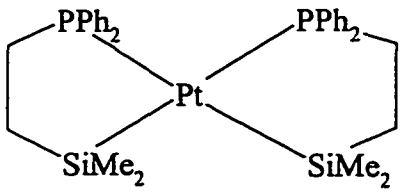

(3-C)

Two mol equivalents of 12 are needed to form product 24 from $Pt(PPh_3)_3$; it was found that addition of only one equivalent of 12 afforded the same compound 24, together with unidentified by-products and about half of the $Pt(PPh_3)_3$ unreacted.

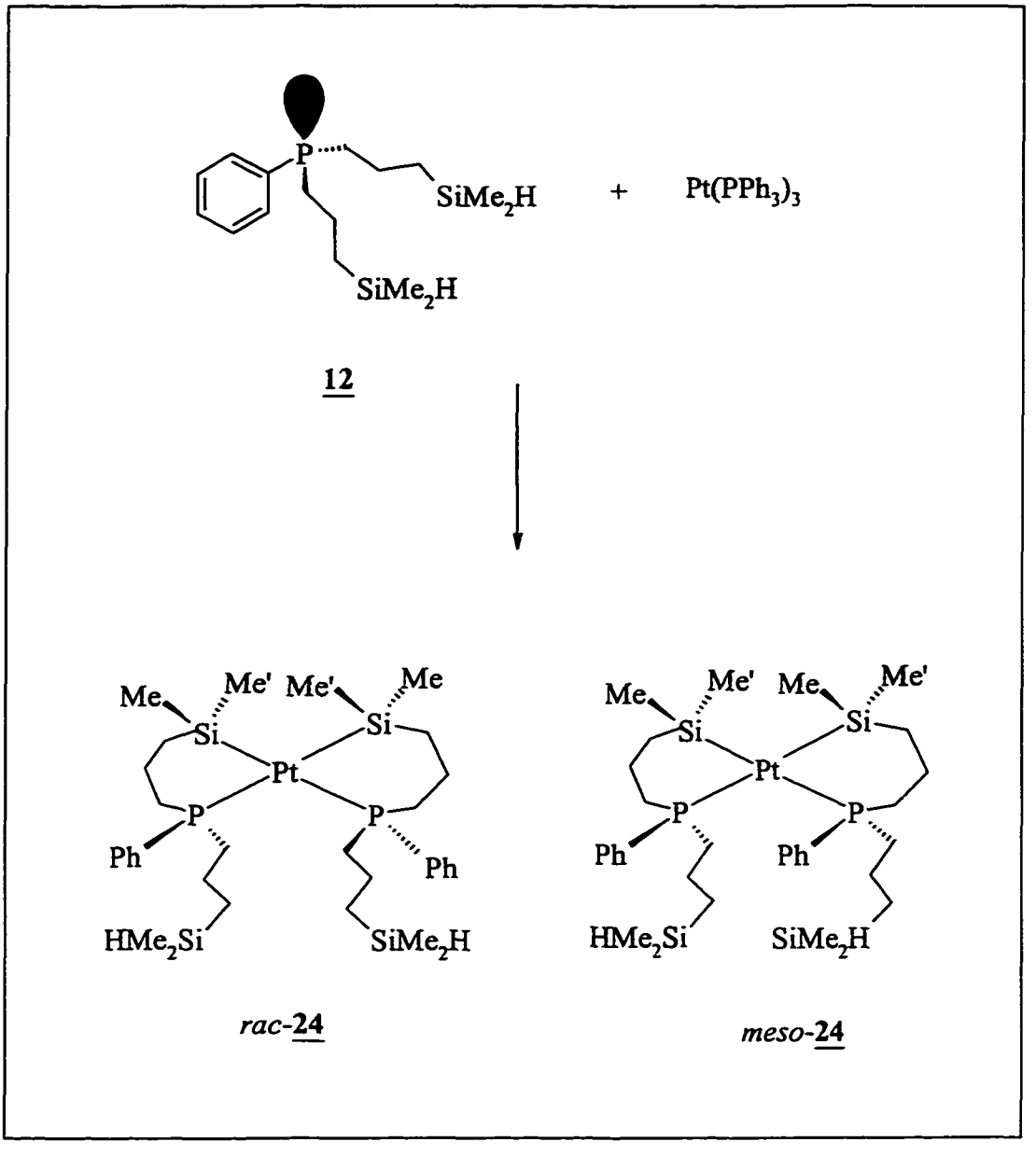

Scheme 3-2. Formation and proposed structure of compound 24

By contrast with the complications encountered in reaction of **12**, addition of one mol equivalent of the more rigid disilaorganophosphine **21** in benzene to $Pt(PPh_3)_3$ led to immediate bubbling of H_2, confirmed by the observation of a weak singlet at δ 4.46 in ^1H NMR spectrum which disappeared on heating the reaction mixture. After heating at 80°C for 20 minutes, a clear yellow solution remained from which a yellow solid **25** (Scheme 3-3) was isolated in quantitative yield. Formation of **25** may involve double oxidative addition of hydridosilane units, to form a six coordinate Pt(IV) intermediate, which then reductively eliminates a H_2 molecule (Scheme 3-3). The Pt(IV) intermediate would be likely to have *cis* dihydrides and *trans* bis(silyl) ligands though it was not observed by NMR spectroscopy in solution under ambient conditions. Compound **25** shows low solubility in hexanes, ether and benzene and medium solubility in dichloromethane. It has been fully characterized by NMR (Table 3-4: ^1H NMR data; Table 3-5: ^{31}P and ^{29}Si NMR data; Table 3-6: ^{13}C NMR data), IR and elemental analysis. The ^1H and ^{31}P NMR spectra are shown in Figures 3-10 and 3-11 respectively.

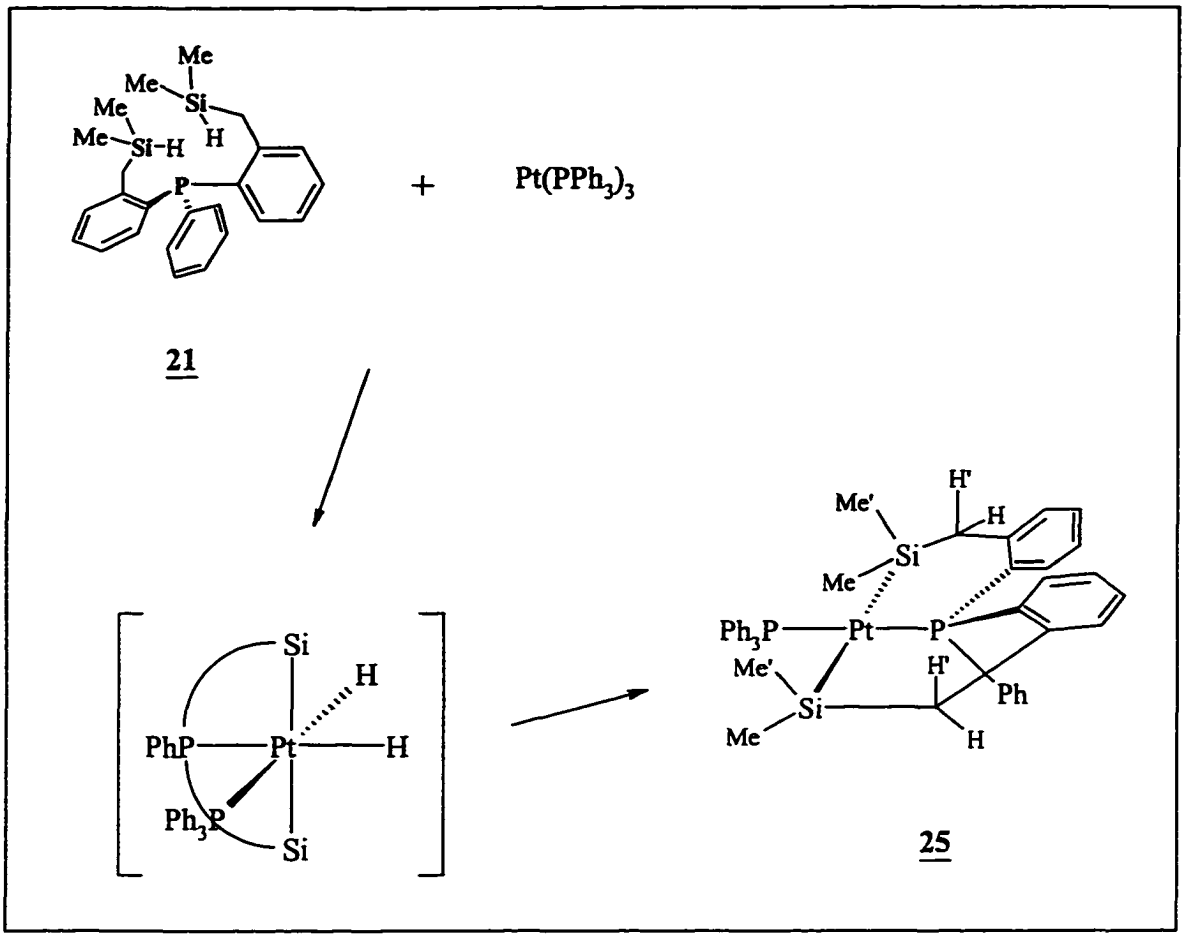

Scheme 3-3. Formation and structure of compound 25

Table 3-4. ^{1}H NMR Data[a] for Compound 25

	^{1}H					
Compd	δ(SiCH_2)	^2J(H*C*H)	^4J(P*C*H_2)	^3J(Pt*C*H_2)	δ(Si*Me*$_2$)	^3J(Pt*Si*Me_2)
	2.31		2.8	29.2	-0.65	10.3
25	2.14	12.4	3.9	20.9	-0.68	9.3

[a] CD_2Cl_2 was used as solvent; coupling constants were measured in Hz

Table 3-5. ^{31}P and ^{29}Si NMR Data[a] for Compounds 25

	^{31}P					^{29}Si		
Compd	$\delta(PtPPh_3)$	$^1J(Pt\text{-}PPh_3)$	$\delta(PtPR_3)$	$^1J(Pt\text{-}PR_3)$	$J_{PP'}$	$\delta(PtSi)$	$^2J_{PSi}$	$^2J_{P'Si}$
25	33.5	3113	10.4	2670	366.4	38.8	16.5	16.6

[a] CD_2Cl_2 was used as solvent; ^{31}P chemical shifts vs external 85% H_3PO_4; ^{29}Si chemical shifts vs external tetramethylsilane; coupling constants were measured in Hz

Table 3-6. ^{13}C NMR Data[a] for Compounds **25**

	^{13}C									
Compd	δ(SiCH$_2$)	$^3J_{PC}$	^2J(*Pt*SiCH$_2$)	δ(SiCH$_2$*C*)	$^2J_{PC}$	δ(SiCH$_2$C=*C*)	$^1J_{PC}$	δ(SiCH$_3$)	*J*(*P*-SiCH$_3$)	^2J(*Pt*SiCH$_3$)
								3.88	0	31.8
25	30.51	16.6	16.0	132.92	6.3	150.14	11.5	3.59	2.7	29.8

[a] CD_2Cl_2 was used as solvent; coupling constants were measured in Hz

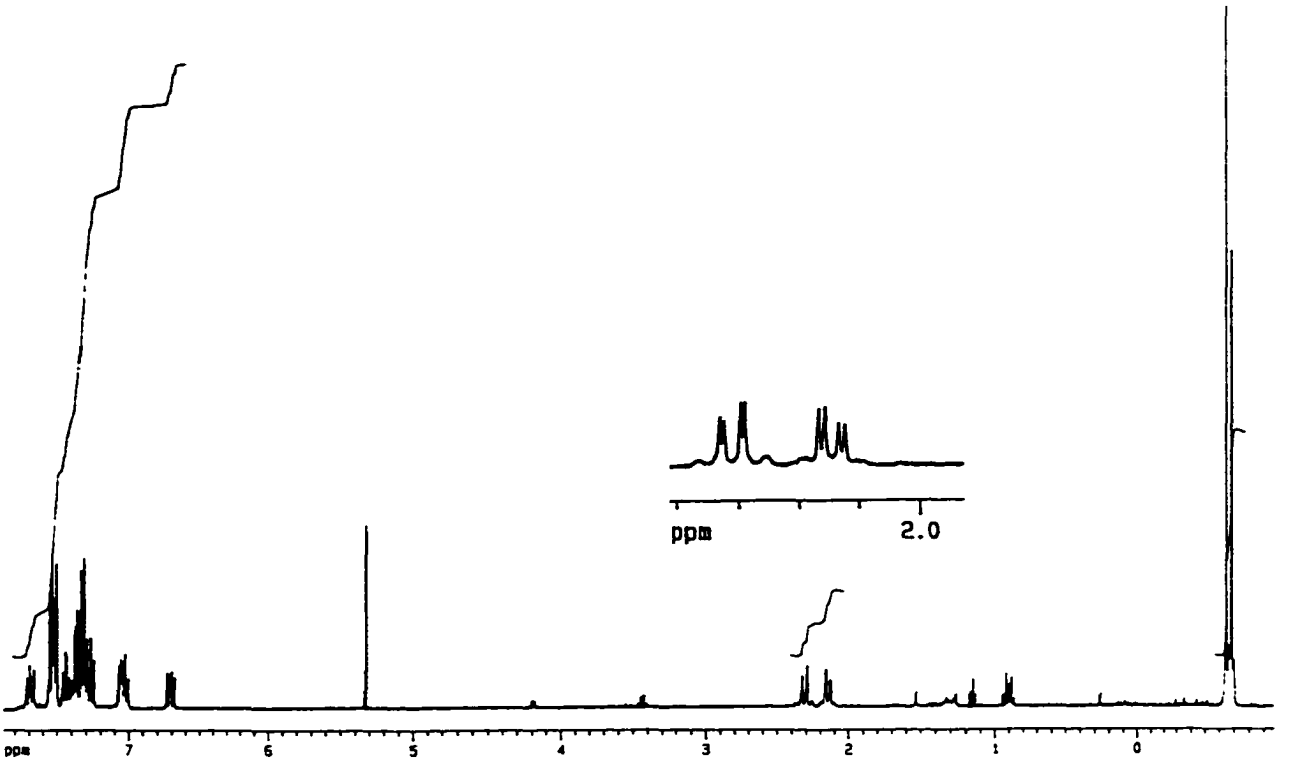

Figure 3-10. ^{1}H NMR spectrum for complex **25**

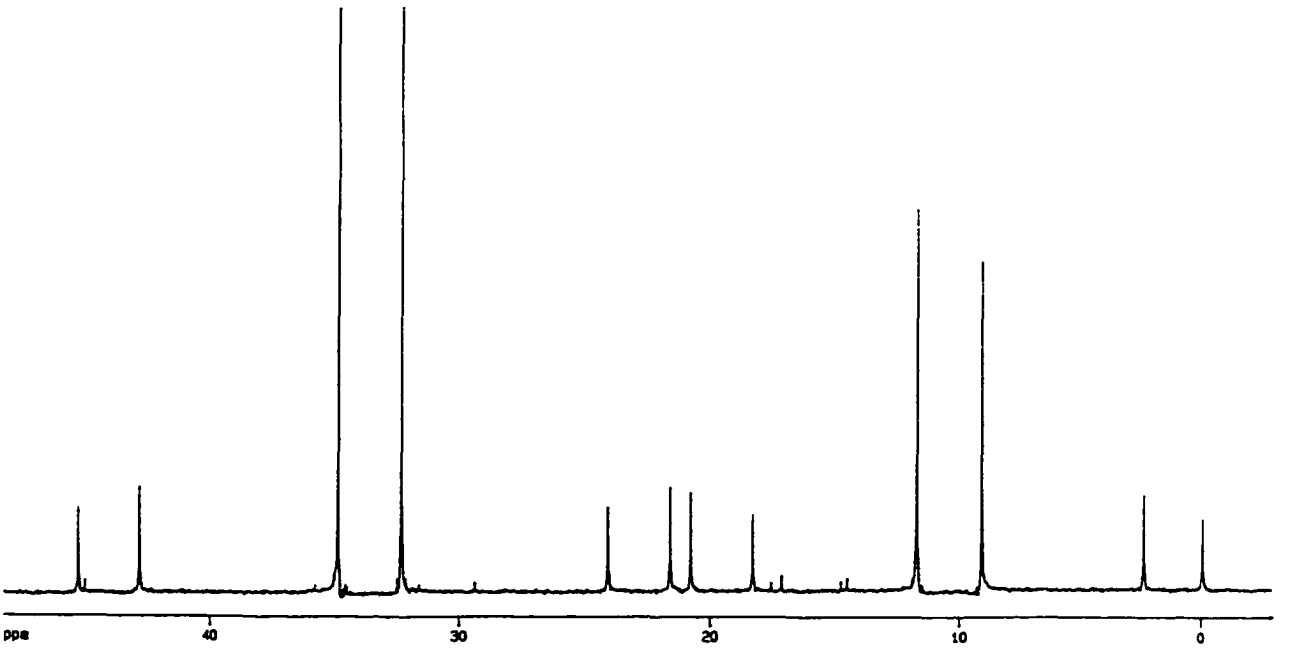

Figure 3-11. ^{31}P NMR spectrum for complex **25**

The bis(silyl) complex 25 is assigned a square planar geometry, like that which most Pt(II) complexes prefer to adopt,[108] and a *trans* stereochemistry. The Si*Me* group and benzylic hydrogen C*H* above the square coordination environment around Pt are chemically inequivalent to those under the latter due to the low symmetry (C_S) of the molecule (see the structure in Scheme 3-3). The geminal CH_2 coupling $^2J_{HH}$ = 12.4 Hz is observed, both components being split by coupling to phosphorus ($^4J_{PH}$ = 2.8, 3.9 Hz) and to platinum ($^3J_{PtH}$ = 29.2, 20.9 Hz). The methyl groups in SiMeMe' fragment are observed as two singlets which are further split by ^{195}Pt ($^3J_{PtH}$ = 10.3, 9.3 Hz). A large *trans* P-P coupling ($^2J_{PP'}$ 366.4 Hz) is found between two inequivalent phosphorus atoms. The corresponding large $^1J_{PtP}$ 3113 and 2670 Hz also confirm the *trans* diphosphine configuration (see Table 3-3).[109] The ^{13}C signal of the benzylic CH_2 group lies at δ 30.51 and is split by one ^{31}P ($^3J_{PC}$ 16.6 Hz) and ^{195}Pt ($^2J_{PtC}$16.0 Hz). The ^{13}C signal of one of the silicon methyl groups (δ 3.59) is split by P into a doublet (2.7 Hz) while the other (δ 3.88) is observed as a singlet; both couple to ^{195}Pt, $^2J_{PtC}$ = 29.8 and 31.8 Hz respectively. The ^{29}Si signal is split by two *cis* phosphorus atoms almost equally ($^2J_{PSi}$ = 16.5, 16.6 Hz) into an overlapping doublet of doublets that resembles a triplet pattern. ^{195}Pt satellites were not observed in the ^{29}Si NMR spectrum.

Similar chemistry using $Pt(PPh_3)_2(\eta\text{-}C_2H_4)$ also gave 25 accompanied by another product that showed resonances due to metal hydrides and ethyl groups in the ^{1}H NMR. For this second species, δ(Pt*H*) = -1.8 with $^1J_{PtH}$ = 1140 Hz, *trans*-$^2J_{PH}$ = 150 Hz, *cis*-$^2J_{PH}$ = 25 Hz, and in the ^{31}P NMR δ(*P*) = 30.6, δ(*P'*) = 20.9; *cis*-$^2J_{PP'}$ = 12 Hz, $^1J_{PtP}$ = 1600 Hz, $^1J_{PtP'}$ = 2390 Hz. The values for J_{PtP} suggests that the complex is a Pt(IV) species. This

reaction which requires further investigation may involve the insertion of ethylene into Pt-H bonds in a Pt(IV) intermediate like that shown in Scheme 3-3.

Reaction of 22 with $Pt(PPh_3)_3$ or $Pt(PPh_3)_2(\eta\text{-}C_2H_4)$ produced a mixture in which a compound having two *trans* phosphines [$\delta(P) = 32.7$, $\delta(P') = 2.1$; *trans*-$^2J_{PP'} = 288.0$ Hz, $^1J_{PtP} = 3192$ Hz, $^1J_{PtP'} = 2510$ Hz] was detected and is assumed to have the similar geometry as 25. Further investigation of this system is in progress.

In square-planar Pt(II) chemistry, a ligand of strong *trans* effect typically avoids a site *trans* to a similar ligand, as discussed in Chapter 1. Such a rule has been proven by many examples.[30a, 37] *Trans* configurations are sometimes formed, however, if other bulky ligands are coordinated and/or strong electron-withdrawing groups are involved to distribute electron density on the metal center. *Trans*-$PtH(R)(PR'_3)_2$ can be isolated readily if R is a substituted phenyl group (R' = Ph)[99] such as *p*-C_6H_4Me, *p*-C_6H_4OMe, *p*-C_6H_4F or *p*-C_6H_4Cl, or if R is methyl and R' is a bulky group such as Cy or ^{i}Pr,[110] or if the σ-donating ability of R is reduced through bonding to electron-withdrawing groups such as R = $-CH(SO_2CF_3)_2$ (R' = Ph).[100] The *trans* dihydrido Pt(II) complexes *trans*-$Pt(H)_2(PR_3)_2$ can be stabilized by coordination of bulky phosphines such as R = Cy, ^{i}Pr or ^{t}Bu.[98, 111] Stannyl groups, also strong *trans* influencing ligands, can form both *cis*- and *trans*-Pt(II) isomers under similar conditions.[101, 112] Square planar Pt(II) complexes containing *trans* hydride and germyl groups or hydride and silyl groups have been isolated (see Table 3-3). Kampf has recently claimed the isolation of the Pt(II) species containing two *trans* germyl groups, though some experimental data including $^1J_{PtP}$ coupling constants have not yet been reported.[113] The silyl group is considered to be a more strongly *trans* influencing ligand than alkyl, hydride or stannyl groups. So far, *trans*

bis(silyl) Pt(II) species have not been reported so compound **25** is the first example of this kind. The successful isolation of **25** can be attributed to the low flexibility of ligand precursor **21**, which forms a rigid Si-P-Si cage to enclose the platinum atom. A strong chelate effect appears to overcome the electronically unfavorable *trans* geometry, so that higher reactivity is expected for this *trans* complex than for related *cis* compounds. In fact, even as a solid, **25** decomposes to a mixture of species that could not be identified by NMR over the course of several weeks. This decomposition process is faster in solution (several days).

For higher oxidation state Pt(IV) complexes which have an octahedral geometry, a very small number of examples exist in which strong *trans* influencing ligands such as silyl and hydride are *trans* to each other.[24, 25, 114] Tanaka has recently reported the isolation of a tetra(silyl) Pt(IV) species (structure 3-D) which has an unusually small $^{1}J_{PtP}$ = 1188 Hz, and for this complex, it was suggested that the silyl groups, as strong σ-donors, help to stabilize the high oxidation state. An obvious area for future investigation will be oxidation of the new compound **25** to Pt(IV) analogues of (3-D).

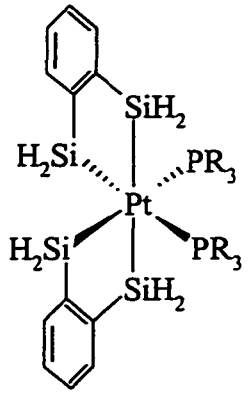

(3-D)

Chapter 4

RUTHENIUM CHEMISTRY OF BIS(DIPHENYLPHOSPHINOPROPYL)SILANE (biPSiH, II)

4.A. Background and Synthesis of Ru(biPSi)(H)(CO)$_2$, 26

Since bis(diphenylphosphinopropyl)silane (biPSiH, II) was prepared in the early 1990s, its coordination chemistry towards platinum group metals has been intensively investigated (see Chapter 1), and the Pt, Rh and Ir complexes that have been isolated from this chemistry have been shown to be active catalysts for the hydroformylation of olefins. Some preliminary work on parallel complexation at Ru started some years ago by Bruce[81] who synthesized complex **26a** by reaction of biPSiH with $Ru_3(CO)_{12}$ under vigorous conditions (140°C, 8 h) but in less than 15% yield. The pale yellow product was isolated as single crystals, however, and the X-ray crystal structure showed that it is the *syn* isomer **26a**.

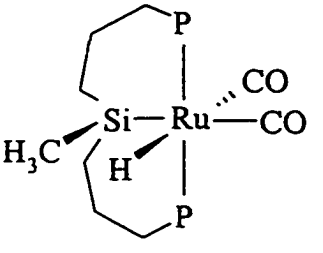

syn **26a**

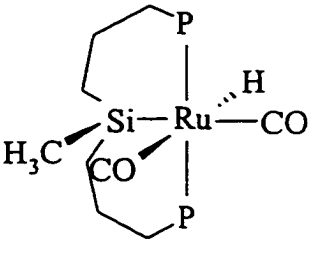

anti **26b**

Much more recently, it was discovered by Zeller that mcbiPSiH (VI) adds smoothly to the mononuclear complex bis(triphenylphosphine)tricarbonylruthenium(0), $Ru(CO)_3(PPh_3)_2$, to give in excellent yield the mcbiPSi analogue of **26** (Section 4.C.). Easy access to biPSiH (II) provided by the chemistry in Chapter 2 allowed the same approach to be used for synthesis of **26** itself.

A quantitative yield is obtained under quite mild conditions, by refluxing reactants biPSiH (II) and $Ru(CO)_3(PPh_3)_2$ together in toluene for 17 h under an inert atmosphere. Prolonged reaction time or higher temperature results in side reactions that have not been investigated in detail (eq 4-1). The ^1H NMR spectrum of the raw product showed two triplets in the high field hydide region, in a ratio of 4.5:1, which can be assigned to the two diastereomers, *syn* **26a** and *anti* **26b**, through comparison with Bruce's data. Washing the raw product with large amounts of ethanol and hexanes left a pale yellow solid which was stable in the solid state in air and was soluble in benzene, THF, toluene or dichloromethane. The ^1H and ^{31}P NMR data demonstrate that the material recovered in this way is almost pure *syn* **26a**, with the ratio of *syn/anti* > 20:1. The diastereomers **26a** and **26b** have now been fully characterized by NMR (Figure 4-1: ^1H NMR spectrum for **26a**; Table 4-1: ^1H, ^{31}P and ^{29}Si NMR data; Table 4-2: ^{13}C NMR data), IR and EA. The triplets assigned to hydrides in the high field of ^1H NMR spectrum have small coupling constants, $^2J_{PH}$, of 19.3 and 22.0 Hz, confirming a *cis* relationship between hydrides and coordinated phosphines. Saturation at the ^{31}P resonant frequencies collapses the hydride triplets into singlets. The ^{13}C NMR spectrum shows *cis* coupling between carbonyls and phosphines ($^2J_{PC}$ = 7-12 Hz), to give two triplets for the two inequivalent carbonyls and virtual coupling between PCH_2 and two *trans* phosphines, to

produce a triplet for PCH_2 groups. No two-bond P-C coupling along the backbones can be observed. The *cis* relationship between coordinated Si nucleus and two phosphines is again confirmed by the small two-bond coupling, $^2J_{PSi}$, of 19.7 Hz for **26a** and 11.2 Hz for **26b**. The IR spectrum shows two strong bands at 1997 and 1960 cm^{-1}, attributed to the stretching absorption of two carbonyl groups, and a weak band at 1889 cm^{-1} due to the metal hydride stretching. The latter assignment has been further confirmed by observation for the deuteride analogues **26a**-*d* and **26b**-*d* of only two strong carbonyl bands in this region (Section 4.B.iv.).

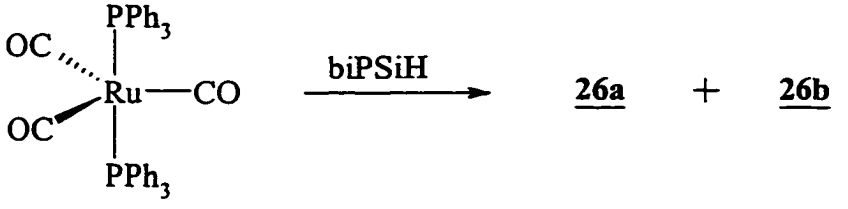

(4-1)

It was found that solution of **26** slowly blackened on exposure to sunlight and that this process was retarded significantly in storage in the dark or under an atmosphere of CO gas; and that pure *syn* **26a** recovered as crystalline material slowly isomerized to the diastereomer *anti* **26b**, reaching equilibrium at a ratio of *ca.* 4.5:1. The equilibrium constant and the diastereoisomerization rate are temperature dependent: higher temperature leads to a smaller *syn*/*anti* ratio and faster isomerization. At ambient temperature (22°C), the equilibrium constant K = 0.22. Detailed kinetic studies on this isomerization and possible mechanisms will be discussed in Section 4.B.v.

A slight excess of biPSiH (1.2 mol equiv), and refluxing in toluene under an inert atmosphere are essential for the reaction to go cleanly to product **26**. Otherwise, a minor second product, which was not isolated, is produced (up to 10% yield) if only one or less than one mol equiv of biPSiH is used, or if the reaction is conducted at a lower temperature. All attempts to separate this complex from **26** by fractional crystallization were not successful. Its conversion to **26** was never observed, even after heating, and interestingly it shows lower reactivity than the latter in substitution reactions where carbonyl groups are replaced with other ligands such as $P(OMe)_3$.

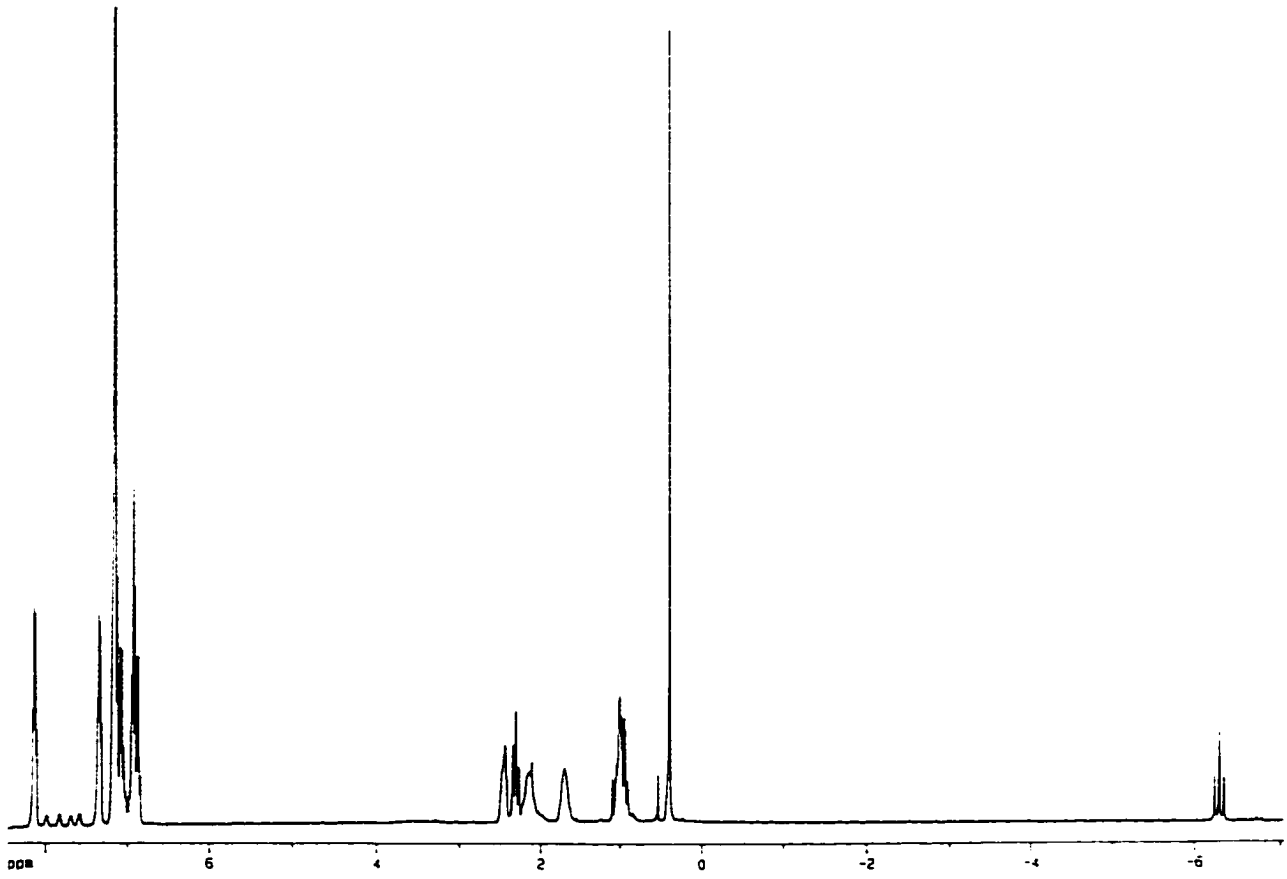

Figure 4-1. ^1H NMR spectrum for *syn* **26a**

Table 4-1. ^{1}H, ^{31}P and ^{29}Si NMR data[a] for compounds **26a** and **26b**

				^{1}H					
Compd	^{31}P	^{29}Si	$^{2}J_{PSi}$	Ru*H*	$^{2}J_{PH}$	RuSi*CH*$_3$	Si*CH*$_2$	SiCH$_2$*CH*$_2$	P*CH*$_2$
							1.00	2.13	2.44
26a	31.4	-2.5(t)	19.7	-6.30(t)	19.3	0.38	1.00	1.69	2.30
	31.3[b]			-6.69(t)[b]		-0.09[b]			
26b	32.9	-1.1(t)	11.2	-6.73(t)	22.0	0.52	-	-	-
	33.0[b]			-7.06(t)[b]		0.08[b]			

[a] C_6D_6 was used as solvent; coupling constants were measured in Hz

[b] THF-d_8 was used as solvent

Table 4-2. ^{13}C NMR data[a] for compounds **26a** and **26b**

	^{13}C						
Compd	RuSi*CH*$_3$	Si*CH*$_2$	SiCH$_2$*CH*$_2$	P*CH*$_2$	^{1}J(*P*-*CH*$_2$)	Ru*CO*	^{2}J(*P*-Ru*CO*)
						205.06(t)	8.7
26a	8.43	20.87	20.87	32.68(t)	16.1	198.23(t)	10.8
	12.62[b]	25.72[b]	25.83(t)[b, c]	37.50(t)[b]	16.3[b]		
						203.92(t)	7.8
26b	7.54	20.50	20.50	32.43(t)	16.8	199.04(t)	11.6

[a] C_6D_6 was used as solvent; coupling constants were measured in Hz

[b] THF-d_8 was used as solvent

[c] $^{2}J_{PC} = 4.0$ Hz

Among modern NMR techniques that have recently been developed a useful routine is the Nuclear Overhauser Enhancement Difference experiment (nOe-diff). This under favorable conditions can allow the proximity of non-coupled magnetic nuclei to be estimated.[115] The magnetic influence that one nucleus has on another occurring "through space" is proportional to the inverse distance between the nuclei (r_o) to the sixth power (i.e. $\propto r_o^{-6}$), and can therefore only be detected at short range (nuclei are separated by less than *ca.* 3 Å); the experiment has been widely used in organic,[116] bioinorganic[117] and organometallic[118, 119] systems to determine the configurations or conformations of molecules. For example, in order to determine rotamer populations of coordinated olefins, Erickson quantitatively applied nOe-diff technique.[120] Scheme 4-1 illustrates one pair of rotamers whose difference was clearly demonstrated by quantitative nOe-diff experimental results. In some cases, the residual intensity in the difference spectrum can result either from close inter-proton distance (nOe) or from chemical exchange ("Spin saturation transfer": SST). Both mechanisms normally give resonances of opposite phases, but they can be distinguished by variable temperature studies. nOe-diff data show little temperature dependence while higher temperature significantly enhances SST results.[121]

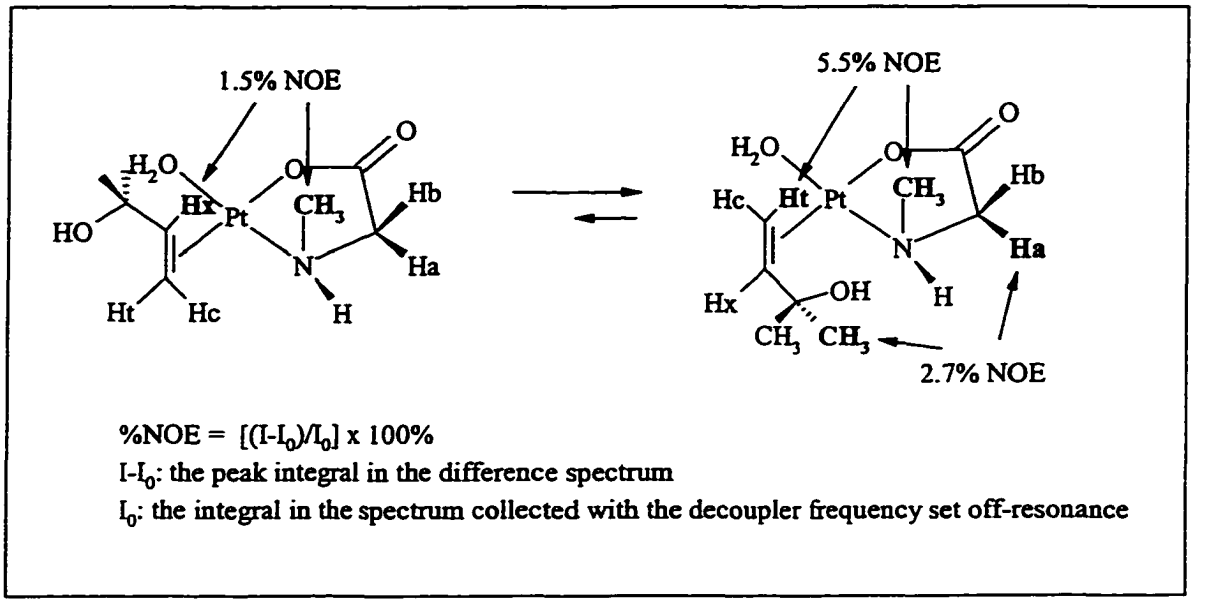

Scheme 4-1. Distinguish rotamers using quantitative nOe-diff technique

In the nOe difference experiment of **26a** and **26b** (Figure 4-2), irradiation into either the SiCH_3 or hydride resonance of **26a** led to observable enhancement of the other's intensity, since they are on the same molecular face (*syn*); while similar irradiation of resonances in **26b** led to no similar enhancement. In both isomers, irradiation of the hydride signals also caused strong nOe effects in the *otho* hydrogen signals on the phenyl groups. Thus, the *syn* configuration observed in solid **26a** X-ray crystallography was also demonstrated in solution, using nOe-diff results. The use of this technique to determine the solution structures of some other biPSi complexes of Ru(II) will be discussed in the following sections.

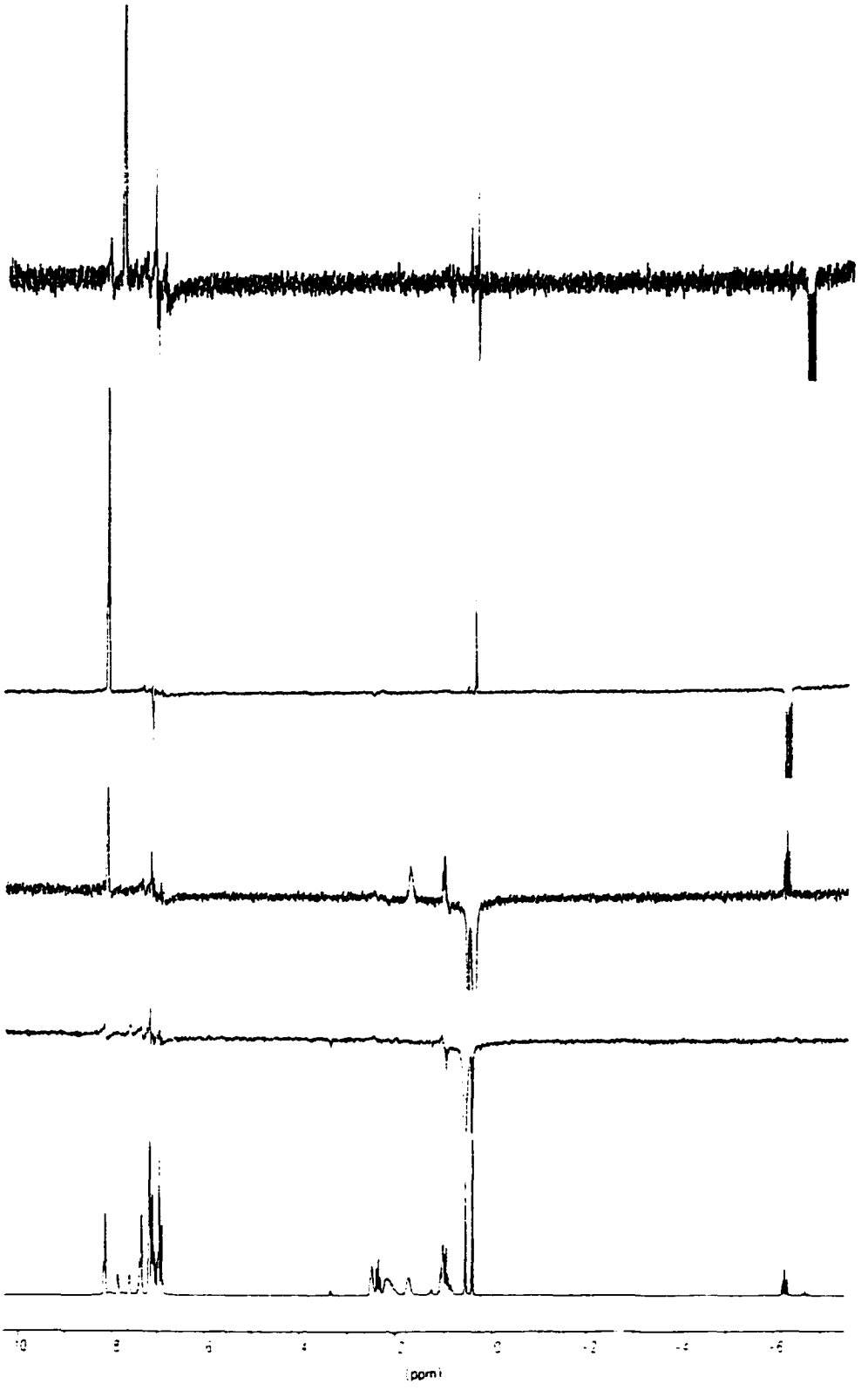

Figure 4-2. nOe-diff experiment for compounds **26a** and **26b** (irradiation at δ 10.00, 0.52, 0.38, -6.30 and -6.73 from bottom to top)

4.B. Chemistry of Complex 26

4.B.i. Ligand Substitution

As discussed in Chapter 1, there is evidence to suggest that silyl groups are stronger *trans* influencing ligands than hydrides. For obvious reasons, ligands that are strong *trans* influencing prefer not to be *trans* to each other. Thus **26** is likely to be the thermodynamically stable isomer for a Ru^{II}(biPSi)(H)$(CO)_2$ composition and it is expected that the carbonyls *trans* to Si atoms may show higher lability than those *trans* to hydrides. The photo-irradiation of the mixture of **26** and excess $P(OMe)_3$ did not result in carbonyl substitution, and the carbonyl could also not be abstracted by $(CH_3)_3N{=}O$ in the presence of phosphites under ambient conditions. Heating a mixture of **26** and excess $P(OMe)_3$ in toluene at 100°C for 2 hours, however, afforded a colorless clear solution, from which a white solid **27** was isolated showing better solubility than **26** in most solvents. Complex **27** has been fully identified with NMR spectroscopy (Figure 4-3: ^{31}P NMR spectrum; Figure 4-4: ^{29}Si NMR spectrum; Table 4-3: ^{1}H NMR data; Table 4-4: ^{31}P and ^{29}Si NMR data; Table 4-5: ^{13}C NMR data), IR and EA. The configuration of this product is assigned on the basis of the *cis* coupling constants $^{2}J(PR_3H)$ 16.4 Hz, $^{2}J[P(OR)_3H]$ 32.1 Hz, $^{2}J_{PP}$' 39.7 Hz, $^{2}J(PR_3Si)$ 21.3 Hz and the *trans* coupling constant $^{2}J[P(OR)_3Si]$ 112.4 Hz. It should be pointed out that the coupling with phosphites usually has a larger value than with phosphines. The ^{13}C signal of the single carbonyl group is detected as a weak multiplet at δ 210.15. The IR spectrum shows a strong band at 1942 cm^{-1} for CO stretching and a weaker band at 1864 cm^{-1} assigned to ν_{RuH}.

Only the *syn* isomer of 27 was obtained in the reaction of 26 with $P(OMe)_3$. In the nOe-diff experiment, irradiation at the frequency of the $SiCH_3$ group enhanced the signal intensities of both hydride and *ortho* hydrogen on phenyl groups; while irradiation of the hydride enhanced the intensities of $SiCH_3$, $P(OMe)_3$ and *ortho* hydrogens (Figure 4-5).

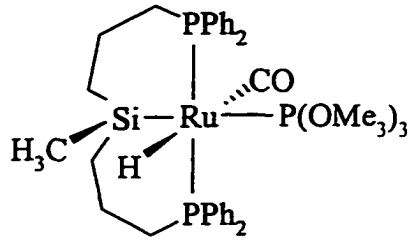

syn 27

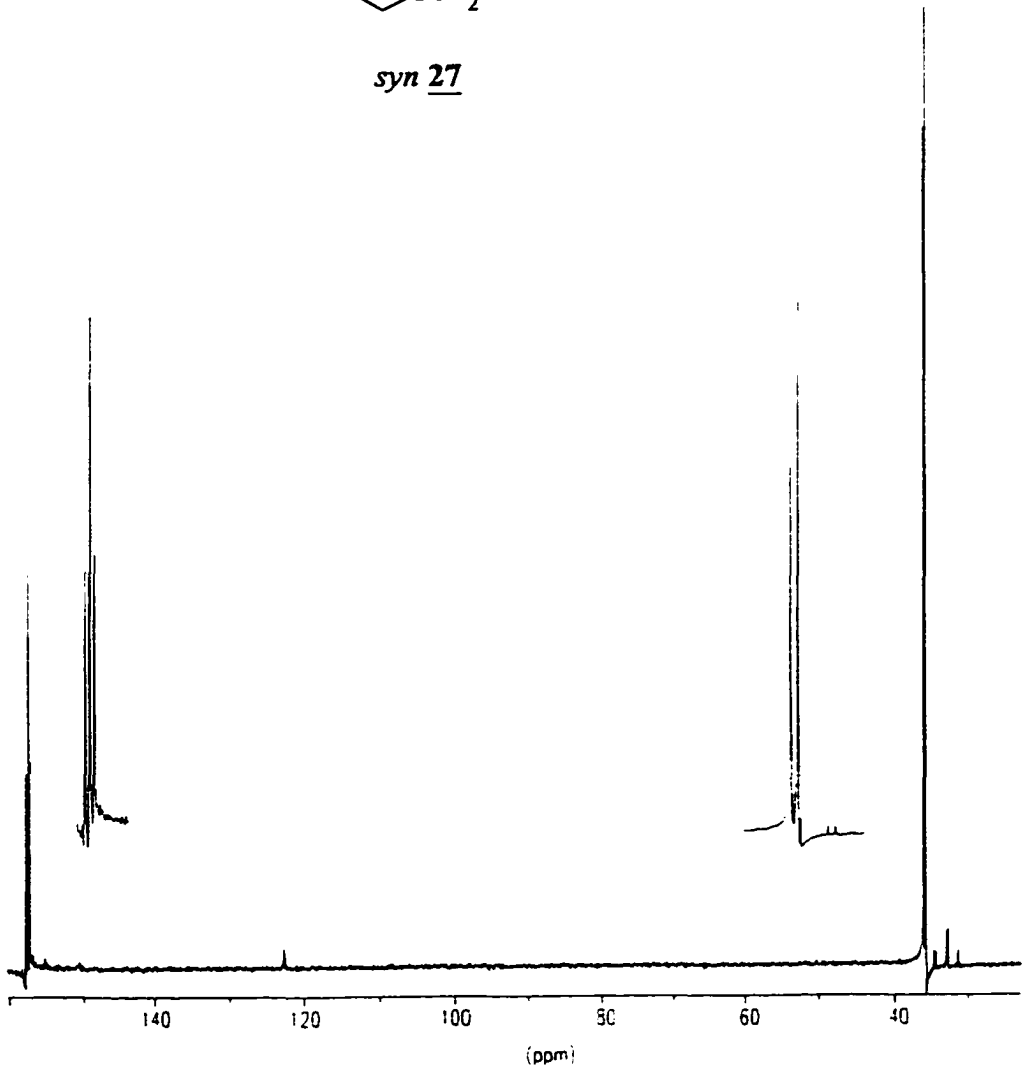

Figure 4-3: ^{31}P NMR spectrum for complex 27

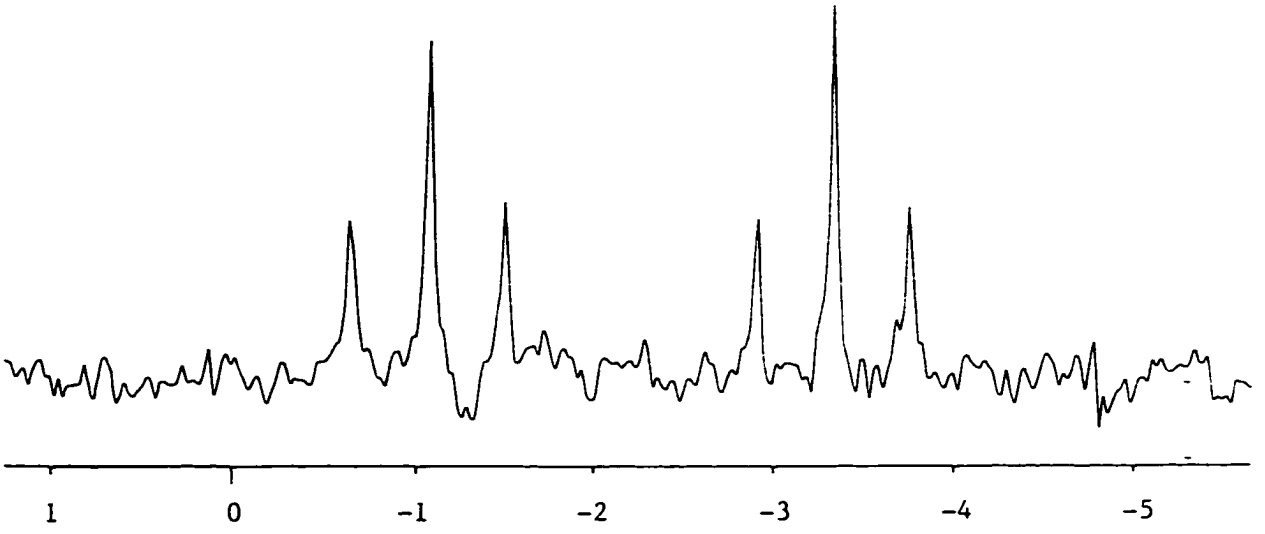

Figure 4-4: ^{29}Si NMR spectrum for complex **27**

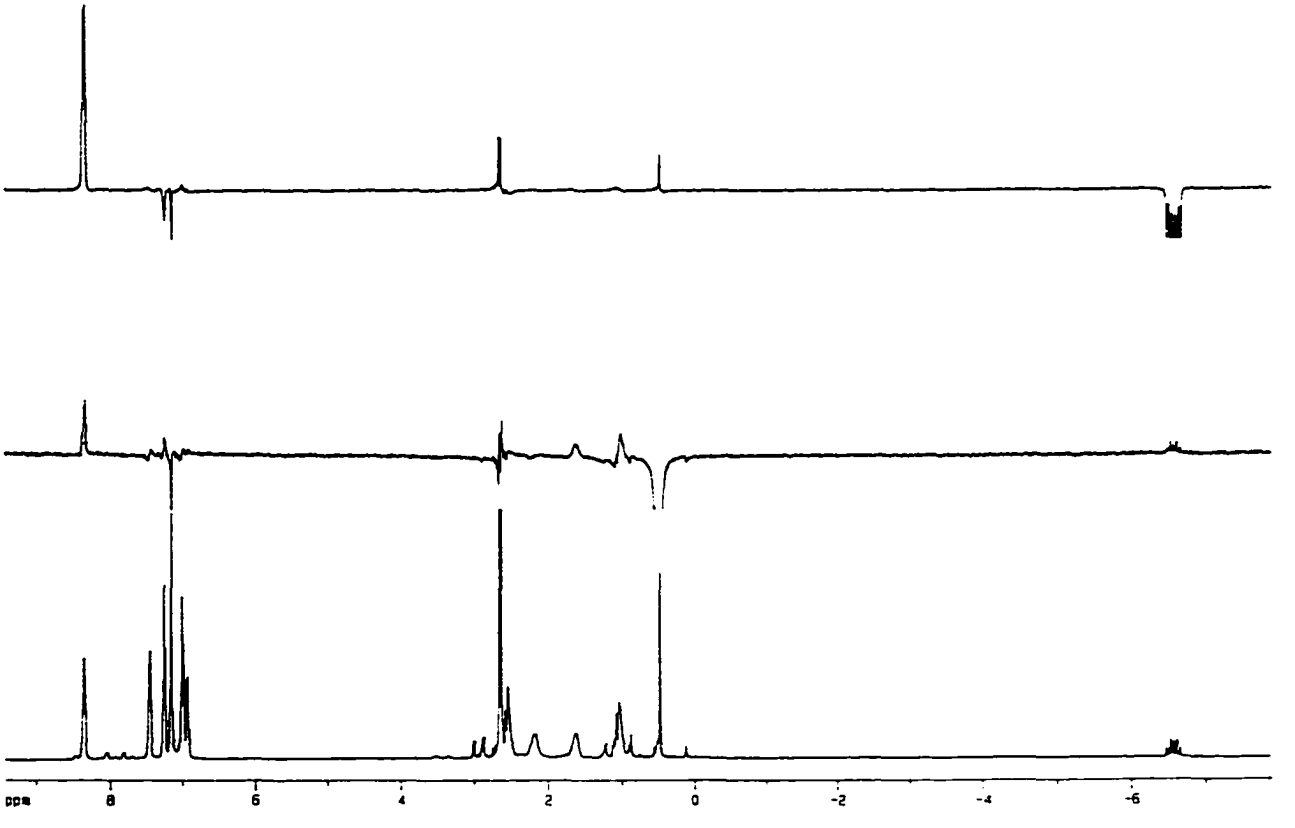

Figure 4-5. nOe-diff experiment for complex 27 (irradiation at δ 10.00, 0.46 and -6.57 from bottom to top)

Table 4-3. ^{1}H NMR data[a] for complex **27**

	^{1}H								
Compd	Ru*H*	$^{2}J_{PH}$	$^{2}J_{P'H}$	RuSiCH_3	SiCH_2	SiCH$_2$CH_2	PCH_2	P(OCH_3)	^{3}J(*P*-OCH_3)
					1.03	1.65	2.57		
27	-6.57(dt)	16.4	32.1	0.46	1.03	2.18	2.57	2.65(d)	8.9

[a] C_6D_6 was used as solvent; coupling constants were measured in Hz; P represents phosphines; P' represents phosphites

Table 4-4. ^{31}P and ^{29}Si NMR data[a] for complex **27**

	^{31}P					
Compd	*P*R$_3$	*P*(OR)$_3$	$^{2}J_{PP'}$	^{29}Si	$^{2}J_{PSi}$	$^{2}J_{P'Si}$
27	36.0(d)	157.6(t)	39.7	-2.2(dt)	21.3	112.4

[a] C_6D_6 was used as solvent; coupling constants were measured in Hz; P represents phosphines; P' represents phosphites

Table 4-5. ^{13}C NMR data[a] for complex 27

	^{13}C											
Compd	RuSi*C*H$_3$	^3J(P'-Si*C*H$_3$)	Si*C*H$_2$	SiCH$_2$*C*H$_2$	^2J(P-*C*H$_2$)	^4J(P'-*C*H$_2$)	P*C*H$_2$	^1J(P-*C*H$_2$)	^3J(P'-*C*H$_2$)	Ru*C*O	P(O*C*H$_3$)	^2J(PO*C*H$_3$)
27	9.86(d)	9.8	21.22	22.32(dt)	4.9	6.1	35.78(dt)	15.9	4.9	210.15 (m)	50.40	2.5

[a] C_6D_6 was used as solvent; coupling constants were measured in Hz; P represents phosphines; P' represents phosphites

Reaction of **26** and excess triethylphosphite $P(OEt)_3$ under the conditions used for the formation of **27** gave a completely different product **28**, the ^1H NMR spectrum of which shows a quintet signal at δ -7.10 split by a coupling constant $^2J_{PH}$ 20.9 Hz. The ^{31}P NMR shows a signal due to displaced phosphine ligands (δ -17.1) and a singlet at δ 165.9 assigned to coordinated $P(OEt)_3$. These data strongly imply that the four neutral ligands, i.e., chelating phosphines and carbonyls, in **26** have been substituted by four phosphite molecules, probably to give the tetrakis(phosphite) complex. A structure such as this is likely to show non-rigid properties. The four phosphites at apical and equatorial positions undergo rapid exchange, becoming equivalent to one another on the NMR time scale. Under milder conditions (<80°C), it was possible to observe formation of an analogue **29** of **27**, present as the major product but unavoidably contaminated with **28**. Important NMR data for **29** are collected in Table 4-6.

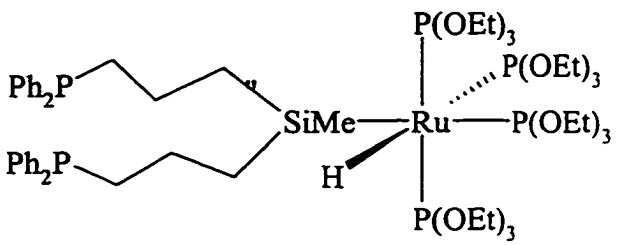

28

Table 4-6. Important NMR data[a] for complex 29

	^{1}H			^{31}P		
Compd	Ru*H*	$^2J_{PH}$	$^2J_{P'H}$	PR_3	$P(OR)_3$	$^2J_{PP'}$
29	-6.65(dt)	17.0	32.4	35.7	151.4	39.7

[a] Toluene-d_8 was used as solvent; coupling constants were measured in Hz; P represents phosphines; P' represents phosphites

As confirmed by the NMR data for complexes 27-29, the coupling between other NMR active nuclei and ^{31}P atoms in phosphites is usually larger than in phosphines. Phosphites are stronger π acids and behave as stronger ligands than either phosphines or carbonyls. This is why the totally substituted phosphite complex 28 can be formed as a stable product. The reason for the difference in reactivity between $P(OMe)_3$ and $P(OEt)_3$ towards 26 remains unclear. Triphenylphosphine was found not to substitute the CO groups in 26, which can be attributed to large steric bulk and the fact that it has poorer coordination ability than CO. Reactions of 26 with other ligands containing unsaturated bonds (including t-butylisocyanide, acetonitrile, benzonitrile, cyclooctene and phenylacetylene) led to the loss of hydrides but no isolable products were obtained.

4.B.ii. Amine Assisted Hydrolysis of the Ru-Si Bond in Ru(biPSi)(H)(CO)$_2$ (26)

Silicon metal bonds, M-Si, in early transition metal complexes are usually sensitive to water. Such hydrolysis of M-Si bonds is favored by the formation of stable M-O bonds (*e.g.*, Zr-O bond energy = 760 ± 8 kJmol^{-1}) in oxo bridged (M-O-M) or in

hydroxo functionalized (M-OH) products.[122] By contrast, late transition metal silyl complexex are usually more stable to hydrolysis and almost all the platinum group metal complexes of phosphinoalkylsilanes synthesized so far are not moisture sensitive.

Activation of water is an active research topic due to its potential importance in solar energy conversion schemes and other homogeneous catalytic cycles. Oxidative addition of water to transition metal precursors can be viewed as controlled hydrolysis of metal complexes and has been observed for $[Ir(PMe_3)_4]^+PF_6^-$,[123] $[Rh(H)(P^iPr_3)_3]$,[124] cyclometalated[125] $Ru(H)(PMe_2CH_2)(PMe_3)_3$ and *in situ* generated $[W(\eta^5\text{-}C_5Me_5)_2]$.[126] Hydrido hydroxy complexes are produced and these may play an important role in the water gas shift reaction, olefin and nitrile hydration, and photodissociation of water.[123] As an example, the reaction of the hydroxoruthenium complex $Ru(H)(OH)(DMPE)_2$ with silanols yields siloxoruthenium complexes (eq 4-2).[127] Other synthetic methods leading to the formation of siloxoruthenium complexes include the substitution of ruthenium chlorides with nucleophiles $KOSiR_3$ (R_3 = Me_3, Ph_3 or Me_2Ph, eq 4-3),[45a] the oxidation and oxygen insertion into Ru-Si bonds (eq 4-4),[128] and the neutralizaton of coordinated silanols with strong bases (eq 4-5).[44]

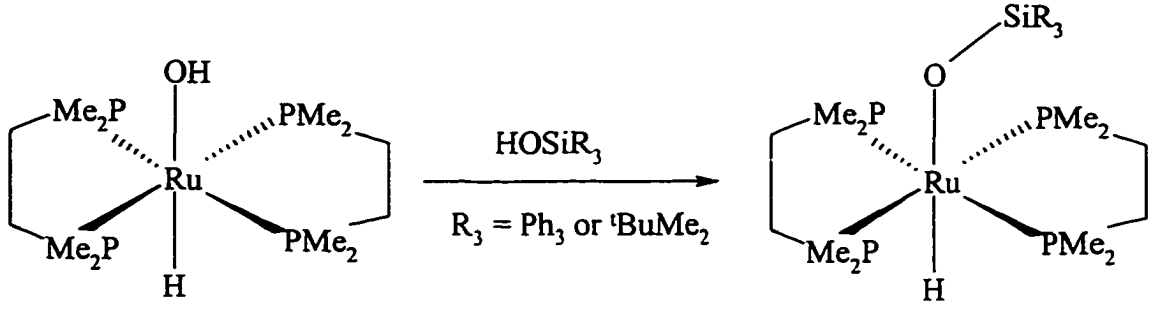

(4-2)

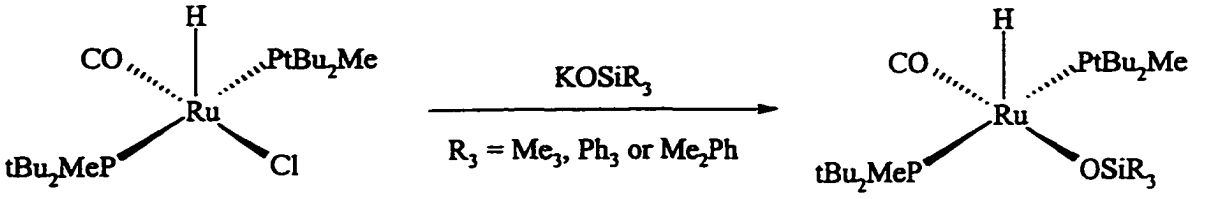

(4-3)

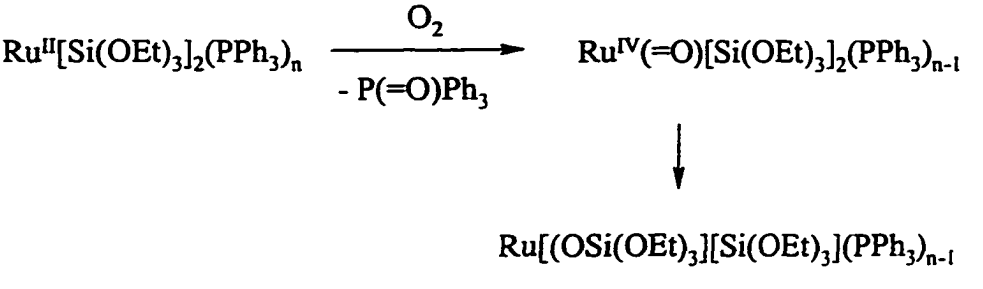

(4-4)

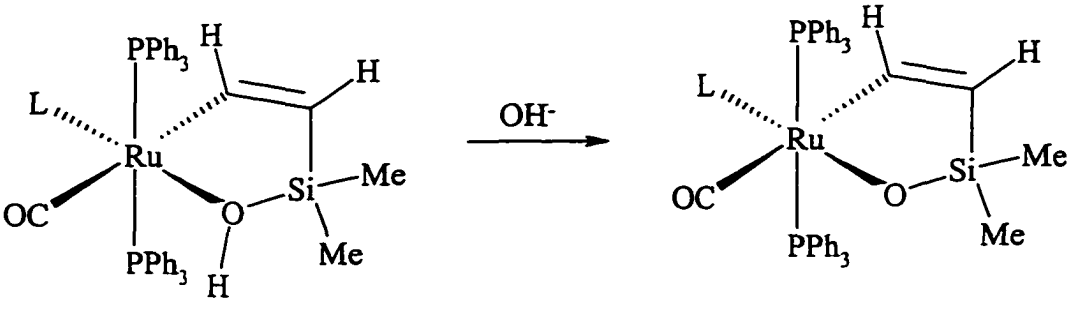

L = CO or CN-*p*-tolyl

(4-5)

Complexes 26 did not react with pure water even at high temperature (100°C, 17 h) so long as both the solvent and water are properly degassed in order to avoid reaction with O_2. It was found, however, that a new species 30 was formed if excess piperidine saturated with water was used under the same experimental conditions. Interestingly, no reaction could be observed with piperidine alone that had been previously dried over

$LiAlH_4$. The product **30** is stable at elevated temperature in the presence of excess piperidine, but can not be isolated since removal of excess piperidine under vacuum led to immediate decomposition. It was characterized *in situ* by ^1H, ^{31}P, ^{13}C and ^{29}Si NMR spectroscopy. The ^1H NMR spectrum has a hydride triplet (δ -12.65) with a $^2J_{PH}$ 21.8 Hz and a Si*Me* singlet (δ 0.36). The ^{31}P NMR spectrum shows a singlet (δ 43.6) while the ^{13}C NMR spectrum has only one carbonyl triplet signal (δ 203.4) with $^2J_{PC}$ 14.5 Hz. An unusually weak singlet (δ 8.1) in the ^{29}Si NMR spectrum recorded in toluene-d_8 suggests that the Si atom is not coordinated to the Ru center. The coordination of piperidine is suggested by the decomposition of the complex on removal of piperidine, and also by the chemical shift of the hydride signal, which is close to those reported for hydride complexes where H is *trans* nitrogen-containing ligands (Figure 4-6).[129] An nOe-diff experiment failed to give definite information about the stereochemistry although a signal enhancement of the *ortho* hydrogens (δ 8.24) on the phenyl groups could be observed using irradiation at the hydride frequency. This suggests that the hydride and the Si*Me* are probably *anti*. No temperature dependent behavior could be observed in the NMR behavior for **30**. Further identification of complex **30** is based on the complete characterization of its phosphite derivative **31**.

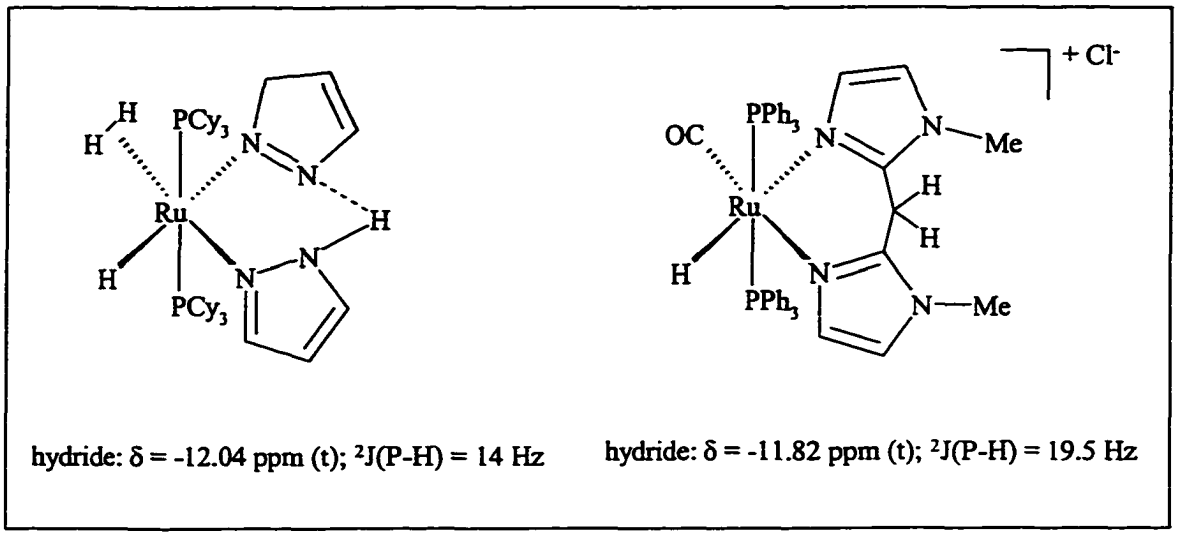

Figure 4-6. Structures and some NMR data of the hydride complexes coordinated by nitrogen-containing ligands

Since **30** decomposes on removal of excess piperidine, weak coordination of piperidine to the Ru center is implied, suggesting that this complex may be useful intermediate for conversion to other Ru(II) species. Investigation of its reactivity confirmed this: the coordinated piperidine was readily substituted by carbon monoxide (22°C, 10 min), trimethylphosphite (78°C, 20 min), t-butylisocyanide (78°C, 2 h) and triphenylphosphine (incomplete even after heating to 100°C for several days), to yield **31**, **32**, **33** and **34** respectively (Scheme 4-2). Nitrogen-containing ligands, which are hard bases, usually bind rather weakly to late transition metal centers. Caulton *et al*, for example, found that pyridine and nitriles (acetonitrile and acrylonitrile) bind reversibly to $RuHX(CO)P_2$ species.[45a, 130]

In the reaction of **30** with CO, piperidine is displaced by CO to give **31** so that the hydride chemical shift moves from δ -12.65 to δ -4.17 ($^2J_{PH}$ = 23.5 Hz), a typical value for

hydride *trans* to CO. Complex 31 was found to be always contaminated by impurities attributed to decomposition of precursor 30 that occurs in the absence of excess piperidine. This is likely to arise because the equilibrium between 31 and 30 is shifted when the concentration of CO in solution is lowered as volatiles are removed during purification. Only one isomer of 31 could be detected, and is assumed to have Ru-O-Si bonding like 30, due to the singlet ^{29}Si resonance (δ 7.9). Two strong IR absorptions were found at 1948 and 2048 cm^{-1} (ν_{CO}) with a weak band (ν_{RuH}) at 2002 cm^{-1} and NMR data are shown in Table 4-7.

Table 4-7. The NMR data[a] for complex 31

			^{1}H			
Compd	^{31}P	^{29}Si	Ru*H*	$^2J_{PH}$	RuOSiC*H*$_3$	SiC*H*$_2$C*H*$_2$C*H*$_2$P
31	33.9	7.9	-4.17(t)	23.5	0.46	3.20, 2.12, 1.86, 1.72, 1.30, 0.51

[a] C_6D_6 was used as solvent; coupling constants were measured in Hz

Both 32 and 33 were isolated as white powders, and were characterized by spectroscopic methods and elemental analysis. The ^{1}H, ^{31}P, ^{29}Si and ^{13}C NMR data for 32 and 33 are collected in Tables 4-8, -9 and -10. In the ^{1}H NMR spectrum for 32, as shown in Figure 4-7, the large *trans* coupling ($^2J_{PH}$ = 185.4 Hz) between hydride and phosphite

ligands establishes a *trans* relationship between these two, and further suggests that piperidine *trans* to hydride in **30** has been selectively substituted by the phosphite. Two isomers can be found in solution for **32**, in a 20:1 ratio, of which the *anti* isomer dominates, on the basis of an nOe-diff experiment in which irradiation at the hydride frequency enhances a proton signal (δ 1.26) assigned to one of the SiCH_2 groups in the ligand backbone and the *ortho* hydrogens on the phenyl groups. This conclusion has been confirmed by a X-ray crystal structure. An unusual-looking doublet ($^3J_{PSi}$ = 8.1 Hz) (*i.e.*, showing no coupling to biPSi P atoms), was found in the ^{29}Si NMR, perhaps due to coupling arising from a *cis* interaction between phosphite and silicon atoms. In the ^{13}C spectrum, the phosphite and phosphines couple with the single carbonyl group almost equally, splitting it into an apparent quartet. The IR spectrum shows only one strong absorption at 1904 cm^{-1}, assigned to CO stretching or overlapped CO and RuH stretching. Complex **32** was fully characterized only after a single crystal had been grown from a saturated ether solution and the structure had been determined by X-ray crystallography. The molecular structure is shown in Figure 4-8. The important bond lengths and bond angles are listed in Table 4-11. Other crystallographic data are collected in Appendix A. The crystal structure shows an oxygen atom has been inserted into the Ru-Si bond, the complex has an *anti* configuration, and the Ru-O-Si bond angle is 121.7(2)° with Ru-O and Si-O bond lengths 2.115(3) and 1.605(4) Å respectively. The Ru-O-Si bond angle is much smaller than that of 168.8(3)° found in the five coordinate complex, $Ru(H)(OSiPh_3)(CO)(P^tBu_2Me)_2$, where a monodentate triphenylsiloxy group is attached to a Ru(II) center and is coordinated by bulky ligands, and the Ru-O and Si-O distances are somewhat longer than those in the latter [2.057(4) and 1.584(4) Å respectively].[45a]

These differences suggest that π-bonding may be less important in six-coordinate 32 than in the square pyramidal analogue.

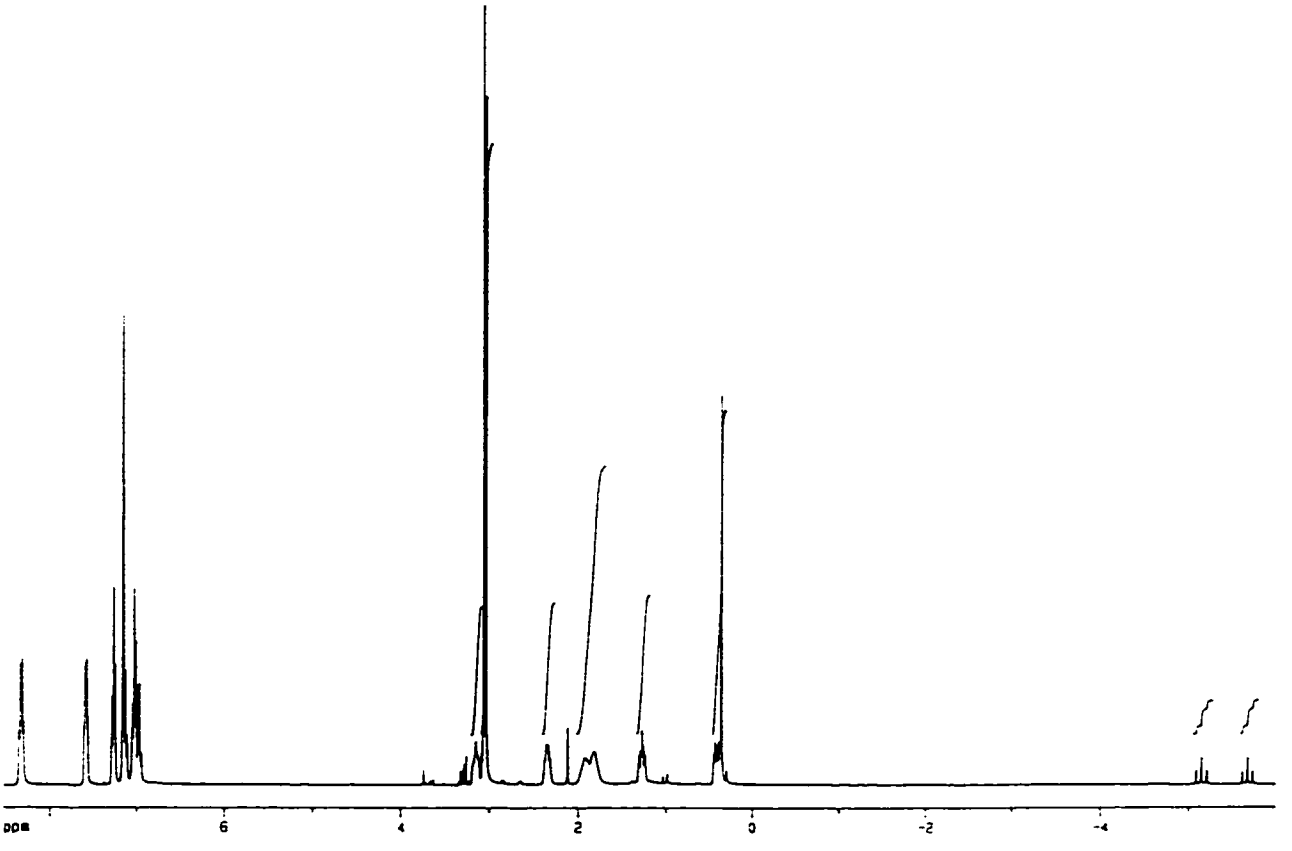

Figure 4-7. ^{1}H NMR spectrum for complex 32

Table 4-8. ^{1}H NMR data[a] for compounds 32 and 33

	^{1}H								
Compd	Ru*H*	$^{2}J_{PH}$	$^{2}J_{P'H}$	RuSi*CH*$_3$	Si*CH*$_2$	SiCH$_2$*CH*$_2$	P*CH*$_2$	P(O*CH*$_3$)	^{3}J(POCH$_3$)
					0.42	1.81	2.36		
32	-5.40(dt)	21.5	185.4	0.35	1.26	1.90	3.15	3.04(d)	10.2
					0.50	1.79	2.21		
33	-5.69(t)	20.5	-	0.47	1.51	1.93	3.28	-	-

[a] C_6D_6 was used as solvent; coupling constants were measured in Hz; P represents phosphines; P' represents phosphites

Table 4-9. ^{31}P and ^{29}Si NMR data[a] for compounds 32 and 33

	^{31}P				
Compd	*P*R$_3$	*P*(OR)$_3$	$^{2}J_{PP'}$	^{29}Si	$^{3}J_{P'Si}$
32	40.0	135.7	24.4	4.6(d)	8.1
33	38.8	-	-	6.0	-

[a] C_6D_6 was used as solvent; coupling constants were measured in Hz; P represents phosphines; P' represents phosphites

Table 4-10. ^{13}C NMR data[a] for compounds 32 and 33

	^{13}C											
Compd	RuSi*C*H$_3$	Si*C*H$_2$	SiCH$_2$*C*H$_2$	P*C*H$_2$	*J*(P-*C*H$_2$)	Ru*C*O	^2J(P-*C*O)	^2J(P'-*C*O)	P(O*C*H$_3$)	^3J(P*O*C*H*$_3$)	C(*C*H$_3$)$_3$	*C*(CH$_3$)$_3$
32	1.14	17.36	19.01	26.18(t)	12.8	203.13(q)	13.2	13.2	50.94(d)	3.6	-	-
33	0.94	17.23	18.46	26.57(t)	12.9	202.56(t)	13.5	-	-	-	29.35	54.95

[a] C_6D_6 was used as solvent; coupling constants were measured in Hz; P represents phosphines; P' represents phosphites

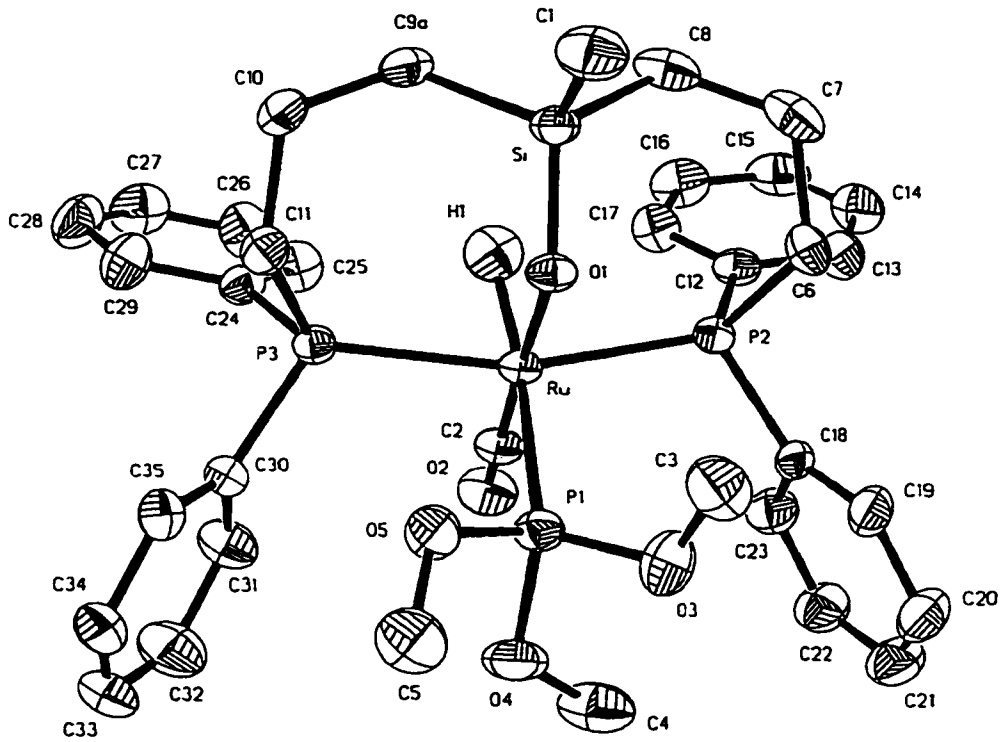

Figure 4-8. Molecular structure of complex 32

Table 4-11. Important bond lengths[a] and bond angles in complex 32

(a) Bond lengths:					
Atoms	Distance (Å)	Atoms	Distance (Å)	Atoms	Distance (Å)
Ru-H(1)	1.615(87)	Ru-P(1)	2.366(2)	Ru-P(2)	2.353(2)
Ru-P(3)	2.348(2)	Ru-O(1)	2.115(3)	Ru-C(2)	1.823(5)
P(1)-O(3)	1.598(6)	P(1)-O(4)	1.600(4)	P(1)-O(5)	1.596(5)

P(2)-C(6)	1.838(6)	P(2)-C(12)	1.834(7)	P(2)-C(18)	1.838(6)
P(3)-C(11)	1.831(5)	P(3)-C(24)	1.829(7)	P(3)-C(30)	1.841(6)
Si-O(1)	1.605(4)	Si-C(1)	1.865(7)	Si-C(8)	1.873(8)
Si-C(9a)	1.885(8)	O(2)-C(2)	1.162(6)	O(3)-C(3)	1.401(9)
O(4)-C(4)	1.399(10)	O(5)-C(5)	1.436(12)		

(b) Bond angles:

Atoms	Angle(°)	Atoms	Angle(°)	Atoms	Angle(°)
H(1)-Ru-P(1)	169.2(26)	H(1)-Ru-P(2)	86.5(27)	H(1)-Ru-P(3)	77.1(27)
P(1)-Ru-P(2)	100.6(1)	P(1)-Ru-P(3)	95.2(1)	P(2)-Ru-P(3)	163.3(1)
H(1)-Ru-O(1)	91.1(25)	P(1)-Ru-O(1)	81.0(1)	P(2)-Ru-O(1)	88.5(1)
P(3)-Ru-O(1)	88.8(1)	H(1)-Ru-C(2)	91.9(25)	P(1)-Ru-C(2)	96.1(2)
P(2)-Ru-C(2)	91.1(2)	P(3)-Ru-C(2)	92.5(2)	O(1)-Ru-C(2)	176.9(2)
O(1)-Si-C(1)	109.3(3)	Ru-O(1)-Si	121.7(2)		

[a] Estimated standard deviations are given in parentheses

Complex **33**, the product formed by reaction of **30** with *t*-butylisocyanide, a better ligand than CO, was found to exist as only one detectable isomer for which the stereochemistry has not been determined directly. The hydride triplet NMR signal moves downfield from δ -12.65 in the piperidine adduct **30** to δ -5.69 ($^2J_{PH}$ = 20.5 Hz), consistent with substitution of piperidine by *t*-butylisocyanide at the site *trans* to hydride. A singlet is observed in the ^{29}Si NMR, indicating a non-coordinated Si atom. Only one carbonyl

group is detected as a triplet (δ 202.56; $^2J_{PC}$ = 13.5 Hz) in the ^{13}C NMR spectrum, while the weak ^{13}C signal for *C*≡N- can not be assigned due to its overlap with phenyl signals. An overlapped IR absorption of carbonyl and hydride was found at 1927 cm^{-1} with a strong band at 2160 cm^{-1} assigned to C≡N stretching. Complex **33** is therefore assumed to have a similar structure as **32**.

The triphenylphosphine adduct **34** was only partially identified in solution, by the NMR data given in Table 4-12. Two isomers (**34a** and **34b**) were formed at an equal ratio. Both of them have large *trans* couplings ($^2J_{PH}$ = 107.2 or 111.2 Hz) between triphenylphosphine and hydrides and small *cis* coupling between the P atom of triphenylphosphine and those of the biPSi framework ($^2J_{PP'}$ = 15.3 Hz). They are assumed to be *syn* and *anti* diastereomers.

Table 4-12. Important ^1H and ^{31}P NMR data for complex **34**

	^1H			^{31}P		
Compd	Ru*H*	$^2J_{PH}$	$^2J_{P'H}$	*P*R$_3$	*P*Ph$_3$	$^2J_{PP'}$
34a	-6.45(dt)	22.6	107.2	42.84(d)	7.47(t)	15.3
34b	-7.00(dt)	23.4	111.2	42.68(d)	5.38(t)	15.3

[a] Toluene-d_8 was used as solvent; coupling constants were measured in Hz; P represents chelating phosphines; P' represents PPh_3

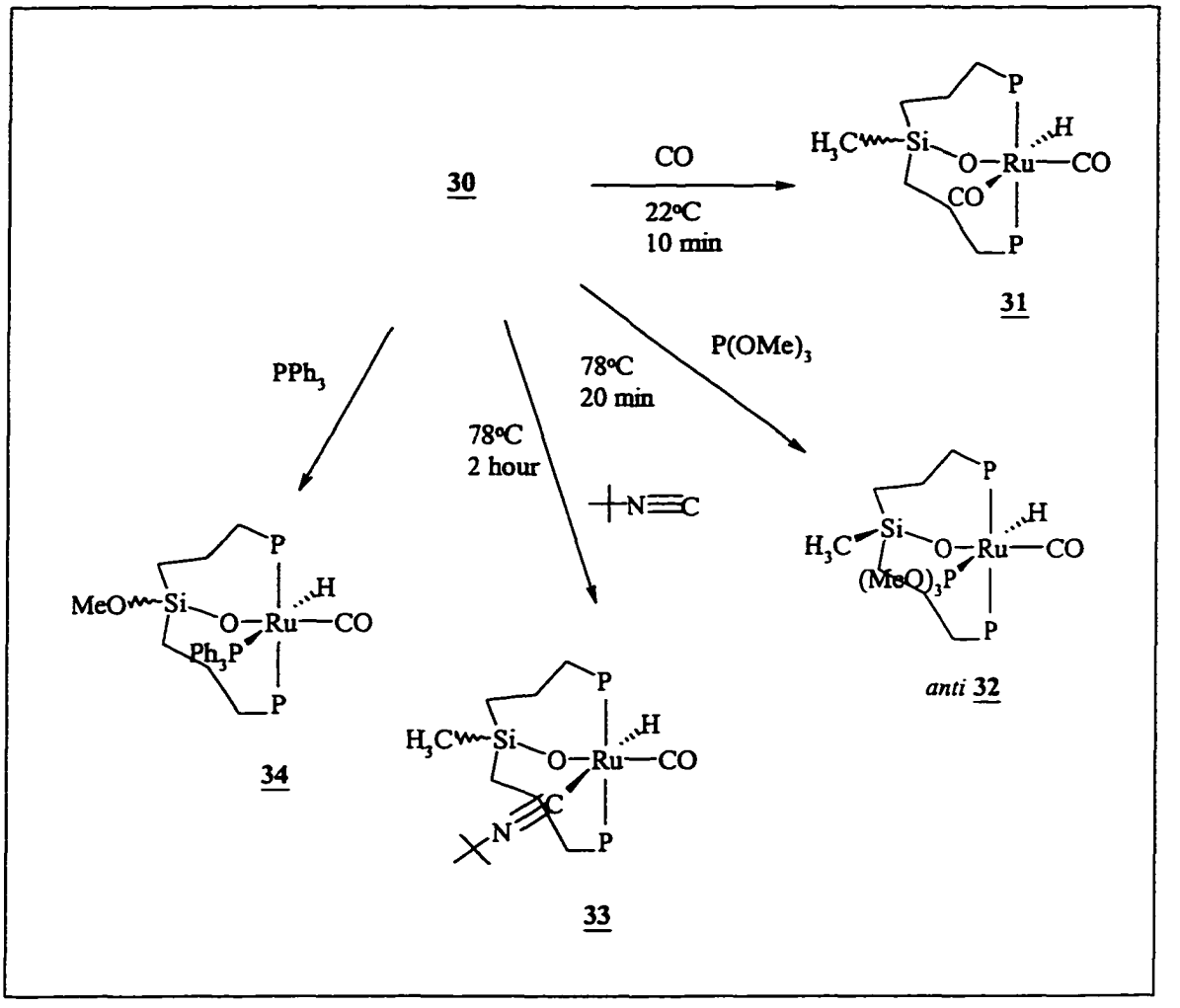

Scheme 4-2. Reaction of 30 with carbon monoxide, trimethylphosphite, *t*-butyl isocyanide, triphenylphosphine

In complexes where hydride is the ligand with the strongest *trans* effect, ligands *trans* to hydrides are expected to be labile. This is the case for complex 31, where the silicon atom is connected to Ru through a bridging oxygen, leaving the hydride exerting the strongest *trans* effect. Thus it is the CO group *trans* to hydride that is expected to be the more reactive, and accordingly substitution of CO by trimethylphosphite, *t*-

butylisocyanide or piperidine occurs in such a way for complex 31, affording the corresponding products 32, 33 and 30 (Scheme 4-3). Similar substitution by triphenylphosphine went to completion only after heating at 78°C for 48 h, affording 34 with formation of significant amounts of other unidentified hydride species (also Scheme 4-3).

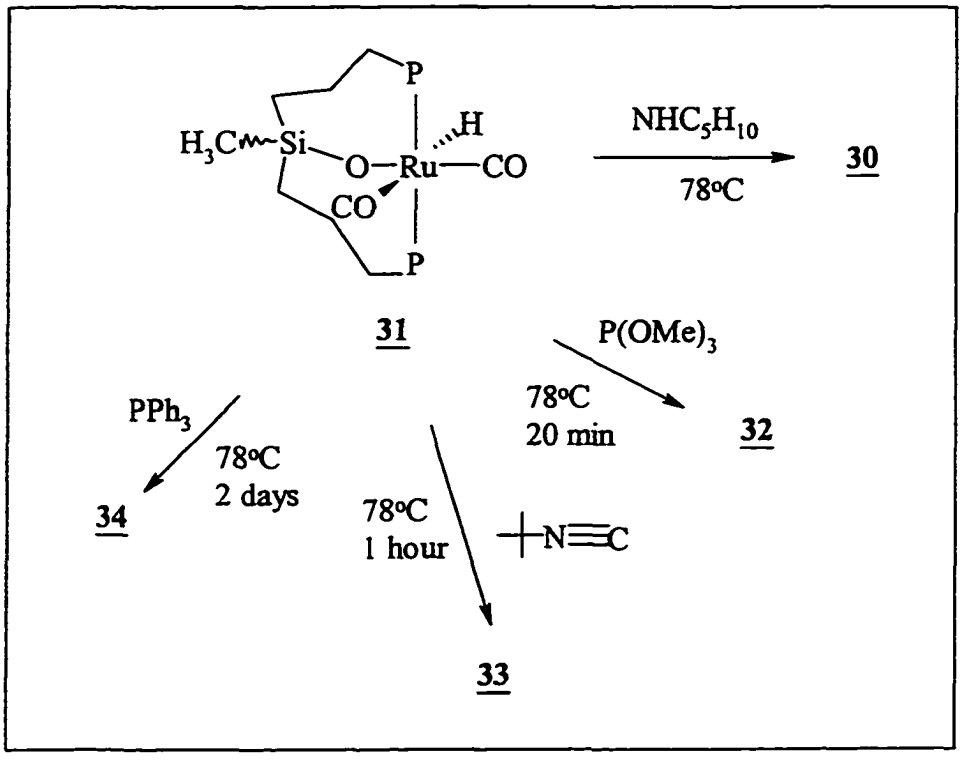

Scheme 4-3. Reactions of complex 31 with $P(OMe)_3$, ^tBuNC, PPh_3 and NHC_5H_{10}

The observation of Ru-O-Si bonding in the X-ray crystal structure of 32 implies that the same bonding arrangement also exits in the precursor 30, accounting for the absence of NMR coupling between phosphines and the ^{29}Si atom. The immediate conversion of 30 to 32 on addition of trimethylphosphite into a solution of the former suggests also that 30 is likely to have *anti* configuration. The formation of 30 from 26 by

reaction with water only in the presence of piperidine further suggests that the latter assists the hydrolysis of the Ru-Si bond in **26**, and that the oxygen atom inserted into the Ru-Si bond comes from water (which is the only oxygen source in the reaction). This interesting transformation was further investigated by using deuterium oxide (D_2O) instead of water. The reaction of **26** with piperidine (pre-dried) saturated with D_2O followed by the addition of $P(OMe)_3$ yielded products that showed weak high field Ru*H* signals for the piperidine intermediate and for the final phosphite complex that were sharply reduced in intensity when integrated against the Si*Me* group. However, when examined using ^2H NMR, a broad deuteride signal at δ -5.40 with a *trans* coupling $^2J_{PD}$ 29.5Hz for the phosphite complex could be detected, strongly suggesting that the metal hydride of **26** is replaced by deuterium during the reaction with piperidine and D_2O. The piperidine deuterio-complex **30**-*d* and the phosphite deuterio-complex **32**-*d* have similar ^{31}P NMR features to their hydride analogues **30** and **32**: a singlet (δ 43.0) in toluene-d_8 for **30**-*d*, which is replaced on addition of $P(OMe)_3$ by a triplet (δ 135.8; assigned to the coordinated phosphite ligand) and a doublet (δ 41.0; attributed to phosphines in biPSi framework) with a $^2J_{PP'}$ 25.8 Hz (*cis*) for **32**-*d*.

Since removing water from starting materials and equipment and keeping them away from moisture is difficult, the reverse isotope incorporation in which the deuteride **26**-*d* (see Section 4.B.iv. for synthesis) was reacted with water and piperidine and then with trimethylphosphite, was also investigated (Scheme 4-4). The intermediate **30** and phosphite final product **32** were detected only as the hydrido-isotopomers, and no deuterium signals could be detected in the final phosphite complex so formed. This

discovery confirms that the hydride in the hydrolyzed siloxo Ru(II) product does not come from starting hydride **26**, but from water. After complex **30** had been formed, the hydride was not observed to exchange with deuterium even after heating at 100°C for 3 h in D_2O-saturated toluene, establishing that the hydride/deuteride crossover happens at the time of the formation of the Ru-O-Si unit.

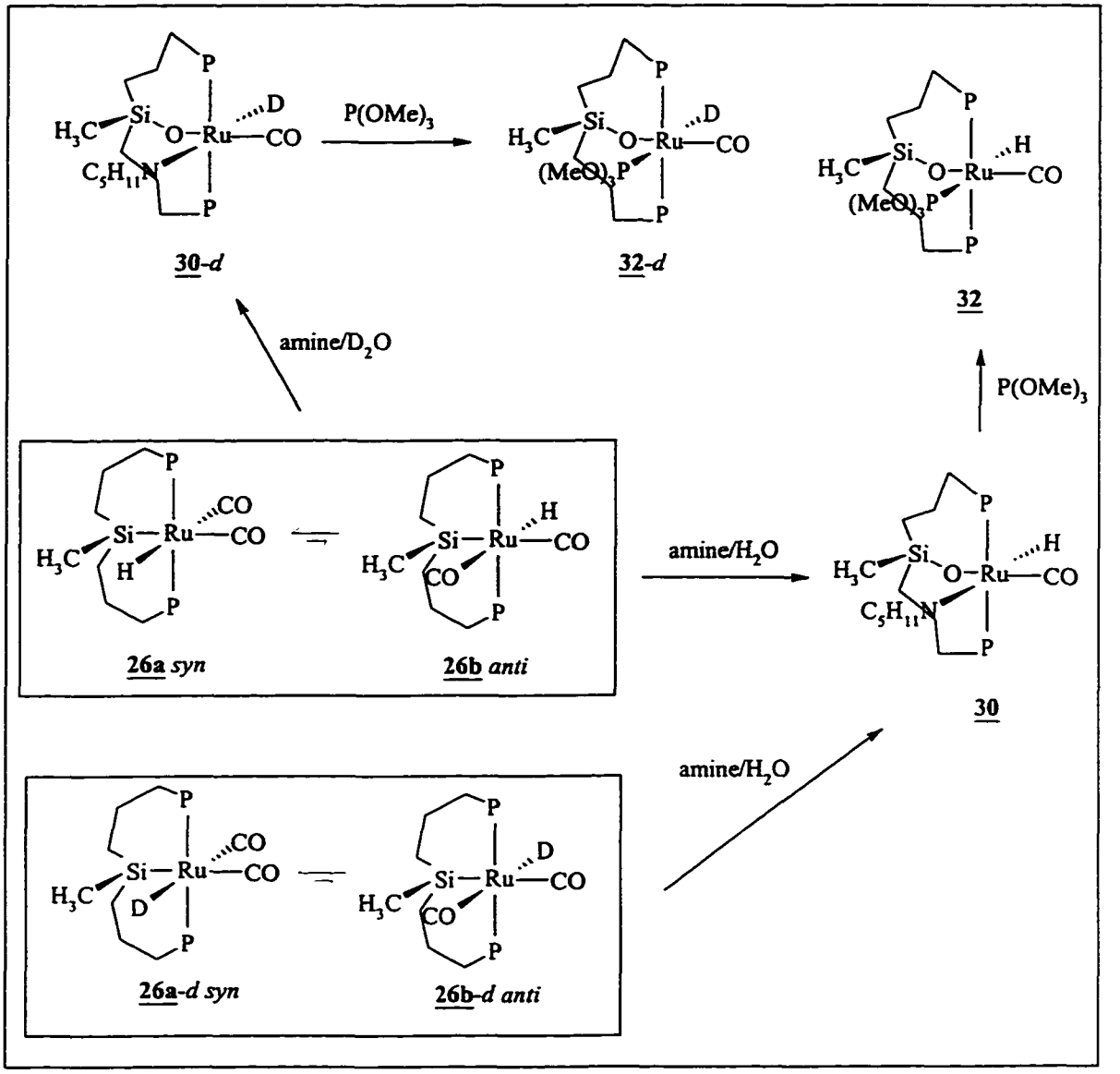

Scheme 4-4. Amine assisted hydrolysis of Ru-Si bonds in **26** and **26**-*d*

Piperidine (pK_a = 11.12 in aqueous solution) is not the only amine leading, in the presence of water, to hydrolysis of the Ru-Si bond in 26. Pyridine, which is a much weaker nitrogen-containing base (pK_a = 5.25), was found to induce the same chemistry. A mixture of complex 26, excess water and pyridine was heated at 100°C for 62 h to produce a pyridine intermediate 35 which, like the piperidine analogue 30, could not be isolated pure but was identified *in situ* using ^1H, ^{31}P and ^{29}Si NMR spectroscopy (Table 4-13). The data obtained suggest that the pyridine complex 35 has a similar structure to that of the piperidine complex 30, in particular showing a high field hydride signal at δ -11.69, indicating Ru*H* *trans* to pyridine, and that the Ru-O-Si bonding has been formed (singlet ^{29}Si NMR δ 7.1). Addition of trimethylphosphite immediately converts 35 to the fully characterized 32. Pyridine, however, is a better ligand than piperidine, and accordingly complex 30 can be completely converted to 35 at 100°C within 30 min. These observations implies that rate of reaction of the Ru-Si bond in 26 with water, to give the Ru-O-Si complex, is dependent on the basicity of the cooperating amine, with the pyridine reaction being about four times slower than for piperidine.

Table 4-13. ^1H and ^{31}P NMR data[a] for complex 35

			^1H		
Compd	^{31}P	^{29}Si	Ru*H*	$^2J_{PH}$	SiCH_3
35	43.9	7.1	-11.69(t)	20.1	0.53

[a] Toluene-d_8 was used as solvent; coupling constants were measured in Hz

Based on the experimental results a mechanism can be proposed for the hydrolysis of the Ru-Si bond (Scheme 4-5). Water in basic medium is more basic, and cleaves the Ru-Si bond, to form a anionic Ru(0) hydride containing a silanol (SiOD) group. The negatively charged hydride is then attacked by acid D^+, to form a molecular dihydrogen (η^2-HD) intermediate that undergoes the oxidative addition of O-D to the reduced Ru(O) center. This leads to a labeled analogue **31**-*d* of **31** in which Si is connected to Ru through a bridging siloxo group and deuterium (only) is attached at Ru. At the same time a molecule of hydrogen HD is liberated. The carbonyl group *trans* to deuteride is labile and can be substituted by piperidine at elevated temperature (see **31** as discussed previously) to produce the piperidine complex **30**-*d* which then converts to the stable phosphite complex **32**-*d* on introduction of $P(OMe)_3$. The proposed second step, i.e., the protonation of the anionic Ru(0) hydride, and later liberation of HD is further confirmed by the reactions of **26** and its deuteride analogue **26**-*d* with the acid HBF_4. The hydride or deuteride is attacked by HBF_4 immediately to liberate H_2 or HD, of which H_2 is detected as a singlet at δ 5.4 in ^1H NMR spectra and HD as a triplet. The same NMR experiment conducted at low temperature suggests that a dihydrido cation molecular dihydrogen complex prior to H_2 elimination may be produced initially. This would implicate intermediacy of Ru(IV) in a manner consistent with suggestions of Crabtree *et al* and Morris *et al.*[131]

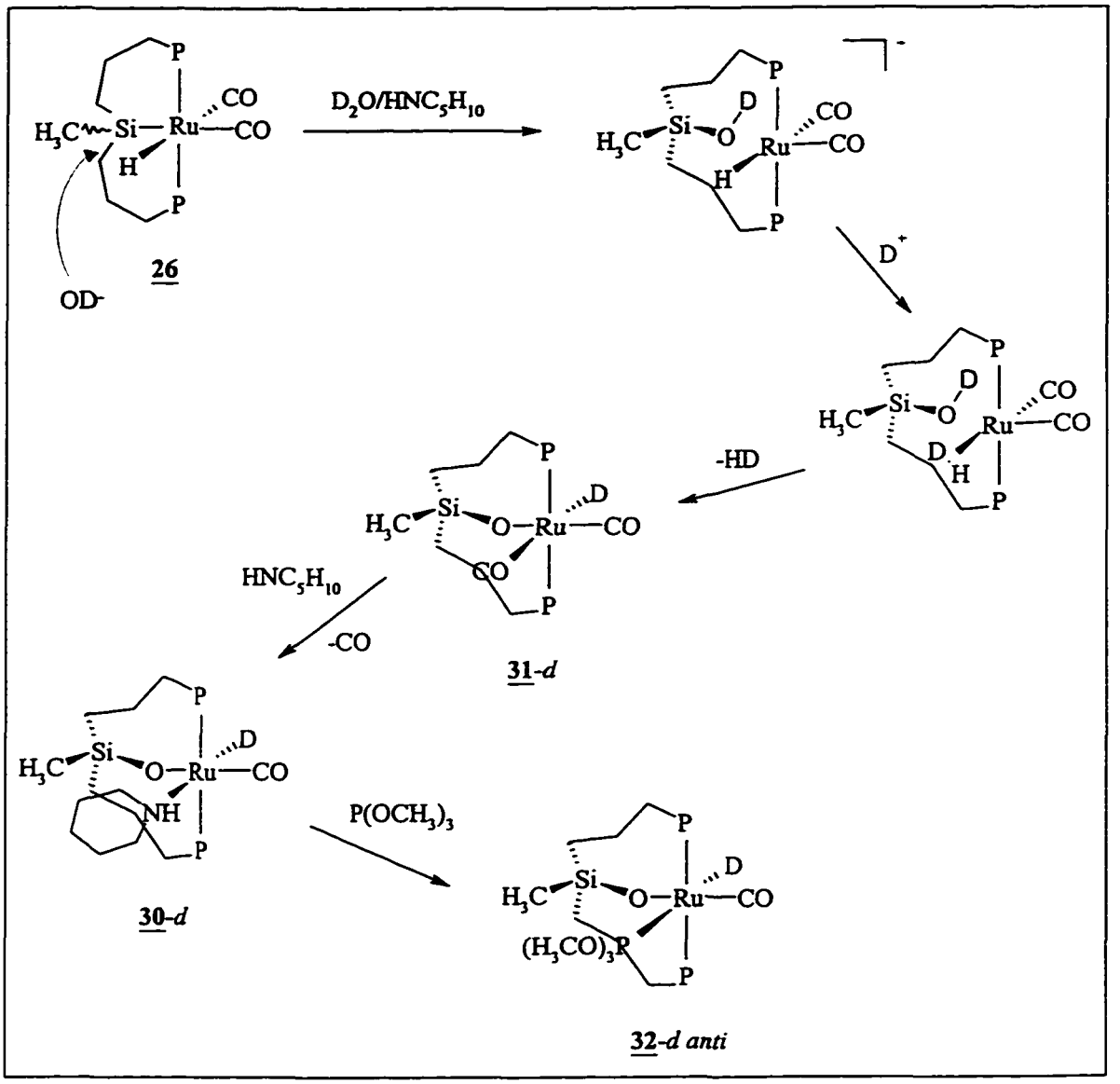

Scheme 4-5. Proposed mechanism for amine assisted hydrolysis of Ru-Si bond in **26**

4.B.iii. Oxidation of Complex 26

Since Vaska first observed the reversible coordination of oxygen to the iridium precursor, *trans*-Ir(CO)Cl(PPh_3)$_2$,[132] the reductive activation of O_2 by transition metal complexes has drawn much attention due to the importance from both synthetic and biological points of view.[133] The activation of oxygen usually leads to oxo (M=O)[128] or peroxo (M-O-O-M[134] or η-O_2-M[135]) metal complexes. Characterization of these oxygen adducts is relatively difficult. The most commonly used analytic methods include elemental analysis to measure oxygen content, mass spectroscopy, ^{17}O (I = ½) labeling experiments,[134] X-ray crystallography and IR spectroscopy.

Compound **26** is inert to oxidation in the solid state and in solution at ambient temperature. Heating at 78°C in benzene under ambient air, however, caused **26** to be slowly (longer than one week) oxidized to give a product **36** that was subsequently fully characterized only after determination of the X-ray crystal structure of the derived trimethylphosphite complex. During the reaction (eq 4-6), a color change was observed as the almost colorless solution of **26** darkened to a greenish color as product **36** was formed. A faster reaction rate was achieved by bubbling pure O_2 through the solution, or by heating to a higher temperature in boiling toluene, but this was unavoidably accompanied by some decomposition to unidentified by-products. After compound **26** had reacted completely, removal of the volatiles left a pale solid that was characterized by NMR and IR spectroscopy. The ^1H, ^{31}P and ^{29}Si NMR and IR data are shown in Table 4-14, and the ^{13}C NMR data are collected in Table 4-15. The product **36** shows high solubility in most common solvents. From the high field proton NMR it was concluded to consist of a mixture of two diastereomers, *syn* **36a** and *anti* **36b**, at a ratio of *ca.* 1:6. The

major isomer distinguished from **26** immediately by unusually low field NMR signals in both ^{1}H (δ 3.75) and ^{13}C (δ 49.64) spectra. The ^{29}Si NMR spectrum shows a singlet (δ -8.2 for **36b**, i.e., not coupled to the phosphorus atoms of the biPSi unit), implying that the Si atom was not bonded to Ru. These observations became fully understandable only after the solution of the X-ray crystal structure of the corresponding phosphite complex, which showed not only insertion of an oxygen atom into the Si-Ru bond but also conversion of the silylmethyl group to a methoxysilyl unit. Six non-first-order signals are found in the ^{1}H NMR for the six protons of the three methlyene units in backbone. Their exact assignment is based on the information from a ^{1}H-^{13}C correlation spectrum. The CO signal at higher field (δ 193.14) in the ^{13}C NMR spectrum can be assigned as a CO group *trans* to hydride, since a large *trans* coupling with hydride was detected on the gated ^{13}C spectrum, while the signal (δ 199.66) is assigned to CO *trans* to the siloxo ligand (identified crystallographically) with only a small *cis* coupling $^{2}J_{CH}$.

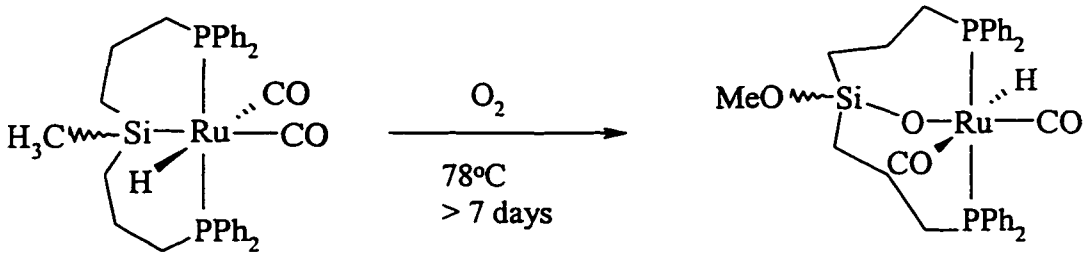

26 **36** (*syn*:*anti* = 1:6)

(4-6)

Table 4-14. ^{1}H, ^{31}P and ^{29}Si NMR and IR data[a] for complex **36**

			^{1}H						IR
Compd	^{31}P	^{29}Si	Ru*H*	$^{2}J_{PH}$	$SiOCH_3$	$SiCH_2$	$SiCH_2CH_2$	PCH_2	ν_{CO}
36a	-	-	-4.15(t)	20.3	-	-	-	-	-
						0.72	1.64	2.11	1954
36b	33.8	-8.2	-4.22	20.3	3.75	1.23	1.88	3.24	2046

[a] C_6D_6 was used as solvent; coupling constants were measured in Hz; IR frequencies were measured in cm^{-1}

Table 4-15. ^{13}C NMR data[a] for complex **36**

	^{13}C						
Compd	$SiOCH_3$	$SiCH_2$	$SiCH_2CH_2$	PCH_2	J(P-CH_2)	Ru*C*O	^{2}J(P-*C*O)
						199.66(t)	11.9
36b	49.64	13.90	18.06	27.80(t)	-	193.14(t)	7.1

[a] C_6D_6 was used as solvent; coupling constants were measured in Hz;

The reaction of **36** with trimethylphosphite afforded a white solid which was found to be a mixture concluded to be *syn* **37a** and *anti* **37b** diastereomers of a phosphite adduct in a 1:6 ratio. The major constituent was selectively crystallized from ether solution and its structure has been determined by X-ray crystallography. The molecular

structure is shown in Figure 4-9 and more crystallographic data are collected in Appendix B. Most surprisingly, two oxygen atoms were found to have become inserted into the Si-C and Ru-Si bonds respectively; the structurally characterized isomer **37b** has an *anti* stereochemistry. Important bond lengths and bond angles are collected in Table 4-16. The structure has a very similar bonding pattern to that of **32**, the mono-oxygen-inserted phosphite product of hydrolysis of **26**. The Ru-O and Si-O(Ru) bond lengths are 2.111(6) and 1.591(6) respectively. The Ru-O-Si bond angle at 127.9(3)° is somewhat larger than that of 121.7(2)° in **32**. The Si-O(Me) and (Si)O-C bond distances were determined at 1.685(9) and 1.217(23) Å respectively, of which the former is slightly longer than that of the coordinated Si-O(Ru) bond and is typical for uncoordinated Si-O bonds [1.647(5), 1.649(5) and 1.624(5) were measured[136] as the Si-O bond lengths in $OsCl(CO)(PPh_3)_2Si(OH)_3$]. The Si-O-C(Me) angle is found to be 137.4(12)°. Complex **37** has also been characterized using spectroscopic methods (Figure 4-10: ^1H NMR spectrum; Tables 4-17, -18 and -19: NMR data). The hydride signals are detected as doublets of triplets (δ -5.40 for **37a**, -5.44 for **37b**), split by *cis* coupling to phosphines ($^2J_{PH}$ = 21.5 Hz for **37a**, 21.3 Hz for **37b**) and *trans* coupling to phosphite ($^2J_{PH}$ = 185.8 Hz for **37a**, 184.7 Hz for **37b**). A downfield singlet (δ 3.73) in the ^1H NMR spectrum is assigned to the methoxy group in **37b**. In the ^{31}P NMR spectrum, **37b** shows a doublet (δ 41.6) assigned to biPSi phosphorus atoms and a triplet (δ 135.9) due to the coordinated phosphite, with a coupling ($^2J_{PP'}$ = 25.0 Hz). Only the biPSi P signal (δ 41.0) was detectable for the minor isomer **37a**. The ^{29}Si NMR signals of both isomers do not show coupling with phosphine ligands, because the Si atom is no longer bound to Ru. In the ^{13}C

NMR spectrum, only one CO group (δ 202.83) is found for 37b, which couples with three phosphorus atoms equally to give a quartet ($^2J_{PC}$ 13.1); the methoxyl ^{13}C frequency for 37b (*anti*) is found at δ 49.25. The IR spectrum of complexes 37 shows the absorption for carbonyl ν_{CO} = 1906 cm^{-1}.

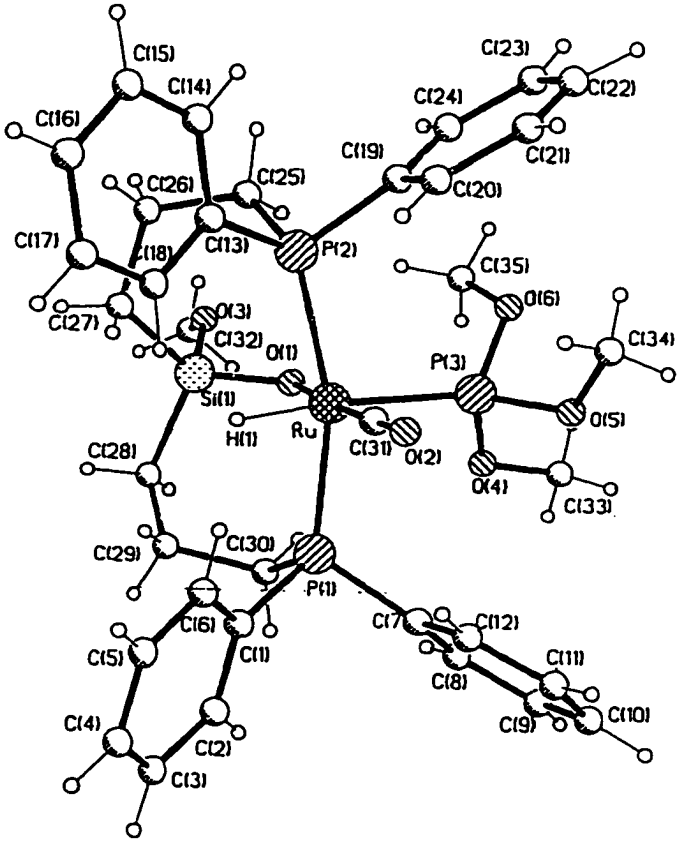

Figure 4-9. Molecular structure of compound 37b

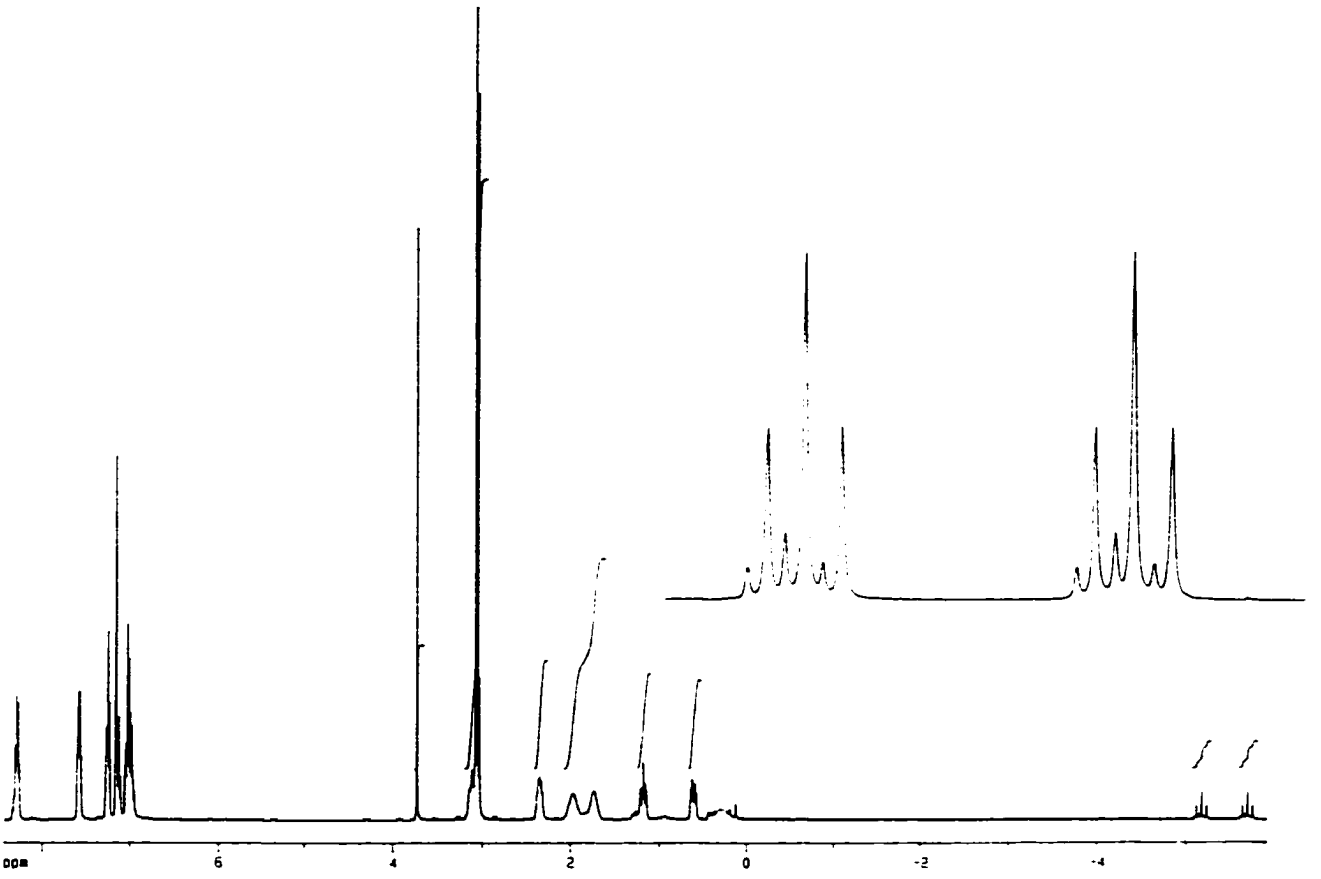

Figure 4-10. ^{1}H NMR spectrum for complex 37

Table 4-16. Important bond lengths[a] and bond angles in complex **37b**

(a) Bond lengths:					
Atoms	Distance (Å)	Atoms	Distance (Å)	Atoms	Distance (Å)
Ru-P(1)	2.351(2)	Ru-P(2)	2.352(2)	Ru-P(3)	2.364(2)
Ru-O(1)	2.111(6)	Ru-C(31)	1.820(10)	Si(1)-O(1)	1.591(6)
Si(1)-O(3)	1.685(9)	Si(1)-C(27)	1.881(9)	Si(1)-C(28)	1.865(11)
P(3)-O(4)	1.591(6)	P(3)-O(5)	1.602(7)	P(3)-O(6)	1.619(7)

O(2)-C(31)	1.157(12)	O(3)-C(32)	1.217(23)	O(4)-C(33)	1.434(12)
O(5)-C(34)	1.398(15)	O(6)-C(35)	1.414(14)		
(b) Bond angles:					
Atoms	Angle(°)	Atoms	Angle(°)	Atoms	Angle(°)
P(1)-Ru-P(2)	162.7(1)	P(1)-Ru-P(3)	94.4(1)	P(2)-Ru-P(3)	102.2
P(1)-Ru-O(1)	89.0(2)	P(2)-Ru-O(1)	88.6(2)	P(3)-Ru-O(1)	80.9(1)
P(1)-Ru-C(31)	92.1(3)	P(2)-Ru-C(31)	91.4(3)	P(3)-Ru-C(31)	95.4(3)
O(1)-Si-C(31)	176.2(3)	O(1)-Si(1)-O(3)	108.3(4)	O(1)-Si(1)-C(27)	112.3(4)
O(3)-Si(1)-C(27)	104.0(4)	O(1)-Si(1)-C(28)	111.5(4)	O(3)-Si(1)-C(28)	108.4(5)
C(27)-Si(1)-C(28)	111.9(4)	Ru-C(31)-O(2)	178.8(9)	Ru-O(1)-Si(1)	127.9(3)
Si(1)-O(3)-C(32)	137.4(12)				

[a] Estimated standard deviations are given in parentheses

The possibility that moisture in the air is the source of oxygen for the formation of **36** can be ruled out since no reaction could be detected between **26** and degassed H_2O in toluene. It is proposed that the dissociation of a ligand in **26** produces an unoccupied site where O_2 can complex to form a peroxo intermediate (Scheme 4-6). It is very possible that insertion of oxygen into Ru-Si and Si-C(Me) bonds is simultaneous, since neither of the complexes **30** or **31** in which the Ru-O-Si connection is already in place could be converted to **40** (piperidine adduct) or **36** in air or by the action of a flow of pure oxygen gas. Thus the involvement of oxo intermediates as proposed in the mechanism for

dioxygen assisted catalyzed hydrosilylation of alkenes seems unlikely (see eq 4-4 in Section 4.B.ii.).[128]

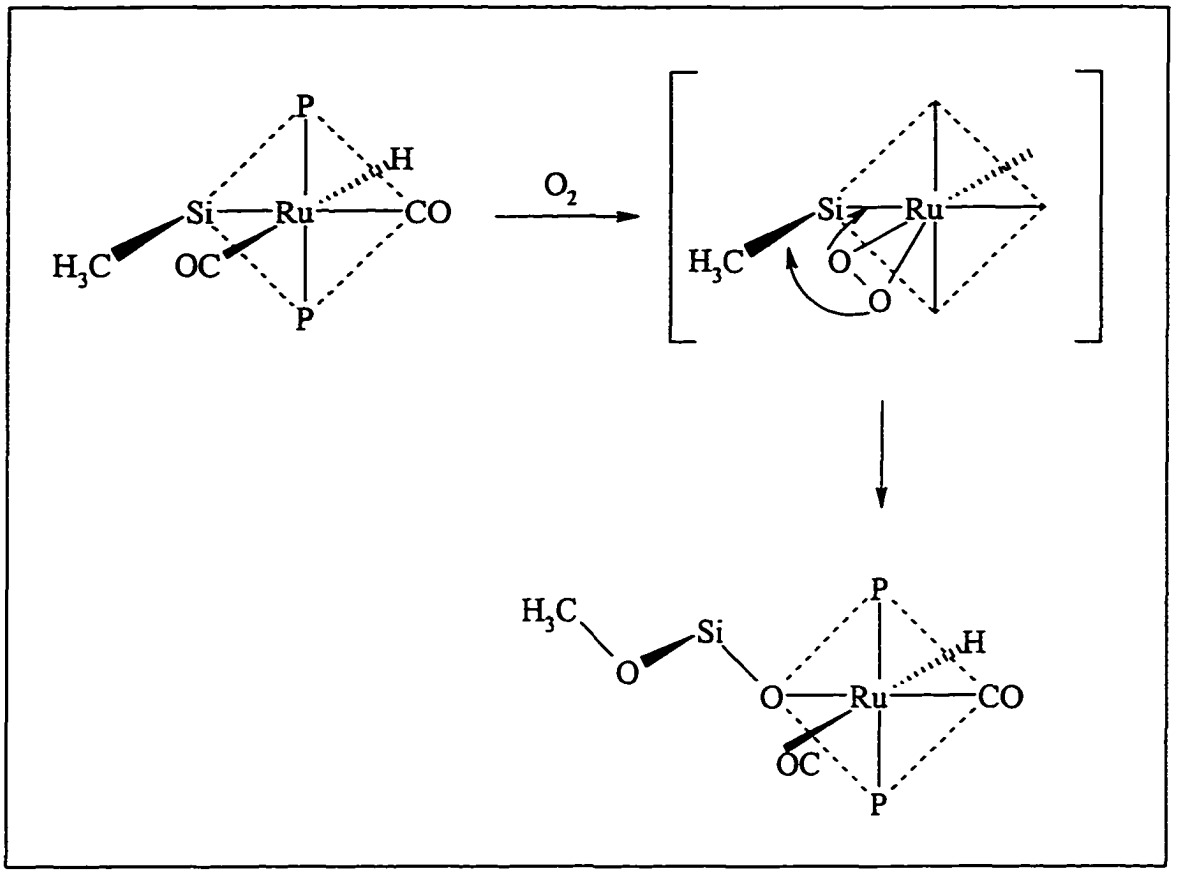

Scheme 4-6. Proposed mechanism of the oxidation of complexes **26**

The insertion of oxygen into an extremely stable and normally unreactive Si-C bond, leaving more sensitive phosphines and hydride centers undisturbed, is unusual: oxidation of coordinated phosphines and metal hydrides to give phosphine oxides[137] and hydroxo metal complexes[127] respectively have commonly been observed. More information is certainly needed for complete elucidation of the mechanism of oxidation of **26**. Further work in this area is likely to include oxygen uptake measurements[138] and

oxygen-labeled NMR experiments.[134] Attempts to selectively oxidize 26 with *t*-butyl hydroperoxide, another commonly used oxidant, at ambient temperature led only to heat evolution with immediate formation of black insoluble materials.

The formation of a phosphite adduct 37 in the reaction of the dicarbonyl complex 36 with trimethylphosphite shows that the CO group *trans* to the hydride in 36 is labile, as was found for the analogue 31. Such a conclusion is further confirmed by similar substitution of CO *trans* to hydride in 36 by *t*-butyl isocyanide, triphenylphosphine, and piperidine, affording analogues 38, 39 and 40 of 33, 34 and 30 (Scheme 4-7).

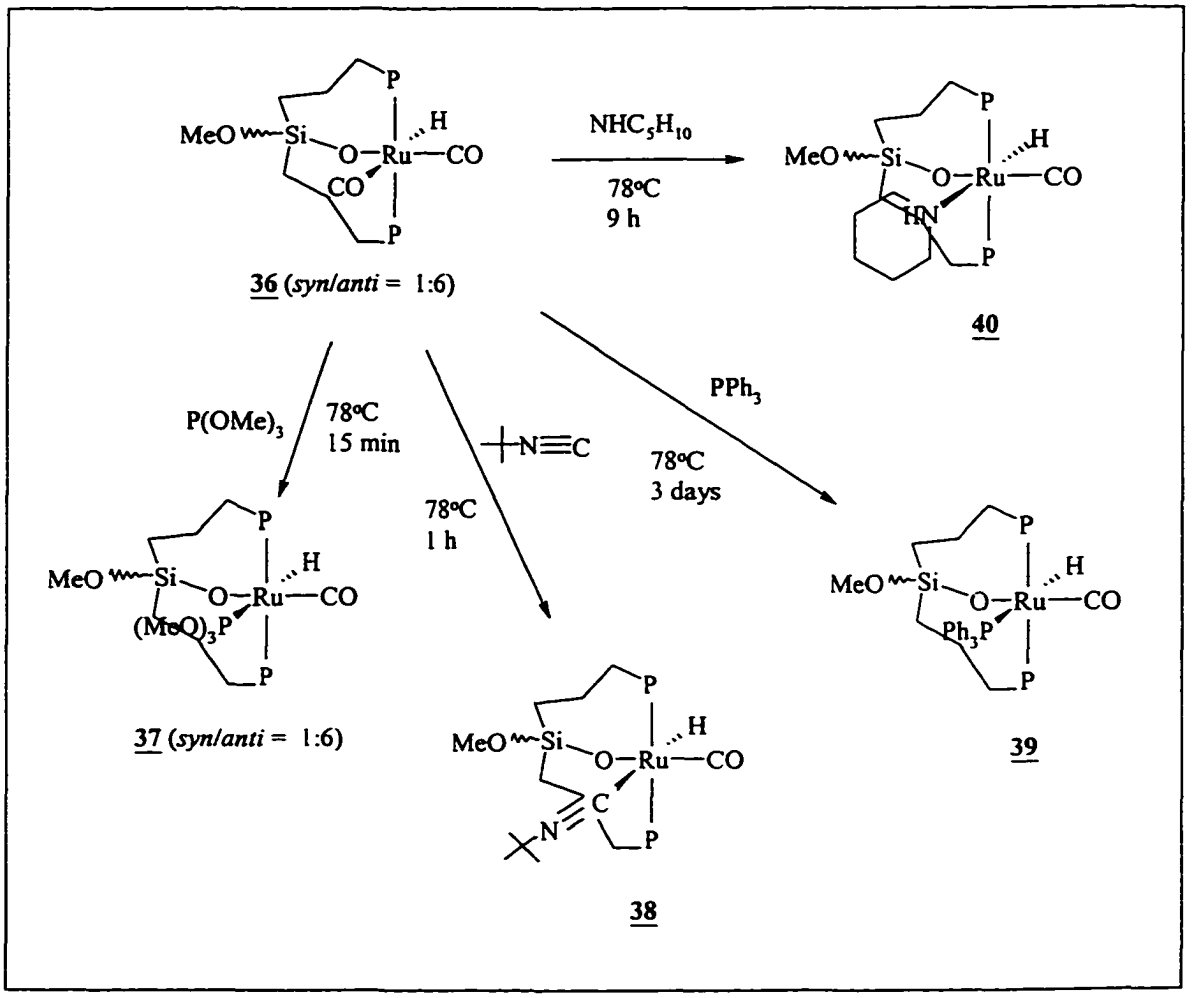

Scheme 4-7. Reactions of complexes 36 with $P(OMe)_3$, ^tBuNC, PPh_3 and NHC_5H_{10}

Complex 38 was isolated as a white solid and characterized with NMR, IR and EA. The ^{1}H NMR data are shown in Table 4-17, ^{31}P and ^{29}Si NMR data are collected in Table 4-18, and ^{13}C NMR data are listed in Table 4-19. A high field triplet (δ -5.76; $^{2}J_{PH}$ 20.3) in the ^{1}H NMR spectrum is assigned to Ru*H*. Both the ^{31}P and ^{29}Si NMR spectra show singlets [δ(^{31}P) 39.2; δ(^{29}Si) -9.2]. A resonance for only one carbonyl ligand is found at δ 202.91 as a triplet ($^{2}J_{PC}$ = 12.6 Hz) in the ^{13}C NMR spectrum, while the peak for the isocyanide carbon *C*N- could not be differentiated from phenyl signals.

The complete formation of 39 took at least 3 days at 78°C in benzene. During this prolonged period of heating, a black solid precipitated suggesting some decomposition. After purification, a greenish solid, which appeared to be a single compound on the basis of NMR data, but gave poor elemental analysis results, was recovered. The ^{1}H NMR spectrum shows a high field doublet of triplets centered at δ -6.86, split by *cis* $^{2}J_{PH}$ 22.9 Hz and *trans* $^{2}J_{PH}$ 111.1 Hz, assigned to Ru*H*. In the $^{31}P\{^{1}H\}$ NMR spectrum, the phosphorus atom in triphenylphosphine couples ($^{2}J_{PP}$, 12.2 Hz) with those in the biPSi unit to give a triplet (δ 6.5) for the former and a doublet (δ 42.6) for the latter. Compared to phosphite adduct 37, coupling with phosphine is smaller than with phosphites, so that the *trans* coupling between hydride and phosphine ($^{2}J_{PH}$ 111.1 Hz) is smaller than the similar coupling with phosphite ($^{2}J_{PH}$ 184.7 Hz), and the *cis* coupling with phosphine ($^{2}J_{PH}$ 12 Hz) is also smaller than the corresponding coupling with phosphite ($^{2}J_{PH}$ 25 Hz)..

Both 38 and 39 have characteristic downfield signals for the methoxyl groups: near δ 3.8 in ^{1}H NMR spectrum and δ 50 in the ^{13}C NMR spectrum. The IR spectra of

these two species show the absorptions for CO stretching: 1922 cm^{-1} for **38** and 1912 cm^{-1} for **39**, while **38** has another strong band at 2157 cm^{-1} for CN group.

Table 4-17. ^{1}H NMR data[a] for compounds 37 - 39

	^{1}H								
Compd	Ru*H*	$^2J_{PH}$	$^2J_{P'H}$	SiOC*H*$_3$	SiC*H*$_2$	SiCH$_2$C*H*$_2$	PC*H*$_2$	P(OC*H*$_3$)	^3J(POC*H*$_3$)
37a	-5.40(dt)	21.5	185.8	-	-	-	-	-	-
					0.64	1.73	2.34		
37b	-5.44(dt)	21.3	184.7	3.73	1.17	1.96	3.11	3.06	10.4
					0.74	1.74	2.19		
38	-5.76(t)	20.3	-	3.75	1.40	1.98	3.28	-	-
					0.69	1.61	2.36		
39	-6.86(dt)	22.9	111.1	4.00	1.12	2.03	3.32	-	-

[a] C_6D_6 was used as solvent; coupling constants were measured in Hz; P represents phosphines; P' represents phosphite for 37, triphenylphosphine for 39

Table 4-18. ^{31}P and ^{29}Si NMR data[a] for compounds 37 - 39

	^{31}P				
Compd	PR_3	$P(OR)_3/PPh_3$	$^2J_{PP'}$	^{29}Si	$^3J_{P'Si}$
37a	41.0(d)	-	25.4	4.5	8.3
37b	41.6(d)	135.9(t)	25.0	-8.8(d)	6.9
38	39.2	-	-	-9.2	-
39	42.6(d)	6.5(t)	12.2	-8.4(d)	4.6

[a] C_6D_6 was used as solvent; coupling constants were measured in Hz; P represents phosphines; P' represents phosphite for 37, triphenylphosphine for 39

Table 4-19. ^{13}C NMR data[a] for compounds 37 - 39

	^{13}C											
Compd	$SiOCH_3$	$SiCH_2$	$SiCH_2CH_2$	PCH_2	$J(P\text{-}CH_2)$	RuCO	$^2J(P\text{-}CO)$	$^2J(P'\text{-}CO)$	$P(OCH_3)$	$^2J(POCH_3)$	$C(CH_3)_3$	$C(CH_3)_3$
37a	50.61	17.02	18.68	-	-	-	-	-	-	-	-	-
37b	49.25	13.95	18.30	26.00(t)	12.5	202.83(q)	13.1	13.1	50.53(d)	4.0	-	-
38	49.92	14.34	18.46	27.26(t)	13.4	202.91(t)	12.6	-	-	-	29.74	55.45
39	49.61	14.38	18.56	26.49(t)	11.3	201.97(m)	-	-	-	-	-	-

[a] C_6D_6 was used as solvent; coupling constants were measured in Hz; P represents phosphines; P' represents phosphite for 37, triphenylphosphine for 39

The reaction of **36** with excess piperidine under mild conditions (78°C; 9 h) again produces two isomers **40a** and **40b**, presumably *syn* and *anti* respectively, in variable ratio (from 1:4 to 4:1) depending on experimental conditions. Both of these have been partially characterized by spectroscopic methods (Table 4-20). The piperidine ligand in **40** is labile and can be displaced by other stronger ligands, e.g., CO, trimethylphosphite, *t*-butyl isocyanide or triphenylphosphine, to form **36** (*syn*:*anti* ≅ 1:6), **37** (*syn*:*anti* ≅ 1:6), **38** (one isomer) and **39** (incomplete conversion) respectively.

Table 4-20. NMR data[a] for compounds **40a** and **40b**

		^{1}H		
Compd	^{31}P	Ru*H*	$^2J_{PH}$	SiOC*H*$_3$
40a	44.5	-12.54(t)	21.1	3.81
40b	45.0	-11.75(t)	19.5	3.84

[a] C_6D_6 was used as solvent; coupling constants were measured in Hz

On the basis of the investigation of substitution reactions of the dicarbonyl complexes **26**, **31** and **36**, one can conclude that both hydride and silyl groups show strong *trans* effects in six coordinate octahedral Ru(II) complexes, with the silyl ligand being the stronger of the two. The *trans* labilization by hydride or silyl groups has also

been observed in other Ru(II) complexes such as $RuHCl(CO)(PPh_3)_3$[139] and *cis*-$Ru(SiR_3)_2(CO)_4$.[140] The Ru(II) complexes discussed in this section can be divided into three categories according to their particular bonding modes. For **26** and **27**, alkylsilyl ligands are attached to Ru centers through Ru-Si bonds , while for **30**, **31**, **32**, **34**, **36**, **37**, **38** and **39** oxygen atoms have inserted into Ru-Si so that Si is connected to Ru through Ru-O-Si bonding. Complexes **36**, **37**, **38** and **39** are differentiated from **30**, **31**, **32** and **34** by a Me-O-Si-O-Ru linkage instead of Me-Si-O-Ru. It has been found that the complexes in each category are related by the similarity of their ^{29}Si NMR chemical shifts and coupling patterns (Table 4-21). The $\delta(^{29}Si)$ for **26** and **27** is close to zero ppm, while $\delta(^{29}Si)$ for **30**, **31**, **32** and **34** is in the range δ 4.5 - 8.5, and $\delta(^{29}Si)$ for **36**, **37**, **38** and **39** is near δ -9. The two-bond coupling between Si and P is much larger than the three-bond coupling.

Table 4-21. Comparison of ^{29}Si NMR data for complexes **26**, **27**, **30**, **31**, **32**, **34**, **36**, **37**, **38** and **39**

Connection	Compd	$\delta(^{29}Si)$ (C_6D_6)	$^2J_{PSi}$ (Hz)	$^3J_{P'Si}$ (Hz)
Ru-Si	**26a**	-2.5(t)	19.7	-
	27	-2.2(dt)	21.3 (*cis*)	-
			112.4 (*trans*)	
Ru-O-Si	**30**	8.1	-	-
	(toluene-d_8)			

	31	7.9	-	-
	32	4.6(d)	-	8.1
	33	6.0	-	-
Ru-O-Si-O-Me	**36b**	-8.2	-	-
	37b	-8.8(d)	-	6.9
	38	-9.2	-	-
	39	-8.4(d)	-	4.6

4.B.iv. Chlorination of Ru(biPSi)(H)(CO)$_2$ (26), Formation of Reactive Ru(II) species and Synthesis of Regiospecifically Labeled Isotopomers

It has been observed that conversion of a metal hydride to the corresponding chloride may occur in chlorinated solvents such as CCl_4 or $CHCl_3$ although the mechanism of this chemistry remains unclear. Accordingly, chlorination of Ru(biPSi)(H)(CO)$_2$ (**26**) takes place with excess CCl_4 in refluxing benzene solution to give a mixture of two chlorides **41a** and **41b**, ratio 1.5:1; complete reaction to pure product requires heating at 60°C for 6 h first then at 70°C for 1.5 h (Scheme 4-8). Monitoring the reaction using ^1H and ^{31}P NMR spectroscopy disclosed that complex **41a** was formed faster than **41b** and that prolonged heating led to the disappearance of both **41a** and **41b** accompanied by formation of some unidentified hydride, although the latter was not observed when **41** alone was heated in benzene. Almost pure **41a** (**41a**:**41b** ≅ 15:1) could be isolated by stopping the experiment at early stage. Either the isomeric

mixture of **41a** and **41b** or pure **41a** could be purified by removing volatiles under vacuum then washing the residue with hexanes. NMR data (Table 4-22: ^{1}H, ^{31}P and ^{29}Si NMR data; Table 4-23: ^{13}C NMR data) and elemental analysis indicate that **41a** and **41b** have the same composition and have two equivalent phosphines (singlet, ^{31}P NMR), one bonded silicon atom (triplet, ^{29}Si NMR), two carbonyl groups (two high-frequency triplets, ^{13}C NMR) and a chloride. The small coupling constants $^{2}J_{PSi}$ 11-16 Hz and $^{2}J_{PC}$ 10-15 Hz indicate that phosphines are *cis* to both the silicon atom and two carbonyl groups. Complex **41a** shows strong IR absorption at 1948 cm^{-1} with a weaker band at 2061 cm^{-1}, assigned to two conjugated CO stretching modes. The corresponding IR absorptions of **41b**, identified by comparison with those of pure **41a**, are found at 1964 cm^{-1} (s) and 2012 cm^{-1} (w). The molecular ion was not detected using fast atom bombardment (FAB) mass spectrometry: instead, an intense fragment ion was found corresponding to loss of one CO group and a chlorine atom from **41**.

When isolated pure, isomer **41a** is converted to a mixture of **41a** and **41b** in variable proportion at elevated temperature. Conversion of **41b** back to **41a** is not observed after a significant amount of **41b** was produced and then the mixture was cooled. These observations suggest that **41a** and **41b** are not in equilibrium, a different situation to that for the diastereoisomeric pair, *syn* **26a** and *anti* **26b**. Based on the fact that **41a** and **41b** have similar spectroscopic and analytical data, and that **41a** can be converted to **41b**, they are concluded to be *syn* and *anti* isomers. In the absence of a probe like the hydride signals of **26**, there is no satisfactory way of deciding which isomer is which by spectroscopic methods. X-ray crystallography would be required to fully identify the structures of **41a** and **41b**, but single crystals have not yet been obtained.

As discussed above, pure **41a** converts to a mixture of **41a** and **41b** on heating, but if this is prolonged or higher temperature is applied, both isomers slowly diminish as indicated by ^{1}H and ^{31}P NMR spectroscopy, while a new species accumulates (Scheme 4-8). Minor production of what may be paramagnetic impurities gives rise to an unresolved broad peak at δ 19 in the ^{31}P NMR, and some broad proton signals are also observed as the overall NMR resolution deteriorates significantly. Subsequent removal of volatiles and washing with methanol left a yellow powder **42**, which is stable for at least several days in air, and was characterized by spectroscopic methods (Figure 4-11: ^{1}H NMR spectrum; Table 4-22: ^{1}H, ^{31}P and ^{29}Si NMR data; Table 4-23: ^{13}C NMR data).

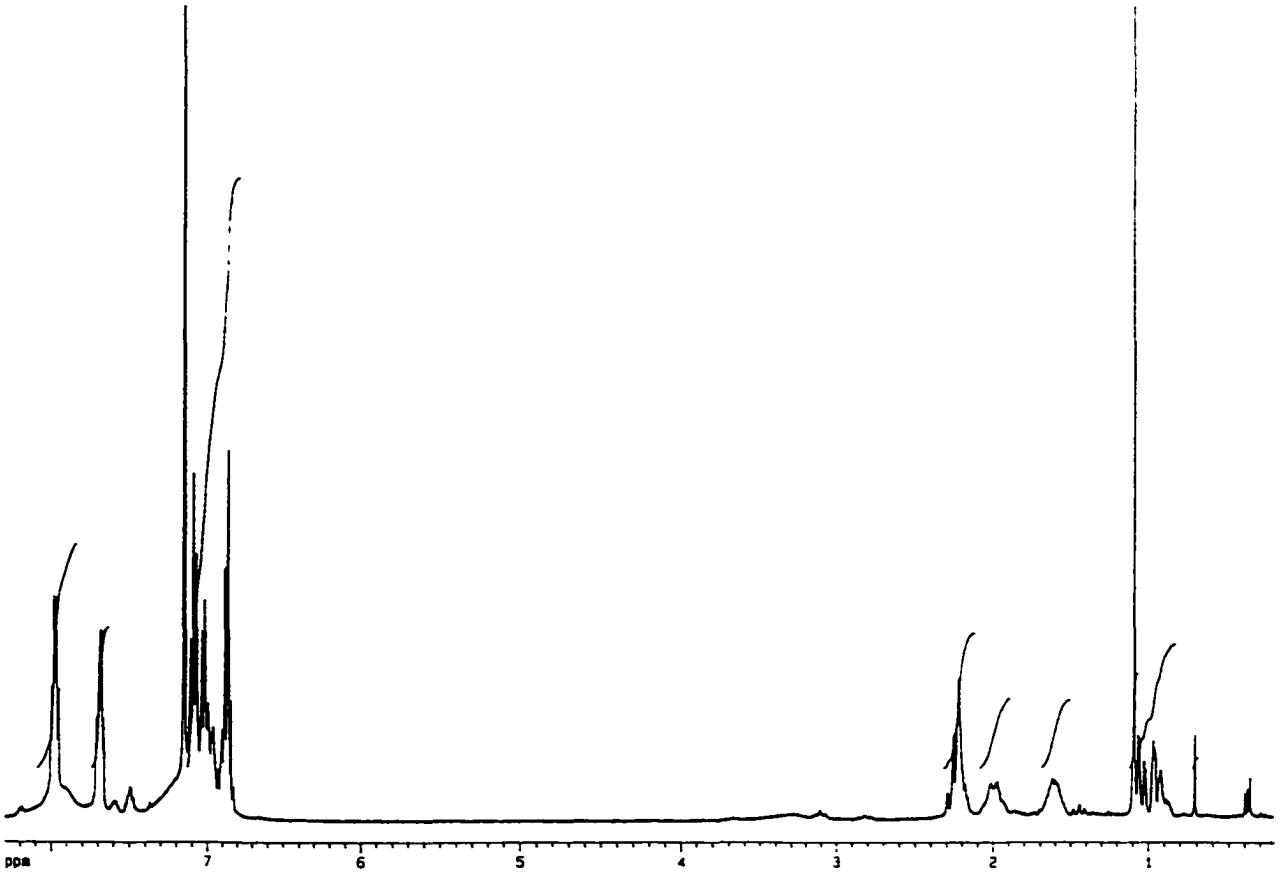

Figure 4-11. ^{1}H NMR spectrum for complex **42**

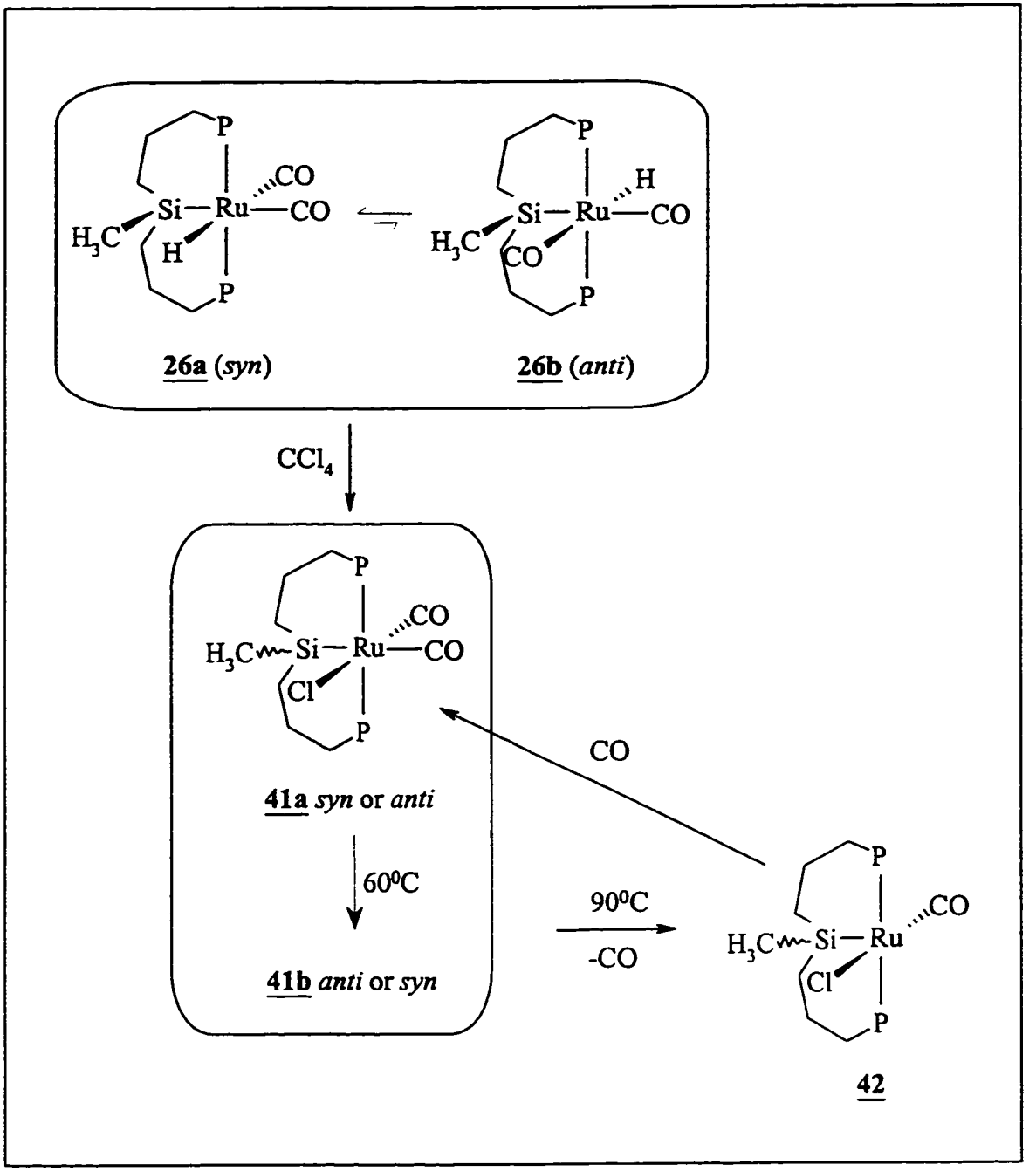

Scheme 4-8. Chlorination of complex **26** and formation of complex **42**

Table 4-22. ^{1}H, ^{31}P and ^{29}Si NMR data[a] for compounds **41a**, **41b** and **42**

				^{1}H	
Compd	^{31}P	^{29}Si	$^{2}J_{PSi}$	$RuSiCH_3$	$PCH_2CH_2CH_2Si$
41a	14.7	10.9(t)	11.0	0.40	2.34, 2.00, 1.86, 1.78, 1.89, 1.89
41b	13.9	1.7(t)	16.0	0.36	2.82, 2.22, 2.14, 1.68, 1.89, 1.89
42	17.6	53.7(t)	12.8	1.09	2.21, 2.21, 1.99, 1.61, 1.00, 1.00

[a] C_6D_6 was used as solvent; coupling constants were measured in Hz

Table 4-23. ^{13}C NMR data[a] for compounds **41a**, **41b** and **42**

				^{13}C			
Compd	$RuSiCH_3$	$SiCH_2$	$SiCH_2CH_2$	PCH_2	$J(P\text{-}CH_2)$	$RuCO$	$^{2}J(P\text{-}CO)$
41a	6.88	19.09	20.74	32.52(t)	15.8	202.41(t) 196.79(t)	14.6 12.2
41b	4.03	17.03	21.21	27.84(t)	15.0	201.70(t) 191.58(t)	11.5 10.4
42	5.38	19.19	21.48	30.77(t)	15.6	201.20(t)	13.4

[a] C_6D_6 was used as solvent; coupling constants were measured in Hz

The spectroscopic data for compound **42** are unusual compared to the six coordinate precursors including **26**, **27**, etc. The ^{1}H NMR shows a singlet at δ 1.09 for the Si*Me* group, which is about 0.5-0.7 further downfield than corresponding resonances in **26**, **27** and **31**. Only one CO signal was found in the ^{13}C NMR spectrum, split into a triplet by two equivalent *cis* phosphines. The extremely low field ^{29}Si NMR signal, δ 53.7, strongly suggests that the Si atom is *trans* to an unoccupied site. Similar low field ^{29}Si signals have been detected for a series of five coordinate Ru(II) complexes $Ru(SiR_3)Cl(CO)(PPh_3)_2$ (R = Me, Et or Ph, Table 4-24),[44] which are considered to have a square pyramidal geometry, as has been established by crystal structures of $Ru(SiR_3)Cl(CO)(PPh_3)_2$ (R = Et or OEt, Structure 4-A)[47] and $Os(SiX_3)Cl(CO)(PPh_3)_2$ (X = Cl, OH or Me).[47b, 136] In the FAB mass spectrum, the biggest intensity peak is at 627.1, due to the fragment ion $[Ru(biPSi)(CO)]^+$ formed by loss of a chlorine atom. The experimental pattern matches the simulated spectrum calculated for the molecular formula $C_{32}H_{35}OP_2SiRu$ (Figure 4-12). All these data strongly suggest a square pyramidal monocarbonyl structure for **42**, formed by CO elimination from the dicarbonyl **41**, where the silyl group lies at the apical site, though confirmation of this will require an X-ray crystal structure if a suitable single crystal can be obtained.

Table 4-24. The ^{29}Si chemical shifts and two bond P-Si coupling constants (in CH_2Cl_2/30% $CDCl_3$) for $Ru(SiR_3)Cl(CO)(PPh_3)_2$ (R = Me, Et or Ph)

R	$\delta(^{29}Si)$	$^2J_{PSi}$ (Hz)
Me	55.7	10.9
Et	71.7	11.7
Ph	40.3	13.1

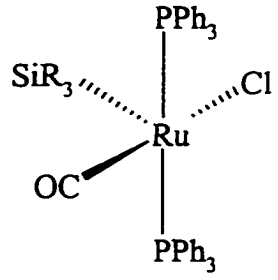

R = Et or OEt

(4-A)

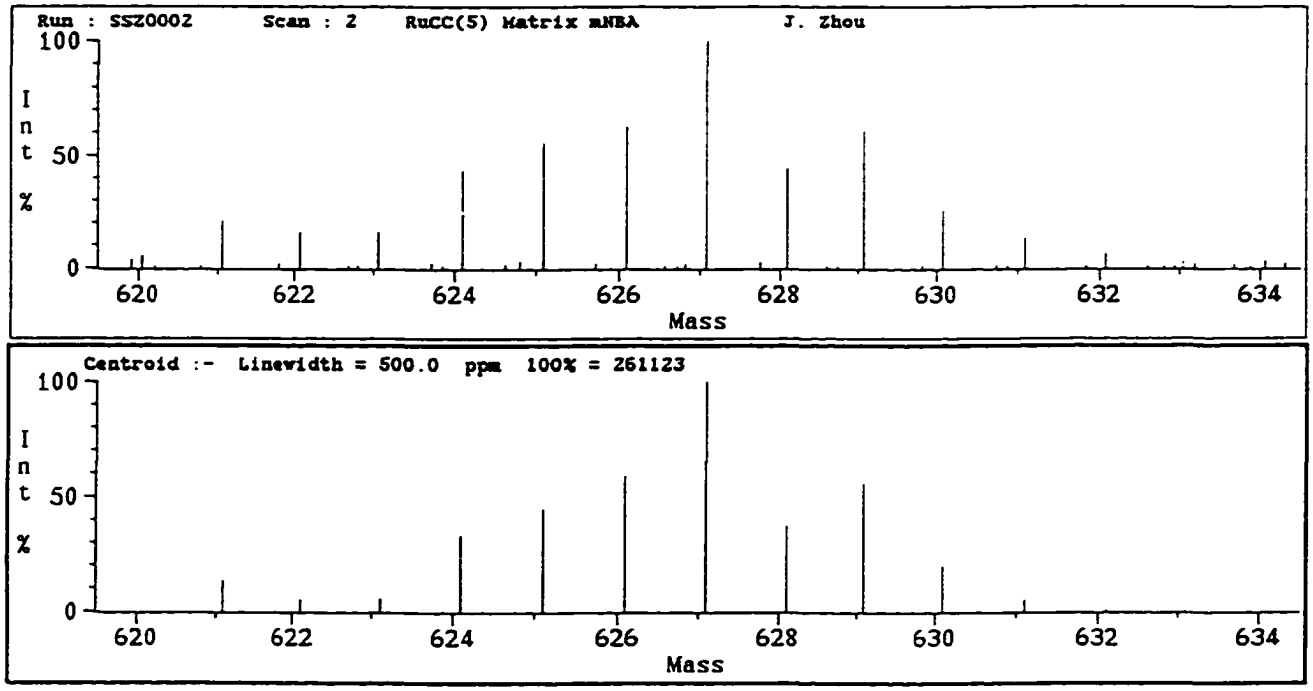

Figure 4-12. Mass spectrum of compound 42: upper, FAB data; lower, simulation for M - Cl fragment

A surprising property of 42 is the existence of three equally strong IR bands (rather than the expected one), at 1911, 1984 and 2048 cm^{-1} (KBr) and at 1911, 1993 and 2055 cm^{-1} (CH_2Cl_2 solution), as shown in Figure 4-13. This may imply the existence of three isomers, which must however be exchanging extremely fast, because only one

stereochemistry could be detected by VT-NMR techniques even at temperatures as low as -105°C in CD_2Cl_2. Roper and co-workers have also observed similar multiple IR bands (Table 4-25) in the series of five coordinate Ru(II) species, $Ru(SiR_3)Cl(CO)(PPh_3)_2$ (structure 4-A: $R_3 = Me_3$, Me_2OEt or Me_2Cl) but no explanation was given.[44]

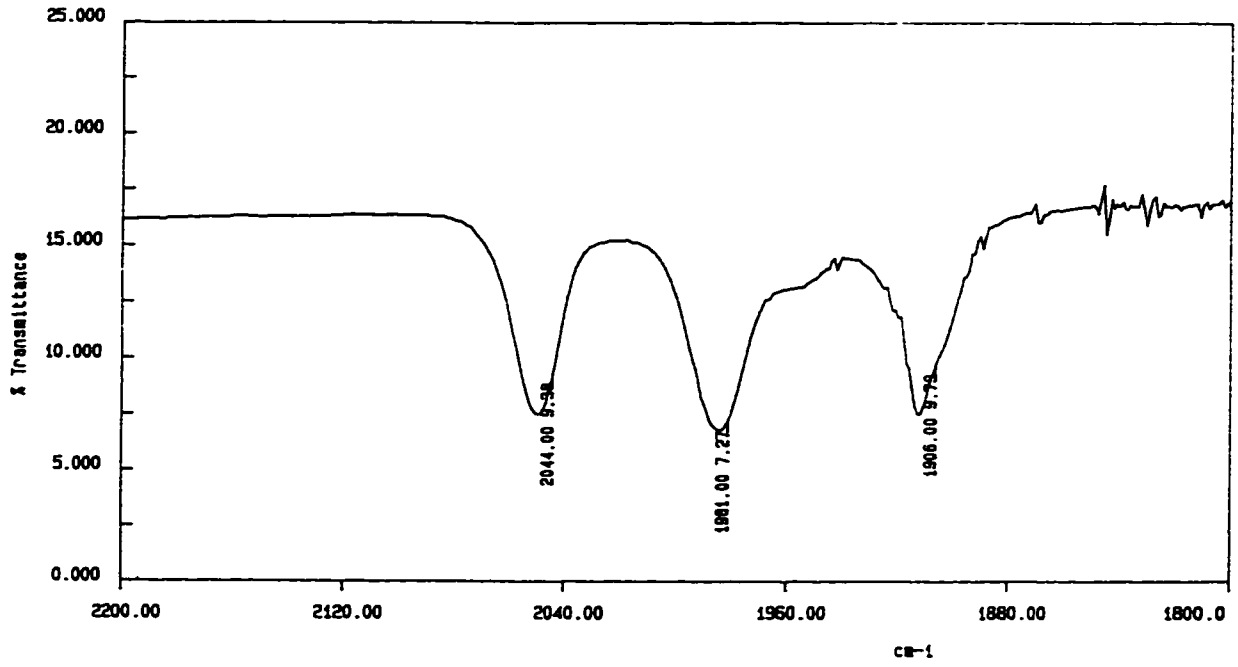

Figure 4-13. CO range of IR spectrum for complex 42

Table 4-25. IR frequencies[a] ν_{CO} for five coordinate $Ru(SiR_3)Cl(CO)(PPh_3)_2$

R_3	ν_{CO} (cm^{-1})
Me_3	1919, 1900, (1911[b])
Et_3	1904
Ph_3	1923

Me_2OEt	1925, 1910, (1923[b])
Me_2OH	1921
Me_2Cl	1944, 1929, 1917, (1933[b])

[a] Spectra recorded as Nujol mulls between KBr plates.

[b] Spectra recorded as dichloromethane solutions between KBr plates.

The formation of compound **42** from compound **41** simply on moderate heating implies that CO ejection from **41** is a thermodynamically favored process. Caulton and co-workers have explained the stability of a series of five coordinate 16e Ru(II) complexes, $RuHX(CO)(P^tBu_2Me)_2$ (X = I, Br, Cl, OR, NR_2, SR, C_2R or C_2H_2R), by proposing that these coordinatively unsaturated complexes are stabilized primarily by the strong σ donation of H and secondarily by π donation from X ligands to metal centers.[45] They also suggest the weak π bonding does not prohibit the complexes from undergoing addition reactions. Compound **42** is closely related to the species $RuHCl(CO)(P^tBu_2Me)_2$, so its thermal stability may be understood in the same way. Significantly, when CO is bubbled into a solution of **42**, it converts back to **41a** immediately, accompanied by the formation of only a small amount of **41b** (~5%; Scheme 4-8). The rapid specific regeneration of **41a** from **42** indicates that the two species may have similar configurations.

Caulton and co-workers have done an *ab initio* calculation and MO analysis in order to understand the reactivity dependence of the model compound $RuHCl(CO)(PH_3)_2$ on the particular ligand positions as shown below.[59c]

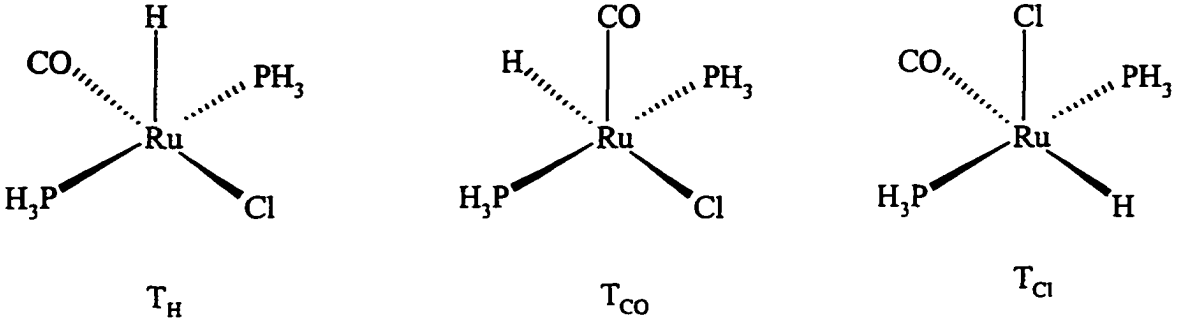

The *ab initio* potential energy surface for this complex, $E = f(\alpha, \beta)$ (where α and β are respectively the H-Ru-Cl and H-Ru-CO angles), shows that the transformation of T_H to T_{CO} corresponding to the opening of the Cl-Ru-H (α) angle, maintaining the H-Ru-CO (β) close to 90°, requires only 28 $kJmol^{-1}$ while the transformation of T_H to T_{Cl} needs 112 $kJmol^{-1}$. Consequently, the structure of the T_{CO}-type (although not of minimum energy) has a sufficiently low energy to be proposed as an active intermediate, together with the T_H configuration. The five coordinate energy surface also implies that attack of an incoming ligand is facile via direction **a** in the HRu(CO) plane.

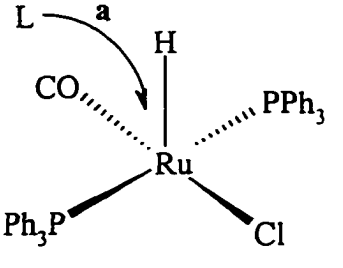

Similar arguments could be applied to silyl analogues, although the calculations have not yet been done and may be relevant to the substitution chemistry of **26**, **31** and **36** if entry of external substrate is channeled through a dissociative mechanism.

The ready thermal loss of CO from **41** accounts for why the FAB mass spectrum of **41** shows the same fragment ion as **42**.

The 18e and 16e chloro complexes **41** and **42** may prove to be useful precursors because substitution of Cl by a range of nucleophilic reagents is expected, including chloride abstraction by reagents such as $NaBF_4$ or silver salts in the presence of electron donors. The simplest reaction of this type is Cl^- displacement by hydride, the most commonly used reagents for which are $NaBH_4$ and $LiAlH_4$. The former is usually used as a milder hydride-transfer reagent in both aqueous and organic media. The latter is more reactive and can only be used under non-aqueous condition. In solutions of $LiAlH_4$, there exists free hydride, while in $NaBH_4$ solution the H^- ions are bonded to the boron center.[141] The reduction of metal chlorides with $NaBH_4$ can form mononuclear metal hydrides,[142] species containing one or two M-H-B bonds[142, 143] or dimers bridged through M-H-B bonds such as $[(P^iPr_3)_2(CO)HM(\mu\text{-}\eta^4\text{-}BH_4)MH(CO)(P^iPr_3)_2]^+$ (M = Ru or Os, Structure 4-B).[144]

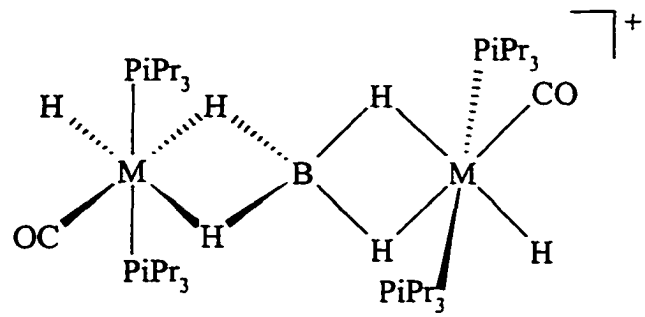

M = Ru or Os

(4-B)

Boron has two spin active isotopes: ^{10}B (natural abundance 19.6%; spin quantum number I = 3) and ^{11}B (80.4%; I = 3/2). Both of them have quadrupolar effects and interact with boron hydride to give broad hydride signals.

Addition of excess $NaBH_4$ to **42** in THF-d_8 immediately produced a yellow solution, which showed a sharp ^{31}P NMR signal at δ 24.2, together with a broad hydride signal at δ -6.8 and a sharp Si*Me* singlet at δ 0.57 in the ^1H NMR at ambient temperature. Further investigation using VT-NMR led to observation of a broad hydride peak at δ -3.3, which gradually narrowed as the temperature was lowered further below -20°C (Figure 4-14). At the same time, multiplets in the range δ -1 - 0.5 assigned to uncoordinated and excess borohydride became better resolved, while there was no change in the hydride signal at δ -6.8 or the ^{31}P resonance. At temperatures lower than -80°C, the two hydride signals (δ -3.3; -6.8) integrated in a 1:1 ratio. These data strongly suggest a structure containing a borohydride ligand attached by two Ru-H-B 3c-2e (three-center-two-electron) bonds for **43** though whether as *syn* or *anti* diastereomer is not obvious (eq 4-7).

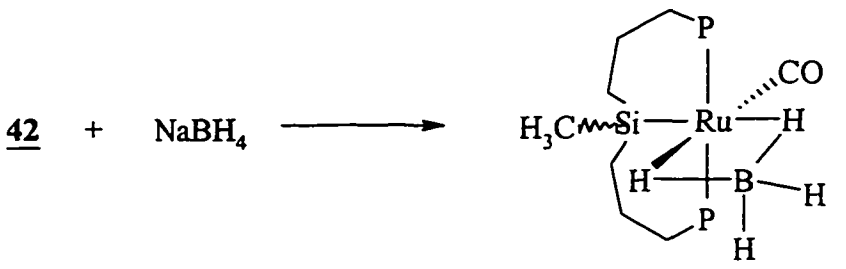

43

(4-7)

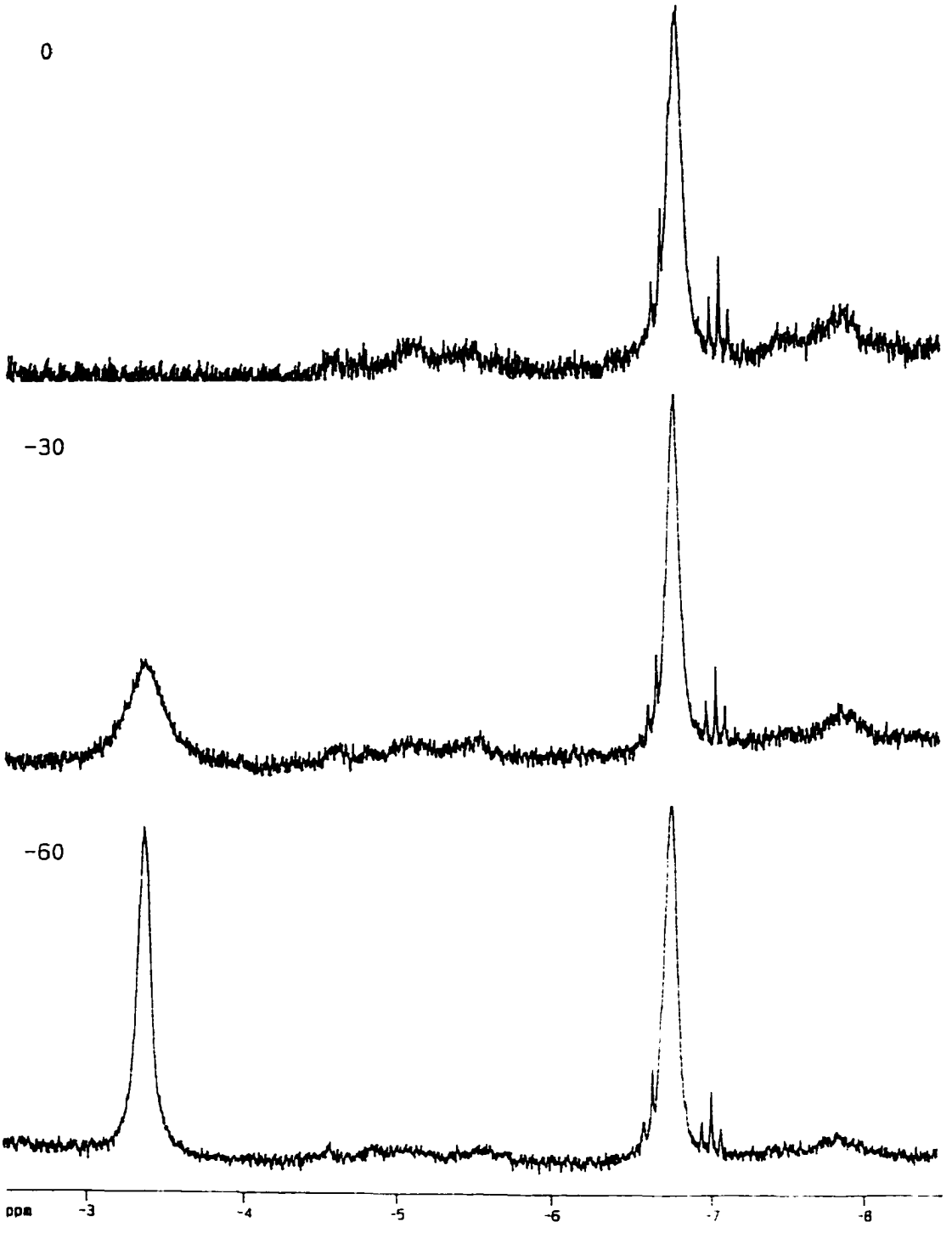

Figure 4-14. ^{1}H VT-NMR spectrum for complex 43

Such a structure for **43** was further suggested by the IR spectrum of the solution in THF-d_8, which showed three strong bands at 1930, 1987 and 2052 cm^{-1} attributable to CO and metal hydride stretching respectively.[141] Complex **43** slowly decomposed in solution, apparently by inter-molecular CO abstraction to give **26**, even under a dry inert-atmosphere. Attempts to isolate **43** left only a mixture in which **26** was the major component.

Bubbling CO through the solution of **43** accelerated this reaction, immediately forming **26** as the *syn* isomer (Scheme 4-9). As evidenced by ^1H and ^{31}P NMR: the formation of **26a** (*syn*) was confirmed by the characteristic ^{31}P (δ 31.3), hydride triplet Ru*H* (δ -6.69) and Si*Me* singlet (δ -0.09) in THF-d_8 solution (Table 4-1). Pure **26a** (*syn*) formed in this way slowly isomerized to an equilibrium mixture of **26a** and **26b** (*anti*) over 24 h. The immediate formation exclusively of **26a** in the reaction of **43** with CO may suggest a similar *syn* relationship in **43**, though an nOe-diff experiment failed to show interaction between the metal hydride (δ -6.79) and the Si*Me* group (δ 0.57).

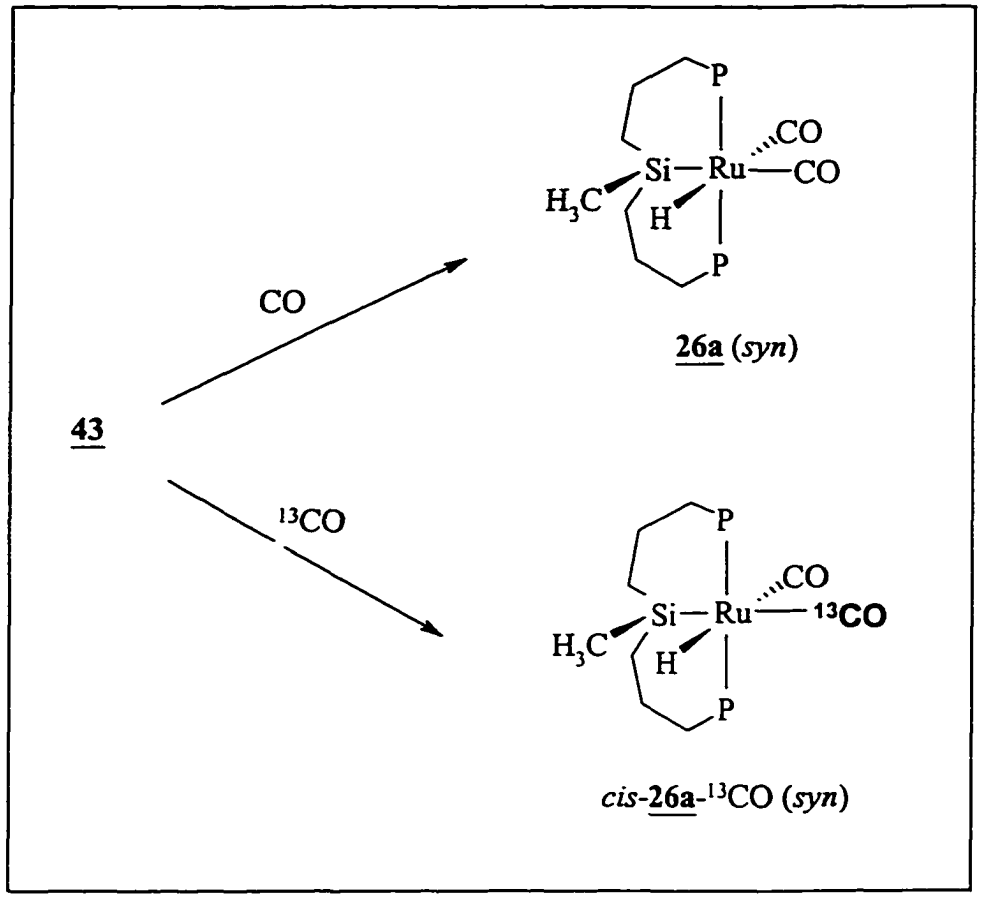

Scheme 4-9. Reaction of 43 with CO and ^{13}CO

The VT-NMR results also indicate one of the metal hydrides (δ -3.3) exchanges with other uncoordinated atoms of the borohydride group while the other (δ -6.8) does not (Figure 4-15). It is logical that the H_a is more labile than H_d since the silyl group has a stronger *trans* effect than CO. Fast exchange occurs between H_a with H_b, H_c at ambient temperature, while H_d is not involved. At low temperatures, the exchange is slowed so that H_a is resolved at δ -3.3. The high-field proton signal that is not involved in the exchange process is assigned to H *trans* to CO on the basis of the chemical shift (δ -6.8). As can be seen from Figure 4-14, the minor signals due to 26 is observed in the same

region. Broadening in the δ -6.8 resonance is consistent with a hydrogen atom attached to B, rather than a terminal Ru-H coupled only to *cis* P atoms.[141] Reaction of **43** with 99% isotope-enriched ^{13}CO led to formation of a labeled product *cis*-**26a**-^{13}CO (*syn*), ^{31}P shift (δ 31.4), doublet of triplet hydride (δ -6.41), as shown in Figure 4-16, and singlet Si*Me* (δ -0.09), in which the ^{13}CO group is introduced regiospecifically, *cis* to H and *trans* to silicon (Scheme 4-9). The mono-^{13}CO-labeled *cis*-**26a**-^{13}CO (*syn*) is unavoidably contaminated by **26** (~ 10%) which is formed in the decomposition of precursor **43**. The isotopomer *cis*-**26a**-^{13}CO (*syn*) was found to slowly scramble the ^{13}CO ligand, affording the three other possible isotopomers *trans*-**26a**-^{13}CO (*syn*), *cis*-**26b**-^{13}CO (*anti*) and *trans*-**26b**-^{13}CO (*anti*) over 24 h. These isotopomerization processes have been kinetically investigated and will be discussed in Section 4.B.v. All measured NMR parameters for *cis*-**26a**-^{13}CO (*syn*), *trans*-**26a**-^{13}CO (*syn*), *cis*-**26b**-^{13}CO (*anti*) and *trans*-**26b**-^{13}CO (*anti*) are compared in Table 4-26. The *trans* coupling constants $^{2}J_{C(13)H}$ of 18-22 Hz are comparable to the *cis* $^{2}J_{PH}$ in *trans*-**26a**-^{13}CO (*syn*) and *trans*-**26b**-^{13}CO (*anti*), giving the hydride signals a quartet-like appearance (overlapping doublet of triplets). By contrast, *cis* $^{2}J_{C(13)H}$ is relatively small, 3-7 Hz. The hydride NMR spectrum (Figure 4-17) for a mixture of these four isotopomers consists of overlapped doublets of triplets for *cis*- and quartets for *trans*-labeled isotopomers, and a triplet due to the contaminant **26**.

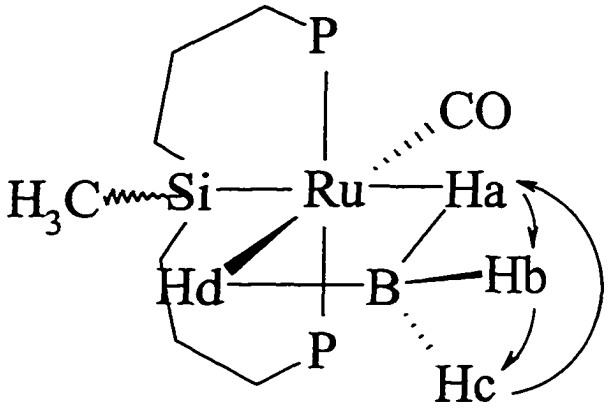

Figure 4-15. Exchange of hydrides in complex 43

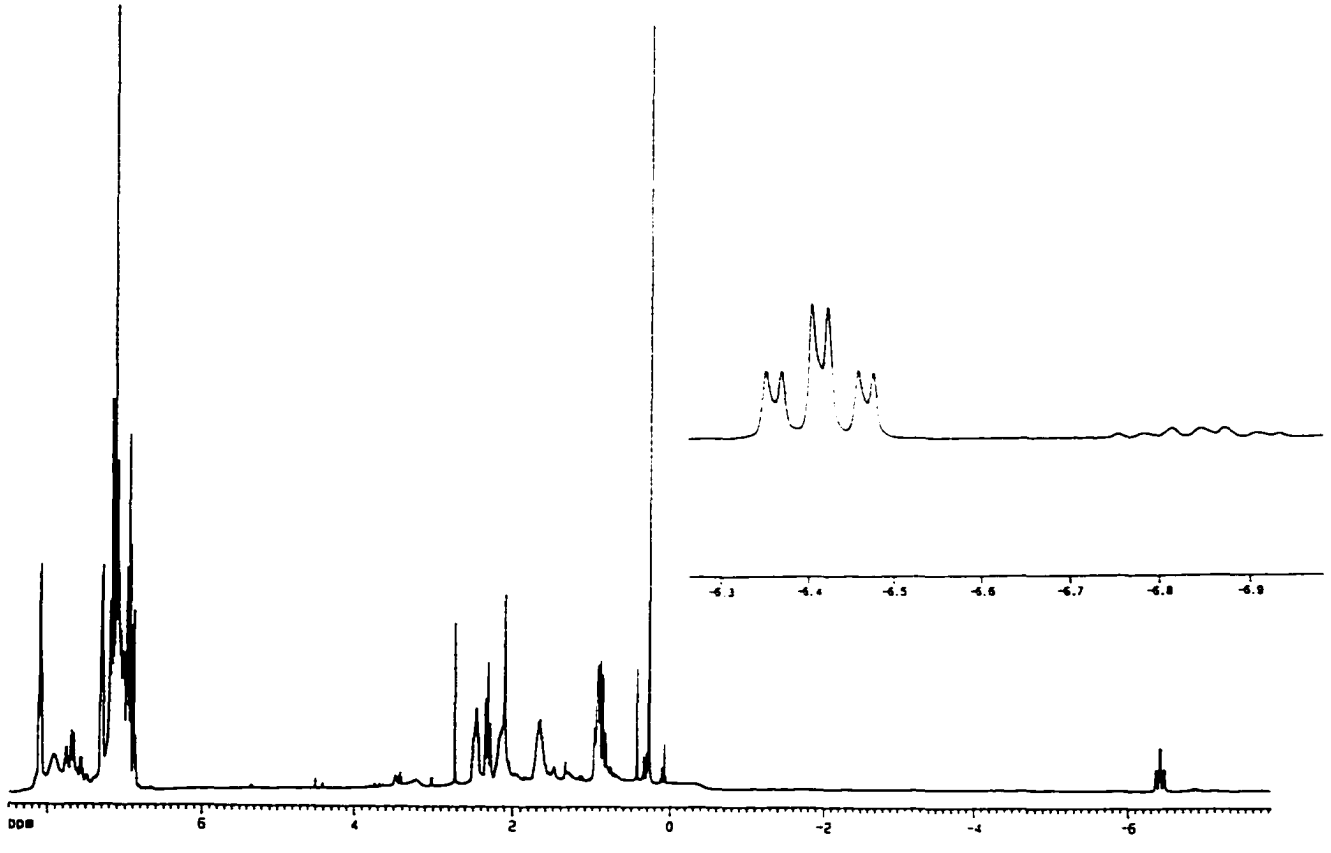

Figure 4-16. ^{1}H NMR spectrum for complex *cis*-26a-^{13}CO (*syn*)

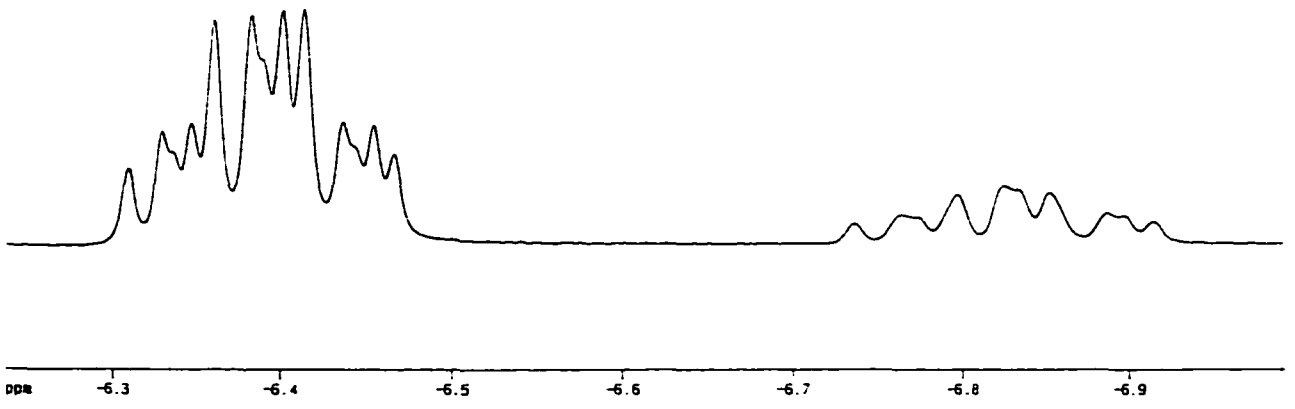

Figure 4-17. The hydride NMR spectrum for a mixture of four mono-^{13}CO-labeled isotopomers of **26**

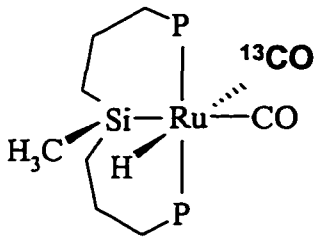

trans-**26a**-^{13}CO (*syn*)

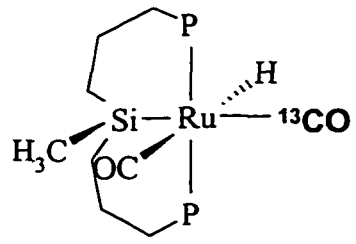

cis-**26b**-^{13}CO (*anti*)

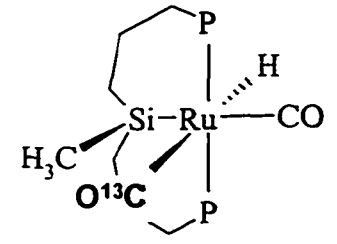

trans-**26b**-^{13}CO (*anti*)

Table 4-26. Important NMR data[a] for isotopomers *cis*-**26a**-^{13}CO (*syn*), *trans*-**26a**-^{13}CO (*syn*), *cis*-**26b**-^{13}CO (*anti*) and *trans*-**26b**-^{13}CO (*anti*)

		^{1}H			^{13}C	
Compd	^{31}P	Ru*H*	$^{2}J_{PH}$	$^{2}J(^{13}CO\text{-}H)$	Ru(^{13}*C*O)	$^{2}J(P\text{-}^{13}CO)$
cis-**26a**-^{13}CO (*syn*)	31.37(d)	-6.41(dt)	19.3	6.4	198.23(t)	10.5
trans-**26a**-^{13}CO (*syn*)	31.40(d)	-6.40(dt)	18.8	18.8	205.06(t)	8.7
cis-**26b**-^{13}CO (*anti*)	32.88(d)	-6.82(dt)	18.3	~3	199.04(t)	11.8
trans-**26b**-^{13}CO (*anti*)	32.90(d)	-6.82(dt)	22.0	21.4	203.92(t)	8.2

[a] C_6D_6 was used as solvent; coupling constants were measured in Hz

Werner has observed similar exchange processes in a Ru(II) system (Scheme 4-10).[145] The five coordinate hydride Ru(H)Cl(CO)$(PR_3)_2$ [R_3 = $^{i}Pr_3$ or $Me^{t}Bu_2$] was treated with $NaBH_4$ to give a non-rigid borohydride species in which H_b exchanges with H_c with H_a not involved below -30°C; H_d does not take part in the exchange at any temperature. Substitution with trimethylphosphine or trimethylphosphite introduces the new ligand at the site *trans* to H_d.

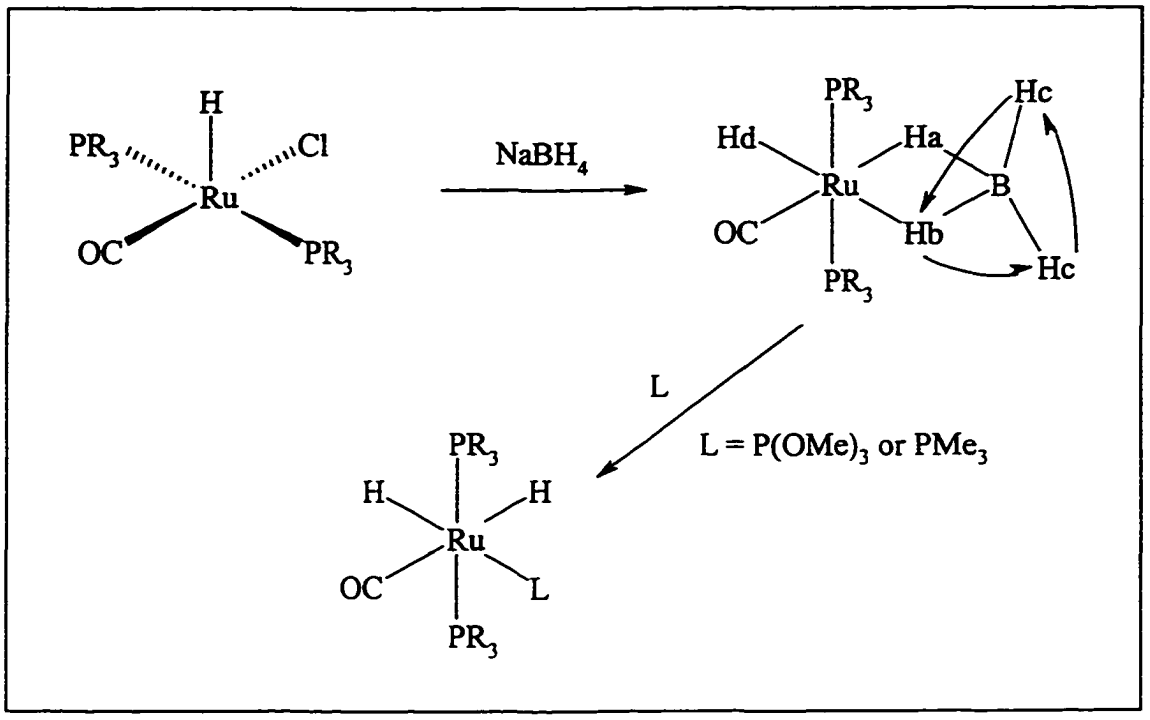

Scheme 4-10. Reduction of $Ru(H)Cl(CO)(PR_3)_2$ with $NaBH_4$

When the five coordinate chloride 42 was heated with excess $LiAlH_4$ in THF (instead of $NaBH_4$), an extremely air sensitive solution was obtained that could be examined only by using *in situ* NMR methods. The most striking feature of the ^1H spectrum is a broadened AB-like signal in the Ru-H range, near δ -10. This non first order hydride resonance is centered at δ -9.94, with the SiMe protons appearing at δ 0.11 as a sharp singlet; the intensity ratio between these two signals is clearly much higher than 1:3 although more accurate integration was not possible due to the presence of $LiAlH_4$. The ^{31}P NMR shows a singlet at δ 36.0; most surprisingly, none of the NMR data showed any temperature dependence, but the symmetrical multiplet hydride signal collapsed to a singlet on irradiation at the ^{31}P frequency. These data imply that more than one H atom is bonded per metal center; from the ^{31}P NMR the two biPSi phosphorus nuclei are

chemically equivalent; and that the hydride sites are also chemically equivalent. Attempts at simulation of an AX_2 or AXX' spin system gave no fit with the observed hydride resonance. A simulated pattern resembling the latter was obtained by using an AA'XX' spin system, and then it was learned that complexes of the type $Os(H)_2(P^iPr_3)_2(PHPh_2)_2$ synthesized by the Esteruelas group at Zergoza give virtually identical high field proton signals.[146] These are molecules in which two metal hydrides and four phosphorus nuclei are mutually all *cis*. Refinement of the computer simulation on the basis of AA'XX' coupling led to acceptable fit between calculated and observed patterns (Figure 4-18) with the coupling constants that are listed in Table 4-27. The mutually *trans* hydride and phosphine give large coupling constants (66 - 68 Hz) and the *cis* hydride and phosphine gives small negative coupling constants (-24 - -27 Hz). The small $^2J_{HH'}$ 4.68 Hz and $^2J_{PP'}$ 11.70 Hz indicates the *cis* relationships between two hydrides and two phosphines respectively.

The product of reaction between **42** and excess $LiAlH_4$ is therefore the novel *fac* anionic complex **44** (eq 4-8). The counterion of this anionic ruthenate(II) species is most likely to be Li^+. Attempts at isolation by removal of the THF led to rapid blackening of the solution, and re-dissolution of the solid residue showed the presence of compounds **26a** and **26b** detected as the only identifiable hydride products of decomposition by ^{31}P NMR spectroscopy. Even under inert and dry atmosphere, it still slowly decomposed to afford **26a** and **26b**. This process was slower at low temperatures.

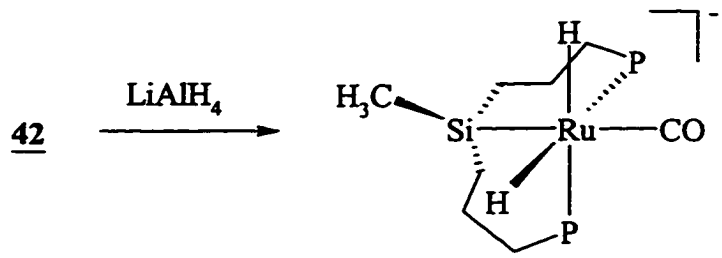

44 (4-8)

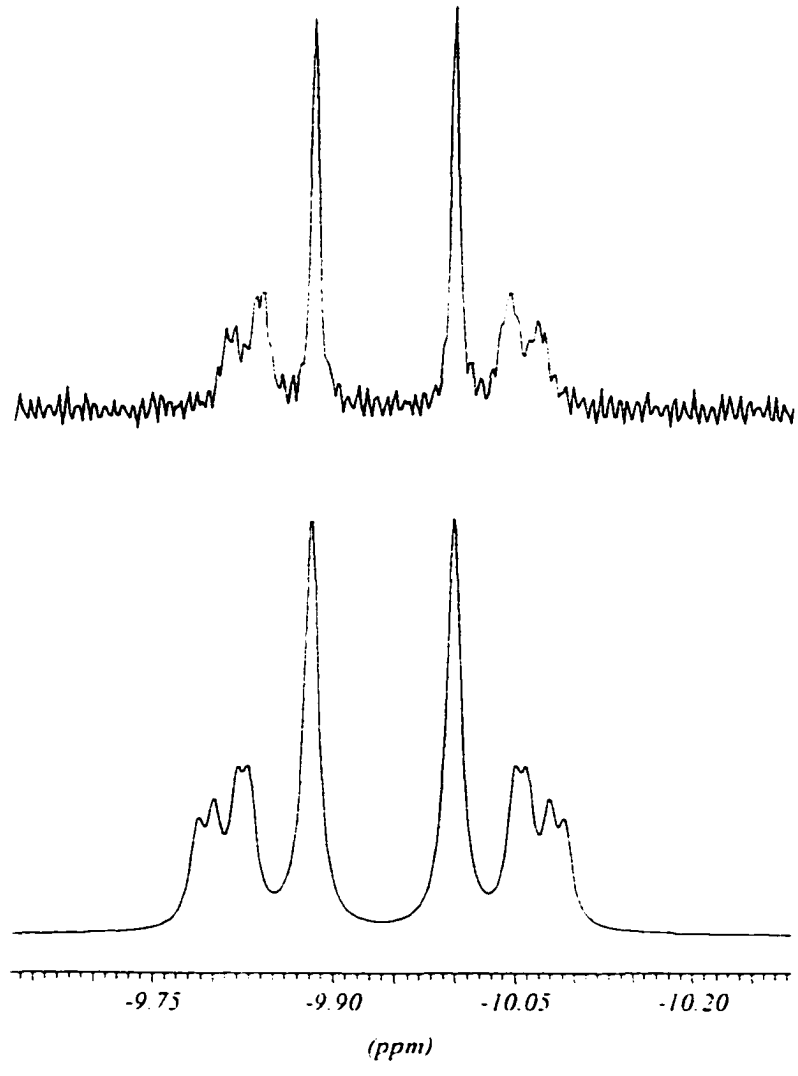

Figure 4-18. Experimental and simulated hydride signal for anion **44**

Table 4-27. The best fit coupling constants (Hz) for anion **44**

	H^1	H^2	P^1	P^2
H^1	-	4.68	68.06	-24.46
H^2	4.68	-	-26.98	66.81

P^1	68.06	-26.98	-	11.70
P^2	-24.46	66.81	11.70	-

Anion **44** was concluded to have a *syn* configuration on the basis of a nOe-diff experiment. Irradiation of the hydride peak at δ -9.94 enhanced significantly the Si*Me* signal at δ 0.11 as well as the *ortho* hydrogen signal on phenyl groups at δ 7.8 (Figure 4-19).

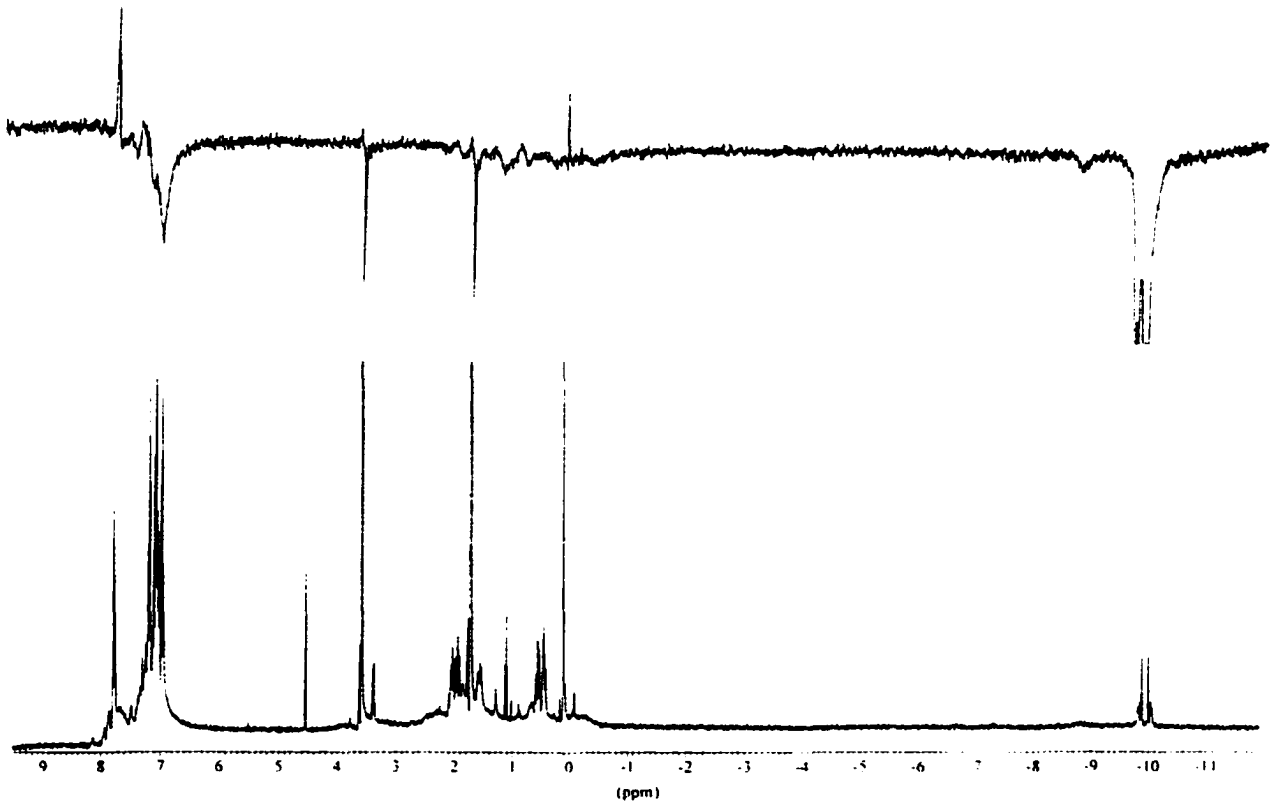

Figure 4-19. nOe-diff experiment for anion **44**

The stereochemistry of **44** was further investigated by synthesis of its deuterio-analogue **44**-d_2. Anion **44**-d_2 was prepared from **42** and $LiAlD_4$ in THF and examined *in situ* using ^2H and ^{31}P NMR spectroscopy. The deuterium nucleus has a spin quantum number I = 1, giving rise to 1:1:1 triplet structure when it couples to other spin active nuclei. The coupling constants of deuterium with other spin active nuclei are usually much smaller than the corresponding couplings to a proton. The ^2H NMR spectrum of **44**-d_2 consists of a broadened doublets resonance at δ -9.87. The corresponding ^{31}P NMR signal is complicated by coupling with two deuterium nuclei and apparent slight inequivalence between the two ^{31}P nuclei. Computer simulation of both ^2H and ^{31}P NMR signals using an AA'XY coupling pattern gave a good fit between calculated and experimental spectra (Figures 4-20 and -21), with the best fit parameters listed in Table 4-28. Comparison of calculated couplings for the deuterio- and protio- (Table 4-27) systems shows agreement between the two except that the *cis*- and *trans*-$^2J_{PD}$ (0.5-2 Hz and 8.5 Hz respectively) are all much smaller than the corresponding $^2J_{PH}$.

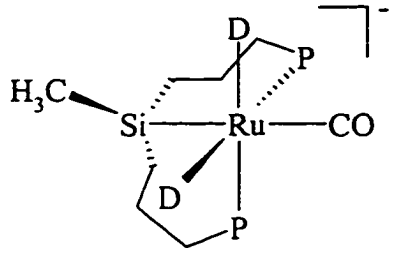

44-d_2

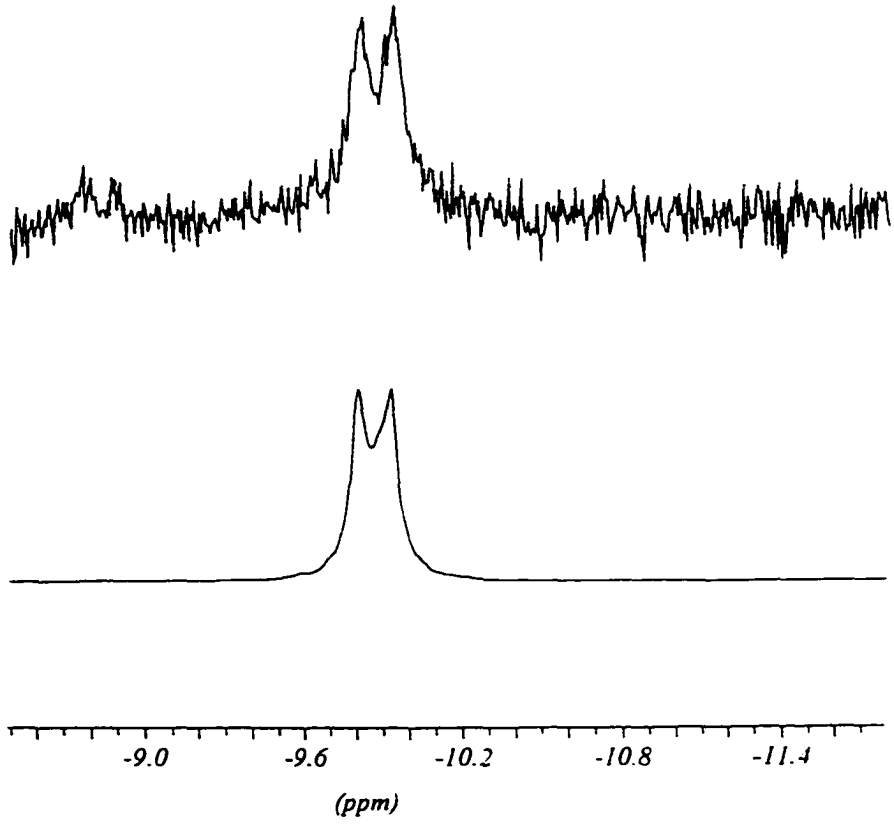

Figure 4-20. Experimental and simulated ^{2}H NMR spectra for anionic deuteride **44**-d_2

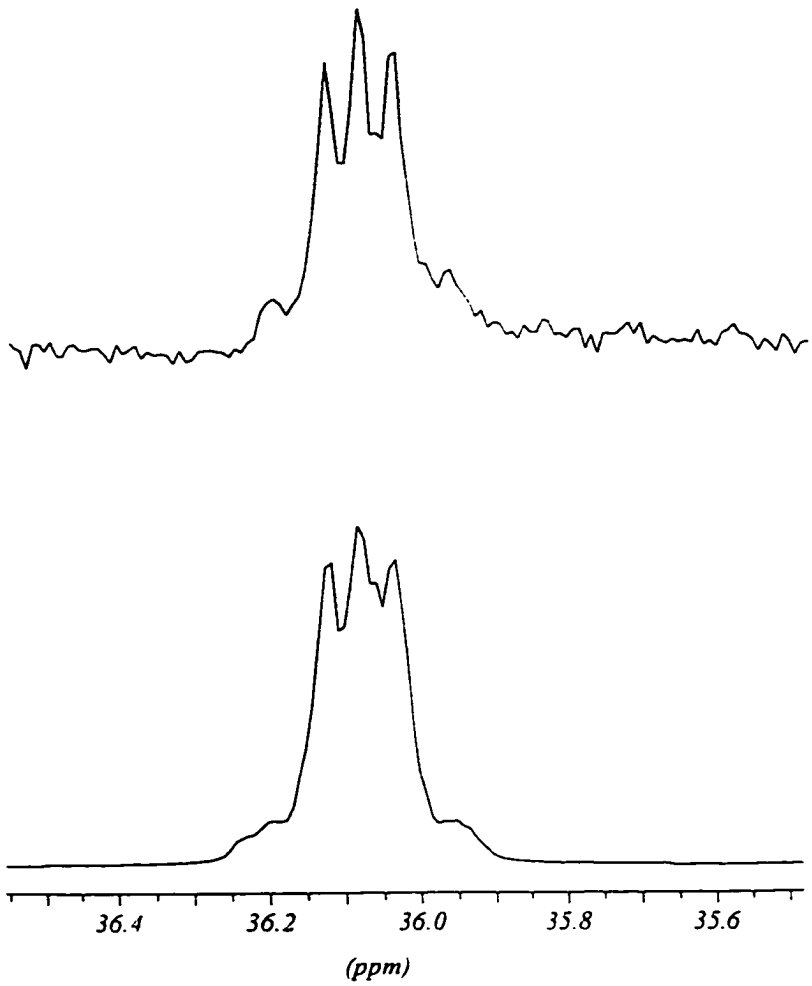

Figure 4-21. Experimental and simulated ^{31}P NMR spectra for anionic deuteride 44-d_2

Table 4-28. The best fit NMR parameters for anionic deuteride 44-d_2

	D^1	D^2	P^1 (δ 36.0)	P^2 (δ 36.1)
D^1	-	-2.46	8.41	-1.86
D^2	-2.46	-	-0.59	8.58

P^1 (δ 36.0)	8.41	-0.59	-	11.43
P^2 (δ 36.1)	-1.86	8.58	11.43	-

Transition metal hydride complexes can range from predominantly acidic ($L_nM^{\delta-}H^{\delta+}$) to hydridic ($L_nM^{\delta+}$-$H^{\delta-}$) in character, depending on the nature of the metal atom and charge-transfer characteristics of the complementary ligands. Some metal carbonyl hydrides, e.g., $HCo(CO)_4$ and $H_2Fe(CO)_4$, behave as acids in aqueous solution and are good examples for the former. Hydridic metal complexes are common in early transition metal chemistry, e.g., $Cp_2Zr(H)Cl$ and Cp^*ZrH_2 and hydridometalates containing strongly π-acid ligands such as $Na^+[HFe(CO)_4]^-$ and $Na_3^+[HCo(CN)_5]^{3-}$ are also well-known,[147a] with electronegative ligands tending to stabilize the electron rich complex anion species. Hydridometalates containing only weakly π-acceptor ligands are relatively rare. Some known examples include $Et_4N^+[ReH_8(PPh_3)]^-$,[147b] K_2TcH_9,[147c] K_2ReH_9,[147d] Li_4RhH_4, Sr_2RuH_6, Sr_2RhH_5,[147e] $Na^+[Ru(dppe)_2H]^-$ [dppe = 1,2-bis(dimethylphosphino)ethane].[147f] Halpern et al prepared two unusual Ru(II) polyhydride anions; *fac*-$[RuH_3(PPh_3)_3]^-$ was isolated as a yellow K^+ salt and the five coordinate $[RuH_3(PPh_3)_2]^-$ was observed only in solution. The hydride ^1H NMR signal of the former has an AA'A''XX'X'' pattern.[148] Caulton reported an Os(II) analogue, $K^+[OsH_3(PMe_2Ph)_3]^-$ and found from its crystal structure that it consists of centrosymmetric $K_2^+[Os(\mu\text{-}H)_3(PMe_2Ph)_3]_2^-$ dimers.[149] Pez found that the potassium hydrido(phosphine)ruthenate complexes $K^+[(Ph_3P)_2Ph_2PC_6H_4RuH_2]^-\cdot C_{10}H_8\cdot(C_2H_5)_2O$ ($C_{10}H_8$ = naphthalene) and dimeric $K_2^+[(Ph_3P)_3(Ph_2P)Ru_2H_4]^{2-}\cdot 2C_6H_{14}O_3$ ($C_6H_{14}O_3$ = diglyme) were good catalysts for the

hydrogenation of ketones, aldehydes and activated carboxylic acid esters.[150] The crystal structures of both these anionic hydrido-complexes were determined.

It is always a problem to stabilize hydridic metal anions as solids since most of them are extremely air sensitive and some are thermodynamically unstable. Two possible approaches are the use of large cations or alternatively, coordination of the cations with an appropriate crown ether. The first of these is illustrated by crystallization of the anion $[RuH(CO)_4]^-$ as its PPN^+ salt,[151] [PPN^+ = bis(triphenylphosphine)iminium]. The second, by isolation of the polyhydridoruthenate anion, $K[RuH_3(PPh_3)_3]$, in high yield on addition of one mole equiv of 18-crown-6 ether.[152a] In crystals of the latter, the potassium cation was found to be trapped and protected by the crown ether. The use of 18-crown-6 even led to stabilization of the potassium salt of first "naked" anionic molybdenum carbide complex.[152b] Effort to produce **44** as its potassium salt has not been successful: the five coordinate chloride **42** was found not to react with potassium hydride. The stabilization and isolation of the electron rich anion **44** through combination with a large cation, such as PPN^+, has not yet been attempted.

The reaction in which **44** is formed appears to be slow, and during hours (at ambient) or a period of minutes (80°C), hydride intermediates which all have poorly resolved hydride signals in the range from δ -7 to -11 were observed, possibly due to intermediates involved in the configurational change from *ax-eq-ax-* **42** to *fac-***44**.

Solutions containing complex **44** reacted with CO immediately to give a mixture of **26a** and **26b**, but in 2.4:1 ratio, *i.e.*, enriched in the less stable *anti* diastereomer (**26b**) compared with the 4.5:1 equilibrium distribution although the mechanism of what is

formally displacement of H^- by CO is not known. The anion **44** is coordinatively saturated, is 18e Ru(II), and carries a negatively charged ligand so that ligand dissociation to produce a free site may be the first step. When a large excess of $LiAlD_4$ was added to solutions containing **44** and AlH_4^- ions, no isotopic substitution of the bound hydrides in **44** was observable, and similarly when the corresponding dideuterio-anion was treated with $LiAlH_4$ no isotopic exchange could be detected. A possible dissociative mechanism that accommodates CO entry may involve temporary displacement of a chelate P atom.

Reduction of the six coordinate chloride **41** with excess $LiAlH_4$ in THF at room temperature gave immediately **26a** and **26b**, along with a small amount (~20%) of a new species **45**. In this reaction, the *anti* isomer **26b** was formed faster than *syn* isomer **26a** so that the ratio of **26a**:**26b** was approximately 2:3. The distribution returned to the equilibrium ratio (4.5:1) only after the solution had stood at room temperature for 24 h. The formation of the new complex **45** was unexpected. It has been only tentatively identified by solution NMR spectroscopy, because it could not be recovered as a pure compound. It is distinguishable by a hydride triplet at δ -7.94 ($^2J_{PH}$ = 16.4 Hz), a silicon methyl singlet at δ 0.12, and a ^{31}P singlet at δ 32.9. It did not convert to **26** over one day at ambient temperature. Interestingly, gently heating the solution (60°C) slowly converted **45** into the previously characterized hydridic anion **44**, which as has been shown reacts readily with CO to give **26**. Based on the these observations, compound **45** is assumed to be another isomer of **26a** and **26b**, in which two carbonyl groups are *trans* to one another.

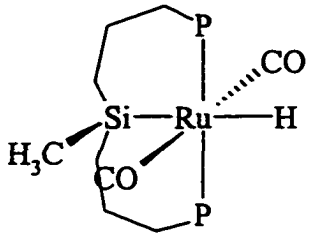

45

The proposed structure for **45** is unusual because it places two strongly *trans* influencing ligands, silyl and hydride, *trans* to each other, implying that it may be thermodynamically unfavorable. Some *trans* dicarbonyl Ru(II) complexes have been reported such as all-*trans*-$[Ru(CO)_2L_2Cl_2]$ (L = PMe_2Ph)[153, 154] and *trans*-$[Ru(CO)_2(PPh_2CH_2CH_2SiR_2)]$ (R_2 = Me_2, Ph_2 or MePh) (Structures 4-C and 4-D).[34] The IR absorption due to CO stretching in (4-C) was found at 2012 cm^{-1}. The all-*trans* isomer of $Ru(CO)_2L_2Cl_2$ was observed to isomerize to the *cis* isomer under heating, and the process was proposed to involve dissociation and re-association of CO. It was also found that one of the carbonyl groups was labile and was displaced by phosphorus-containing ligands, pyridine, ammonia, piperidine, acetonitrile or ethlyene. Low IR frequencies (1910-1940 cm^{-1}) were observed for the carbonyl groups in structure 4-D, indicating stronger M-C bonds. The carbonyl groups were found not to be affected by the neutral substrates such as ethylene, triphenylphosphine and trimethylphosphite using thermal or photochemical activation. Clearly the *trans* dicarbonyl complex **45** undergoes substitution of one CO with H^- on heating, giving the *fac* dihydrido anion **44**, but since this chemistry takes place *in situ* with excess $LiAlH_4$ present no further CO displacement chemistry could be explored.

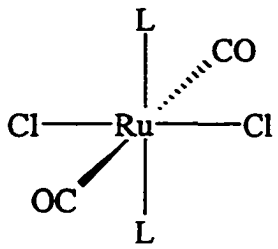

L = PMe_2Ph

(4-C)

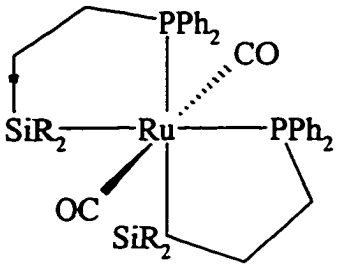

R_2 = Me_2, Ph_2 or MePh

(4-D)

The Ru chemistry discussed above opens up two synthetic routes to the deuterium-labeled analogues *syn* **26a**-*d* and *anti* **26b**-*d* of the hydrido complexes *syn* **26a** and *anti* **26b**. One of these involves a four-step synthesis, through the sequence **26** - **41** - **42** - **44** - **26**-*d*; while the other takes place in three steps, by the sequence **26** - **41** - **45** - **26**-*d*. The second process was found to produce cleaner labeled products. Complexes **26a**-*d* and **26b**-*d* have been characterized using ^1H, ^{31}P and ^2H NMR and IR spectroscopy, and elemental analysis. The ^1H NMR spectrum recorded in toluene-d_8 is the same as that for **26** except there are no hydride signals. Two singlets at δ 31.5 and 32.8 in the ^{31}P NMR are assigned to **26a**-*d* and **26b**-*d* respectively. The ^2H NMR spectrum shows two unresolved broad peaks, at δ -6.34 for the major diastereomer and δ -6.79 for the minor product. The equilibrium ratio **26a**-*d*:**26b**-*d* is approximately 4.5:1, identical with the distribution for hydride analogue. The IR spectrum shows two strong bands at 1995 and 1932 cm^{-1} for carbonyl stretching, while ν_{RuD} was not found.

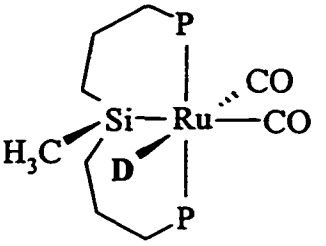

syn 26a-*d*

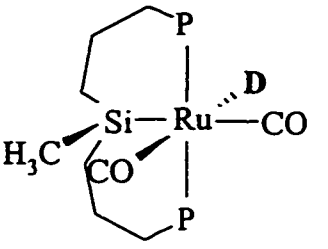

anti 26b-*d*

4.B.v. Isomerization and Inter/intra-molecular CO Exchange in Ru(biPSi)(H)(CO)$_2$ (26)

The tridentate chelating framework of bisphosphinoalkylsilyl (biPSi) ligand presents two different molecular faces by ax-eq-ax attachment in a TBP complex or mer-complexation in octahedral geomerty. This differentiates *syn* and *anti* diastereomers in platinum group metal complexes. It is a feature of these systems that the energy difference between *syn* and *anti* isomers appears to be quite small, so that equilibrium distributions are controlled by *syn*:*anti* diastereoisomerization. Such an isomerization process that converts the 5-coordinate complex *syn*-RhH(biPSi)Cl [biPSi = bis(diphenylphosphinopropyl)methylsilyl] to its *anti* isomer has been observed to be slow and has been kinetically investigated by Gossage and Wang in earlier work in this laboratory.[55] Both *syn* and *anti* isomers are of comparable thermodynamic stability (ΔG_{298}° ~ 5 kJmol^{-1}) so an equilibrium exists between them. The *syn* isomer of RhH(biPSi)Cl was observed to slowly isomerize to the *anti* isomer through an observable Rh(III) intermediate (Scheme 4-11). A kinetic analysis identified the isomerization as a first-order process and gave the activation parameters as $\Delta G_{298}^{\ddagger}$ = 95(4) kJmol^{-1}, $\Delta H^{\ddagger}$ =

71(2) kJmol^{-1}, $\Delta S^{\neq}$ = -82(7) JK^{-1}mol^{-1} and E_a = 70 kJmol^{-1}, and a mechanism was proposed to involve intra-molecular rearrangement without bond-breaking.

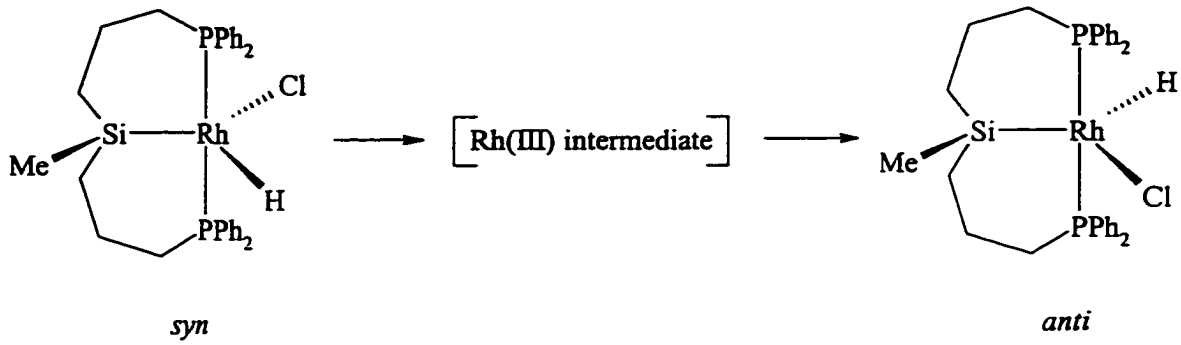

syn *anti*

Scheme 4-11. Isomerization of a Rh(III) system

The octahedral RuH(biPSi)(CO)$_2$ (**26**), which is closely related to the dist-TBP complex RhH(biPSi)Cl referred to above, can be isolated as the pure *syn* isomer **26a** by repeatedly washing the original mixture of *syn* **26a** and *anti* **26b** with hexanes. No isomerization occurs in the solid state, but in solution **26a** obtained in this way isomerizes over several hours to an equilibrium mixture of **26a** and **26b**, in 4.5:1 ratio at ambient temperature (22°C). Lower equilibrium *syn*:*anti* ratios were formed at higher temperature, e.g., 4.0 at 34°C and 3.6 at 45°C. Monitoring the isomerization [**26a** (*syn*) → **26b** (*anti*)] in toluene-d_8 by using ^{1}H NMR spectroscopy (Figure 4-22 and Appendix D.i.), and applying the method for kinetic analysis shown in Appendix C, this isomerization was found to be independent of concentration (1.06 x 10^{-1}, 5.33 x 10^{-2} and 2.56 x 10^{-2} M) and was shown to be a first-order process. There is no significant solvent effect, since a rate difference of only 18% could be observed between non-polar toluene-d_8 (k_{295} = 5.25 x 10^{-6}

s^{-1}) and polar THF-d_8 ($k_{295} = 6.30 \times 10^{-6}$ s^{-1}). By contrast, the ratio k(toluene-d_8)/k(CD_2Cl_2) was found to be in the range 2.9-3.8 for the intra-molecular fluxional behavior of $Ir(H)_2X(P^tBu_2Ph)_2$ (X = Cl, Br or I) at 200 K.[155] The rate constants of isomerization of **26** were measured to be 5.25×10^{-6}, 3.58×10^{-5} and 1.72×10^{-4} s^{-1} respectively at 295, 307 and 318 K (Figure 4-23). An Eyring plot of ln(k/T) *vs* T^{-1} gives the activation parameters as $\Delta G^{\ddagger}_{295} = 102 \pm 5$ kJmol^{-1}, $\Delta H^{\ddagger} = 113 \pm 7$ kJmol^{-1}, $\Delta S^{\ddagger} = 37.4 \pm 2.0$ JK^{-1}mol^{-1} (Figure 4-24).

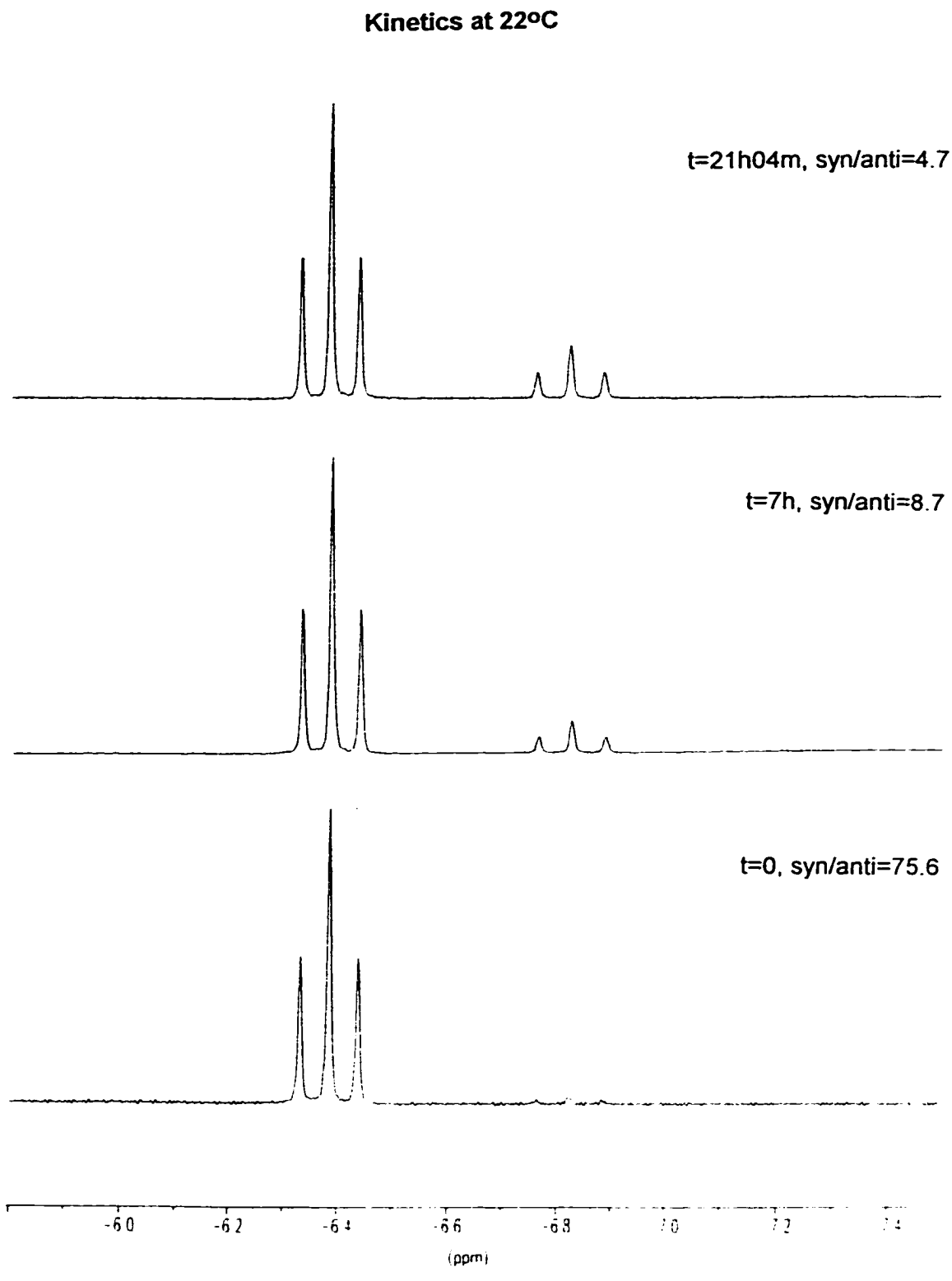

Figure 4-22. ^{1}H NMR spectra for isomerization *syn* **26a** → *anti* **26b**

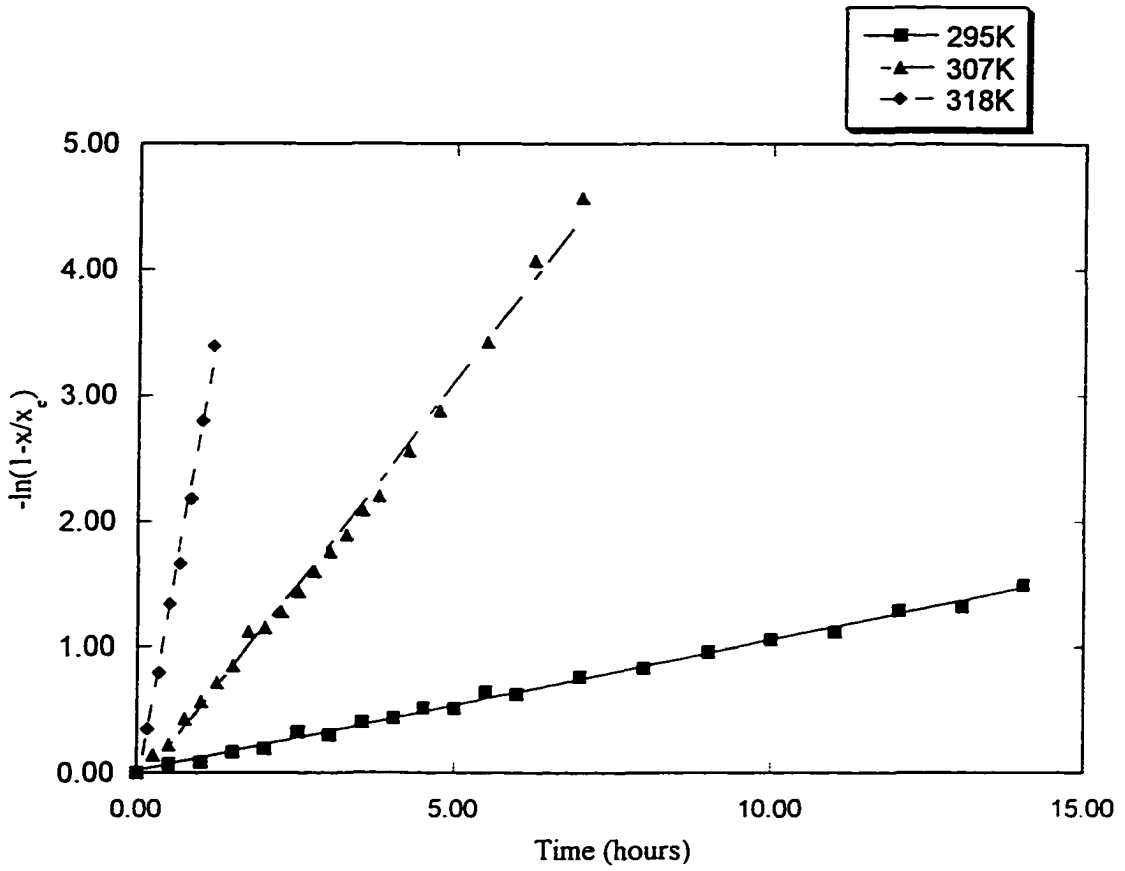

Figure 4-23. Plot of $-\ln(1-x/x_e)$ *vs* time (hours) at different temperatures - determination of reaction rates - for *syn* **26a** → *anti* **26b** isomerization

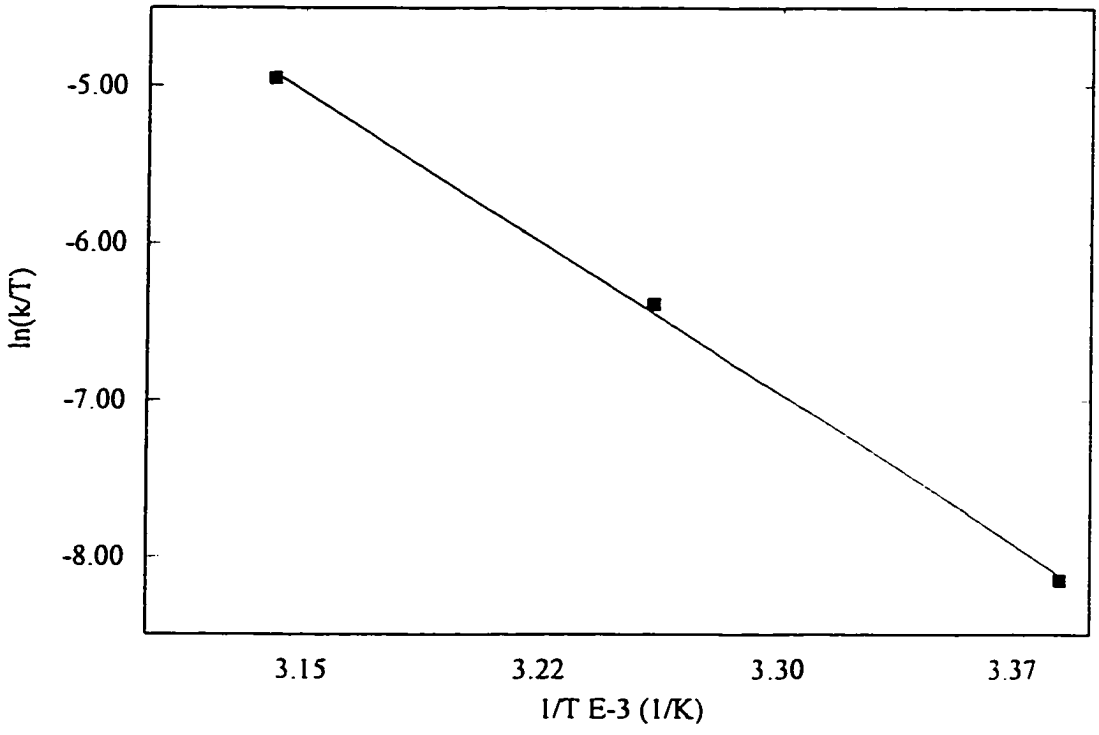

Figure 4-24. Eyring plots of ln(k/T) *vs* T^{-1} for *syn* **26a** → *anti* **26b** isomerization

The significant positive $\Delta S^{\neq}$ and $\Delta H^{\neq}$ suggests a dissociative process involving bond cleavage since the intra-molecular mechanism suggested for the 5-coordinate rhodium biPSi complex without bond-breaking has negative entropy term and a smaller enthalpy change. By comparison, the measured $\Delta S^{\neq}$ and $\Delta H^{\neq}$ for the intra-molecular fluxional behavior of five coordinate $Ir(H)_2X(P^tBu_2Ph)_2$ are 0.4±5.0 $JK^{-1}mol^{-1}$ and

32.8±0.8 kJmol^{-1} respectively.[66] In the fluxional seven coordinate trihydride complex, Ir(acac)(H)$_3$(SiEt$_3$)(PCy$_3$) (acac = acetylacetonato), the $\Delta S^{\neq}$ and $\Delta H^{\neq}$ for the exchange of hydrides were found to be -6.02±7.64 JK^{-1}mol^{-1} and 50.75±3.15 kJmol^{-1} (quoted directly from the literature).[156] Five and seven coordinate species are known for their stereochemical nonrigidity.[157] The fluxional trihydride species may also undergo rearrangement through a molecular hydrogen complex as the intermediate. By contrast, dissociative processes usually involve large positive entropy changes with the enthalpy change varying with strength of the bond being broken. The activation parameters for the loss of dihydrogen ligand from *trans*-Os(H)Cl(η^2-H$_2$)(CO)(P^{i}Pr$_3$)$_2$ to give the five coordinate Os(H)Cl(CO)(P^{i}Pr$_3$)$_2$ and free hydrogen are: $\Delta S^{\neq}$ = 41.08±2.08 JK^{-1}mol^{-1} and $\Delta H^{\neq}$ = 60.59±0.83 kJmol^{-1} (quoted directly from the literature).[158] The trimerization of Ru(CO)$_5$ to form Ru$_3$(CO)$_{12}$ with liberation of 3 mol equivalents of CO was found to have activation parameters as follows: $\Delta S^{\neq}$ = 53±15 JK^{-1}mol^{-1} and $\Delta H^{\neq}$ = 109±15 kJmol^{-1}.[159] Similarly, isomerization going through dissociative pathway also has positive $\Delta S^{\neq}$. The activation parameters for the isomerization of all-*trans*-Ru(CO)$_2$Cl$_2$(PBz$_2$Ph)$_2$ to the *cis* isomer were measured as: $\Delta S^{\neq}$ = 39.4±8.3 JK^{-1}mol^{-1} and $\Delta H^{\neq}$ = 72.71±4.15 kJmol^{-1} (quoted directly from the literature).[153] This isomerization was believed to involve dissociation and re-association of CO,[154] while the isomerization *cis*-M(CO)$_4$(SiCl$_3$)$_2$ → *trans*-M(CO)$_4$(SiCl$_3$)$_2$ (M = Ru or Os) at elevated temperature was concluded to go through a non-dissociative intra-molecular mechanism due to the negative or near-zero entropy changes: $\Delta S^{\neq}$ = -28.6±12.4 JK^{-1}mol^{-1} and $\Delta H^{\neq}$ = 103.3±4.2 kJmol^{-1} for the Ru system; $\Delta S^{\neq}$ = 6.6±7.0 JK^{-1}mol^{-1} and $\Delta H^{\neq}$ = 74.3±2.5 kJmol^{-1} for the Os system.[160] These

latter systems are unusual because the energy barrier for non-dissociative intra-molecular rearrangement in octahedral complexes is generally assumed to be high. This is also the reason why *syn*:*anti* diastereoisomerization of octahedral **26a**:**26b** at a rate qualitatively similar to that of the related Rh system is a surprising observation.

While all six bonds to the Ru center of **26a** could be broken in a dissociative mechanism for isomerization, further experiments ruled out the cleavage of Ru-H, Ru-CO and Ru-Si bonds, leaving reversible dissociation of P as the only remaining possibility. The hydride in **26a** was not substituted by either positively (CD_3OD) or negatively ($LiAlD_4$) charged deuterium centers even at elevated temperature.[161] This evidence indicates that the Ru-H bond remains unchanged during isomerization. Measuring the rate of isomerization of the deuteride anologues **26a**-*d* (*syn*) → **26b**-*d* (*anti*) at 22°C gave k = 4.36×10^{-6} s^{-1}, which is only 9% slower than the rate determined for isomerizaton of the hydride **26a**. This is a negligible kinetic isotopic effect, compared with typical k_H/k_D values that are in the range 3-10,[155, 158, 162] and strongly suggests that any process involving the Ru-H bond (including reductive elimination and oxidative re-addition of the Si-H bond) is unlikely. Loss of coordinated CO to produce a five coordinate intermediate can be ruled out because the replacement of CO in **26** with ^{13}CO was observed to be very slow, with only a trace of incorporation into **26** after 24 h exposure (C_6D_6 solution, *ca.* 760 mmHg ^{13}CO). For comparison, the two equatorial carbonyl ligands in *cis*-$Ru(CO)_4(SiCl_3)_2$ exchange completely under similar conditions to give labeled di-^{13}CO-substituted and mono-^{13}CO-substituted *cis* isotopomers within 18 hours.[140] This labeling process has been suggested to occur through a five coordinate intermediate which is

produced from the dissociation of one equatorial CO (labilized *trans* to a silyl group). This leaves only cleavage of Ru-P bonds as a dissociative step in the *syn* **26a** → *anti* **26b** isomerization, which may therefore be occurring through dissociation of one of the biPSi phosphine groups, followed by a configurational change at the resulting five coordinate center, then re-association of the phosphorus to generate the diastereomeric geometry.

Labeling **26** with ^{13}CO is faster at elevated temperature, although it is still much slower than *syn* → *anti* isomerizaton under the same conditions (Scheme 4-12). This process has been monitored by using ^{1}H, ^{31}P and ^{13}C NMR spectroscopy. Figures 4-25, -26 and -27 demonstrate the enrichment of the mono-^{13}CO-labeled complexes, *cis*-**26a**-^{13}CO (*syn*), *trans*-**26a**-^{13}CO (*syn*), *cis*-**26b**-^{13}CO (*anti*) and *trans*-**26b**-^{13}CO (*anti*), and di-^{13}CO-labeled complexes, *syn* **26a**-$(^{13}CO)_2$ and *anti* **26b**-$(^{13}CO)_2$, after **26** was exposed to ^{13}CO (760 mmHg) at 70°C for 10 h. After careful analysis, the coupling patterns for all species involved could be identified since the four mono-^{13}CO isotopomers *cis/trans*-**26a/b**-^{13}CO have previously been characterized (Section 4.B.iv.). The di-labeled species **26**-$(^{13}CO)_2$ (*syn* and *anti*) can also be identified in the NMR spectra in spite of their low abundance. They are expected to show doublets of doublets of triplets through splitting by *cis* $^{2}J_{CH}$, *trans* $^{2}J_{CH}$ and *cis* $^{2}J_{PH}$. The $^{1}H\{^{31}P\}$ NMR suggests the existence of *cis/trans*-**26**-^{13}CO (two doublets) and **26**-$(^{13}CO)_2$ (doublet of doublets). Such an assignment is also supported by ^{31}P NMR in which the doublet is attributed to mono-label isotopomers and the two further partially resolved peaks on the edge of the main contour may represent di-labeled species. The two CO signals are observed at the same intensities for each

diastereomer in the ^{13}C NMR spectrum, indicating that the two CO groups in **26** are displaced by ^{13}CO at comparable rates.

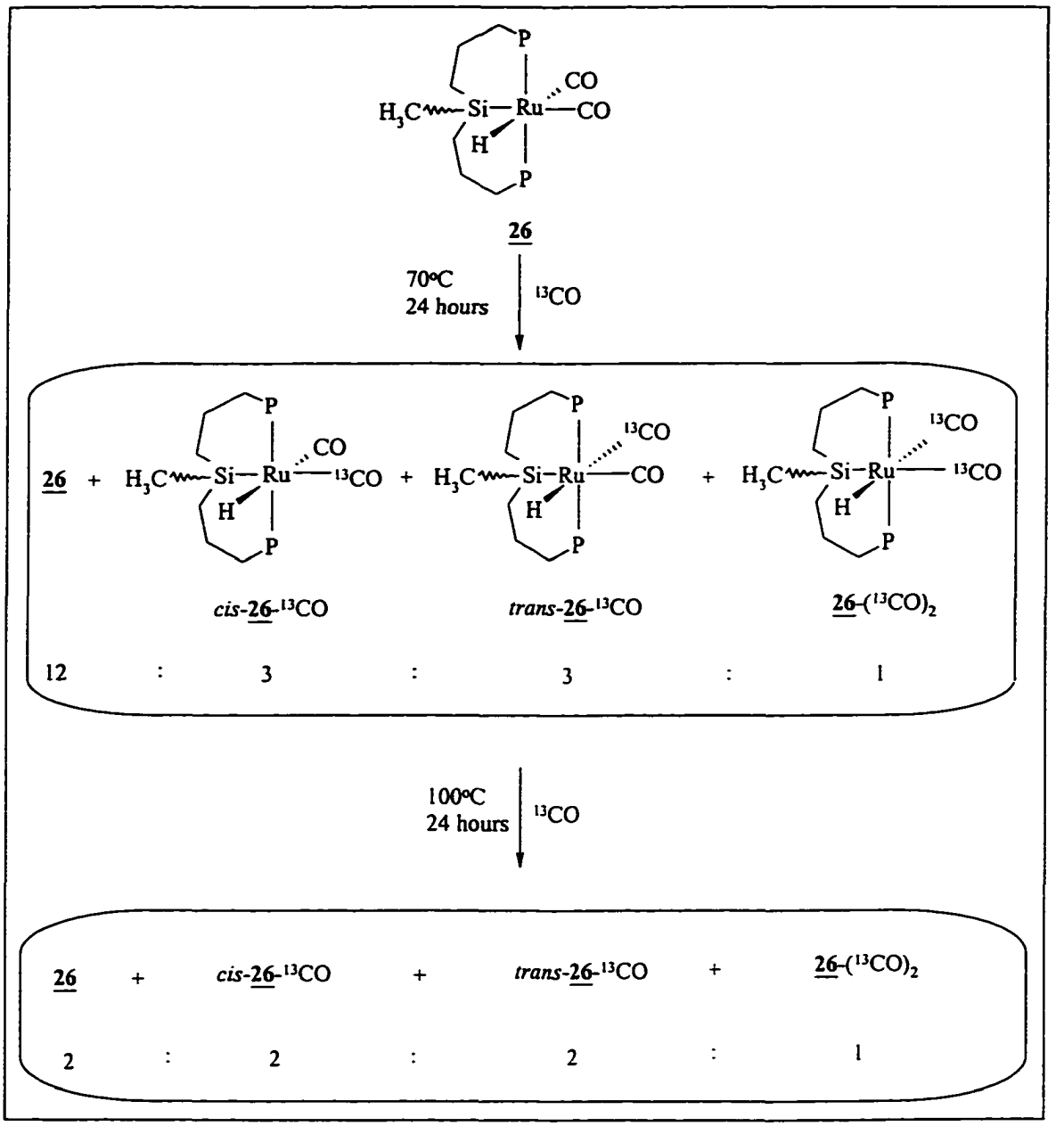

Scheme 4-12. The ^{13}CO-labeling reaction of complexes **26**

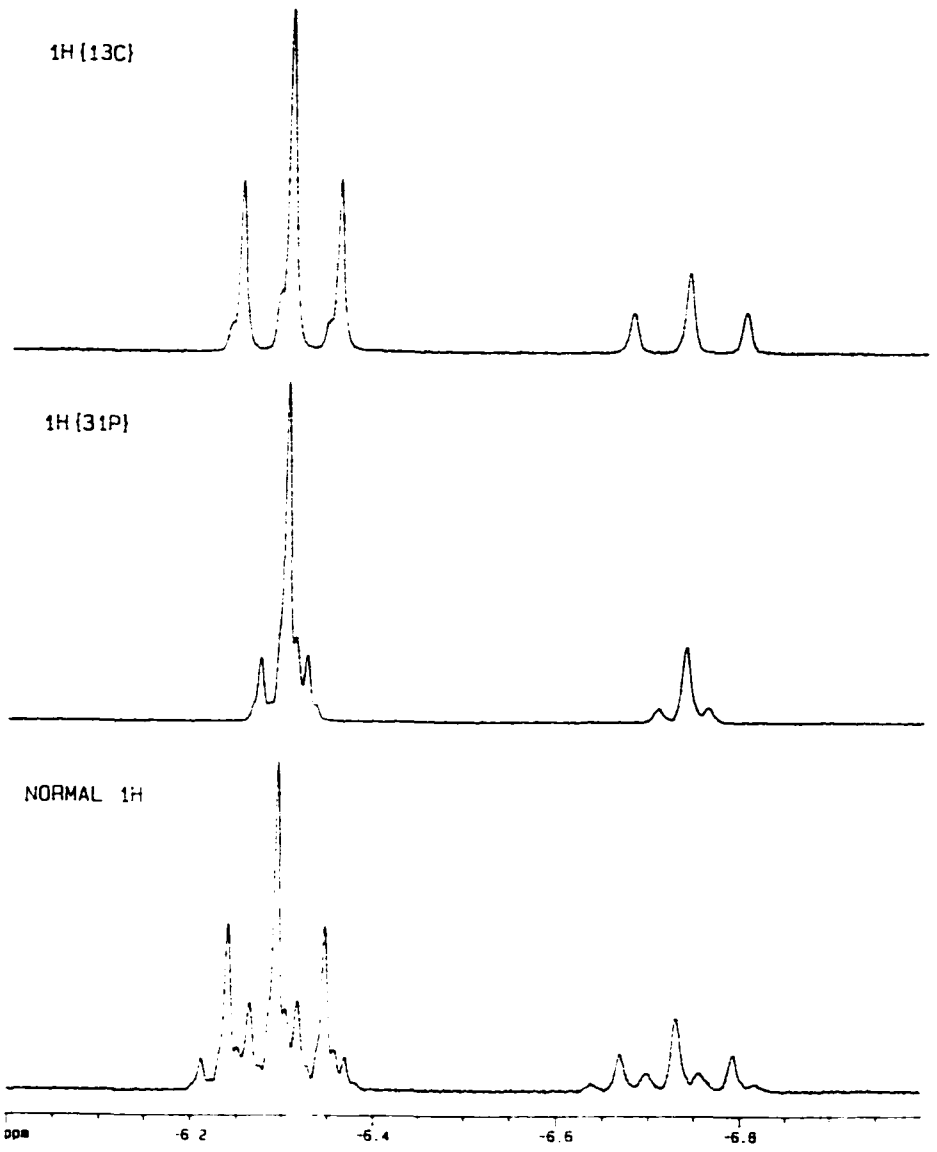

Figure 4-25. ^{1}H NMR for ^{13}CO-labeling experiment of complex **26**

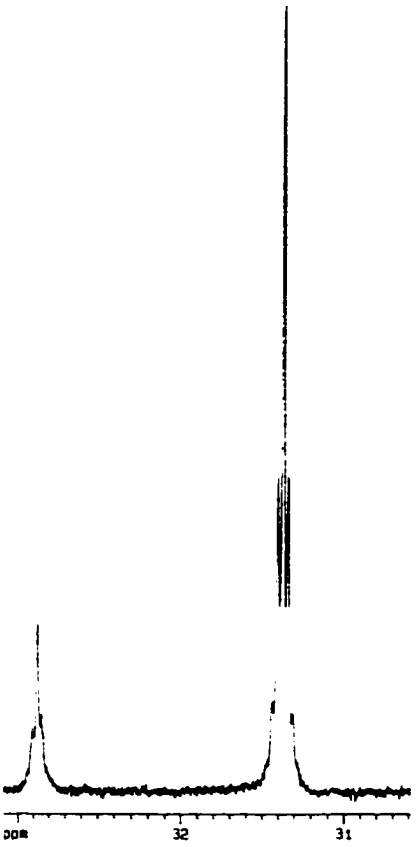

Figure 4-26. ^{31}P NMR for ^{13}CO-labeling experiment of complex 26

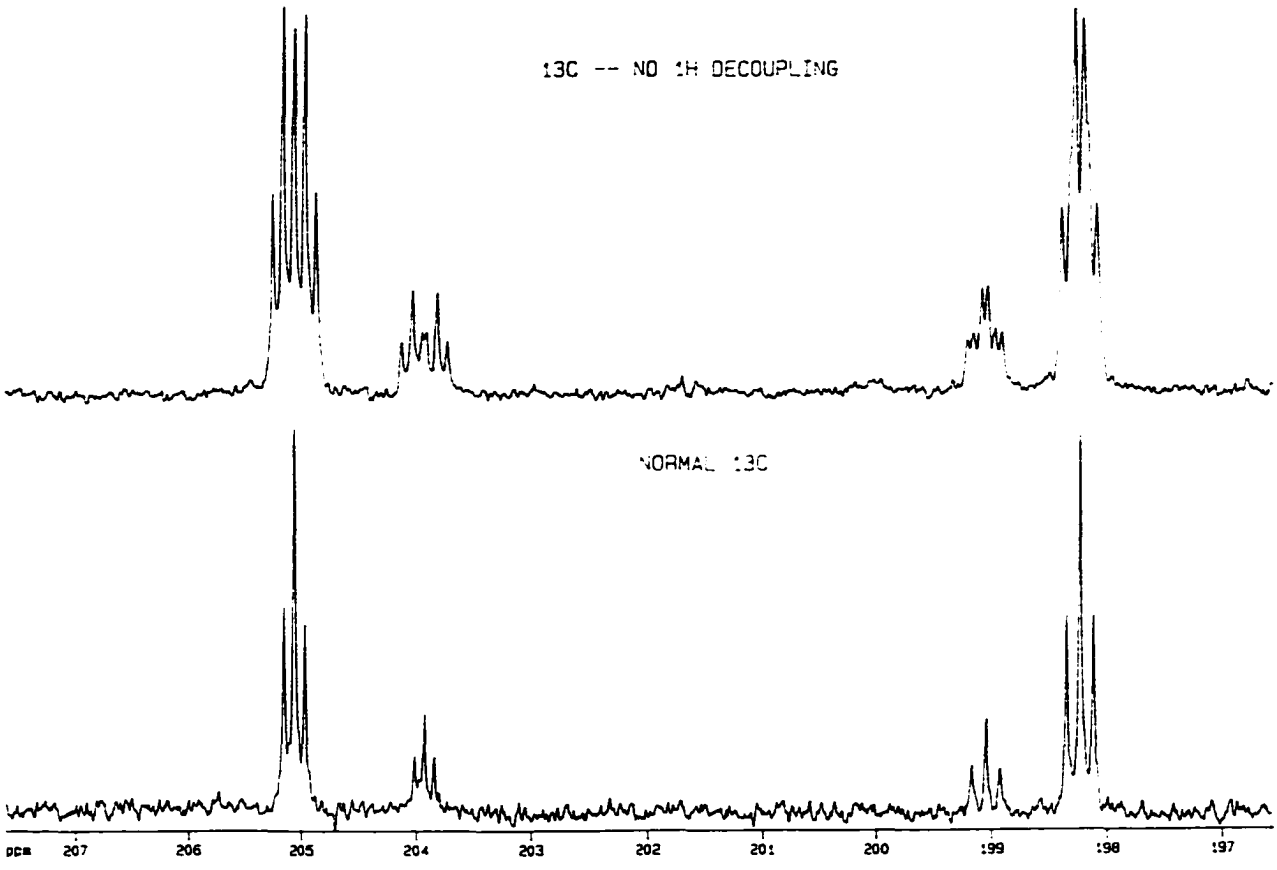

Figure 4-27. ^{13}C NMR ^{13}CO-labeling experiment of complex **26**

The mono-labeled *cis*-**26a**-^{13}CO (*syn*), isolated from the reaction of **43** with ^{13}CO, isomerizes to the other three isotopomers *trans*-**26a**-^{13}CO (*syn*), *cis*-**26b**-^{13}CO (*anti*) and *trans*-**26b**-^{13}CO (*anti*). This process involves two competing isomerization steps: (a) isomerization from *syn* to *anti* isomers, and (b) isomerization from *cis* to *trans* isotopomers. The former reaches an equilibrium ratio of 4.5:1 at 22°C within 48 h, while

the latter leads to an equilibrium ratio of 1:1 during the same time, and has been determined to be a first-order process as well. A kinetic study by using ^{1}H NMR spectroscopy (Appendix D.ii.)gave the approximate activation parameters as: $\Delta G^{\ddagger}_{295} \cong$ 105±20 kJmol^{-1}, $\Delta H^{\ddagger} \cong$ 98.9±22 kJmol^{-1}, $\Delta S^{\ddagger} \cong$ -22±8 JK^{-1}mol^{-1} (Figure 4-28: an Eyring plot). The similarity of the free energy change to that measured for *syn* → *anti* isomerization suggests that the two processes undergo the same or similar pathway, i.e., involve the same intermediates or intermediates at similar energy level. In Scheme 4-13 a mechanism is proposed for the simultaneous isomerization and isotopomerization from *cis*-**26a**-^{13}CO (*syn*) to the other three isotopomers, involving dissociation of chelate phosphine, configurational change, clock-wise face rotation and re-association of phosphine.

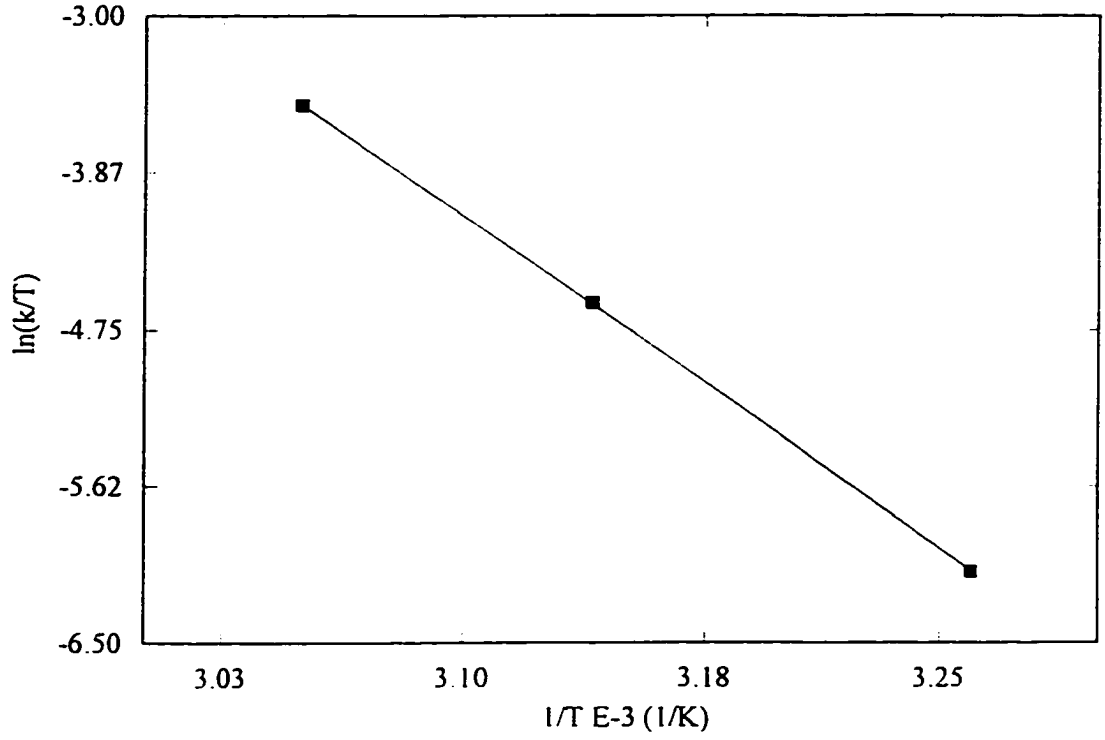

Figure 4-28. Eyring plots of ln(k/T) *vs* T^{-1} for *cis*-**26a**-^{13}CO → *trans*-**26a**-^{13}CO isotopomerization

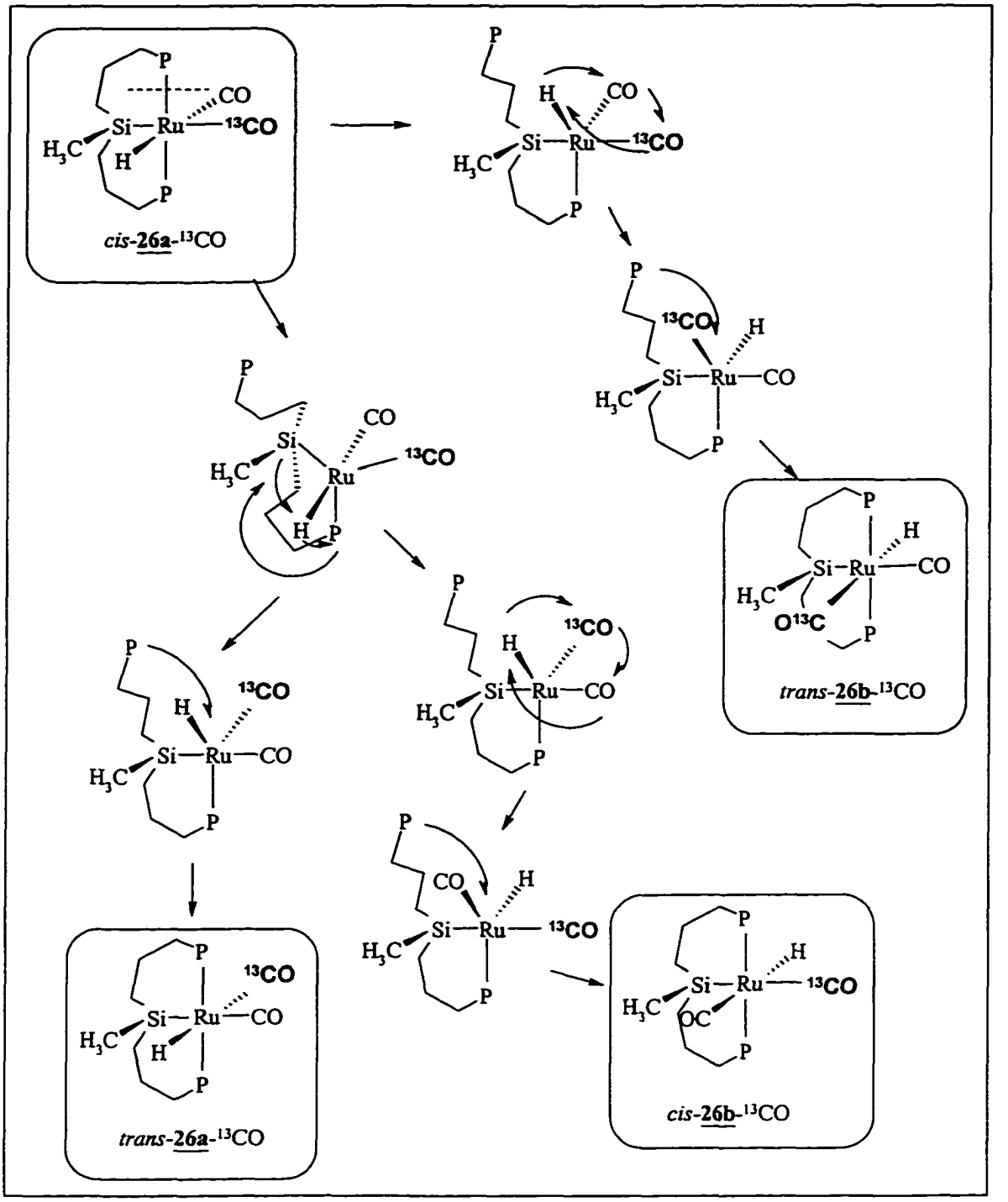

Scheme 4-13. Proposed mechanism of isomerization and isotopomerization

The inter-molecular transfer of ^{13}CO was not observed since the concentration of mono-^{13}CO-labeled **26**-^{13}CO did not increase as a mixture of enriched di-^{13}CO-labeled complexes **26**-$(^{13}CO)_2$ and unlabeled **26** was heated in solution. Thus the two intra-molecular isomerization processes, *syn* → *anti* and *cis* → *trans*, run at comparable rates simultaneously and are probably part of the same process, involving the dissociation and re-association of chelate phosphines.

4.C. Parallel Chemistry of Ru(mcbiPSi)(H)$(CO)_2$ (46)

As discussed in Chapter 1, a series of new phosphinoorganosilanes ligand precursors containing more rigid backbones than the polymethylene-bridged prototypes has been synthesized from treatment of benzylic anions with organochlorosilanes. Coordination behavior with platinum group metals including Ir, Rh and Pt, (*via* the oxidative addition of Si-H bonds assisted by chelate phosphine complexation), has been found to give similar products to those formed from normal flexible phosphinoalkylsilanes.[52, 55] Complexation of the modified rigid tridentate unit derived from mcbiPSiH, **VI** at ruthenium(II) has also been examined in order to draw comparisons with **26** and its derivatives.

The reaction of mcbiPSiH (**VI**) with $Ru(CO)_3(PPh_3)_2$, after refluxing in toluene for 19 h, gave a pale white solid which was found to have two triplets (δ -6.89, -6.64) in 10:1 ratio and an unresolved multiplet centered at δ -6.0 in the ^1H NMR spectrum (eq 4-9). The two triplets are assigned to *syn* and *anti* diastereomers of **46**, which is an analogue of **26**, while the remaining peak is attributed to a kinetic hydride intermediate, since it was found that conversion to complexes **46** occured at 78°C during 4 h. A recent nOe-diff

experiment conducted by Wang in this laboratory has shown that the major isomer [δ(RuH) = -6.64; δ(13P) = 40.7] has an *anti* configuration (**46b**), leaving the other hydride triplet (δ -6.89) and ^{31}P singlet (δ 42.3) to be assigned to the corresponding *syn* diastereomer **46a**. Non first order signals (δ 2.5) consistent with an AB coupling pattern is observed for the SiCH_2 groups in ^1H NMR spectrum, as shown in Figure 4-29. The IR spectrum (KBr) has two strong bands at 1999 and 1963 cm^{-1} (ν_{CO}) and one weak band at 1891 cm^{-1} (ν_{RuH}). The NMR spectroscopic data are collected in Table 4-30.

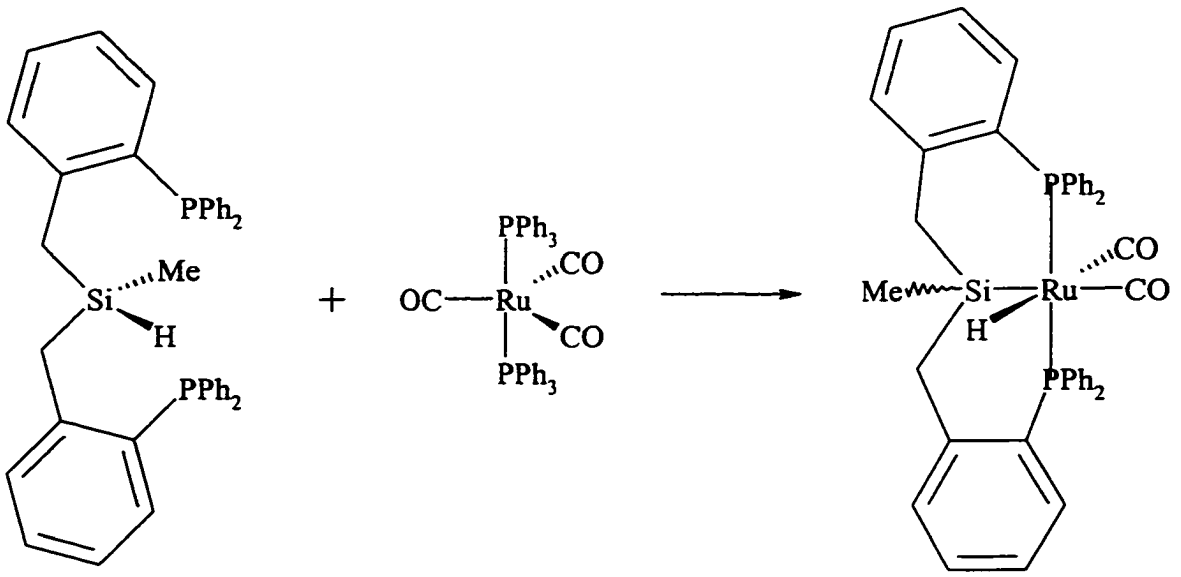

mcbiPSiH, **VI** **46**

(4-9)

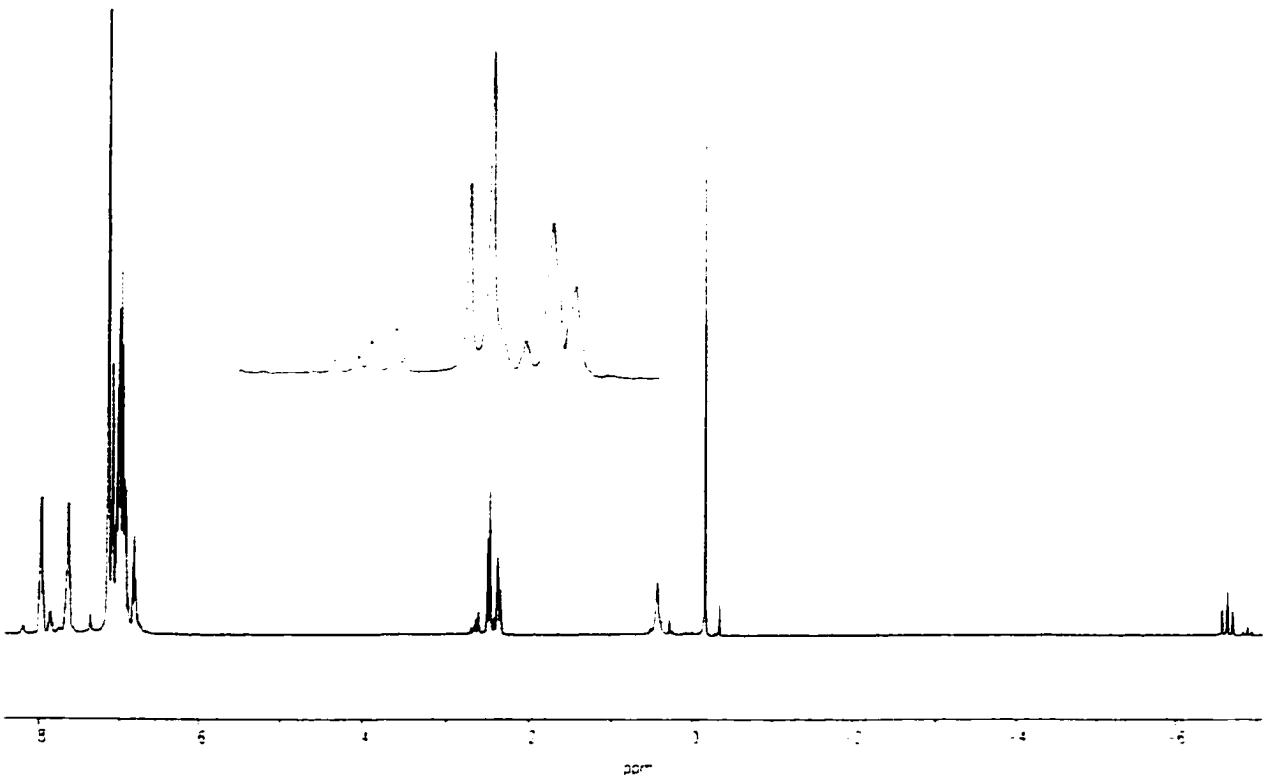

Figure 4-29. ^{1}H NMR spectrum for complex **46**

Table 4-29. The NMR data[a] for complexes **53a** and **53b**

				^{1}H				^{13}C				
Compd	^{31}P	^{29}Si	$^2J_{PSi}$	Ru*H*	$^2J_{PH}$	SiC*H*$_3$	SiC*H*$_2$	Si*C*H$_3$	Si*C*H$_2$	J_{PC}	Ru*C*O	$^2J_{PC}$
53a	42.3	-	-	-6.89(t)	20.4	0.44	2.52(m)	-	-	-	-	-
53b	40.7	42.6(t)	17.5	-6.64(t)	24.3	-0.16	2.41(m)	0.43	32.40(t)	6.9	204.04 (t)	7.8
											200.02 (t)	11.0

[a] C_6D_6 was used as solvent; coupling constants were measured in Hz

The *anti* isomer **46b** could be recovered pure after **46** was washed with alcohols or hexanes (*syn*:*anti* < 1:20). It was observed to isomerize to its diastereomer **46a** in solution over a period of three days, to give an equilibrium ratio of *syn*:*anti* = 1:10 at 22°C. The ratio was measured as 1:6 at 50°C. Complex **46** is soluble in aromatic and halogenated solvents. It was found to be more unstable than its analogue **26**, slowly blackening even when stored under inert atmosphere conditions in the dark. This difference in stability has not yet been investigated but may be associated with the less flexible ligand framework. Some molecular distortion may be caused by the rigid mcbiPSi ligand in the evident structures of appropriate platinum, iridium and rhodium complexes.[210]

Complex **46** shows lower reactivity than **26**. Substitution of the CO group *trans* to Si by phosphites is very slow at room temperature. After photo-irradiation or refluxing in toluene for 16 h, a triethylphosphite derivative **47** was recovered from a mixture of **46** and excess triethylphosphite. Complex **47** may have a similar configuration to the trimethylphosphite adduct **27**, and only one isomer was detected. In the ^{31}P NMR spectrum for **47**, the *cis* coupling $^{2}J_{PP'}$ between chelate phosphine (δ 45.5) and coordinated triethylphosphite (δ 141.5) is 37.1 Hz. The coupling ($^{2}J_{PH} = {}^{2}J_{P'H}$ = 22.0 Hz) between the ruthenium hydride (δ -6.68) and *cis* phosphorus nuclei in the phosphine and phosphite ligands splits the hydride signal into a quartet-like doublet of triplets. The SiCH_3 and SiCH_2 groups are found at δ -0.17 and 2.49 respectively. Reaction of **46** with piperidine and water led to only decomposition, with a signal due to uncoordinated chelate phosphine observed at δ -14 in the ^{31}P NMR spectrum. No oxidation similar to that of **26**

took place even after pure oxygen gas was bubbled through a benzene solution of **46**. Chlorination of **46** using CCl_4 progressed slowly (80°C, 5.5 h), giving one product **48** that is presumably the analogue of the six coordinate chloride **39**, since it showed no hydride signal and the $SiCH_3$ and $SiCH_2$ groups lie at δ -0.38 and 2.54 respectively in the ^1H NMR spectrum. The latter shows an AB coupling pattern in which the two-bond coupling $^2J_{HH'}$ between geminal hydrogens is ~15 Hz. A ^{31}P singlet at δ 26.2 is assigned to **48**. Prolonged heating of **48** in toluene-d_8 appeared to convert it to another isomer (δ 28.8 in the ^{31}P NMR spectrum), but attempts to prepare a five coordinate analogue of **42** from **48** by removal of CO at elevated temperture led to significant decomposition.

Differences in reactivity observed between biPSi and mcbiPSi Ru(II) systems are likely to be a result of different rigidity of each ligand framework, since similar differences have been observed for the Ir and Rh biPSi and mcbiPSi systems.[55, 60]

4.D. Catalytic Oxidation of Alkenes by Ru(biPSi) Complexes

Catalytic oxidation of saturated and unsaturated hydrocarbons is an area that has recently attracted much attention both from the synthetic and biological points of view.[163] The most commonly used oxidants include hydroperoxide, *t*-butyl peroxide, and dioxygen. In most systems metal complexes are used as catalysts while in some cases, oxidation is effected by other medium such as a mixture of N-hydroxyphthalimide (NHPI) and acetaldehyde in the absence of metal catalysts.[164] The metal catalysts can be porphyrin-type[165] or non-porphyrin-type, e.g. $RuCl_2(PPh_3)_3$ and $RuH_2(PPh_3)_4$,[166] complexes and the metals that have been investigated cover most of the transition series but in particular Fe, Ru, Cu, Mn and Co.[166a, 167] The oxidation of hydrocarbons converts

saturated substrates to ketones or alcohols and olefins to epoxides, ketones and/or alcohols.[168, 169] It is known that the oxidation cycle involve changes in the metal oxidation state and formation of reactive free radicals in some cases.[170]

Though the optimum conditions for catalytic oxidation of hydrocarbons with alkyl hydroperoxide systems varies according to the metals, ligands, substrates, etc., chemistry named the GIF system by Barton and co-workers is attractive due to its mild operating conditions, relatively high efficiency and high selectivity.[171] Most of the GIF prototypes use an iron salt as a catalyst, hydrogen peroxide or *t*-butyl hydroperoxide as the primary oxidant and a pyridine/acetic acid mixture as the solvent. The reactivity of the catalyst is frequently enhanced by the addition of picolinic acid.[172] Barton has proposed a radical-free mechanism in which a high valent iron-oxo species [formally Fe(V)=O] is formed, which can insert into an unactivated C-H bond to give an alkyl-Fe(V)-OH complex. This complex is the supposed precursor of the observed organic reaction products (mainly ketones from cycloalkanes; alcohols from *t*-CH bonds).[173] Later investigation suggested that in some specific GIF systems, free-radicals and Fe(III)/Fe(IV) couples are involved.[174] The use of large quantities of pyridine as solvent in GIF chemistry limits its practical application. A similar system without solvent has been developed by combining *t*-butyl hydroperoxide and catalytic amount of soluble Fe(III) or Cu(II) chelates.[175] GIF chemistry is still under development.[176]

By comparison with alkyl hydroperoxides, gaseous dioxygen is a more desirable oxidizing source because it is inexpensive and its reduced product is usually H_2O, but oxidation of diamagnetic organic molecules by O_2, a two electron oxidant, is slow since organic molecules can only provide one electron or one hydrogen atom per molecule. The

reaction of O_2 with some metal complexes can, however, activate O_2 in a way that facilitates its reaction with organic compounds.[177]

Typically, oxidation by activated O_2 can be achieved by a) bonding to a metal center as O_2, e.g. $LCoO_2$, b) formation of metal oxo compounds, e.g. LM=O, c) formation of metal peroxo compounds, e.g. LM-O-OR or LM-O-OH or d) generation of high oxidation state metal complexes.[178] Co complexes have been found to catalyze oxidation of olefins to give ketones and alcohols[179] or epoxides in high yield.[180, 181] Ru complexes are also found to catalyze oxidition of alkanes to ketones or alcohols,[182, 183] and olefins to ketones, alcohols and epoxides.[184, 185]

The observation of the reaction of dioxygen with Ru(biPSi) complex **26** and isolation of the oxygen insertion product **32** led us to investigate in a preliminary way the possible catalytic activity of Ru(biPSi) complexes in oxidation of unsaturated hydrocarbons. Cyclohexene and 1,2-dichloroethane were chosen as the model substrate and solvent respectively. The catalysis was monitored using ^1H NMR spectroscopy. The conversion was calculated by integration of the signals attributed to starting materials and products. The catalysis was achieved either by bubbling pure O_2 through substrate solution at a flow rate of approximately 1 cm^3/second or by using a steel bomb filled with 5 atm of O_2. In the ambient method, a medium fine glass frit was used to split the gas flow into small bubbles in order to increase the gas-liquid interface. In the pressured system, the solution was not stirred.

It was found that complex **26** catalyzed the oxidation of cyclohexene under ambient or pressured O_2 to give a mixture of four organic compounds, 2-cyclohexen-1-one, 2-cyclohexen-1-ol, cyclohexene oxide and *trans*-1,2-cyclohexanediol (eq 4-10) and

water. Of the product mixture, 2-Cyclohexen-1-one and 2-cyclohexen-1-ol accounted for 90% while cyclohexene oxide constituted about 10%. Cyclohexene oxide was slowly hydrolyzed under the experimental conditions used to form *trans*-1,2-cyclohexanediol if the reaction time was prolonged. The four products were identified through comparison with standard ^1H NMR spectra and by mixing with commercially available pure compounds. The experimental results are summarized in Table 4-30. The conversion represents the percentage yield of total products. The turnover number is the number of molecules of substrates oxidized per catalyst molecule within the specific reaction time.

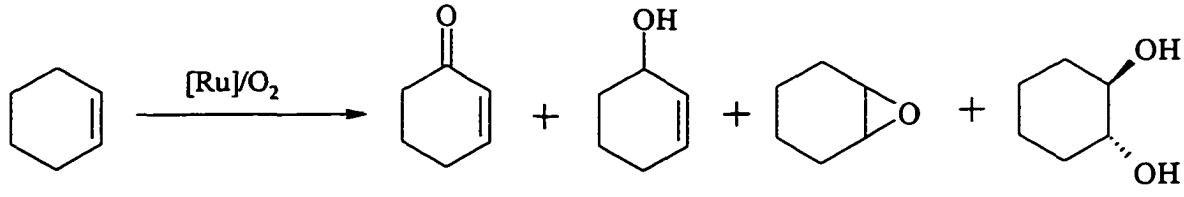

(4-10)

Table 4-30. The results of the oxidation of cyclohexene catalyzed by **26**

Pressure of O_2 (atoms)	Moles of cat./ moles of sub.	Time (hours)	Conversion (%)	Turnover number (sub./per cat.)
1	1/2000	4	15	300
	1/400	4	21	85

5	1/2000	14	21	420
	1/400	14	24	97

Catalysis started as soon as the catalyst precursor **26** was added, with the color of the solution turned from colorless to yellow, then red and finally deep red as oxygen was bubbled. The appearance of the deep red color was often accompanied by deposition of some black precipitate, possibly due to decomposition of the catalytic species. After 4 h bubbling or 14 h in bomb, the solution turned to clear and colorless again and the catalysis was finished.

The mechanism of this oxidation chemistry is not yet known, but it is believed to involve a free radical pathway since the free radical quencher BHT, 2,6-di-^{t}butyl-4-methylphenol, stopped the catalysis. Furthermore, the red color appears to be a characteristic of the catalytically active species, which may be a Ru(IV) species complexed with cyclohexene since it was only formed in the presence of both **26** and cyclohexene.

The increased pressure (5 atms) of O_2 did not significantly improve the catalysis so that similar efficiency was possible by bubbling in oxygen gas at ambient conditions. Pressures higher than 5 atms have not been investigated due to safety considerations. The turnover number was found to decrease significantly with higher catalyst/substrate ratio. This unusual behavior implies the catalyst decomposes faster at higher concentration,

which may limit the value of this system for practical analysis. Further research will be required to evaluate its potential more fully.

Chapter 5

EXPERIMENTAL

5.A. General

All compounds were manipulated in an atmosphere of dry argon gas, using standard bench-top inert-atmosphere (Schlenk) techniques.

Solvents were dried and redistilled under argon gas immediately before use from the following drying agents: THF, diethyl ether, benzene, toluene, hexanes from sodium/benzophenone; dichloromethane from lithium aluminum hydride.

The transition-metal reagent complexes were prepared according to literature methods (Table 5-1).

Table 5-1. The transition-metal reagent complexes

Compound	Reference
$ZrCp_2(H)Cl$	66
$Ru(CO)_3(PPh)_2$	186
$Fe(CO)_3(PPh)_2$	187
$Pt(PPh_3)_2(\eta\text{-}C_2H_4)$	188
$Pt(PPh_3)_4$	189

Microanalysis data were supplied by Canadian Microanalytical Services Ltd., Vancouver, British Columbia. Crystal structure determination was carried out by Dr.

R.A. Toscano at UNAM, Mexico City, Mexico. All instruments employed in this work are listed in Table 5-2.

Table 5-2. Instruments

Technique	Instrument[a]
IR	Bruker IFS25 FTIR
^{1}H NMR	Bruker AMX 360 (360.1MHz)
	Bruker AC300 (300.1MHz)
	Bruker WM 250 (250.1MHz)
^{13}C NMR	Bruker AMX 360 (90.6MHz)
	Bruker AC300 (75.4MHz)
	Bruker WM 250 (62.9MHz)
^{31}P NMR	Bruker AMX 360 (145.8MHz)
	Bruker WM 250 (101.2MHz)
^{29}Si NMR	Bruker WM 250 (49.69MHz)
MS	Kratos Concept-H (FAB)
	Finnegan 3300 (EI, CI)
GC	Varian gas chromatographs

[a] Operating frequencies of the NMR spectrometers are given in parentheses.

5.B. Synthesis of Compounds

5.B.i. Synthesis and purification of silane precursors

Some allylsilanes were synthesized via the reaction of Grignard reagents and chlorosilanes. In a typical Grignard reagent preparation reaction, a two neck round bottom flask with magnesium turnings, a pressure equalized dropping funnel and a reflux condensor were assembled, evacuated and flushed with dry argon. Small pellets of iodine were added as initiator. Magnesium turnings were covered with diethyl ether. Allylbromide was transferred into the dropping funnel and dissolved in diethyl ether. A small amount of allylbromide solution was then added and the reactants were stirred until the reaction was initiated. The reaction vessel was cooled down to 0 °C and allylbromide solution was added dropwise. After addition, reactants were warmed to ambient temperature and allowed to stand for 12 h. Yield for the Grignard reagents was 80-89% based on the amount of unreacted magnesium. An allylmagnesiumbromide reagent, which does not contain unreacted allylbromide, could be prepared through removal of diethyl ether and unreacted allylbromide *in vacuo* (10^{-2} mmHg) to afford a white solid and subsequent re-dissolution of the solid in dried diethyl ether.

$HSi(CH_3)_2(CH_2CH=CH_2)$

To allylmagnesiumbromide (0.60 mol) in diethyl ether (350 mL) was added dropwise chlorodimethylsilane (50 mL, 0.45 mol) in diethyl ether (250 mL) at 0 °C. A white precipitate was formed in this procedure. After addition, the reaction mixture was allowed to warm up to ambient temperature and stand for 12 hours. Excess Grignard reagent was then quenched with 1% ammonium chloride aqueous solution. The ether

layer was washed with 4 x 200 mL distilled water till the washing showed neutral and then was dried over magnesium sulfate (0.5 h). After most of the ether was removed by simple distillation, solution was further concentrated (90 °C, 0.5 h) to give a colorless liquid containing 10% ether (48 mL, 75%).

$HSi(CH_3)(CH_2CH=CH_2)_2$

Using the procedures that paralleled those detailed in preparation of allyldimethylsilane, after dichloromethylsilane (15 mL, 0.14 mol) in diethyl ether (150 mL) was added dropwise to allylmagnesiumbromide (0.38 mol) in diethyl ether (300 mL) at 0 °C, the reaction mixture was warmed to ambient temperature and allowed to stand for 12 hours. Then excess Grignard reagent was quenched and ether layer was washed and dried to afford a clear solution, from which ether was removed by simple distillation and subsequent further concentration (95 °C, 1.5 h) to give a colorless liquid (20 mL, 85%). Purer diallylmethylsilane could be distilled out at 130 °C (17 mL, 71%).

$HSi(CH_2CH=CH_2)_3$

In a manner similar to that described in preparation of allyldimethylsilane, trichlorosilane (10 mL, 0.099 mol) in diethyl ether (100 mL) was added dropwise to allylmagnesiumbromide (0.45 mol) in diethyl ether (300 mL) at 0 °C. After reaction mixture warmed up to ambient temperature and stood for 12 hours, excess Grignard reagent was quenched and ether layer was washed and dried. Removal of ether by simple distillation and further concentration (105 °C, 2.5 h) left a colorless liquid (16 mL, 86%).

$H_2Si(CH_2CH=CH_2)_2$

To a solution of previously prepared trimethoxylsilane (13.9 g, 0.11 mol) in diethyl ether (100 mL) was added dropwise allylmagnesiumchloride (0.22 mol) in diethyl ether (230 mL). A white precipitate was formed immediately. After stirring (25 °C, 12 h), the mixture was filtered through a glass frit affording a clear colorless solution. Ether was then removed by roto-evaporation leaving a clear liquid from which diallylmethoxylsilane was transferred under vacuum and trapped at -78 °C (12.3 g, 86 mmol, 79%).

Diallylmethoxylsilane (5.0 g, 35 mmol), prepared in the above procedures, in diethyl ether (50 mL) was added dropwise to lithiumaluminumhydride (0.83 g, 22 mmol) in diethyl ether (80 mL), which was previously filtered through a celite frit, at -78 °C. A white precipitate was formed immediately. After addition, reaction mixture was allowed to warm to ambient temperature and stirred (6 h). Then removal of ether by roto-evaporation left a liquid from which diallylsilane was transferred under vacuum and trapped at -78 °C as a colorless liquid (1.5 g, 13 mmol, 38%).

$Si(CH_2CH_3)_3(CH=CH_2)$

To ethylmagnesiumiodide, which was prepared in the reaction of iodoethane (13.2 mL, 0.165 mol) in diethyl ether (60 mL) with magnesium turnings (4.81 g, 0.198 mol) in diethyl ether (40 mL), was added dropwise trichlorovinylsilane (5.0 mL, 0.039 mol) in diethyl ether (40 mL). After stirring (25 °C, 48 h), excess Grignard reagent was quenched with 1% ammonium chloride aqueous solution; the ether layer was washed with distilled

water and dried over magnesium sulfate. Roto-evaporation of ether left a colorless liquid (4.4 g, 0.031 mmol, 80%).

5.B.ii. Synthesis and purification of halophosphine precursors

$$ClP[(CH_2)_5CH_3]_2$$

The "hexylmagnesiumchloride was previously prepared in the reaction, which was initiated by iodomethane (~0.1 mL), of 1-chlorohexane (5.0 mL, 36.4 mmol) in diethyl ether (60 mL) with magnesium turnings (1.06 g, 43.7 mmol) in diethyl ether (20 mL). After refluxing (1 d), the Grignard reagent was added dropwise to phosphorus trichloride (1.59 mL, 18.2 mol) in diethyl ether (30 mL) at -78 °C. Then the mixture was warmed to ambient temperature, stirred (12 h), and filtered through a short celite column to afford a clear solution. Removal of volatiles *in vacuo* afforded a yellowish liquid (yield was not measured) which was not further purified.

$$ClP(CH_2C_6H_5)(C_6H_5)$$

Benzylmagnesiumchloride, which was previously prepared from benzyl chloride (5.0 mL, 43.4 mmol) in diethyl ether (70 mL) and magnesium turnings (1.27 g, 52.2 mmol) in diethyl ether (10 mL) under refluxing (1 h), was added dropwise to dichlorophenylphosphine (5.22 mL, 38.5 mmol) in diethyl ether (50 mL) at -78 °C. After the reaction mixture was warmed to ambient temperature and stirred (12 h), it was filtered through a short celite column to afford a clear solution. Removal of volatiles *in vacuo* gave a colorless liquid (yield was not measured) which was used without further purification.

5.B.iii. Synthesis and purification of ligands and ligand precursors

$HSi(CH_3)_2(CH_2CH_2CH_2PPh_2)$, I

Allyldimethylsilane (0.30 mL, 2.1 mmol) in benzene (5 mL) was added to a slurry of zirconocene chloride hydride (0.544 g, 2.1 mmol) in benzene (10 mL). The suspension gradually dissolved to give a yellow or brown solution. After further stirring (25 °C, 16 h) with the reaction mixture protected from the light, chlorodiphenylphosphine (0.38 mL, 2.1 mmol) in benzene (5 mL) was added with a syringe. During stirring (25 °C, 20 h), color faded and a white solid precipitated. Then volatiles were removed to leave a sticky residue which was extracted with hexanes (15 mL). The supernatant was transferred with a syringe, concentrated to 3 mL and stirred (10 h) for further precipitation of zirconocene dichloride. Clear solution was then transferred again and solvent was removed *in vacuo* (10^{-2} mmHg) leaving a colorless oil which was identified to be (diphenylphosphinopropyl)dimethylsilane (0.45 g, 1.6 mmol, 79%) reported elsewhere.[50a]

$HSi(CH_3)(CH_2CH_2CH_2PPh_2)_2$, 'biPSiH', II

See the synthesis of compound 6

$HSi(CH_2CH_2CH_2PPh_2)_3$, 'triPSiH', III

See the synthesis of compounds 7 and 8

$Ph_2P(CH_2CH_2CH_2Cl)$, IV

To a suspension of zirconocene chloride hydride (1.4 g, 5.6 mmol) in benzene (20 mL) was added allylchloride (0.45 mL, 5.6 mmol) in benzene (10 mL). After overnight stirring (25 °C) in dark, chlorodiphenylphosphine (1.0 mL, 5.6 mmol) in benzene (10 mL) was added. After further stirring (25 °C, 24 h), volatiles were removed *in vacuo* and the residue was extracted with hexanes (15 mL). Removal of hexanes left a colorless oil from which impurities were further distilled at reduced pressure (85 °C /10^{-2} mmHg). The pure product was isolated as a viscous oily residue (0.85g, 3.2 mmol, 56%).

$(EtO)_3Si(CH_2CH_2CH_2PPh_2)$, V

Hydrozirconation of allyltriethoxylsilane (0.50 mL, 2.2 mmol) with zirconocene chloride hydride (0.60 g, 2.3 mmol) in benzene (20 mL) was complete after stirring overnight (25 °C). Then chlorodiphenylphosphine (0.40 mL, 2.2 mmol) in benzene (10 mL) was added. After another stirring (25 °C, 24 h), volatiles were removed *in vacuo* and residue was extracted with hexanes (15 mL). Removal of hexanes *in vacuo* left a colorless oil which was identified to be (diphenylphosphinopropyl)triethoxylsilane (0.62 g, 1.6 mmol, 73%) reported elsewhere.[85] Anal. Calcd (found): C, 64.58 (64.09); H, 8.00 (7.29).

$HSi(CH_3)(o\text{-}CH_2C_6H_4PPh_2)_2$, 'mcbiPSiH', VI

To a suspension of diphenyl(*o*-tolyl)phosphine (1.5 g, 5.4 mmol) and tetramethylethlenediamine (0.9 mL) in hexanes (20 mL) was added dropwise 1.6 M ^{n}butyllithium (5.1 mL, 8.1 mmol) in hexanes. A red precipitate was formed immediately.

After stirring (25 °C, 4 h), the supernatant was removed with a syringe and residue was washed with 3 x 5 mL hexanes. Removal of hexanes *in vacuo* afforded a red solid lithium salt which was then re-dissolved in benzene (20 mL) to form a red suspension. After addition of dichloromethylsilane (0.22 mL, 2.2 mmol), the color was gradually discharged. After another stirring (25 °C, 1 d), hexanes (20 mL) was added to produce more fine white precipitate which was then removed by filtration through a short celite/silica column giving a colorless clear solution. Removal of volatiles left a waxy product which was found to contain the target product reported elsewhere[52] and diphenyl(*o*-tolyl)phosphine (~20%).

$Et_3Si(CH_2CH_2PPh_2)$, 2

Triethylvinylsilane (0.52 mL, 2.8 mmol) in benzene (10 mL) was added to a slurry of zirconocene chloride hydride (0.72 g, 2.8 mmol) in benzene (15 mL). After overnight stirring (25 °C) in dark, chlorodiphenylphosphine (0.50 mL, 2.8 mmol) in benzene (10 mL) was added. After another overnight stirring (25 °C), volatiles were *removed in vacuo* and residue was extracted with hexanes (15 mL). Removal of hexanes left a colorless oily residue (0.69g, 2.1 mmol, 75%). Anal. Calcd (found): C, 73.12 (73.08); H, 8.90 (8.24).

$HSi(CH_3)_2(CH_2CH_2CH_2Br)$, 4

Allyldimethylsilane (0.90 mL, 6.36 mmol) in tetrahydrofuran (10 mL) was added to a suspension of zirconocene chloride hydride (1.8 g, 7.0 mmol) in tetrahydrofuran (20 mL). After stirring (25 °C, 16 h) in dark, addition of NBS (1.2 g, 7.0

mmol) in tetrahydrofuran (20 mL) was followed by another stirring (25 °C, 2 d). Then THF was removed *in vacuo* leaving a brown waxy residue which was extracted with ^{n}pentane (20 mL). Removal of ^{n}pentane by simple distillation left a yellow liquid from which (ω-bromopropyl)dimetylsilane was transferred under vacuum and trapped at -78°C as a colorless liquid (0.11 g, 0.61 mmol, 8.5%).

$HSi(CH_3)_2(CH_2CH_2CH_2I)$, 5

After allyldimethylsilane (0.50 mL, 3.5 mmol) in tetrahydrofuran (10 mL) was hydrozirconated (as detailed in the preparation of 4) with zirconocene chloride hydride (0.91 g, 3.5 mmol) in tetrahydrofuran (20 mL), iodine (0.90 g, 3.5 mmol) in tetrahydrofuran (20 mL) was added. A yellow solution was formed after stirring (25 °C, 2 d). THF was then roto-evaporated leaving a yellow waxy residue which was extracted with hexanes (20 mL). Evaporation of solvents left a yellow liquid mixture in which (ω-iodopropyl)dimethylsilane was identified by NMR spectroscopy.

$HSi(CH_3)(CH_2CH_2CH_2PPh_2)_2$, 'biPSiH', II and

$HSi(CH_3)(C_3H_7)(CH_2CH_2CH_2PPh_2)$, 6

Using the procedures that paralleled those detailed in preparation of (Diphenyphosphinopropyl)dimethylsilane, I, diallylmethylsilane (1.2 mL, 7.6 mmol) in benzene (20 mL) was hydrozirconated with zirconocene chloride hydride (4.0 g, 16 mmol) in benzene (30 mL). After stirring (25 °C, 16 h), chlorodiphenylphosphine (2.71 mL, 15 mmol) in benzene (20 mL) was added. After another stirring (25 °C, 1 d),

volatiles were removed *in vacuo* and residue was extracted with hexanes (20 mL). Removal of hexanes left a colorless oil from which (diphenylphosphinopropyl)propylmethylsilane, 6 (0.50 g, 1.6 mmol) was distilled out at reduced pressure (120 °C /10^{-2} mmHg) leaving a viscous oily residue (1.9 g, 3.8 mmol, 51%) identified to be bis(diphenylphosphinopropyl)methylsilane, II reported elsewhere.[50b]

$HSi(CH_2CH_2CH_2PPh_2)_3$, 'triPSiH', III, $HSi(C_3H_7)_2(CH_2CH_2CH_2PPh_2)$, 7 and $HSi(C_3H_7)(CH_2CH_2CH_2PPh_2)_2$, 8

Hydrozirconation of triallylsilane (0.50 mL, 2.63 mmol) in benzene (5 mL) with zirconocene chloride hydride (2.24 g, 8.7 mmol) in benzene (20 mL) afforded a yellow solution after stirring (25 °C, 18 h). Then chlorodiphenylphosphine (1.56 mL, 8.7 mmol) in benzene (15 mL) was added and the reaction mixture was stirred for one day (25 °C). Removal of volatiles *in vacuo*, extraction of residue with hexanes (20 mL) and subsequent evaporation of hexanes left a viscous oil, from which (diphenylphosphinopropyl)dipropylsilane, 7 (0.20 g, 0.58 mmol) was distilled out under vacuum (170 °C/10^{-2} mmHg) leaving a viscous oily residue identified to be a mixture of reported tris(diphenylphosphinopropyl)silane, III and bis(diphenylphosphinopropyl)propylsilane, 8 (~2:1, 1.0 g).

$H_2Si(CH_2CH_2CH_2PPh_2)_2$, 9

Diallylsilane (0.45 mL, 3.0 mmol) in benzene (10 mL) was completely hydrozirconated with zirconocene chloride hydride (1.6 g, 6.3 mmol) in benzene (20 mL)

after overnight stirring (25 °C). Subsequent addition of chlorodiphenylphosphine (1.1 mL, 6.3 mmol) in benzene (10 mL) and stirring (25 °C, 1 d) led to the formation of a yellow solution. After volatiles were removed *in vacuo*, residue was extracted with hexanes (15 mL). Evaporation of hexanes and further removal of volatile impurities at reduced pressure (120 °C /10^{-2} mmHg) afforded a viscous oily residue (0.86 g, 1.8 mmol, 59%). Anal. Calcd (found): C, 74.35 (73.38); H, 7.07 (7.26).

$HSi(CH_3)[CH_2CH_2CH_2P(C_6H_{13})_2]_2$, 10

Chlorodi^{n}hexylphosphine (1.0 mL, 4.0 mmol) in benzene (10 mL) was added after a reaction mixture of diallylmethylsilane (0.33 mL, 2.0 mmol) and zirconocene chloride hydride (1.0 g, 4.0 mmol) in benzene (15 mL) was stirred for 16 hours (25 °C). After another stirring (25 °C, 1 d), volatiles were removed *in vacuo* and residue was extracted with hexanes (15 mL). Subsequent evaporation of hexanes and further removal of volatile impurities at reduced pressure (120 °C /10^{-2} mmHg) left an oily residue (0.49 g, 0.92 mmol, 46%). Anal. Calcd (found): C, 70.13 (69.75); H, 12.91 (12.70).

$HSi(CH_3)[CH_2CH_2CH_2P(C_6H_5)(CH_2C_6H_5)]_2$, 11

Diallylmethylsilane (0.45 mL, 2.7 mmol) in benzene (10 mL) was hydrozirnated by zirconocene chloride hydride (1.4 g, 5.6 mmol) in benzene (20 mL) after overnight stirring (25 °C, 16 h). Then benzylchlorophenylphosphine (1.3 g, 5.6 mmol) in benzene (10 mL) was added and the reaction mixture was stirred (25 °C, 1.5 d). Removal of volatiles *in vacuo*, extraction of residue with hexanes (20 mL) and subsequent evaporation of hexanes afforded a colorless oil, which was further purified by distillation

at reduced pressure (130 °C /10^{-2} mmHg) leaving the pure product as a viscous oily residue (0.80 g, 1.5 mmol, 56%). Anal. Calcd (found): C, 75.25 (74.09); H, 7.66 (7.45).

$PhP[CH_2CH_2CH_2Si(CH_3)_2H]_2$, 12

Allyldimethylsilane (1.7 mL, 12 mmol) in benzene (20 mL) was added to a slurry of zirconocene chloride hydride (3.2 g, 12 mmol) in benzene (40 mL). After overnight stirring (25 °C, 16 h), dichlorophenylphosphine (0.80 mL, 5.9 mmol) in benzene (15 mL)was added. After another overnight stirring (25 °C, 18 h) in dark, volatiles were removed *in vacuo* (25 °C/10^{-2} mmHg). Residue was extracted with 30 mL hexanes. Removal of hexanes left an oil from which the pure product was distilled out at reduced pressure (110 °C /10^{-2} mmHg) as a colorless liquid (0.58 g, 1.7 mmol, 29%). Anal. Calcd (found): C, 61.88 (62.51); H, 10.06 (9.78).

$P[CH_2CH_2CH_2Si(CH_3)_2H]_3$, 13

After allyldimethylsilane (1.1 mL, 7.9 mmol) in benzene (10 mL) was hydrozirconated with zirconocene chloride hydride (2.1 g, 8.0 mmol) in benzene (40 mL), phosphorus tribromide (0.25 mL, 2.6 mmol) in benzene (5 mL) was added and the reaction mixture was stirred (75 °C, 18 h). Then volatiles were removed *in vacuo* (25 °C/10^{-2} mmHg) and residue was extracted with hexanes (20 mL). Subsequent evaporation of hexanes left an oil from which the pure product was distilled out at reduced pressure (75 °C/10^{-2} mmHg) as a yellow liquid (0.13 g, 0.39 mmol, 15%). Anal. Calcd (found): C, 53.82 (53.29); H, 11.74 (11.28).

$Ph_2P(CH_2CH_2CH_2CH_2Br)$, 15 and $Ph_2P(=O)(CH_2CH_2CH_2CH_2Br)$, 18

A benzene (10 mL) solution of 4-bromobutene (0.30 mL, 3.0 mmol) was added to a suspension of zirconocene chloride hydride (0.76 g, 3.0 mmol) in benzene (10 mL). After a short period of stirring (25 °C, 3 h), chlorodiphenylphosphine (0.53 mL, 3.0 mmol) in benzene (10 mL) was added. After another short period of stirring (2 h, 25 °C), volatiles were removed *in vacuo* and residue was extracted with hexanes (7 mL). Evaporation of hexanes quickly *in vacuo* was followed by re-dissolving residue 15 in acetone (6 mL), adding 10% hydrogen peroxide aqueous solution (1.51 g, 4.4 mmol) which was previously warmed to 40-50 °C, stirring (2 h, 40-50 °C), and refluxing (2 h). Then distilled water (12 mL) was added and product was extracted wtih diethyl ether (3 x 12 mL). After ether layer was dried over $MgSO_4$ (0.5 h), ether was removed and product was washed with hexanes (10 mL) to afford a gray solid (0.45 g, 1.3 mmol, 45%). Anal. Calcd (found): C, 56.99 (56.54); H, 5.38 (5.11).

$Ph_2P(CH_2CH_2CH_2CH_2CH_2Br)$, 16 and $Ph_2P(=O)(CH_2CH_2CH_2CH_2CH_2Br)$, 19

In a manner similar to that described in the preparation of 18, 5-Bromopentene (0.30 mL, 2.5 mmol) in benzene (10 mL) was mixed with zirconocene chloride hydride (0.65 g, 2.5 mmol) in benzene (10 mL). After overnight stirring (12 h, 25 °C) in the dark, chlorodiphenylphosphine (0.46 mL, 2.5 mmol) in benzene (10 mL) was added. After another period of stirring (3 h, 25 °C), volatiles were removed *in vacuo* and residue was extracted with hexanes (5 mL). Then quick evaporation of hexanes and immediate re-dissolution of residue 16 in acetone (5 mL) was followed by adding 10% hydrogen peroxide aqueous solution (1.3 g, 3.8 mmol) which was previously warmed to 40-50 °C,

stirring (2 h, 40-50 °C), and refluxing (2 h), adding distilled water (10 mL), extracting product with diethyl ether (3 x 10 mL), and drying ether layer over $MgSO_4$ (0.5 h). Evaporation of ether afforded a yellow viscous oil (0.42 g, 1.2 mmol, 48%). Anal. Calcd (found): C, 58.13 (58.29); H, 5.74 (5.68).

$Ph_2P(CH_2CH_2CH_2CH_2CH_2CH_2Br)$, 17 and

$Ph_2P(=O)(CH_2CH_2CH_2CH_2CH_2CH_2Br)$, 20

In a reaction similar to that described in preparation of **18**, a mixture of 6-Bromohexene (0.30 mL, 2.2 mmol) and zirconocene chloride hydride (0.58 g, 2.2 mmol) in benzene (17 mL) was stirred overnight (12 h, 25 °C). Then chlorodiphenylphosphine (0.40 mL, 2.2 mmol) in benzene (10 mL) was added and the reaction mixture was stirred for another 12 hours (25 °C). Removal of volatiles *in vacuo*, extraction of residue with hexanes (5 mL) and subsequent evaporation of hexanes afforded a yellowish liquid **17** which was stable for at least one day (25 °C). After it was re-dissolved in acetone (5 mL), 10% hydrogen peroxide aqueous solution (1.1 g, 3.4 mmol) which was previously warmed to 40-50°C was added and the solution was heated (2 h, 40-50 °C) and then refluxed (2 h). Addition of distilled water (10 mL), extraction of product with diethyl ether (3 x 10 mL), and evaporation of solvents afforded a yellow viscous oil (0.44 g, 1.2 mmol, 55%). Anal. Calcd (found): C, 59.19 (58.02); H, 6.07 (6.02).

PhP[*o*-$C_6H_4CH_2Si(CH_3)_2H]_2$, 21

To a solution of bis(*o*-tolyl)phenylphosphine (0.50 g, 1.7 mmol) and tetramethylethlenediamine (0.65 mL, 4.3 mmol) in hexanes (10 mL) was added dropwise 1.6 M "butyllithium (2.7 mL, 4.3 mmol) in hexanes. During stirring (25 °C, 1 d), a red solid precipitated slowly. Supernatant was then removed with a syringe and red solid was dried quickly *in vacuo*. This lithium salt was re-dissolved in 10 mL tetrahydrofuran to form a red clear solution to which chlorodimethylsilane (0.48 mL, 4.3 mmol) was added at -78 °C. Color was discharged immediately and a white solid precipitated. After another stirring (25 °C, 12 h), volatiles were removed *in vacuo* and residue was extracted with hexanes (20 mL). Solution was then filtered through a short celite/silica column. Removal of solvent left a colorless viscous oil in quantitative yield. Anal. Calcd (found): C, 70.89 (71.77); H, 7.68 (7.60).

P[*o*-$C_6H_4CH_2Si(CH_3)_2H]_3$, 22

Using procedures that paralleled those described in preparation of 21, to a solution of tris(*o*-tolyl)phosphine (0.3 g, 0.99 mmol) and tetramethylethlenediamine (0.52 mL) in hexanes (10 mL) was added dropwise 1.6 M "butyllithium (2.2 mL, 3.4 mmol) in hexanes. After stirring (25°C, 1 d), supernatant was removed and a red solid was quickly dried *in vacuo* and then re-dissolved in tetrahydrofuran (10 mL) to form a red clear solution to which chlorodimethylsilane (0.38 mL, 3.4 mmol) was added at -78°C. Color was discharged immediately and a white solid precipitated. After another stirring (25°C, 12 h), volatiles were removed *in vacuo* and residue was extracted with hexanes (20 mL). Solution was filtered through a short celite/silica column to remove insolibles.

Evaporation of solvents left a white powder in quantitative yield. Anal. Calcd (found): C, 67.72 (67.86); H, 8.21 (8.06).

5.B.iv. Synthesis and purification of metal complexes

Due to the viscous and air sensitive nature of some ligand precursors, special techniques were employed to weigh small quantities accurately. Typically, a capped glass via containing a micro stirring bar was weighed, placed in a wide mouth schlenk tube without the cap, evacuated and placed under an argon atmosphere. A nickle spatula was dipped in the viscous ligand precursors to collect some of the material, and rapidly transferred to the glass vial. More compound could be obtained by repeated transfers. Evacuation of the sample gave rise to minimal oxidation of phosphine groups. The glass vial was capped after refilled with argon gas and weighed again. Once the mass of the ligand precursor was known, the right amount of the metal precursor could be calculated.

$Pt\{PPh[o\text{-}C_6H_4CH_2Si(CH_3)_2]_2\}(PPh_3)$, 25

To solid $Pt(PPh_3)_4$ (0.31 g, 0.32 mmol) was added $PhP[o\text{-}C_6H_4CH_2Si(CH_3)H]_2$, 21 (0.15 g, 0.38 mmol) in benzene (5 mL). A gas was liberated and color changed from yellow to red. After stirring (25 °C, 20min), the mixture was heated (80 °C, 20 min). Removal of volitiles left a reddish oil which was washed with hexanes (3 x 3 mL) and ether (4 x 3 mL) to afford a yellow solid in quantitative yield. Anal. Calcd (found): C, 58.52 (58.58); H, 5.14 (5.23).

$Ru[(PPh_2CH_2CH_2CH_2)_2Si(CH_3)](H)(CO)_2$, 26

To bis(triphenylphosphine)tricarbonylRu(0) (0.21 g, 0.30 mmol) in toluene (20 mL) at refluxing point was added $HSi(CH_3)(CH_2CH_2CH_2PPh_2)_2$, 'biPSiH', II (0.23 g, 0.46 mmol) in toluene (7 mL). Refluxing (17 h) led to the formation of a clear yellowish solution. Removal of volatiles afforded an oily residue which was washed with 100% ethanol (5 x 3 mL) and hexanes (5 x 3 mL) and dried *in vacuo* to yield a pale yellow solid in quantitative yield. Anal. Calcd (found): C, 60.44 (60.55); H, 5.53 (5.47).

$Ru[(PPh_2CH_2CH_2CH_2)_2Si(CH_3)](H)(CO)[P(OCH_3)_3]$, 27

To $Ru[(PPh_2CH_2CH_2CH_2)_2Si(CH_3)](H)(CO)_2$, 26 (0.28 g, 0.42 mmol) in toluene (12 mL) was added excess trimethoxylphosphite (0.25 mL, 2.1 mmol). After heating (80 °C, 30 min), solvent and un-consumed trimethylphosphite were removed *in vacuo*, and residue was washed with hexanes (2 x 2 mL) to afford a white solid in quantitative yield. Anal. Calcd (found): C, 55.91 (55.65); H, 6.03 (6.06).

$Ru[(PPh_2CH_2CH_2CH_2)_2SiO(CH_3)](H)(CO)(NHC_5H_{10})$, 30

To $Ru[(PPh_2CH_2CH_2CH_2)_2Si(CH_3)](H)(CO)_2$, 26 in toluene-$d_8$ was added excess piperidine which was previously saturated with degassed water. After heating (105 °C, 16 h), complex 30 was formed in solution and characterized *in situ*. Attempted isolation of 30 led to decomposition.

$Ru[(PPh_2CH_2CH_2CH_2)_2SiO(CH_3)](D)(CO)(NHC_5H_{10})$, 30-*d*

To $Ru[(PPh_2CH_2CH_2CH_2)_2Si(CH_3)](H)(CO)_2$, **26** in toluene was added excess piperidine which was previously dried over $LiAlH_4$ and then saturated with D_2O. After heating (105 °C, 16 h), **30**-*d* in a yellow solution was characterized *in situ* with NMR spectroscopy.

$Ru[(PPh_2CH_2CH_2CH_2)_2SiO(CH_3)](H)(CO)_2$, 31

After carbon mono-oxide gas was bubbled through $Ru[(PPh_2CH_2CH_2CH_2)_2SiO(CH_3)](H)(CO)(NHC_5H_{10})$, **30** in toluene (25 °C, 20 min), volatiles were removed *in vacuo* to afford a yellowish residue from which a white solid was recovered by washing with minimum amount of methanol. The ^1H and ^{31}P NMR spectra showed it was contaminated by small amount of unidentified impurities.

$Ru[(PPh_2CH_2CH_2CH_2)_2SiO(CH_3)](H)(CO)[P(OCH_3)_3]$, 32

To $Ru[(PPh_2CH_2CH_2CH_2)_2SiO(CH_3)](H)(CO)(NHC_5H_{10})$, **30** in toluene was added largely excess trimethylphosphite. Color was discharged immediately. After heating (60 °C, 10 min), volatiles were removed *in vacuo* to afford a yellow wax from which a white solid was isolated by washing with methanol (3 x 2 mL). Anal. Calcd (found): C, 55.91 (54.53); H, 6.03 (5.54).

$Ru[(PPh_2CH_2CH_2CH_2)_2SiO(CH_3)](D)(CO)[P(OCH_3)_3]$, 32-*d*

To $Ru[(PPh_2CH_2CH_2CH_2)_2SiO(CH_3)](D)(CO)(NHC_5H_{10})$, **30**-*d* in toluene was added excess trimethylphosphite (25 °C). Color was discharged immediately. Products were characterized with NMR spectroscopy and compared to the analogue **32**.

$Ru[(PPh_2CH_2CH_2CH_2)_2SiO(CH_3)](H)(CO)[CNC(CH_3)_3]$, 33

After excess *t*-butyl isocyanide was added to $Ru[(PPh_2CH_2CH_2CH_2)_2SiO(CH_3)](H)(CO)(NHC_5H_{10})$, **30** in toluene and the reaction mixture was heated (76 °C, 1 h), color was discharged slowly and a white solid precipitated. Then supernatant was transferred with syringe. Removal of volatiles *in vacuo* afforded a white wax from which a white solid was recovered by washing with methanol (3 x 2 mL). Anal. Calcd (found): C, 59.82 (59.67); H, 6.11 (5.97); N, 1.88 (1.80).

$Ru[(PPh_2CH_2CH_2CH_2)_2SiO(CH_3)](H)(CO)(NC_5H_5)$, 35

To $Ru[(PPh_2CH_2CH_2CH_2)_2Si(CH_3)](H)(CO)_2$, **26** in toluene-$d_8$ was added excess wet pyridine. After heating (105 °C, 62 h), a yellow solution was formed in which complex **35** was characterized *in situ* with NMR spectroscopy.

$Ru[(PPh_2CH_2CH_2CH_2)_2SiO(OCH_3)](H)(CO)_2$, 36

While exposed to air, $Ru[(PPh_2CH_2CH_2CH_2)_2Si(CH_3)](H)(CO)_2$, **26** in benzene was gently heated (78 °C, 7d). The color gradually changed from yellow to green. Removal of solvent left a gray solid which was soluble in most solvents and has been characterized by spectroscopic methods.

$Ru[(PPh_2CH_2CH_2CH_2)_2SiO(OCH_3)](H)(CO)[P(OCH_3)_3]$, 37

After $Ru[(PPh_2CH_2CH_2CH_2)_2SiO(OCH_3)](H)(CO)_2$, 36 was formed in benzene, excess trimethylphosphite was added. Color was discharged immediately. After heating (78 °C, 15 min), volatiles were removed *in vacuo* to afford a white wax from which a white solid was isolated by washing with methanol. Anal. Calcd (found): C, 53.63 (53.21); H, 5.79 (5.62).

$Ru[(PPh_2CH_2CH_2CH_2)_2SiO(OCH_3)](H)(CO)[CNC(CH_3)_3]$, 38

To $Ru[(PPh_2CH_2CH_2CH_2)_2SiO(OCH_3)](H)(CO)_2$, 36 in benzene, excess *t*-butyl isocyanide was added. Color was gradually discharged. After heating (78°C, 2 h), volatiles were removed *in vacuo* to afford a white wax which was washed with methanol yielding a white solid. Anal. Calcd (found): C, 59.82 (59.67); H, 6.11 (5.97); N, 1.88 (1.80).

$Ru[(PPh_2CH_2CH_2CH_2)_2SiO(OCH_3)](H)(CO)(PPh_3)$, 39

To $Ru[(PPh_2CH_2CH_2CH_2)_2SiO(OCH_3)](H)(CO)_2$, 36 in benzene, excess triphenylphosphine was added. During heating (78°C, 3 d), color was gradually discharged. Solvent was then removed *in vacuo* affording a dark solid which was washed with ethanol and hexanes to yield a pale white solid identified by spectroscopic methods.

$Ru[(PPh_2CH_2CH_2CH_2)_2SiO(OCH_3)](H)(CO)(NHC_5H_{10})$, 40

A mixture of $Ru[(PPh_2CH_2CH_2CH_2)_2SiO(OCH_3)](H)(CO)_2$, 36 and excess wet piperidine in C_6D_6 was heated (78 °C, 9 h). Complex 40 in a yellow solution was identified *in situ*.

$Ru[(PPh_2CH_2CH_2CH_2)_2Si(CH_3)](Cl)(CO)_2$, 41

A mixture of $Ru[(PPh_2CH_2CH_2CH_2)_2Si(CH_3)](H)(CO)_2$, 26 and excess carbon tetrachloride in benzene was heated (60 °C, 2 h). The volatiles were removed *in vacuo* and residue was washed with hexanes leaving a yellowish solid which was dried under vacuum for approximately 20 hours (10^{-2} mmHg). NMR spectroscopy showed that there was only one isomer. Anal. Calcd (found): C, 57.42 (57.10); H, 5.11 (5.00).

The solid was re-dissolved in benzene and the solution was heated (78 °C, 6 h). Removal of volatiles left a yellowish solid which was found to contain two isomers.

$Ru[(PPh_2CH_2CH_2CH_2)_2Si(CH_3)](D)(CO)_2$, 26-*d*

Excess $LiAlD_4$ was added to $Ru[(PPh_2CH_2CH_2CH_2)_2Si(CH_3)](Cl)(CO)_2$, 41 in THF (25 °C, 1 h). Carbon mono-oxide gas was then bubbled through the solution (25 °C, 10 min). Removal of volatiles left a yellow solid residue which was re-dissolved in benzene and treated with excess methanol to quench excess $LiAlD_4$. Yellow supernatant was transferred and concentrated *in vacuo* to give a yellow residue which was washed with methanol and hexanes leaving a pale yellow solid. Anal. Calcd (found): C, 60.35 (59.49); H, 5.37 (5.63).

$Ru[(PPh_2CH_2CH_2CH_2)_2Si(CH_3)](Cl)(CO)$, 42

After a toluene solution of $Ru[(PPh_2CH_2CH_2CH_2)_2Si(CH_3)](Cl)(CO)_2$, 41 was heated (1 d, 95 °C), volatiles were removed *in vacuo* and residue was washed with methanol affording a yellow solid which has been characterized by spectroscopic methods.

$Ru[(PPh_2CH_2CH_2CH_2)_2Si(CH_3)](H)(CO)(\mu\text{-}\eta^2\text{-}H_2BH_2)$, 43

To $Ru[(PPh_2CH_2CH_2CH_2)_2Si(CH_3)](Cl)(CO)$, 42 in THF-d8 was added excess $NaBH_4$. Complex 43 was formed immediately and characterized with NMR spectroscopy *in situ*.

***syn/cis*-$Ru[(PPh_2CH_2CH_2CH_2)_2Si(CH_3)](H)(^{13}CO)(CO)$, *cis*-26a-$^{13}CO$ (*syn*)**

After $Ru[(PPh_2CH_2CH_2CH_2)_2Si(CH_3)](CO)(H_2BH_2)$, 43 in THF was exposed to ^{13}CO (1 atm, 25 °C, 0.5 h), volatiles were removed *in vacuo* and residue was extracted with benzene. Evaporation of benzene left a pale yellow solid which has been characterized with spectroscopic methods.

***fac*-$Ru[(PPh_2CH_2CH_2CH_2)_2Si(CH_3)](H)_2(CO)$ anion, 44**

To $Ru[(PPh_2CH_2CH_2CH_2)_2Si(CH_3)](Cl)(CO)$, 42 in THF-d8 was added excess $LiAlH_4$. Complex 44 was formed within 2 hours and characterized with NMR spectroscopy *in situ*.

fac-Ru[($PPh_2CH_2CH_2CH_2$)$_2$Si(CH_3)](D)$_2$(CO) anion, 44-d_2

To Ru[($PPh_2CH_2CH_2CH_2$)$_2$Si(CH_3)](Cl)(CO), **42** in THF was added excess $LiAlD_4$. Complex 44-d_2 was formed within 2 hours and characterized with NMR spectroscopy *in situ*.

Ru[(*o*-$PPh_2C_6H_4CH_2$)$_2$Si(CH_3)](H)(CO)$_2$, 46

To bis(triphenylphosphine)tricarbonylRu(0) (0.20 g, 0.28 mmol) in toluene (10 mL) at refluxing point was added HSi(CH_3)(*o*-$CH_2C_6H_4PPh_2$)$_2$, 'mcbiPSiH', **VI** (0.25 g, 0.42 mmol) in toluene (10 mL). After refluxing (19 h), a clear colorless solution was formed. Removal of volatiles *in vacuo* left an oily residue which was washed with methanol (5 x 3 mL) and hexanes (5 x 3 mL) and dried under vacuum to yield a white solid in quantitative yield.

Ru[(*o*-$PPh_2C_6H_4CH_2$)$_2$Si(CH_3)](H)(CO)[P(OCH_2CH_3)$_3$], 47

To Ru[(*o*-$PPh_2C_6H_4CH_2$)$_2$Si(CH_3)](H)(CO)$_2$, **46** in toluene was added excess triethylphosphite. After heating (100 °C, 2 h), volatiles were removed *in vacuo* and residue was washed with hexanes (2 x 2 mL) to afford a white solid.

References

1. Bazant, V.; Chvalovsky, V.; Rathousky, J. Organosilicon Compounds, Academic Press, New York, **1965**
2. (a) Cotton, F.A.; Wilkinson, G. Advanced Inorganic Chemistry, 5th Edition, John Wiley & Sons: Toronto, **1988**, P266; (b) *ibid*, P202; (c) *ibid*, P1255
3. Rendina, L.M.; Puddephatt, R.J. Chemical Reviews **1997**, 97, 1735
4. Tanaka, M.; Uchimaru, Y.; Lautenschlager, H.-J. Organometallics **1991**, 10, 16
5. Wilkinson, G.; Stone, F.G.A.; Abel, E.W. Comprehensive Organometallic Chemistry, Volume 2, Pergamon Press: Toronto, **1982**, P117
6. Stobart, S.R.; Grundy, S.L.; Joslin, F.L. US Patent 4950798, **1990**
7. Stobart, S.R.; Grundy, S.L.; Joslin, F.L. Canadian Patent 1,327,365, **1994**
8. (a) Schubert, U.; Ackermann, K.; Worle, B. J. Amer. Chem. Soc. **1982**, 104, 7378; (b) Schubert, U.; Scholz, G.; Muller, J.; Ackermann, K.; Worle, B. J. Organomet. Chem. **1986**, 306, 303
9. Bruce, M.I. Angew. Chem. Int. Ed. Engl. **1977**, 16, 73
10. (a) Bergman, R.G. Science **1984**, 223, 902. (b) Hoyano, J.K.; McMaster, A.D.; Graham, W.A.G. J. Am. Chem. Soc. **1983**, 105, 7190
11. (a) Arndtsen, B.A.; Bergman, R.G. Science **1995**, 270, 1970. (b) Bromberg, S.E.; Yang, H.; Asplund, M.C.; Lian, T.; McNamara, B.K.; Kotz, K.T.; Yeston, J.S.; Wilkens, M.; Frei, H.; Bergman, R.G.; Harris, C.B. Science **1997**, 278, 260
12. Hofler, F. Topics in Current Chemistry **1974**, 50, 129

13. (a) Fink, W. Helvetica Chimica Acta **1976**, 59, 606; (b) Nagashima, H.; Tatebe, K.; Ishibashi, T.; Nakaoka, A.; Sakakibara, J.; Itoh, K. Organometallics **1995**, 14, 2868

14. (a) Eaborn, C.; Metham, T.N.; Pidcock, A. J. Organomet. Chem. **1973**, 54, C3; (b) Eaborn, C.; Metham, T.N.; Pidcock, A., *ibid*, **1973**, 63, 107; (c) Tanaka, M.; Uchimaru, Y.; Lautenschlager, H.-J. Organometallics **1991**, 10, 16

15. (a) Vancea, L.; Graham, W.A.G. Inorg. Chem. **1974**, 13, 511; (b) Corriu, R.J.P.; Moreau, J.J.E. J. Chem. Soc., Chem. Comm. **1980**, 278; (c) Carre, F.H.; Moreau, J.J.E. Inorg. Chem. **1982**, 21, 3099; (d) Corriu, R.J.P.; Moreau, J.J.E.; Pataud-Sat, M. Organometallics **1985**, 4, 623

16. Kang, Y.; Kim, K.I.; Kang, S.O.; Ko, J.; Heaton, B.T.; Barkley, J.V. J. Organomet. Chem. **1997**, 532, 79

17. Osakada, K.; Hataya, K.; Nakamura, Y.; Tanaka, M.; Yamamoto, T. J. Chem. Soc., Chem. Comm. **1993**, 576

18. Tamso, K.; Miyake, N.; Kiso, Y.; Kumada, M. J. Amer. Chem. Soc. **1975**, 97, 5603

19. (a) Fernandez, M.-J.; Bailey, P.M.; Bentz, P.O.; Ricci, J.S.; Koetzle, T.F.; Maitlis, P.M. J. Am. Chem. Soc. **1984**, 106, 5458; (b) Millan, A.; Towns, E.; Maitlis, P.M. J. Chem. Soc., Chem. Commun. **1981**, 673

20. (a) Kobayashi, T.-a.; Hayashi, T.; Yamashita, H.; Tanaka, M. Chem. Lett. **1989**, 467; (b) Uchimaru, Y.; Lautenschlager, H.-J.; Wynd, A.J.; Tanaka, M.; Goto, M. Organometallics **1992**, 11, 2639; (c) Tanaka, M.; Uchimaru, Y.; Lautenschlager,

H.-J. J. Organomet. Chem. **1992**, 428, 1; (d) Reddy, N.P.; Uchimaru, Y.; Lautenschlager, H.-J.; Tanaka, M. Chem. Lett. **1992**, 45

21. (a) Fernandez, M.-J.; Maitlis, P.M. Organometallics **1983**, 2, 164; (b) Isobe, K.; Bailey, P.M.; Maitlis, P.M. J. Chem. Soc., Chem. Comm. **1981**, 808

22. (a) Duckett, S.B.; Haddleton, D.M.; Jackson, S.A.; Perutz, R.N.; Poliakoff, M.; Upmacis, R.K. Organometallics **1988**, 7, 1526; (b) Duckett, S.B.; Perutz, R.N. J. Chem. Soc., Chem. Comm. **1991**, 28

23. (a) Tanke, R.S.; Crabtree, R.H. J. Chem. Soc., Chem. Comm. **1990**, 1056; (b) Tanke, R.S.; Crabtree, R.H. Organometallics **1991**, 10, 415; (c) Loza, M.; Faller, J.W.; Crabtree, R.H. Inorg. Chem. **1995**, 34, 2937

24. Heyn, R.H.; Tilley, T.D. J. Am. Chem. Soc. **1992**, 114, 1917

25. (a) Shimada, S.; Tanaka, M.; Honda, K. J. Am. Chem. Soc. **1995**, 117, 8289; (b) Shimada, S.; Tanaka, M.; Shiro, M. Angew. Chem. Int. Ed. Engl. **1996**, 35, 1856; (c) Tanaka, M.; Shimada, S. 30th Organosilicon Symposium **1997**, B-15

26. (a) Cotton, F.A.; Wilkinson, G. Advanced Inorganic Chemistry, 5th Edition, John Wiley & Sons, **1988**, P1299. (b) Appleton, T.G.; Clark, H.C.; Manzer, L.E. Coord. Chem. Rev. **1973**, 10, 335. (c) Gofman, M.M.; Nefedov, V.I. Inorg. Chim. Acta. **1978**, 28, 1

27. Koga, N.; Morokuma, K. J. Am. Chem. Soc. **1993**, 115, 6883

28. Latif, L.A.; Eaborn, C.; Pidcock, A.P.; Weng, N.S. J. Organomet. Chem. **1994**, 474, 217

29. Lichtenberger, D.L.; Rai-Chaudhuri, A. J. Am. Chem. Soc. **1991**, 113, 2923

30. (a) Murakami, M.; Yoshida, T.; Kawanami, S.; Ito, Y. J. Am. Chem. Soc. **1995**, 117, 6408; (b) Murakami, M. Yoshida, T.; Ito, Y. Organometallics **1994**, 13, 2900

31. Esteruelas, M.A.; Lahoz, F.J.; Olivan, M.; Onate, E.; Oro, L.A. Organometallics **1994**, 13, 4246

32. Michalczyk, M.J.; Recatto, C.A.; Calabrese, J.C.; Fink, M.J. J. Am. Chem. Soc. **1992**, 114, 7955

33. Ozawa, F.; Sugawara, M.; Hayashi, T. Organometallics **1994**, 13, 3237

34. Holmes-Smith, R.D.; Stobart, S.R.; Vefghi, R.; Zaworotko, M.J. J. Chem. Soc., Dalton Trans. **1987**, 969

35. Pomeroy, R.K.; Wijesekera, K.S. Can. J. Chem. **1980**, 58, 206

36. Auburn, M.J.; Holmes-Smith, R.D.; Stobart, S.R. J. Am. Chem. Soc. **1984**, 106, 1314

37. Grundy, S.L.; Holmes-Smith, R.D.; Stobart, S.R.; Williams, M.A. Inorg. Chem. **1991**, 30, 3333

38. Holmes-Smith, R.D.; Stobart, S.R.; Cameron, T.S.; Jochem, K. J. Chem. Soc., Chem. Comm. **1981**, 937

39. (a) Brookhart, M.; Green, M.L.H.; Wong, L.K. Prog. Inorg. Chem. **1988**, 36, 1. (b) Brookhart, M.; Green, M.L.H. J. Organomet. Chem. **1983**, 250, 395. (c) Crabtree, R.H.; Hamilton, D.G. Adv. Organomet. Chem. **1988**, 28, 299. (d) Schubert, U.; Adv. Organomet. Chem. **1990**, 30, 151

40. Jia, G.; Lee, H.M.; Xia, H.P.; Williams, I.D. Organometallics **1996**, 15, 5453

41. (a) Poulton, J.R.; Folting, K.; Streib, W.E.; Caulton, K.G. Inorg. Chem. **1992**, 31, 3190; (b) Huang, D.; Heyn, R.H.; Bollinger, J.C.; Caulton, K.G. Organometallics **1997**, 16, 292

42. Hill, A.F. J. Chem. Soc., Chem. Comm. **1995**, 741

43. Esteruelas, M.A.; Lahoz, F.J.; Onate, E.; Oro, L.A.; Zeier, B. Organometallics **1994**, 13, 4258

44. Maddock, S.M.; Rickard, C.E.F.; Roper, W.R.; Wright, L.J. Organometallics **1996**, 15, 1793

45. (a) Poulton, J.T.; Sigalas, M.P.; Folting, K.; Streib, W.E.; Eisenstein, O.; Caulton, K.G. Inorg. Chem. **1994**, 33, 1476; (b) Heyn, R.H.; Macgregor, S.A.; Nadasdi, T.T.; Ogasawara, M.; Eisenstein, O.; Caulton, K.G. Inorg. Chim. Acta **1997**, 259, 5

46. Wakatsuki, Y.; Yamazaki, H.; Nakano, M.; Yamamoto, Y. J. Chem. Soc., Chem. Comm. **1991**, 703

47. (a) Rickard, C.E.F.; Roper, W.R.; Salter, D.M.; Wright, L.J. Organometallics **1992**, 11, 3931; (b) Clark, G.R.; Rickard, C.E.F.; Roper, W.R.; Salter, D.M.; Wright, L. J. Pure Appl. Chem. **1990**, 62, 1039

48. Heyn, R.H.; Huffman, J.C.; Caulton, K.G. New J. Chem. **1993**, 17, 797

49. Joslin, F.L. Ph.D. Dissertation, University of Victoria, **1983**

50. (a) Holmes-Smith, R.D.; Osei, R.D.; Stobart, S.R. J. Chem. Soc., Perkin Trans. I **1983**, 861; (b) Joslin, F.L.; Stobart, S.R. Inorg. Chem. **1993**, 32, 2221

51. (a) Schubert, D.M.; Norman, A.D. Inorg. Chem. **1984**, 23, 4130. (b) Hackney, M.L.J.; Norman, A.D. J. Chem. Soc., Chem. Comm. **1986**, 850. (c) Hackney,

M.L.J.; Haltiwanger, R.C.; Brandt, P.F.; Norman, A.D. J. Organomet. Chem. **1989**, 359, C36. (d) Schubert, D.S.; Brandt, P.F.; Norman, A.D. Inorg. Chem. **1996**, 35, 6204. (e) Hackney, M.L.J.; Schubert, D.M.; Brandt, P.F.; Haltiwanger, R.C.; Norman, A.D., *ibid*, **1997**, 36, 1867

52. Gossage, R. A.; McLennan, G. D.; Stobart, S. R. *Inorg. Chem.* **1996**, *35*, 1729

53. Fantucci, P.; Chini, P.; Canziani, F. Gazz. Chim. Ital. **1974**, 104, 249

54. Albricht, von H.P.; Isslieb, K. Z. Anorg. Allg. Chem. **1976**, 422, 237

55. Gossage, R.A. Ph.D. Dissertation, University of Victoria, **1996**

56. Bruce, G.C. Ph.D. Dissertation, University Of Victoria, **1984**

57. (a) Auburn, M. J.; Stobart, S.R. J. Chem. Soc., Chem. Commun. **1984**, 281; (b) Auburn, M.J.; Holmes-Smith, R.D.; Stobart, S.R.; Bakshi, P.K.; Cameron, T.S. Organometallics **1996**, 15, 3032

58. For the recent discussion, see (a) Musaev, D.G.; Morokuma, K. J. Orgnanomet. Chem. **1995**, 504, 93. (b) Caulton, K.G. New J. Chem. **1994**, 18, 25. (c) Paulton, J.T.; Hauger, B.E.; Kuhlmann, R.L.; Caulton, K.G. Inorg. Chem. **1994**, 33, 3325. (d) Harlow, R.D.; Thorn, D.L.; Baker, R.T.; Jones, N.L. Inorg. Chem. **1992**, 31, 993. (e) Chin, B.; Lough, A.J.; Morris, R.H.; Schweitzer, C.T.; D'Agostino, C. Inorg. Chem. **1994**, 33, 6278. (f) Burrel, A.K.; Bryan, J.C.; Kubas, G.J.; J. Am. Chem. Soc. **1994**, 116, 1575. (g) Wang, K.; Emge, T.J.; Goldman, A.S.; Li, C.; Nolan, S.P. Organometallics **1995**, 14, 4929

59. Wang, J. Ph.D. Dissertation, University of Victoria, **1996** and also experimental results in Section 4.G. of this thesis

60. Houri, A.F.; Didiuk, M.T.; Xu, Z.; Horan, N.R.; Hoveyda, A.H. J. Am. Chem. Soc. **1993**, 115, 6614

61. Guram, A.S.; Guo, Z.; Jordan, R.F. J. Am. Chem. Soc. **1993**, 115, 4902

62. (a) Temple, J.S.; Riediker, M.; Schwartz, J. J. Am. Chem. Soc. **1982**, 104, 1310; (b) Schwartz, J. Bull. de la Société Chimique de France **1980**, II332; (c) Hart, D.W.; Schwartz, J. J. Am. Chem. Soc. **1974**, 96, 8115; (d) Schwartz, J.; Labinger, J.A. Angew. Chem. Int. Ed. Engl. **1976**, 15, 333; (e) Carr, D.B.; Schwartz, J. J. Am. Chem. Soc. **1979**, 101, 3521

63. Negishi, E.-I.; Takahashi, T. Aldrichimica Acta **1985**, 18, 31

64. Wang, M.; Lu, S.; Bei, M.; Guo, H.; Jin, Z. J. Organomet. Chem. **1993**, 447, 227

65. Endo, J.; Koga, N.; Morokuma, K. Organometallics **1993**, 12, 2777

66. (a) Buchwald, S.L.; LaMarie, S.J.; Nielsen, R.B.; Watson, B.T.; King, S.M. Tetrahedron Letters **1987**, 28, 3895; (b) King, R.B.; Stone, F.G.A. Inorganic Synthesis, **1963**, 7, 100

67. (a) Kautzner, B.; Wailes, P.C.; Weigold, H. J. Chem. Soc., Chem. Comm. **1969**, 1105; (b) Wailes, P.C.; Weigold, H. J. Organomet. Chem. **1970**, 24, 405

68. Engel R. Synthesis of Carbon-Phosphorus Bonds, CRC Press: Boca Raton, Florida, **1988**

69. (a) Fryzuk, M.D.; Stone, C.; Alex, R.F. Tetrahedron Letters **1988**, 29, 3915. (b) Fryzuk, M.D.; Bates, G.S.; Stone, C., *ibid*, **1986**, 27, 1537. (c) Fryzuk, M.D.; Bates, G.S.; Stone, C. J. Org. Chem. **1987**, 52, 2334. (d) Fryzuk, M.D.; Bates, G.S.; Stone, C. J. Org. Chem. **1988**, 53, 4425

70. (a) Negishi, E.; Cederbaum, F.E.; Takahashi, T. Tetrahedron Lett. **1986**, 27, 2829. (b) Swanson, D.R.; Negishi, E. Organometallics **1991**, 10, 825

71. (a) Fagan, P.J.; Nugent, W.A.; Calabrese, J.C. J. Am. Chem. Soc. **1994**, 116, 1880. (b) Fagan, P.J.; Nugent, W.A., *ibid*, **1988**, 110, 2310

72. Group 14 elements: (a) Dufour, P.; Dubac, J.; Dartiguenave, Y. Organometallics **1990**, 9, 3001. (b) Dufour, P.; Dartiguenave, M.; Dartiguenave, Y.; Dubac, J. J. Orgnaomet. Chem. **1990**, 384, 61. (c) Meier-Brocks, F.; Weiss, E. J. Organomet. Chem. **1993**, 453, 33

73. Group 15 elements: (a) Douglas, T.; Theopold, K.H. Angew. Chem., Int. Ed. Engl. **1989**, 28, 1367. (b) Buchwald, S.L.; Fisher, R.A.; Foxman, R.A. Angew. Chem., Int. Ed. Engl. **1990**, 29, 771. (c) Schenk, W.A.; Voss, E. J. Organomet. Chem. **1990**, 396, C8. (d) Sendlinger, S.C.; Haggarty, B.S.; Rheingold, A.L.; Theopold, K.H. Chem. Ber. **1991**, 124, 372. (e) Ashe, A.J.; Kampf, J.W.; Altaweel, S.M. J. Am. Chem. Soc. **1992**, 114, 372. (f) Ashe, A.J.; Kampf, J.W.; Altaweel, S.M. Organometallics **1992**, 11, 1491. (g) Spence, R.E.V.; Hsu, D.P.; Buchwald, S.L. Organometallics **1992**, 11, 3492

74. Group 16 elements: (a) Buchwald, S.L.; Qun, F. J. Org. Chem. **1989**, 54, 2793. (b) Tour, J.M.; Wu, R.L.; Shcumm, J.S. J. Am. Chem. Soc. **1990**, 112, 562. (c) Cuny, G.D.; Gutierrez, A.; Buchwald, S.L. Organometallics **1991**, 10, 537. (d) Mohamadi, F.; Spees, M.M. Organometallics **1992**, 11, 1398

75. (a) Zablocka, M.; Igau, A.; Majoral, J.-P.; Pietrusiewicz, K.M. Organometallics **1993**, 12, 603; (b) Majoral, J.-P.; Zablocka, M.; Igau, A.; Cenac, N. Chem. Ber. **1996**, 129, 879

76. Labinger, J.-A. Comprehensive Organic Synthesis, Pergamon Press, Oxford, England, **1991**, 8, P667

77. Tebby, J.C. Handbook of Phosphorus-31 Nuclear Magnetic Resonance Data, CRC Press: Boca Raton, Florida, **1991**, P131

78. Jordan, R.F. Adv. Organomet. Chem. **1991**, 32, 325

79. (a) Yamamoto, A. Organotransition Metal Chemistry - Fundamental Concepts and Applications, John Wiley & Sons: New York, **1986**, P208; (b) Li, C.; Ogasawara, M.; Nolan, S.P.; Caulton, K.G. Organometallics **1996**, 15, 4900

80. Brost, R.D.; Bruce, G.C.; Joslin, F.L.; Stobart, S.R. Organometallics **1997**, in press

81. Walker, B.J. Organophosphorus Chemistry, William Clowes & Sons Limited, **1972**

82. (a) Sommer, H.; Hietkamp, S.; Stelzer, O. Chem. Ber. **1984**, 117, 3414; (b) Grim, S.O.; Barth, R.C. J. Organomet. Chem. **1975**, 94, 327

83. Ihara, T.; Nakayama, M.; Murata, M.; Nakano, K.; Maeda, M. J. Chem. Soc., Chem. Comm. **1997**, 1609

84. (a) Blumel, J. J. Am. Chem. Soc. **1995**, 117, 2112; (b) Deschler,U.; Kleinschmit, P.; Panster, P. Angew. Chem. Int. Ed. Engl. **1986**, 25, 236

85. (a) Okano, T.; Kobayashi, T.; Konishi, H.; Kiji, J. Bull. Chem. Soc. Jpn. **1982**, 55, 2675; (b) Deschler, U.; Kleinschmit, P.; Panster, P. Angew. Chem. Int. Ed. Engl. **1986**, 25, 236; (c) Blumel, J. Inorg. Chem. **1994**, 33, 5050

86. Uriarte, R.; Mazanec, T.J.; Tau, K.D.; Meek, D.W. Inorg. Chem. **1980**, 19, 79

87. (a) Blundell, T.L.; Powell, H.M. J. Chem. Soc., Chem. Comm. **1967**, 763; (b) Antberg, M.; Prengel, C.; Dahlenburg, L. Inorg. Chem. **1984**, 23, 4170; (c) Mayer, H.A.; Kaska, W.C. Chem. Rev. **1994**, 94, 1239

88. Chadwell, S.J.; Coles, S.J.; Edwards, P.G.; Hursthouse, M.B. J. Chem. Soc., Dalton Trans. **1996**, 1105

89. (a) Blower, P.J.; Dilworth, J.R.; Leigh, G.J.; Neaves, B.D.; Normanton, F.B. J. Chem. Soc., Dalton Trans. **1985**, 2647; (b) Block, E.; Ofori-Okai, G.; Zubieta, J. J. Am. Chem. Soc. **1989**, 111, 2327; (c) Dilworth, J.R.; Hutson, A.J.; Lewis, J.S.; Miller, J.R.; Zheng, Y.; Chen, Q.; Zubieta, J. J. Chem. Soc., Dalton Trans. **1996**, 1093

90. Benkeser, R.A.; Riel, F.J. J. Am. Chem. Soc. **1951**,73, 3472

91. (a) Gallagher, D.J.; Du, H.; Long, S.A.; Beak, P. J. Am. Chem. Soc. **1996**, 118, 11391; (b) Park, Y.S.; Boys, M.L.; Beak, P., *ibid*, **1996**, 118, 3757; (c) Beak, P.; Kerrick, S.T.; Wu, S.; Chu, J., *ibid*, **1994**, 116, 3231

92. Winkler, U.; Schieck, M.; Pritzkow, H.; Driess, M.; Hyla-Krysp, I.; Lange, H.; Gleiter, R. Chem. Eur. J. **1997**, 3, 874

93. (a) Yin, J.; Klosin, J.; Abboud, K.A.; Jones, W.M. J. Am. Chem. Soc. **1995**, 117, 3298; (b) Procopio, L.J.; Carroll, P.J.; Berry, D.H. J. Am. Chem. Soc. **1994**, 116, 177

94. Kane, K.M.; Lemke, F.R. Inorg. Chem. **1997**, 36, 1354

95. Carre, F.H.; Corriu, R.J.P.; Lanneau, G.F.; Merle, P.; Soulairol, F.; Yao, J. Organometallics **1997**, 16, 3878

96. (a) Breliere, C.; Corriu, R.J.P.; Royo, G.; Zwecker, J. Organometallics **1989**, 8, 1834; (b) Brook, M.A.; Chau, D.; Roth, M.J.; Yu, W.; Penny, H.B., *ibid*, **1994**, 13, 750; (c) Kim, B.-K.; Kloos, S.D.; Boudjouk, P. 30th Organosilicon Symposium **1997**, P-73

97. Abraham, R.J.; Fisher, J.; Loftus, P. Introduction to NMR Spectroscopy, John Wiley & Sons: Toronto, **1988**, P196

98. Clark, H.C.; Goel, A.B.; Goel, R.G.; Ogini, W.O. J. Organomet. Chem. **1978**, 157, C16

99. Crespo, M.; Sales, J.; Solans, X.; Altaba, M.F. J. Chem. Soc., Dalton Trans. **1988**, 1617

100. Siedle, A.R.; Newmark, R.A.; Gleason, W.B. J. Am. Chem. Soc. **1986**, 108, 767

101. Weichmann, H. J. Organomet. Chem. **1982**, 238, C49

102. Ebsworth, E.A.V.; Marganian, V.M.; Reed, F.J.S.; Gould, R.O. J. Chem. Soc., Dalton Trans. **1978**, 1167

103. Han, L.-B.; Shimada, S.; Tanaka, M. J. Am. Chem. Soc. **1997**, 119, 8133

104. Litz, K.E.; Henderson, K.; Gourley, R.W.; Holl, M.M.B. Organometallics **1995**, 14, 5008

105. Mann, B.E.; Musco, A. J. Chem. Soc., Dalton Trans. **1980**, 776

106. (a) Tolman, C.A.; Seidel, W.C.; Gerlach, D.H. J. Am. Chem. Soc. **1972**, 94, 2669; (b) Camalli, M.; Caruso, F. Helvetica Chimica Acta **1990**, 73, 2263

107. (a) Cook, C.D.; Jauhal, G.S. J. Am. Chem. Soc. **1968**, 90, 1464; (b) Cheng, P.-T.; Nyberg, S.C. Can. J. Chem. **1972**, 50, 912; (c) Birk, J.P.; Halpern, J.; Pickard,

A.L. J. Am. Chem. Soc. **1968**, 90, 4491; (d) Cheng, P.-T.; Cook, C.D.; Nyburg, S.C.; Wan, K.Y. Inorg. Chem. **1971**, 10, 2210

108. Maresca, L.; Natile, G. Comments Inorg. Chem. **1993**, 14, 349

109. (a) Ang H.G.; Chang, B.; Kwik, W.L. J. Chem. Soc., Dalton Trans. **1992**, 2161; (b) Atherton, M.J.; Fawcett, J.; Holloway, J.H.; Hope, E.G.; Russell, D.R.; Saunders, G.C. J. Chem. Soc., Dalton Trans. **1997**, 2217

110. Abis, L.; Santi, R. J. Organomet. Chem. **1981**, 215, 263

111. (a) Ferguson, G.; Siew, P.Y.; Goel, A.B. J. Chem. Research (S) **1979**, 362; (b) Clark, H.C.; Goel, A.B.; Wong, C.S. J. Organomet. Chem. **1978**, 152, C45

112. Muller, C.; Schubert, U. Chem. Ber. **1991**, 124, 2181

113. Bender IV, J.E.; Litz, K.E.; Giarikos, D.; Wells, N.J.; Holl, M.M.B.; Kampf, J.W. Chem. Eur. J. **1997**, in press

114. Paonessa, R.S.; Trogler, W.C. J. Am. Chem. Soc. **1982**, 104, 1138

115. (a) Kemp, W. Organic Spectroscopy, 3rd Ed. W.H. Freeman and Co.: New York, **1991**, P157. (b) Brunner, H. Angew. Chem. Int. Ed. Engl. **1983**, 22, 897. (c) Brunner, H.; Agrifoglio, G.; Benn, R.; Rufinska, A. J. Organomet. Chem. **1981**, 217, 365. (d) Benn, R.; Rufinska, A.; Schroth, G. J. Organomet. Chem. **1981**, 217, 91

116. Bundle, D. Biochemistry, **1994**, 33, 5183

117. Frey, M.H.; Wagner, G.; Vasak, M.; Sorensen, O.W.; Neuhaus, D.; Worgotter, E.; Kagi, J.H.R.; Ernst, R.R.; Wuthrich, K. J. Am. Chem. Soc. **1985**, 107, 6847

118. Brunner, H.; Beier, P.; Riepl, G.; Bernal, I.; Reisner, G.M.; Benn, R.; Rufinska, A. Organometallics **1985**, 4, 1732

119. Schlaf, M.; Morris, R.H. J. Chem. Soc., Chem. Comm **1995**, 625

120. Morris, K.F.; Erickson, L.E.; Panajotova, B.V.; Jiang, D.W.; Ding, F. Inorg. Chem. **1997**, 36, 601

121. Gusev, D.G.; Nadasdi, T.T.; Caulton, K.G. Inorg. Chem. **1996**, 35, 6772

122. Hillhouse, G.L.; Bercaw, J.E. J. Am. Chem. Soc. **1984**, 106, 5472

123. Milstein, D.; Calabrese, J.C.; Williams, I.D. J. Am. Chem. Soc. **1986**, 108, 6387

124. Yoshida, Y.; Okano, T.; Saito, K.; Otsuka, S. Inorg. Chim. Acta. **1980**, 44, L135

125. Burn, M.J.; Fickes, M.G.; Hartwig, J.F.; Hollander, F.J.; Bergman, R.G. J. Am. Chem. Soc. **1993**, 115, 5875

126. Yoon, M.; Tyler, D.R. J. Chem. Soc., Chem. Comm. **1997**, 639

127. Kaplan, A.W.; Bergman, R.G. Organometallics **1997**, 16, 1106

128. Gulinski, J.; James, B.R.; Marciniec, B. J. Organomet. Chem. **1995**, 499, 173

129. (a) Christ, M.L.; Sabo-Etienne, S.; Chung, G.; Chaudret, B. Inorg. Chem. **1994**, 33, 5316. (b) Elgafi, S.; Field, L.D.; Messerle, B.A.; Hambley, T.W.; Turner, P. J. Chem. Soc., Dalton Trans. **1997**, 2341

130. Pedersen, A.; Tilset, M.; Folting, K.; Caulton, K.G. Organometallics **1995**, 14, 875

131. (a) Crabtree, R.H. Acc. Chem. Res. **1990**, 23, 95; (b) Morris, R.H.; Jessop, P.G. Coord. Chem. Rev. **1992**, 121, 155

132. (a) Vaska, L.; DiLuzio, J.W. J. Am. Chem. Soc. **1962**, 84, 679. (b) Vaska, L. ibid. **1966**, 88, 5325

133. Sheldon, R.A.; Kochi, J.K. Metal-Catalyzed Oxidations of Organic Compounds, Academic Press: New York, **1981**

134. Duncan, D.C.; Hill, C.L. J. Am. Chem. Soc. **1997**, 119, 243

135. (a) Vigalok, A.; Shimon, L.J.W.; Milstein, D. J. Chem. Soc., Chem. Comm. **1996**, 1673. (b) Maddock, S.M.; Rickard, C.E.F.; Roper, W.R.; Wright, L.J. J. Organomet. Chem. **1996**, 510, 267. (c) Maddock, S.M.; Rickard, C.E.F.; Roper, W.R.; Wright, L.J. J. Organomet. Chem. **1996**, 510, 267

136. Rickard, C.E.F.; Roper, W.R.; Salter, D.M.; Wright, L.J. J. Am. Chem. Soc. **1992**, 114, 9682

137. Marciniec, B.; Pietraszuk, C. Organometallics **1997**, 16, 4320

138. (a) Boyar, E.B.; Moore, D.S.; Robinson, S.D.; James, B.R.; Preece, M.;Thorburn, I. J. Chem. Soc., Dalton Trans. **1985**, 617. (b) James, B.R.; Rempel, G.L. Can. J. Chem. **1966**, 44, 233

139. Sanchez-Delgado, R.A.; Rosales, M.; Andriollo, A. Inorg. Chem. **1991**, 30, 1170

140. Pomeroy, R.K.; Gay, R.S.; Evans, G.O.; Graham, W.A.G. J. Am. Chem. Soc. **1972**, 94, 272

141. Bianchini, C.; Perez, P.J.; Peruzzini, M.; Zanobini, F.; Vacca, A. Inorg. Chem. **1991**, 30, 279

142. Holah, D.G.; Hughes, A.N.; Hui, B.C. Can. J. Chem. **1976**, 54, 320

143. Crabtree, R.H.; Pearman, A.J. J. Organomet. Chem. **1978**, 157, 335

144. Esteruelas, M.A.; Garcia, M.P.; Lopez, A.M.; Oro, L.A.; Ruiz, N.; Schlunken, C.; Valero, C.; Werner, H. Inorg. Chem. **1992**, 31, 5580

145. Werner, H.; Esteruelas, M.A.; Meyer, U.; Wrackmeyer, B. Chem. Ber. **1987**, 120, 11

146. Private communication with S.R. Stobart

147. (a) Kwiatek, J. Catal. Rev. **1967**, 1, 40. (b) Ginsberg, A.P. J. Chem. Soc., Chem. Comm. **1968**, 857. (c) Abrahams, S.C.; Ginsberg, A.P.; Knox, K. Inorg. Chem. **1964**, 3, 558. (d) Ginsberg, A.P. Inorg. Chem. **1964**, 3, 567. (e) Moyer, R.O., Jr.; Lindsay, R.; Marks, D.N. "Tansition Metal Hydrides"; Bau, R., Ed.; American Chemical Society: Washington, DC, **1970**, P366. (f) Chatt, J.; Davidson, J. M. J. Chem. Soc. **1965**, 843

148. Wilczynski, R.; Fordyce, W.A.; Halpern, J. J. Am. Chem. Soc. **1983**, 105, 2066

149. Huffman, J.C.; Green, M.A.; Kaiser, S.L.; Caulton, K.G. J. Am. Chem. Soc. **1985**, 107, 5111

150. (a) Pez, G.P.; Grey, R.A.; Corsi, J. J. Am. Chem. Soc. **1981**, 103, 7528. (b) Grey, R.A.; Pez, G.P.; Wallo, A. J. Am. Chem. Soc. **1981**, 103, 7536

151. Walker, H.W.; Ford, P.C. J. Organomet. Chem. **1981**, 214, C43

152. (a) Chan, A.S.C.; Shieh, H.-S. J. Chem. Soc., Chem. Comm. **1985**, 1379. (b) Peters, J.C.; Odom, A.L.; Cummins, C.C. Chem. Comm. **1997**, 1995

153. Wilkes, L.M.; Nelson, J.H.; Mitchener, J.P.; Babich, M.W.; Riley, W.C.; Helland, B.J.; Jacobson, R.A.; Cheng, M.Y.; Seff, K.; McCusker, L.B. Inorg. Chem. **1982**, 21, 1376

154. (a) Barnard, C.F.J.; Daniels, J.A.; Jeffery, J.; Mawby, R.J. J. Chem. Soc., Dalton Trans. **1976**, 953. (b) Barnard, C.F.J.; Daniels, J.A.; Mawby, R.J. J. Chem. Soc., Dalton Trans. **1976**, 961

155. Hauger, B.E.; Gusev, D.; Caulton, K.G. J. Am. Chem. Soc. **1994**, 116, 208

156. Esteruelas, M.A.; Lahoz, F.J.; Onate, E.; Oro, L.A.; Rodriguez, L. Organometallics **1996**, 15, 823

157. Ogasawara, M.; Maseras, F.; Gallego-Planas, N.; Kawamura, K.; Ito, K.; Toyota, K.; Streib, W.E.; Komiya, S.; Eisenstein, O.; Caulton, K.G. Organometallics **1997**, 16, 1979

158. Bakhmutov, V.I.; Bertran, J.; Esteruelas, M.A.; Lledos, A.; Maseras, F.; Modrego, J.; Oro, L. A.; Sola, E. Chem. Eur. J. **1996**, 2, 815

159. Hastings, W.R.; Roussel, M.R.; Baird, M.C. J. Chem. Soc., Dalton Trans. **1990**, 203

160. Pomeroy, R.K.; Graham, W.A.G. J. Am. Chem. Soc. **1972**, 94, 274

161. Jessop, P.G.; Rastar, G.; James, B.R. Inorg. Chim. Acta **1996**, 250, 351

162. Espenson, J.H. Chemical Kinetics and Reaction Mechanism, McGraw-Hill, Inc.: Toronto, **1995**, P217

163. Barton, D.H.R.; Martell, A.E.; Sawyer, D.T. The Activation of Dioxygen and Homogeneous Catalytic Oxidation, Plenum Press, New York, **1993**

164. Einhorn, C.; Einhorn, J.; Marcadal, C.; Pierre, J.-L. J. Chem. Soc., Chem. Comm. **1997**, 447

165. Nam, W.; Ho, R.; Valentine, J.S. J. Am. Chem. Soc. **1991**, 113, 7052

166. (a) Murahashi, S.-I.; Naota, T.; Miyaguchi, N.; Noda, S. J. Am. Chem. Soc. **1996**, 118, 2509. (b) Murahashi, S.-I.; Oda, Y.; Naota, T.; Kuwabara, T. Tetrahedron Letters **1993**, 34, 1299

167. Vos, D.D.; Bein, T. J. Chem. Soc., Chem. Comm. **1996**, 917

168. James, B.R. Dioxygen Activation and Homogeneous Catalytic Oxidation, Elsevier Science Publishers B.V., **1991**, 195

169. Robbins, M.H.; Drago, R.S. J. Chem. Soc., Dalton Trans. **1995**, 100

170. Groves, J.T.; Bonchio, M.; Carofiglio, T.; Shalyaev, K. J. Am. Chem. Soc. **1996**, 118, 8961

171. Barton, D.H.R.; Gastiger, M.J.; Motherwell, W.B. J. Chem. Soc., Chem. Comm. **1983**, 41

172. Barton, D.H.R.; Doller, D. Acc. Chem. Res. **1992**, 25, 504

173. (a) Barton, D.H.R.; Chavasiri, W. Tetrahedron **1994**, 50, 19. (b) Barton, D.H.R.; Beviere, S.D.; Chavasiri, W. Tetrahedron **1994**, 50, 31

174. (a) Snelgrove, D.W.; MacFaul, P.A.; Ingold, K.U.; Wayner, D.D.M. Tetrahedron Letters **1996**, 37, 823. (b) Minisci, F.; Fontana, F.; Araneo, S.; Recupero, F.; Banfi, S.; Quici, S. J. Am. Chem. Soc. **1995**, 117, 226

175. Barton, D.H.R.; Beviere, S.D.; Hill, D.R. Tetrahedron **1994**, 50, 2665

176. Singh, B.; Long, J.R.; Biani, F.F.; Gattteschi, D.; Stavropoulos, P. J. Am. Chem. Soc. **1997**, 119, 7030

177. Sheldon, R.A.; Kochi, J.K. Metal-Catalyzed Oxidations of Organic Compounds, Academic Press, New York, **1981**

178. Drago, R.S.; Beer, R.H. Inorg. Chim. Acta **1992**, 198-200, 359

179. Hamilton, D.E.; Drago, R.S.; Zombeck, A. J. Am. Chem. Soc. **1987**, 109, 374

180. Nam, W.; Kim, H.J.; Kim, S.H.; Ho, R.Y.N.; Valentine, J.S. Inorg. Chem. **1996**, 35, 1045

181. Reetz, M.T.; Tollner, K. Tetrahedron Letters **1995**, 36, 9461

182. Murahashi, S.-I.; Oda, Y.; Naota, T. J. Am. Chem. Soc. **1992**, 114, 7913

183. Goldstein, A.S.; Beer, R.H.; Drago, R.S. J. Am. Chem. Soc. **1994**, 116, 2424

184. Boelrijk, A.E.M.; Velzen, M.M.; Neenan, T.X.; Reedijk, J.; Kooijman, H.; Spek, A.L. J. Chem. Soc., Chem. Comm. **1995**, 2465

185. Bailey, A.J.; Griffith, W.P.; White, A.J.P.; William, D.J. J. Chem. Soc., Chem. Comm. **1994**, 1833

186. Ahmad, N.; Levison, J.J.; Robinson, S.D.; Uttley, M.F. Inorganic Synthesis **1974**, 15, 50

187. Brunet J.-J.; Kindela, F.B.; Neibecker, D. Inorganic Synthesis **1992**, 29, 153

188. Nagel, U. Chem. Ber. **1982**, 115, 1998

189. Ugo, R.; Cariati, F.; Monica, G.L. Inorganic Synthesis **1968**, 11, 107

Appendices

A. Crystallographic data for compound 32

Empirical formula:	$C_{35}H_{45}O_5P_3RuSi$	Formula weight:	767.8
Crystal system:	triclinic	Space group:	P1
Unit cell dimensions:	a = 9.042(1) Å	Z:	2
	b = 12.040(1) Å	Diffractometer:	Siemens P4/PC
	c = 18.046(2) Å	Temperature:	293 K
	α = 95.11(1)°	R:	5.12%
	β = 101.65(1)°	R_w:	5.64%
	γ = 106.57(1)°		

Table A-1. Atomic coordinates (x 10^4) and equivalent isotropic displacement coefficients ($Å^2$ x 10^3) for 32

Atom	x	y	z	U(eq)
Ru	1132(1)	2647(1)	2521(1)	32(1)
P(1)	-40(2)	3803(1)	3194(1)	44(1)
P(2)	1067(2)	3461(1)	1381(1)	38(1)
P(3)	1285(2)	1383(1)	3433(1)	38(1)
Si	-1809(2)	477(1)	1469(1)	43(1)
O(1)	-1285(4)	1658(3)	2077(2)	39(1)

O(2)	4488(5)	4150(4)	3171(3)	67(2)
O(3)	-1189(6)	4456(5)	2761(3)	70(2)
O(4)	1052(7)	4895(4)	3832(3)	70(2)
O(5)	-1081(6)	3051(4)	3701(3)	61(2)
C(1)	-4021(8)	-128(6)	1198(4)	66(3)
C(2)	3180(7)	3567(5)	2920(3)	45(2)
C(3)	-2681(10)	3827(8)	2286(4)	80(4)
C(4)	1950(11)	5934(7)	3639(5)	91(4)
C(5)	-1840(10)	3541(8)	4213(5)	80(4)
C(6)	-847(7)	2920(6)	670(3)	52(2)
C(7)	-1236(9)	1735(7)	176(3)	67(3)
C(8)	-1024(9)	723(6)	593(4)	65(3)
C(9A)	-824(10)	-604(6)	1860(4)	50(3)
C(9B)	-1877(36)	-945(23)	1958(15)	30(8)
C(10)	-869(9)	-866(5)	2646(4)	61(3)
C(11)	-542(7)	155(5)	3298(3)	48(2)
C(12)	2467(7)	3291(5)	806(3)	45(2)
C(13)	2484(9)	3831(6)	151(4)	61(3)
C(14)	3506(10)	3718(7)	-303(4)	74(3)
C(15)	4521(10)	3089(7)	-123(5)	75(3)
C(16)	4513(9)	2547(7)	514(5)	75(3)
C(17)	3481(8)	2637(6)	978(4)	58(3)

C(18)	1563(8)	5068(5)	1520(3)	45(2)
C(19)	405(9)	5622(6)	1439(4)	57(3)
C(20)	840(12)	6843(7)	1609(5)	78(4)
C(21)	2367(14)	7504(7)	1865(5)	86(4)
C(22)	3541(12)	6962(6)	1947(5)	79(4)
C(23)	3139(9)	5750(6)	1779(4)	61(3)
C(24)	2844(7)	681(5)	3503(3)	47(2)
C(25)	4021(8)	964(7)	3104(4)	63(3)
C(26)	5239(10)	464(8)	3194(5)	77(4)
C(27)	5279(10)	-343(8)	3676(5)	80(4)
C(28)	4097(10)	-667(7)	4061(5)	76(3)
C(29)	2912(9)	-145(6)	3996(5)	68(3)
C(30)	1707(8)	2049(5)	4442(3)	48(2)
C(31)	3180(10)	2848(7)	4753(4)	75(3)
C(32)	3541(13)	3448(9)	5495(5)	101(4)
C(33)	2429(15)	3241(8)	5928(4)	97(5)
C(34)	1018(14)	2450(7)	5626(4)	85(4)
C(35)	597(10)	1837(6)	4884(4)	62(3)

Table A-2. Anisotropic displacement coefficients ($Å^2 \times 10^3$) for **32**

Atom	U_{11}	U_{22}	U_{33}	U_{12}	U_{13}	U_{23}
Ru	30(1)	32(1)	33(1)	7(1)	7(1)	-1(1)

P(1)	49(1)	43(1)	45(1)	17(1)	16(1)	2(1)
P(2)	38(1)	39(1)	37(1)	12(1)	10(1)	2(1)
P(3)	37(1)	38(1)	40(1)	12(1)	11(1)	4(1)
Si	46(1)	36(1)	41(1)	11(1)	5(1)	-3(1)
O(1)	30(2)	36(2)	43(2)	6(1)	5(1)	-4(1)
O(2)	39(2)	70(3)	75(3)	-1(2)	7(2)	-2(2)
O(3)	62(3)	72(3)	84(3)	30(3)	17(3)	24(3)
O(4)	89(4)	54(3)	60(3)	18(3)	19(3)	-13(2)
O(5)	77(3)	64(3)	59(3)	29(2)	39(2)	15(2)
C(1)	51(4)	63(4)	70(4)	-3(3)	16(3)	-7(3)
C(2)	40(3)	43(3)	43(3)	7(2)	8(2)	-4(2)
C(3)	76(5)	109(7)	66(4)	49(5)	16(4)	6(4)
C(4)	88(6)	75(5)	91(6)	-5(5)	36(5)	-21(4)
C(5)	88(6)	95(6)	78(5)	37(5)	51(5)	15(4)
C(6)	42(3)	65(4)	43(3)	14(3)	1(2)	9(3)
C(7)	62(4)	83(5)	36(3)	-2(4)	11(3)	-3(3)
C(8)	61(4)	69(4)	53(3)	7(3)	18(3)	-21(3)
C(9A)	55(5)	36(3)	56(4)	14(3)	8(3)	-5(3)
C(10)	78(5)	35(3)	62(4)	17(3)	1(3)	6(3)
C(11)	44(3)	44(3)	52(3)	4(2)	14(3)	11(2)
C(12)	43(3)	45(3)	47(3)	10(2)	18(2)	-2(2)
C(13)	72(4)	67(4)	52(3)	22(4)	30(3)	17(3)

C(14)	86(6)	73(5)	60(4)	6(4)	38(4)	14(4)
C(15)	75(5)	73(5)	75(5)	5(4)	47(4)	-11(4)
C(16)	63(4)	79(5)	91(6)	25(4)	38(4)	2(4)
C(17)	51(4)	71(4)	58(4)	22(3)	24(3)	13(3)
C(18)	63(4)	39(3)	39(3)	21(3)	19(3)	11(2)
C(19)	67(4)	54(3)	61(4)	29(3)	18(3)	17(3)
C(20)	110(7)	62(4)	81(5)	46(5)	31(5)	21(4)
C(21)	133(9)	47(4)	83(5)	24(5)	37(6)	12(4)
C(22)	94(6)	47(4)	85(5)	3(4)	26(5)	9(4)
C(23)	60(4)	51(3)	68(4)	10(3)	18(3)	6(3)
C(24)	45(3)	42(3)	54(3)	15(2)	7(2)	3(2)
C(25)	54(4)	76(4)	68(4)	32(3)	22(3)	14(4)
C(26)	67(5)	102(6)	78(5)	48(5)	21(4)	20(5)
C(27)	65(5)	81(5)	99(6)	41(4)	12(4)	5(5)
C(28)	79(5)	60(4)	90(5)	32(4)	4(4)	21(4)
C(29)	61(4)	65(4)	87(5)	26(4)	19(4)	25(4)
C(30)	62(4)	44(3)	37(3)	17(3)	9(2)	3(2)
C(31)	68(5)	81(5)	57(4)	11(4)	1(4)	-10(4)
C(32)	101(7)	99(7)	67(5)	12(6)	-19(5)	-22(5)
C(33)	162(11)	81(6)	43(4)	45(7)	7(5)	-10(4)
C(34)	149(9)	68(4)	49(4)	32(5)	47(5)	13(3)
C(35)	86(5)	52(3)	50(3)	18(3)	25(3)	15(3)

Table A-3. H-atom coordinates (x 10^4) and isotropic displacement coefficients ($Å^2$ x 10^3) for 32

Atom	x	y	z	U
H(1)	1693(90)	1650(65)	2102(42)	80(24)
H(1A)	-4533	429	1337	80
H(1B)	-4269	-816	1438	80
H(1C)	-4293	-406	657	80
H(3A)	-3467	4107	2458	80
H(3B)	-2932	3004	2313	80
H(3C)	-2734	3941	1762	80
H(4A)	2373	5768	3210	80
H(4B)	2796	6351	4074	80
H(4C)	1282	6417	3520	80
H(5A)	-1634	4362	4186	80
H(5B)	-1433	3439	4728	80
H(5C)	-2965	3153	4074	80
H(6A)	-884	3495	337	80
H(6B)	-1674	2874	937	80
H(7A)	-575	1834	-184	80
H(7B)	-2319	1508	-113	80
H(8A)	-1494	10	233	80
H(8B)	96	835	740	80

H(9A)	272	-324	1841	80
H(9B)	-1296	-1333	1515	80
H(9C)	-1698	-1505	1602	80
H(9D)	-2939	-1271	2018	80
H(10A)	-96	-1262	2792	80
H(10B)	-1891	-1412	2623	80
H(11A)	-1421	462	3205	80
H(11B)	-526	-155	3771	80
H(13)	1788	4293	23	80
H(14)	3493	4080	-756	80
H(15)	5244	3029	-436	80
H(16)	5226	2097	639	80
H(17)	3479	2250	1420	80
H(19)	-693	5162	1260	80
H(20)	30	7220	1539	80
H(21)	2640	8340	1994	80
H(22)	4638	7425	2122	80
H(23)	3950	5374	1836	80
H(25)	3975	1511	2751	80
H(26)	6061	694	2923	80
H(27)	6121	-690	3742	80
H(28)	4093	-1262	4382	80

H(29)	2123	-345	4288	80
H(31)	3961	2978	4453	80
H(32)	4566	4015	5708	80
H(33)	2663	3650	6440	80
H(34)	244	2304	5929	80
H(35)	-434	1273	4680	80

B. Crystallographic data for compound 37b

Empirical formula:	$C_{34.5}H_{45}O_6P_3RuSi$	Formula weight:	777.8
Crystal system:	monoclinic	Space group:	$P2_1/n$
Unit cell dimensions:	a = 9.045(2) Å	Z:	4
	b = 22.524(2) Å	Diffractometer:	Siemens P4/PC
	c = 18.356(2) Å	Temperature:	293 K
	β = 99.63(2)°	R:	6.16%
		R_w:	6.38%

Table A-4. Atomic coordinates (x 10^4) and equivalent isotropic displacement coefficients ($Å^2$ x 10^3) for **37b**

Atom	x	y	z	U(eq)
Ru	1283(1)	877(1)	2573(1)	34(1)
P(1)	934(2)	-157(1)	2486(1)	40(1)

P(2)	1146(2)	1900(1)	2315(1)	37(1)
P(3)	3438(2)	815(1)	3496(1)	43(1)
Si(1)	2700(3)	818(1)	1011(1)	47(1)
O(1)	2933(5)	804(3)	1889(3)	44(2)
O(2)	-871(7)	1005(3)	3624(4)	68(3)
O(3)	4310(9)	1049(4)	755(5)	101(4)
O(4)	4321(7)	214(3)	3416(3)	52(2)
O(5)	3273(8)	778(3)	4351(3)	65(3)
O(6)	4737(7)	1317(3)	3582(4)	55(3)
C(1)	-997(9)	-427(4)	2192(5)	44(3)
C(2)	-1221(12)	-1016(5)	1999(7)	75(5)
C(3)	-2683(13)	-1230(5)	1750(7)	82(5)
C(4)	-3879(11)	-868(6)	1727(7)	80(5)
C(5)	-3661(12)	-293(5)	1934(8)	81(5)
C(6)	-2225(10)	-63(4)	2152(6)	60(4)
C(7)	1422(10)	-593(4)	3325(5)	47(3)
C(8)	2627(12)	-982(4)	3463(6)	63(4)
C(9)	2983(15)	-1277(5)	4126(8)	83(5)
C(10)	2157(18)	-1197(5)	4683(8)	88(6)
C(11)	978(15)	-808(6)	4555(6)	85(5)
C(12)	602(12)	-519(5)	3892(6)	67(4)
C(13)	-706(9)	2230(4)	1956(5)	40(3)

C(14)	-825(11)	2840(4)	1893(5)	56(4)
C(15)	-2175(13)	3104(5)	1590(6)	70(4)
C(16)	-3413(12)	2763(5)	1376(6)	67(4)
C(17)	-3315(10)	2161(5)	1432(5)	59(4)
C(18)	-1955(10)	1890(4)	1720(5)	49(3)
C(19)	1713(10)	2378(4)	3115(5)	46(3)
C(20)	735(12)	2463(4)	3610(6)	59(4)
C(21)	1176(14)	2781(5)	4276(6)	69(5)
C(22)	2607(14)	2988(5)	4433(6)	71(5)
C(23)	3581(13)	2923(4)	3952(7)	67(4)
C(24)	3144(11)	2617(4)	3298(5)	52(4)
C(25)	2283(10)	2155(4)	1641(5)	47(3)
C(26)	1671(11)	2038(4)	814(5)	57(4)
C(27)	1282(11)	1390(4)	606(5)	50(3)
C(28)	2241(13)	66(5)	610(6)	71(5)
C(29)	1268(12)	-306(5)	998(5)	64(4)
C(30)	1945(11)	-484(4)	1812(5)	51(3)
C(31)	-40(10)	949(4)	3214(5)	45(3)
C(32)	5217(21)	859(10)	392(11)	69(6)
C(33)	5644(12)	39(5)	3914(6)	78(5)
C(34)	2819(14)	1269(6)	4725(7)	92(6)
C(35)	5583(11)	1409(5)	3010(6)	71(5)

Table A-5. Anisotropic displacement coefficients ($Å^2 \times 10^3$) for **37b**

Atom	U_{11}	U_{22}	U_{33}	U_{12}	U_{13}	U_{23}
Ru	33(1)	31(1)	35(1)	2(1)	-1(1)	-2(1)
P(1)	36(1)	34(1)	48(1)	2(1)	1(1)	-1(1)
P(2)	38(1)	35(1)	37(1)	1(1)	0(1)	-3(1)
P(3)	43(1)	43(1)	40(1)	2(1)	-4(1)	-2(1)
Si(1)	53(1)	45(2)	42(1)	-1(1)	7(1)	-8(1)
O(1)	35(3)	50(4)	45(3)	4(3)	2(2)	-2(3)
O(2)	55(4)	84(6)	67(5)	7(4)	15(4)	-2(4)
O(3)	74(5)	102(7)	142(8)	-12(5)	60(5)	-29(6)
O(4)	50(4)	42(4)	57(4)	10(3)	-12(3)	-8(3)
O(5)	77(5)	73(6)	42(4)	11(4)	0(3)	2(4)
O(6)	49(4)	50(4)	64(5)	-12(3)	3(3)	-8(3)
C(1)	42(5)	40(5)	47(5)	-7(4)	3(4)	1(4)
C(2)	52(6)	57(8)	116(10)	-9(5)	14(6)	-16(6)
C(3)	75(8)	59(8)	110(11)	-28(6)	12(7)	-25(7)
C(4)	49(6)	76(8)	106(10)	-14(7)	-9(6)	-1(9)
C(5)	53(7)	60(8)	123(11)	4(5)	-3(7)	-7(7)
C(6)	50(6)	43(6)	79(8)	1(5)	-10(5)	-8(5)
C(7)	53(6)	35(5)	47(6)	-12(4)	-5(5)	4(4)
C(8)	71(7)	51(7)	63(7)	6(5)	0(5)	6(5)
C(9)	86(9)	59(8)	88(10)	8(6)	-30(8)	16(7)

C(10)	137(13)	41(7)	73(9)	-12(7)	-17(9)	19(6)
C(11)	118(10)	86(10)	48(7)	-14(9)	10(6)	-5(7)
C(12)	69(7)	66(8)	62(7)	1(6)	1(6)	-3(6)
C(13)	43(5)	38(5)	40(5)	12(4)	9(4)	7(4)
C(14)	55(6)	49(6)	58(6)	9(5)	-8(5)	7(5)
C(15)	81(8)	53(7)	74(8)	26(6)	5(6)	14(6)
C(16)	52(6)	66(8)	78(8)	16(6)	-1(6)	9(6)
C(17)	40(5)	74(8)	59(7)	12(5)	-1(5)	3(6)
C(18)	48(5)	43(5)	54(6)	0(4)	6(4)	0(5)
C(19)	52(5)	35(5)	49(6)	4(4)	3(4)	0(4)
C(20)	73(7)	46(6)	55(7)	5(5)	3(5)	-7(5)
C(21)	90(9)	65(8)	54(7)	15(6)	16(6)	-13(6)
C(22)	92(9)	55(7)	56(7)	-7(6)	-12(7)	-15(6)
C(23)	72(7)	44(6)	76(8)	-13(5)	-11(6)	3(6)
C(24)	63(6)	39(5)	53(6)	-7(5)	4(5)	-11(5)
C(25)	44(5)	50(6)	50(6)	-12(4)	12(4)	0(5)
C(26)	61(6)	56(7)	55(6)	6(5)	13(5)	6(5)
C(27)	64(6)	53(6)	32(5)	1(5)	3(4)	0(4)
C(28)	93(8)	71(8)	45(7)	-10(7)	-1(6)	-20(6)
C(29)	66(7)	79(8)	47(6)	-27(6)	9(5)	-28(6)
C(30)	58(6)	36(5)	62(6)	-2(4)	17(5)	0(5)
C(31)	44(5)	44(6)	47(5)	4(4)	6(4)	6(5)

C(33)	71(7)	78(8)	75(8)	26(6)	-15(6)	2(7)
C(34)	94(9)	125(12)	54(8)	26(8)	5(7)	-11(8)
C(35)	50(6)	72(8)	82(9)	-5(5)	-8(6)	3(6)

C. Derivation of kinetic equations

For the first-order reaction,

$$\underset{}{} \quad \underset{}{\textit{syn}} \quad \underset{k_{-1}}{\overset{k_1}{\rightleftharpoons}} \quad \underset{}{\textit{anti}}$$

$t = 0$	a	b
$t = t$	a - x	b + x
$t = t_e$	$a - x_e$	$b + x_e$

where a and b are the initial concentrates; x is the concentrate change at the time t; $(a - x_e)$ and $(b + x_e)$ are the concentrations at equilibrium,

the reaction rate can be expressed as:

$$\frac{dx}{dt} = k_1(a - x) - k_{-1}(b + x)$$

At equilibrium:

$$k_1(a - x_e) = k_{-1}(b + x_e)$$

$$k_{-1} = \frac{k_1(a - x_e)}{b + xe}$$

Therefore:

$$\frac{dx}{dt} = k_1(a - x) - \frac{k_1(a - x_e)(b + x)}{b + x_e}$$

$$= \frac{k_1(a + b)(x_e - x)}{b + x_e}$$

$$= \frac{k_1(a + b)(x_e - x)dt}{b + x_e}$$

$$\frac{dx}{x_e - x} = \frac{k_1(a + b)dt}{b + x_e}$$

Integrating both sides from 0 to x and from 0 to t:

$$-\ln(1-x/x_e) = \frac{k_1(a + b)t}{b + x_e}$$

(Equation A-1)

The *syn* → *anti* isomerization was monitored by ^{1}H NMR spectroscopy. The most straight-forward data from the spectra was the ratio of two isomers.

Assuming: $b/a = n$; $(b + x_e)/(a - x_e) = K$; $(b + x)/(a - x) = y$ (K was measured after the equilibrium had been achieved; n and y were determined from the integration of hydride or silicon methyl signals),

Then:

$$(1 - x/x_e) = \left[\frac{1 + n}{K - n}\right]\left[\frac{K - y}{1 + y}\right]$$

(Equation A-2)

$$\frac{a + b}{b + x_e} = (1 + K)/K$$

(Equation A-3)

-ln(1-x/xe) varies with the ratio y which changes with time t (Equation A-2). Plotting $-\ln(1-x/x_e)$ *vs* t gave a straight line (Equation A-1). k_1 can be calculated from the slope since $(a + b)/(b + x_e)$ is a constant (Equation A-3). The slope is independent of concentration for first-order reaction. It changes with concentration for any other reaction orders. If assuming a second-order process for the isomerization, for example, a relationship as: $-\ln(1-x/x_e) = 2k_1(a + b)t$ can be derived.

After the k_1 values at three different temperatures were measured, plot ln(k/T) *vs* 1/T to give the slope ($-\Delta H^{\ddagger}/R$) and the intercept [($\Delta S^{\ddagger}/R$) + ln(k/h)] based on the equation: $k = (kT/h)\exp(\Delta S^{\ddagger}/R)\exp[-\Delta H^{\ddagger}/(RT)]$ (k = Boltzmann's constant; h = Plank's constant).

D. Kinetic Data for Isomerization *syn* 26a → *anti* 26b and Isotopomerization *cis*-26a-^{13}CO (*syn*) → *trans*-26a-^{13}CO (*syn*)

D.i. Isomerization

T = 295 K		Solvent = toluene-d_8	$(b + x_e)/(a - x_e) = 4.5$		$(a + b) = 2.56E\text{-}2$ M		
t (h)	0	0.5	1	2	3	4	5
syn:*anti*	34.0	26.8	21.5	16.1	11.7	10.7	9.2
t (h)	6	7	8	9	10	11	12
syn:*anti*	8.3	7.6	7.1	6.6	6.7	5.9	5.6
t (h)	13						
syn:*anti*	5.6						

T = 295 K		Solvent = toluene-d_8	$(b + x_e)/(a - x_e) = 4.5$		$(a + b) = 5.33E\text{-}2$ M		
t (h)	0	0.5	1	1.5	2	2.5	3
syn:*anti*	75.6	40.1	36.1	24.6	22.4	15.6	16.5
t (h)	3.5	4	4.5	5	5.5	6	7
syn:*anti*	13.5	12.8	11.4	11.4	9.8	10.0	8.7

t (h)	8	9	10	11	12	13	14
syn:anti	8.2	7.6	7.1	6.9	6.4	6.3	6.0

T = 295 K		Solvent = toluene-d_8	$(b + x_e)/(a - x_e) = 4.5$		$(a + b) = 1.06E\text{-}1$ M	
t (h)	0	0.5	1	1.5	2	2.5	3
syn:anti	29.1	22.9	19.2	16.2	14.0	13.3	11.9
t (h)	3.5	4	4.5	5	6	7	8
syn:anti	11.1	10.1	9.1	8.5	8.1	7.4	6.8
t (h)	9	10	11	12			
syn:anti	6.4	6.1	5.8	5.6			

T = 307 K		Solvent = toluene-d_8	$(b + x_e)/(a - x_e) = 4.0$			
t (h)	0	0.25	0.5	0.75	1	1.25	1.5
syn:anti	36.4	19.1	15.2	10.4	8.8	7.6	6.9
t (h)	1.75	2	2.25	2.5	2.75	3	3.25
syn:anti	6.5	5.9	5.5	5.2	5.0	4.8	4.7
t (h)	3.5	3.75	4.25	4.75	5.5	6.25	7
syn:anti	4.6	4.5	4.3	4.2	4.1	4.0	4.0

T = 318 K		Solvent = toluene-d_8		$(b + x_e)/(a - x_e) = 3.6$			
t (h)	0	0.167	0.333	0.500	0.667	0.833	1.00
syn:*anti*	17.7	8.8	6.0	4.8	4.4	4.1	3.8
t (h)	1.17						
syn:*anti*	3.8						

T = 295 K		Solvent = THF-d_8		$(b + x_e)/(a - x_e) = 4.1$			
t (h)	0	0.5	1	1.5	2	2.5	3
syn:*anti*	40.9	31.8	24.7	16.4	16.5	14.5	12.7
t (h)	3.5	4	4.5	5	5.5	6	6.5
syn:*anti*	11.5	10.5	9.7	9.2	8.8	8.4	8.0
t (h)	7	7.5	8	8.5	9	9.5	10.5
syn:*anti*	7.6	7.3	7.0	6.8	6.6	6.5	6.2
t (h)	11.5						
syn:*anti*	5.9						

26-*d*		T = 295 K		Solvent = toluene-d_8	$(b + x_e)/(a - x_e) = 4.5$		
t (h)	0	1	2	3	4	5	6
syn:*anti*	15.8	13.1	11.1	10.5	9.7	8.9	8.5
t (h)	8	10	14	16.5			

syn:anti	7.3	6.6	6.0	5.5			

D.ii. Isotopomerization

T = 307 K		Solvent = toluene-d_8		$(b + x_e)/(a - x_e) = 1$		$(a + b) = 1.81E\text{-}2$ M	
t (h)	0	1	2	3	4	5	6
syn/trans :*syn/cis*	0	0.073	0.11	0.13	0.15	0.21	0.23
t (h)	7	8	9	10	11	12	13
syn/trans :*syn/cis*	0.27	0.31	0.33	0.36	0.39	0.42	0.45
t (h)	14	15	16	17	18	19	20
syn/trans :*syn/cis*	0.47	0.49	0.50	0.54	0.54	0.58	0.58

T = 307 K		Solvent = toluene-d_8		$(b + x_e)/(a - x_e) = 1$		$(a + b) = 6.44E\text{-}2$ M	
t (h)	0	1	2	3	4	5	6
syn/trans :*syn/cis*	0	0.060	0.087	0.093	0.13	0.17	0.21
t (h)	7	8	9	10	11	12	13
syn/trans :*syn/cis*	0.25	0.28	0.31	0.35	0.39	0.42	0.46

t (h)	14	15	16	17	18	19	20
syn/trans :*syn/cis*	0.47	0.51	0.53	0.56	0.57	0.59	0.62

t (h)	21
syn/trans :*syn/cis*	0.63

T = 307 K		Solvent = toluene-d_8	$(b + x_e)/(a - x_e) = 1$		$(a + b) = 1.68E\text{-}2$ M	
t (h)	0	1	2	3	4	5	6
syn/trans :*syn/cis*	0.25	0.28	0.29	0.32	0.33	0.36	0.40
t (h)	7	8	9	10	11	12	13
syn/trans :*syn/cis*	0.42	0.42	0.47	0.47	0.49	0.50	0.55
t (h)	14	15					
syn/trans :*syn/cis*	0.53	0.57					

T = 318 K		Solvent = toluene-d_8	$(b + x_e)/(a - x_e) = 1$		$(a + b) = 1.68E\text{-}2$ M	
t (h)	0	0.33	0.66	1	1.33	1.66	2

syn/trans :*syn/cis*	0.25	0.27	0.30	0.33	0.38	0.41	0.44
t (h)	2.33	2.66	3.66	4			
syn/trans :*syn/cis*	0.47	0.53	0.57	0.59			

T = 328 K		Solvent = toluene-d_8	$(b + x_e)/(a - x_e) = 1$		$(a + b) = 1.68E\text{-}2$ M	
t (h)	0	0.25	0.5	0.75	1	1.25	1.5
syn/trans :*syn/cis*	0.26	0.33	0.40	0.49	0.54	0.57	0.63
t (h)	1.75						
syn/trans :*syn/cis*	0.68						